ISSN 1881-7815 Online ISSN 1881-7823

BST
BioScience Trends

Volume 14, Number 5
October, 2020

IRCA
BSSA

IACMHR

www.biosciencetrends.com

BST
BioScience Trends

ISSN: 1881-7815
Online ISSN: 1881-7823
CODEN: BTIRCZ
Issues/Year: 6
Language: English
Publisher: IACMHR Co., Ltd.

BioScience Trends is one of a series of peer-reviewed journals of the International Research and Cooperation Association for Bio & Socio-Sciences Advancement (IRCA-BSSA) Group and is published bimonthly by the International Advancement Center for Medicine & Health Research Co., Ltd. (IACMHR Co., Ltd.) and supported by the IRCA-BSSA and Shandong University China-Japan Cooperation Center for Drug Discovery & Screening (SDU-DDSC).

BioScience Trends devotes to publishing the latest and most exciting advances in scientific research. Articles cover fields of life science such as biochemistry, molecular biology, clinical research, public health, medical care system, and social science in order to encourage cooperation and exchange among scientists and clinical researchers.

BioScience Trends publishes Original Articles, Brief Reports, Reviews, Policy Forum articles, Case Reports, News, and Letters on all aspects of the field of life science. All contributions should seek to promote international collaboration.

Editorial Board

Editor-in-Chief:

Norihiro KOKUDO
National Center for Global Health and Medicine, Tokyo, Japan

Co-Editors-in-Chief:

Xue-Tao CAO
Nankai University, Tianjin, China
Takashi KARAKO
National Center for Global Health and Medicine, Tokyo, Japan
Arthur D. RIGGS
Beckman Research Institute of the City of Hope, Duarte, CA, USA

Senior Editors:

Xunjia CHENG
Fudan University, Shanghai, China
Yoko FUJITA-YAMAGUCHI
Beckman Research Institute of the City of Hope, Duarte, CA, USA
Jianjun GAO
Qingdao University, Qingdao, China
Na HE
Fudan University, Shanghai, China
Kiyoshi KITAMURA
The University of Tokyo, Tokyo, Japan
Misao MATSUSHITA
Tokai University, Hiratsuka, Japan
Munehiro NAKATA
Tokai University, Hiratsuka, Japan
Takashi SEKINE
Toho University, Tokyo, Japan
Fanghua QI
Shandong Provincial Hospital, Ji'nan, China
Ri SHO
Yamagata University, Yamagata, Japan
Yasuhiko SUGAWARA
Kumamoto University, Kumamoto, Japan
Ling WANG
Fudan University, Shanghai, China

Web Editor:

Yu CHEN
The University of Tokyo, Tokyo, Japan

Proofreaders:

Curtis BENTLEY
Roswell, GA, USA
Thomas R. LEBON
Los Angeles, CA, USA

Editorial Office

Pearl City Koishikawa 603,
2-4-5 Kasuga, Bunkyo-ku, Tokyo 112-0003, Japan
E-mail: office@biosciencetrends.com

BioScience Trends

Editorial and Head Office

Pearl City Koishikawa 603, 2-4-5 Kasuga, Bunkyo-ku,
Tokyo 112-0003, Japan

E-mail: office@biosciencetrends.com
URL: www.biosciencetrends.com

Editorial Board Members

Girdhar G. AGARWAL
(Lucknow, India)
Hirotsugu AIGA
(Geneva, Switzerland)
Hidechika AKASHI
(Tokyo, Japan)
Moazzam ALI
(Geneva, Switzerland)
Ping AO
(Shanghai, China)
Hisao ASAMURA
(Tokyo, Japan)
Michael E. BARISH
(Duarte, CA, USA)
Boon-Huat BAY
(Singapore, Singapore)
Yasumasa BESSHO
(Nara, Japan)
Generoso BEVILACQUA
(Pisa, Italy)
Shiuan CHEN
(Duarte, CA, USA)
Yuan CHEN
(Duarte, CA, USA)
Naoshi DOHMAE
(Wako, Japan)
Zhen FAN
(Houston, TX, USA)
Ding-Zhi FANG
(Chengdu, China)
Xiaobin FENG
(Beijing, China)
Yoshiharu FUKUDA
(Ube, Japan)
Rajiv GARG
(Lucknow, India)
Ravindra K. GARG
(Lucknow, India)
Makoto GOTO
(Tokyo, Japan)
Demin HAN
(Beijing, China)
David M. HELFMAN
(Daejeon, Korea)
Takahiro HIGASHI
(Tokyo, Japan)
De-Fei HONG
(Hangzhou, China)
De-Xing HOU
(Kagoshima, Japan)
Sheng-Tao HOU
(Ottawa, Canada)
Yong HUANG
(Ji'ning, China)
Hirofumi INAGAKI
(Tokyo, Japan)
Masamine JIMBA
(Tokyo, Japan)
Chunlin JIN
(Shanghai, China)
Kimitaka KAGA
(Tokyo, Japan)
Ichiro KAI
(Tokyo, Japan)
Kazuhiro KAKIMOTO
(Osaka, Japan)
Kiyoko KAMIBEPPU
(Tokyo, Japan)
Haidong KAN
(Shanghai, China)
Bok-Luel LEE
(Busan, Korea)
Mingjie LI
(St. Louis, MO, USA)
Shixue LI
(Ji'nan, China)
Ren-Jang LIN
(Duarte, CA, USA)
Lianxin LIU
(Hefei, China)
Xinqi LIU
(Tianjin, China)
Daru LU
(Shanghai, China)
Hongzhou LU
(Shanghai, China)
Duan MA
(Shanghai, China)
Masatoshi MAKUUCHI
(Tokyo, Japan)
Francesco MAROTTA
(Milano, Italy)
Yutaka MATSUYAMA
(Tokyo, Japan)
Qingyue MENG
(Beijing, China)
Mark MEUTH
(Sheffi eld, UK)
Satoko NAGATA
(Tokyo, Japan)
Miho OBA
(Odawara, Japan)
Xianjun QU
(Beijing, China)
John J. ROSSI
(Duarte, CA, USA)
Carlos SAINZ-FERNANDEZ
(Santander, Spain)
Yoshihiro SAKAMOTO
(Tokyo, Japan)
Erin SATO
(Shizuoka, Japan)
Takehito SATO
(Isehara, Japan)
Akihito SHIMAZU
(Tokyo, Japan)
Zhifeng SHAO
(Shanghai, China)
Judith SINGER-SAM
(Duarte, CA, USA)
Raj K. SINGH
(Dehradun, India)
Peipei SONG
(Tokyo, Japan)
Junko SUGAMA
(Kanazawa, Japan)
Zhipeng SUN
(Beijing, China)
Hiroshi TACHIBANA
(Isehara, Japan)
Tomoko TAKAMURA
(Tokyo, Japan)
Tadatoshi TAKAYAMA
(Tokyo, Japan)
Shin'ichi TAKEDA
(Tokyo, Japan)
Sumihito TAMURA
(Tokyo, Japan)
Puay Hoon TAN
(Singapore, Singapore)
Koji TANAKA
(Tsu, Japan)
John TERMINI
(Duarte, CA, USA)
Usa C. THISYAKORN
(Bangkok, Thailand)
Toshifumi TSUKAHARA
(Nomi, Japan)
Kohjiro UEKI
(Tokyo, Japan)
Masahiro UMEZAKI
(Tokyo, Japan)
Junming WANG
(Jackson, MS, USA)
Xiang-Dong Wang
(Boston, MA, USA)
Hisashi WATANABE
(Tokyo, Japan)
Jufeng XIA
(Tokyo, Japan)
Lingzhong XU
(Ji'nan, China)
Masatake YAMAUCHI
(Chiba, Japan)
Aitian YIN
(Ji'nan, China)
George W-C. YIP
(Singapore, Singapore)
Xue-Jie YU
(Galveston, TX, USA)
Rongfa YUAN
(Nanchang, China)
Benny C-Y ZEE
(Hong Kong, China)
Yong ZENG
(Chengdu, China)
Chengchao ZHOU
(Ji'nan, China)
Xiaomei ZHU
(Seattle, WA, USA)

(*as of February, 2020*)

CONTENTS

Volume 14, Number 5, 2020

Editorial

Review

Original Article

Editorial

DOI: 10.5582/bst.2020.03364

Realizing 5G- and AI-based doctor-to-doctor remote diagnosis: opportunities, challenges, and prospects

Kenji Karako[1], Peipei Song[2,*], Yu Chen[1,*], Wei Tang[3]

[1] Department of Human and Engineered Environmental Studies, Graduate School of Frontier Sciences, The University of Tokyo, Chiba, Japan;
[2] Institute for Global Health Policy Research, National Center for Global Health and Medicine, Tokyo, Japan;
[3] International Health Care Center, National Center for Global Health and Medicine, Tokyo, Japan.

SUMMARY Fifth Generation (5G) mobile communications technology became available in Japan as of the end of March 2020. The Ministry of Internal Affairs and Communications (MIC) is proceeding with a plan to use 5G for a doctor-to-doctor remote diagnosis system. This remote diagnosis offers patients the benefit of receiving advanced medical care without having to travel long distances. The provision of a remote diagnosis will provide elderly patients in rural areas with an earlier diagnosis without burdening patients in Japan where the aging population and the uneven distribution of doctors are increasing. However, the system will increase the burden on specialists by expanding the doctor's catchment area. As a solution to that problem, deep learning-based artificial intelligence (AI) is expected to reduce the burden on doctors. In order to realize 5G- and AI-based real-time diagnostic support, diagnostic imaging using AI and an AI model that provides instructions are required. This is because ultrasonography and endoscopy, which can be used for remote diagnosis, do not acquire data on fixed areas like a CT or MRI scan. The AI model needs to instruct the doctor at the patient's home in order to collect appropriate information in accordance with the patient's symptoms and status. In order to build an interactive AI model, the interactions between doctors who are making a remote diagnosis should be recorded as training data and a 5G-based remote diagnosis system should be created. A remote diagnostic support system incorporating 5G and interactive diagnostic imaging incorporating AI will result in a system that places less of a burden on patients and doctors.

Keywords remote diagnosis, 5G mobile communications, artificial intelligence, ultrasonography, endoscopy, Japan

1. Doctor-to-doctor remote diagnosis

A remote diagnosis means that a doctor provides medical care to a distant patient *via* the Internet. This is expected to remedy regional differences in the quality of medical care and to provide high-level medical care to patients on isolated islands and in remote areas. In addition to conventional remote diagnostic imaging and remote pathological diagnosis, new types of remote care such as remote surgical support and remote intensive care, which can be called "urban medicine delivered remotely", have emerged in recent years. The demand for online medical care is also increasing because of COVID-19. In Japan, online medical care was clearly defined by the revision of "Guidelines for Proper Implementation of Online Medical Care" in July 2019 (*1*). In addition, medical fees were revised this year (*2*), and the case where a doctor in a remote location provides medical treatment using an information communication device under some conditions will be counted as a medical fee.

There are two major formats for telemedicine, "Doctor-to-Doctor-to-Patient" and "Doctor-to-Patient with Doctor". The first doctor is a specialist who has richer knowledge and clinical experience but works at the hospital located away from the attending physician and the patient. The second doctor is the patient's attending physician who can actually contact the patient. The major difference between the two methods is the way in which a specialist is involved. In the "Doctor-to-Doctor-to-Patient" format, the attending physician and the specialist exchange information based on information obtained from the patient by the attending physician, and the attending physician conducts a formal examination and makes a diagnosis based on the advice of the specialist. In contrast, in the "Doctor-to-Patient with Doctor" format, the specialist examines and diagnoses the patient with support and information shared by the attending physician near the patient. The

attending physician conducts examinations using testing equipment while receiving specialized knowledge and technical guidance from the specialist.

2. The 5G era: Opportunities for doctor-to-doctor remote diagnosis

In Japan, 5th Generation (5G) mobile communications technology became available from Japan's telecommunications carriers, DoCoMo, au, and SoftBank as of the end of March 2020 (*3-5*). In conjunction with this, the Ministry of Internal Affairs and Communications (MIC) is proceeding with a plan to use 5G for telemedicine (*6*). 5G is a new generation of mobile communications and has a higher communication speed than the conventional 4th Generation. The main impact of 5G is the improvement in Internet speed. The maximum downstream speed is about 3.4 Gbps and the maximum upstream speed is about 182 Mbps (*3*), enabling real-time transmission of 4K and high-quality video. This facilitates Doctor-to-Doctor with Patient remote diagnosis, whereby a specialist diagnoses the patient with the attending physician while watching video of the examination performed at the patient's home in real time. This remote diagnostic support gives patients the benefit of receiving advanced medical care without having to travel long distances. The provision of remote diagnostic support will provide elderly patients in rural areas with an earlier diagnosis without burdening patients in Japan where the aging population and the uneven distribution of doctors are increasing.

5G is expected to allow real-time remote diagnosis *via* high-quality video. However, there is no great advantage in using it in hospitals that can use optical communications because 5G is for mobile communications. 5G is effective when video or data needs to be communicated in real time from a place other than a hospital. Situations involving 5G and its advantages and requirements are summarized in Table 1. The mobility of equipment for each examination used in remote diagnosis is summarized in Table 2. Table 1 shows communication between hospitals does not require 5G if there are existing wired connections. In contrast, 5G is highly useful when making a remote diagnosis at a patient's home, and especially when making a diagnosis based on imaging such as ultrasonography or endoscopy. Aging of the population is progressing and the number of doctors is unevenly distributed in Japan. Here, remote diagnostic support will make it easier for elderly people living in areas far away from hospitals with specialists to receive a diagnosis. In addition, in the new era of COVID-19, the elderly - who are highly susceptible – can benefit from remote diagnostic support without crowding into hospitals. Preparations for such a remote diagnosis system are underway. In China, patients with COVID-19 underwent ultrasonography using a 5G-based robot-assisted remote ultrasound system between temporary hospitals and specialists at a hospital 700 km away (*7*).

Table 1. Comparison of whether 5th Generation (5G) mobile technology is required to facilitate real-time remote diagnosis between two points

Location		Necessity of 5G	Advantages of using 5G	Types of examinations available
Site of diagnosis	Site of examination			
Hospital	Hospital	× It is not necessary if an optical communications network is available at both hospitals.	None	Ultrasonography, Endoscopy, Skin examination, MRI, CT Scan, X-Ray
Hospital	Ambulance	○ It is necessary because conventional mobile communications cannot handle high-quality video in real time.	Real-time remote diagnosis can be provided by an emergency specialist	Ultrasonography, Endoscopy, Skin examination
Hospital	Patient's home	Δ It is not necessary if the patient's home has an optical communications network.	Real-time remote diagnosis can be provided regardless of location or region.	Ultrasonography, Endoscopy, Skin examination

Table 2. Comparison of the mobility of equipment for type of examination used in remote diagnosis

Type of examination	Need to be performed in real time	Type of data	Mobility
Ultrasonography	○	Video	○ Mobile examination equipment is being developed.
Endoscopy	○	Video	○ Mobile examination equipment is being developed.
Skin examination	×	Multiple images	○ Examination is possible if using a camera and a PC.
MRI	×	Multiple images	Δ Examination is possible if there is a vehicle equipped with the equipment.
CT Scan	×	Multiple images	Δ Examination is possible if there is a vehicle equipped with the equipment.
X-Ray	×	Multiple images	Δ Examination is possible if there is a vehicle equipped with the equipment.

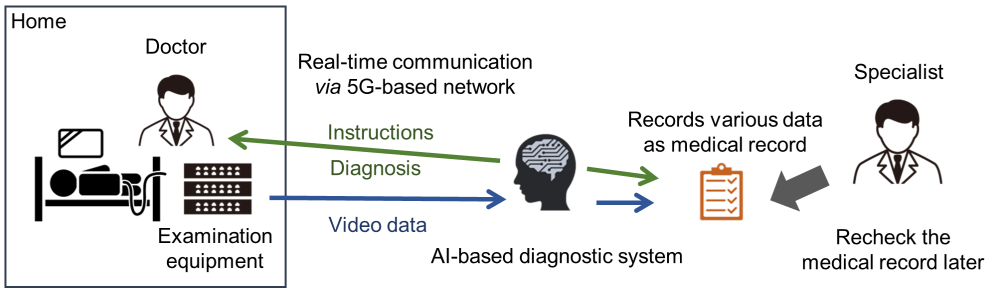

Figure 1. An overview of a 5G-based remote diagnosis system using AI. 5G, 5th Generation; AI, artificial intelligence.

3. 5G era: Challenges for doctor-to-doctor remote diagnosis

Remote diagnosis is likely to benefit the elderly, especially those living in rural areas, but it is likely to increase the burden on doctors. Remote diagnosis requires at least two doctors: an attending physician who visits the patient's home directly and a specialist who diagnoses the disease and instructs the attending physician. Although the area covered by the attending physician remains the same, remote diagnosis will force a specialist to spend more time diagnosing patients who live in a wider area in addition to his/her current patients.

On the other hands, one of the challenges is securing specialists can realize the remote diagnosis service using 5G communications technology. By providing remote diagnostic support, mid-sized hospitals are predicted to see patients from an even larger area. However, the number of specialists is limited, and the number of patients per specialist will increase. In other words, remote diagnostic support will decrease the burden on elderly in rural areas and increase the burden on doctors. Faced with this challenge, deep learning is expected to be widely used as a technology to reduce the burden on doctors. In recent years, deep learning has performed well in image recognition. Many deep learning applications involving CT (*8*) or MRI (*9*) scans have been proposed, resulting in highly accurate image interpretation. In addition, deep learning applications using ultrasonography and endoscopy image are also being studied. CT and MRI scans cannot be performed at the patient's home, but ultrasonography and endoscopy can be performed using mobile devices. By combining these mobile devices with 5G communications technology and deep learning, real-time simple remote diagnostic support can be provided without the actual contact between a specialist and the patient.

4. Prospects: Realizing 5G- and AI-based doctor-to-doctor remote diagnosis

Deep learning has been studied for various applications in medicine, though the main one is image recognition (*10-12*). This is effective when combined with 5G-based remote diagnosis, which mainly uses diagnostic imaging. Figure 1 shows an overview of a 5G-based remote diagnosis system in which a specialist and an attending physician are supported by deep learning. Deep learning replaces the diagnosis conventionally performed by a specialist, and the specialist performs a final check after the remote diagnosis is made. This reduces the burden on specialists. Because the obtained images can be saved, the images that deep learning has used to make a diagnosis can be checked again. Not only can the burden on the doctor be reduced, but the patient's waiting time can also be greatly shortened through the convenient application of remote diagnosis.

However, it is difficult to realize 5G-based artificial intelligence (AI) remote diagnosis support by combining the current technologies. There are two reasons. The first is the types of images that are mainly obtained using ultrasonography or endoscopy in remote diagnosis, but well-calibrated deep learning applications in medicine involve CT and MRI. Ultrasonography and endoscopy do not acquire data on fixed areas like a CT or MRI scan, the angle and position of imaging change depending on the state of the operator and the patient. This means that more varied images are expected to be obtained, and more training data are required to construct a highly accurate AI model. The second reason is that the specialist not only makes a diagnosis based on images but also gives additional instructions to the operator depending on examination results and the patient's condition obtained in remote diagnosis. Similarly, AI needs to make a diagnosis based on the received video and to give instructions to the operator who lacks specialized knowledge in 5G-based AI remote diagnosis. Little research has been conducted in this area, while diagnostic imaging is currently being studied in multiple areas of medicine. In order to provide a remote diagnosis incorporating AI in the future, instructions given to the operator depending on the patient's condition should be recorded and collected as learning data.

Finally, the potential of introducing AI into a remote diagnosis is expected to be used not only for diagnosis but also for matching specialists and patients. As 5G-based remote diagnosis removes the distance between

patients and specialists, patients will have more choices. At that time, AI could also be used to find the specialist suitable for the patient's symptoms and condition.

In conclusion, 5G communications technology allows a specialist to make a diagnosis remotely in real time using images from examinations such as ultrasonography and endoscopy. This will reduce the burden of travel for patients and make it easier for people in the suburbs and the elderly to receive an expert diagnosis. The obstacles posted by distance have disappeared, but specialists must oversee more patients, and the burden on specialists may increase. Remote diagnostic support using AI is expected to be a solution to this problem. Real-time diagnosis using AI enables an examination in accordance with the patient's schedule. In addition, video can be saved so a specialist can check the examination results later.

Funding: None.

Conflict of Interest: The authors have no conflict of interest to disclose.

References

1. Ministry of Health, Labor, and Welfare. Guidelines for Proper Implementation of Online Medical Care. *https://www.mhlw.go.jp/content/000534254.pdf* (accessed September 28, 2020) (in Japanese)
2. Ministry of Health, Labor, and Welfare. An overview of revised medical fees. *https://www.mhlw.go.jp/content/12400000/000616842.pdf* (accessed September 28, 2020) (in Japanese)
3. NTT docomo. Press Release: "5G" service launched. *https://www.nttdocomo.co.jp/info/news_release/2020/03/18_00.html* (accessed September 30, 2020) (in Japanese)
4. KDDI. "UNLIMITED WORLD au 5G" starts. 5G mobile communication service "au 5G" starts on March 26. *https://news.kddi.com/kddi/corporate/newsrelease/2020/03/23/4326.html* (accessed September 30, 2020) (in Japanese)
5. SoftBank. Press Release: The commercial service "SoftBank 5G" starts on March 27. *https://www.softbank.jp/corp/news/press/sbkk/2020/20200305_05/* (accessed September 30, 2020) (in Japanese)
6. Ministry of Internal Affairs and Communications. Report on a survey of the status of implementation of doctor-to-doctor remote medicine *https://www.soumu.go.jp/main_content/000699422.pdf* (accessed September 28, 2020) (in Japanese)
7. Ye R, Zhou X, Shao F, Xiong L, Hong J, Huang H, Tong W, Wang J, Chen S, Cui A, Peng C, Zhao Y, Chen L. Feasibility of a 5G-based robot-assisted remote ultrasound system for cardiopulmonary assessment of patients with COVID-19. Chest. 2020; S0012-3692(20)31870-5.
8. Domingues I, Pereira G, Martins P, Duarte H, Santos J, Abreu P. Using deep learning techniques in medical imaging: A systematic review of applications on CT and PET. Artif Intell Rev. 2019; 53:4093-4160.
9. Mazurowski MA, Buda M, Saha A, Bashir MR. Deep learning in radiology: An overview of the concepts and a survey of the state of the art with focus on MRI. J Magn Reson Imaging. 2019; 49:939-954.
10. Milletari F. Navab N, Ahmadi S. V-Net: Fully convolutional neural networks for volumetric medical image segmentation. 2016; arXiv:1606.04797.
11. Zhang J, Xie Y, Wu Q, Xia Y. Medical image classification using synergic deep learning. Med Image Anal. 2019; 54:10-19.
12. Ker J, Wang L, Rao J, Lim T. Deep learning applications in medical image analysis. IEEE Access. 2018; 6:9375-9389.

Received October 2, 2020; Revised October 18, 2020; Accepted October 21, 2020.

**Address correspondence to:*
Peipei Song, Institute for Global Health Policy Research, National Center for Global Health and Medicine, Tokyo, Japan.
E-mail: ppsong-tky@umin.ac.jp

Yu Chen, Department of Human and Engineered Environmental Studies, Graduate School of Frontier Sciences, The University of Tokyo, Chiba, Japan.
E-mail: chen@edu.k.u-tokyo.ac.jp

Released online in J-STAGE as advance publication October 25, 2020.

Review

DOI: 10.5582/bst.2020.03345

An overview of potential therapeutic agents to treat COVID-19

Xueqin Dong[1], Zhenxue Tian[2], Chengwu Shen[3], Cuirong Zhao[3,*]

[1] Community Health Service Center of the Qianfo Mountain Office, the People's Hospital of Lixia District of Jinan, Ji'nan, Shandong, China;
[2] Department of Pharmacy, Qingdao Municipal Hospital, Qingdao, Shandong, China;
[3] Department of Pharmacy, Shandong Provincial Hospital Affiliated to Shandong First Medical University, Ji'nan, Shandong, China.

SUMMARY The emerging novel coronavirus disease (COVID-19), caused by severe acute respiratory syndrome coronavirus 2 (SARS-CoV-2), has swept across the world and become a global threat to public health. More than 200 countries and territories worldwide are suffering from this COVID-19 pandemic. Worryingly, no specific vaccines or drugs have been approved for the prevention or treatment of COVID-19. Under the pressure of a sustained rise in the incidence and mortality of COVID-19, an unprecedented global effort is being implemented to identify effective drugs to combat the current coronavirus. As the understanding of SARS-CoV-2 virology, the underlying mechanism by which it attacks host cells, and the host response to the infection rapidly evolves, drugs are being repurposed and novel drugs are being identified and designed to target the SARS-CoV-2 pathogenesis. Presented here is a brief overview of both virus-based and host-based potential therapeutic drugs that are currently being investigated.

Keywords coronavirus, COVID-19, severe acute respiratory syndrome coronavirus 2, potential therapeutic agents, virus-based, host-based

1. Introduction

Since China first reported an unusual type of pneumonia on December 31, 2019, the number of people identified with this pneumonia has been increasing at an alarming rate, leading to a worldwide public health emergency. This new infectious disease, officially named coronavirus disease (COVID-19) on February 11, 2020 by the World Health Organization (WHO), is caused by severe acute respiratory syndrome coronavirus 2 (SARS-CoV-2). On March 11, 2020, the COVID-19 outbreak was officially declared a pandemic by the WHO. The disease is characterized by flu-like symptoms, such as cough, fever, myalgia, and fatigue. Although some infections are asymptomatic, many patients develop pneumonia, and some patients even develop severe and fatal respiratory diseases. As noted by the WHO, a total of 32,029,704 confirmed cases and 979,212 deaths worldwide were caused by COVID-19 as of September 25, 2020 (*1*). Nevertheless, there are no approved vaccines or specific drugs available for the prevention and treatment of COVID-19 at this moment. Given the threat of the pandemic and urgent need for effective vaccines and antivirals, vigorous efforts are being made globally to stop the COVID-19 epidemic. Compared to *de novo* drug development, drug repurposing offers advantages in taking less time and involving less cost, so it may be an ideal strategy for finding and identifying effective and safe potential therapeutic agents for the disease (*2*).

A better understanding of SARS-CoV-2 virology, the underlying mechanisms by which it attacks host cells, and the host response to the infection is crucial to drug discovery and repurposing. Like severe acute respiratory syndrome coronavirus (SARS-CoV) that emerged in 2002 and Middle East respiratory syndrome coronavirus (MERS-CoV) that was identified in 2012, SARS-CoV-2 is a lipid-enveloped, single-stranded, positive sense RNA virus that is a zoonotic β-coronavirus (*3*). The SARS-CoV-2 genome, first published on January 24, 2020 (*4*), shares a nucleotide identity of 82% with SARS-CoV (*5*). Studies have confirmed that SARS-CoV-2 and SARS-CoV bind to the same host cell surface receptor, angiotensin-converting enzyme 2 (ACE2), *via* their structural spike glycoprotein (S protein) (*6*). Host transmembrane serine protease 2 (TMPRSS2), along with ACE2 and virus S protein, is responsible for virus fusion and entry, and the three have been studied as potential targets for screening therapeutic compounds and repurposing drugs (*7,8*). In addition, many agents have been studied and identified based on virus-specific nucleic acids or proteins such as RNA-dependent RNA polymerase (RdRp), 3-chymotrypsin-like protease 3Clpro (also termed Mpro), and papain-like proteases (PLpro), which play an important role in virus replication

(*8,9*). The mechanism of host response to the infection also offers attractive targets for potential therapies (*8,10*). The possible life cycle of SARS-CoV-2 in host cells and host immune responses is shown in Figure 1. Presented here is a brief overview of both virus-based and host-based potential therapeutic drugs that are being investigated. Some examples are listed in Table 1 and their potential targets are shown in Figure 1.

2. Therapeutic agents targeting SARS-CoV-2 entry

The recognition and docking between virus S protein and host receptor ACE2 is the first step – and a critical one – for SARS-CoV-2 entry into susceptible cells (*11*). The binding process also requires the priming of the S protein by cleaving S protein by TMPRSS2 into two functional subunits, S1 and S2 (*7*). S1 is responsible for

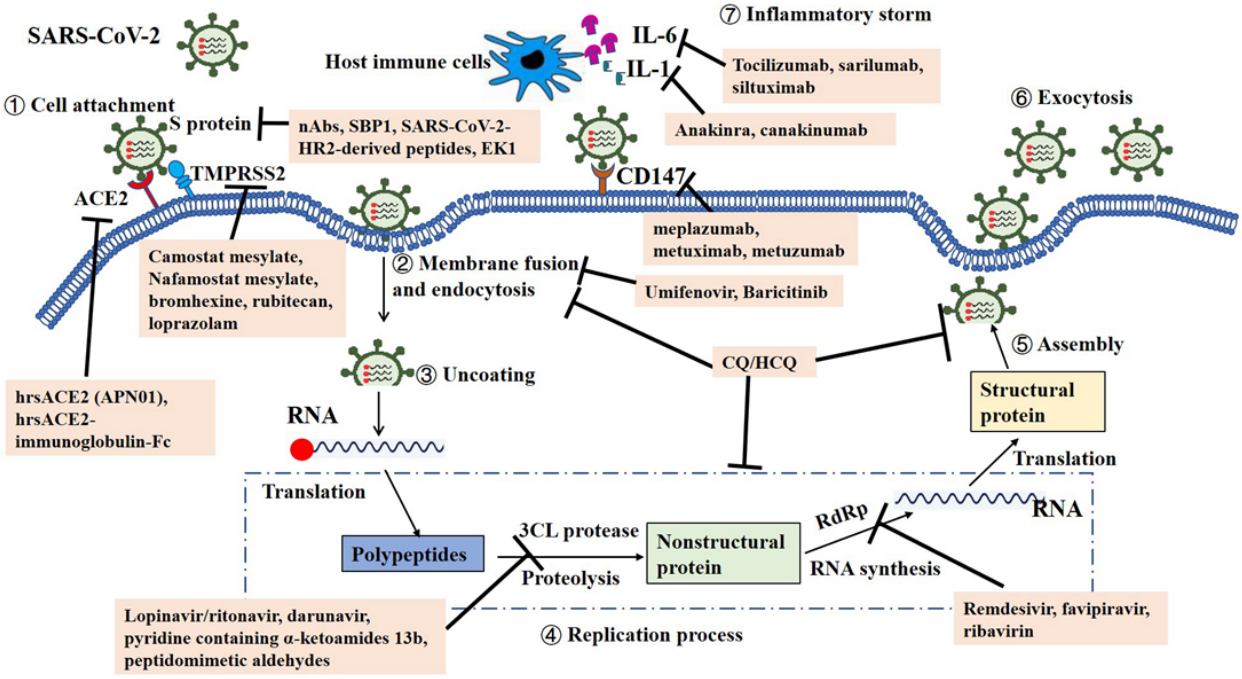

Figure 1. Possible life cycle of SARS-CoV-2 and potential agents. ① SARS-CoV-2 attaches to the host cell through the bind between the virus S protein and cellular receptors, such as angiotensin-converting enzyme 2 (ACE2) or transmembrane glycoprotein CD147. ② At this point, transmembrane protease serine 2 (TMPRSS2) cleaves and activates the S protein, leading to membrane fusion and virus entry *via* an endosomal pathway. ③ After entering the host cell, the viral RNA is introduced into the cytoplasm. ④ Then, with the help of encoded proteases including 3C-like protease (3CLpro) and RNA-dependent RNA polymerase (RdRP), SARS-CoV-2 produces new genomic RNA. ⑤ The assembled virion is formed and ⑥ released from the infected cells *via* exocytosis. ⑦ Uncontrolled replication promotes infection with SARS-CoV-2 and causes host immune responses and inflammatory cytokine storms. Proposed potential agents to treat SARS-CoV-2 and their possible targets are shown with bold lines. (CQ/HCQ: Chloroquine and hydroxychloroquine; nAbs: S protein-neutralizing antibodies; SBP1: peptide binder targeting the receptor-binding domain (RBD) of the S protein; EK1: a peptide fusion inhibitor; hrsACE2 (APN01): recombinant human soluble ACE2 protein)

Table 1. Potential agents for SARS-CoV-2

Mechanisms	Targets	Potential agents
Inhibiting SARS-CoV-2 entry	S protein	S protein-neutralizing antibodies (nAbs), peptide binder SBP1, SARS-CoV-2-HR2-derived peptides, peptide fusion inhibitor EK1
	ACE2	hrsACE2 (APN01), hrsACE2-immunoglobulin-Fc
	TMPRSS2	Camostat mesylate, nafamostat mesylate, bromhexine, rubitecan, loprazolam
	CD147	Meplazumab, metuximab, and metuzumab
	membrane lipids	Umifenovir
	AAK1	Baricitinib
Interrupting the process of SARS-CoV-2 replication	3CL protease	Lopinavir/ritonavir, darunavir, pyridine containing α-ketoamides 13b, peptidomimetic aldehydes
	RdRp	Remdesivir, favipiravir, ribavirin
Affecting host immune responses	IL-6 receptor	Tocilizumab, sarilumab, siltuximab
	IL-1 receptor/ IL-1β	Anakinra, canakinumab
Potential therapeutic agents with multiple mechanisms		Chloroquine and hydroxychloroquine, Interferons

viral attachment to the target host cells. The S2 subunit facilitates viral fusion with the cellular membrane, allowing virus entry *via* endocytosis (*7*). This complex process provides insights with which to screen potential drugs.

2.1. Screening for virus-based therapeutic agents targeting SARS-CoV-2 entry

The screening of virus-based therapeutic agents targeting SARS-CoV-2 entry is mostly focused on the virus' structural S protein. S protein-neutralizing antibodies (nAbs) could prevent SARS-CoV-2 infection *via* passive immunization and may become a better strategy for COVID-19 treatment (*12*). In molecular docking experiments, Pandey *et al.* found that 10 natural compounds (flavonoids/non-flavonoids) effectively bind to the C-terminal region of the SARS-CoV-2 S protein's two subunits, displaying a higher affinity than that of hydroxychloroquine (HCQ) (*13*). This binding likely interferes with interaction between the virus S protein and host ACE2 receptor or internalization during fusion (*14*). That study also suggested that fisetin, quercetin, and kamferol bind to the complex of hACE2-S with a low binding free energy and exhibit drug-like properties (*13*). A study has indicated that the S protein binds to the ACE2 receptor in its receptor-binding domain (RBD) (*15*). The peptide binder SBP1, which was synthesized to target the RBD of the S protein, could potentially keep SARS-CoV-2 from entering into host cells (*16*). A functional analysis of the S2 subunit revealed that the fusion of the viral and host cell membranes is mediated by the formation of a six-helical bundle (6-HB) from the interaction between heptad repeat 1 (HR1) and HR2 of S2 (*17*). The HR1 region is conserved among various human coronaviruses. Therefore, HR1 and HR2 may good targets for identifying fusion inhibitors against SARS-CoV-2. Based on experience with SARS-CoV (*18*), HR1- and HR2-derived peptides (named SARS-CoV-2-HR1P and SARS-CoV-2-HR2P, respectively) were designed to act as a SARS-CoV-2 membrane fusion inhibitor (*19*). Although their actual effect and safety need to be verified further, SARS-CoV-2-HR2P with potent fusion-inhibiting activity was found to be a promising therapeutic for treatment of SARS-CoV-2. In contrast, HR1P did not markedly inhibit virus fusion (*19*). The peptide fusion inhibitor EK1, which was designed based on the HR1 region, exhibited obvious fusion inhibitory activity with lower immunogenicity and better safety (*20*). Thus, EK1 may also be a potential treatment for COVID-19, although it needs to be verified.

2.2. Screening of host-based therapeutic agents targeting SARS-CoV-2 entry

The ACE2 receptor and TMPRSS2 are valuable targets for host-based therapeutic drug development involving the inhibition of SARS-CoV-2 entry. The recombinant human soluble ACE2 protein (hrsACE2, APN01) dose-dependently bound to cellular ACE2, suppressed SARS-CoV-2 replication, and significantly reduced viral loads in Vero cells (*21*). A point worth noting is that APN01 also inhibited SARS-CoV-2 infection in human kidney organoids and engineered blood vessels. The actual efficacy with which APN01 reduces the viral load and mitigates symptoms in patients with COVID-19 is being verified in a randomized, multicenter clinical trial (NCT04335136). In addition, the hrsACE2-immunoglobulin-Fc, formed by fusing hrsACE2 to an immunoadhesin, may be a good choice to suppress SARS-CoV-2 infection *in vitro* and potentially *in vivo* (*22*).

Given the key role of host cell serine protease TMPRSS2 in virus entry, protease inhibitors may be a treatment option for patients with COVID-19 (*7*). By inhibiting the activity of TMPRSS2, the clinically-proven serine protease inhibitors camostat mesylate and nafamostat mesylate have been found to drastically reduce SARS-CoV-2 infection in human lung Calu-3 cells (*7*) and simian Vero E6 cells (*9*), respectively. Both marketed drugs have already been approved to treat other diseases in Japan for many years and are clinically safe, suggesting that they should be considered as promising therapeutic drugs to treat SARS-CoV-2 without safety concerns. Moreover, the approved mucolytic cough suppressant bromhexine was also found to inhibit TMPRSS2 (*23*). These three marketed drugs are currently being tested in clinical trials as promising therapeutic agents against COVID-19 (*10*). In addition, the approaches of *in silico* structure-based virtual screening and molecular docking have identified the oral topoisomerase I inhibitor rubitecan and benzodiazepine loprazolam as potent candidates for combating SASRS-CoV-2 by inhibiting TMPRSS2 (*24*). Besides host ACE2 receptor and its partner protease TMPRSS2, transmembrane glycoprotein CD147 was found to mediate another novel route for SASRS-CoV-2 invasion of host cells (*25*). Thus, the humanized anti-CD147 antibodies meplazumab, metuximab, and metuzumab are considered promising host-based therapeutic agents for treating COVID-19, though they need to be verified and examined further (*26,27*).

The wide-spectrum antiviral drug umifenovir (arbidol) is another therapeutic agent targeting SARS-CoV-2 entry predominantly by intercalating into membrane lipids and inhibiting viral fusion with host cell membranes (*28*). Currently, several phase IV clinical trials have been completed or are underway in China to confirm the efficacy of arbidol in the treatment of COVID-19 (*29*). Arbidol was recommended to treat COVID-19 in the latest therapy guidelines issued by the National Health Commission of the People's Republic of China on August 8, 2020 (*30*). Baricitinib, the small

molecule inhibitor of Janus kinase subtype 1 and 2 (JAK1/2) approved for the treatment of rheumatoid arthritis, has been selected as a potential therapeutic agent in clinical trials involving patients with COVID-19 because of its interaction with endocytosis kinase regulator AP2-associated protein kinase 1 (AAK1), whereby it interrupts endocytosis and virus entry (*31*).

3. Potential therapeutic agents targeting SARS-CoV-2 replication

Following SARS-CoV-2 entry into the host cell, the viral RNA is introduced and the process of replication begins. Some functional proteins, such as RdRP, helicase 3CL protease, and PL protease, are vital for SARS-CoV-2 replication and have become potential targets for virus-based drug development to treat COVID-19 (*8*).

3.1. Potential therapeutic agents targeting proteases

The replicase complex, involving 3CLpro and the secondary papain-like protease 2 (PL2pro), facilitates viral replication (*32*). Since 96% of the SARS-CoV-2 3Clpro sequence is identical to that of SARS-CoV (*33*) and there is no human homolog of 3CLpro, 3CLpro has become an ideal target for drug discovery and repurposing (*34*). The combination of lopinavir/ritonavir (LPV/RTV), with LPV acting against 3CLpro and RTV increasing the LPV half-life by inhibiting cytochrome P450, was approved for treatment of human immunodeficiency virus (HIV) (*35*). Based on its efficacy against SARS-CoV and MERS-CoV (*36,37*), LPV/RTV was tested for the treatment of SARS-CoV-2. Although one *in vitro* study tested lopinavir against SARS-CoV-2 (*38*), only a few clinical trials have noted clinical improvement in patients with COVID-19 receiving lopinavir/ritonavir (*39,40*). Most clinical trials have found no clinical benefit from lopinavir/ritonavir in patients with mild, moderate, or severe COVID-19 (*41,42*). There may be benefits when lopinavir/ritonavir is combined with other drugs or used in the early stage of COVID-19. Currently, routine use of lopinavir/ritonavir is not recommended, and further studies are needed to confirm its efficacy. Despite the discouraging results with lopinavir and ritonavir, 3CLpro is still a potential therapeutic target for screening agents against SARS-CoV-2. Eleven approved or investigational drugs, such as the tyrosine kinase inhibitors poziotinib and fostamatinib, the antipsychotic drug ziprasidone, and the detoxification drug folinic acid, were identified as potential covalent inhibitors of SARS-CoV-2 3CLpro according to the steric-clashes alleviating receptors (SCAR) protocol (*43*). Other marketed drugs identified as SARS-CoV-2 3Clpro covalent inhibitors include lurasidone, talampicillin, ribavirin, and telbivudine (*24,44*). With the help of target-based virtual ligand screening, Wu *et al.* found that the anti-hypertensive drugs telmisartan and nicardipine, anti-bacterial agents including doxycycline, lymecycline, demeclocycline, and oxytetracycline, and conivaptan for treatment of hyponatremia displayed the highest binding affinity to 3CLpro (*45*). A growing number of marketed drugs, investigational compounds, and phytochemicals were identified as potent inhibitors of SARS-CoV-2 3CLpro according to computational methods (*46,47*), suggesting promising strategies for drug repurposing. The Michael acceptor inhibitor N3 and the organoselenium compound ebselen were found to inhibit SARS-CoV-2 in simian Vero E6 cells (*46*). A newly designed pyridine containing α-ketoamides (13b) displayed a strong inhibitory effect on purified recombinant SARS-CoV-2 3CLpro, favorable pharmacokinetic properties, and strong lung tropism in mice (*33*), suggesting a role for this specific type of 3CLpro inhibitor in COVID-19 therapy. Two newly designed and synthesized peptidomimetic aldehydes, termed 11a and 11b, displayed excellent inhibitory action against 3Clpro in simian Vero E6 cells infected with SARS-CoV-2 and SARS-CoV-2 (*34*). Because of its favorable pharmacokinetic properties and low toxicity in beagles and Sprague Dawley rats, 11a is considered a promising agent for COVID-19 therapy (*34*).

Another protease PLpro, which is crucial for correcting virus replication (*48*), is considered a potential target for developing therapeutic agents against SARS-CoV-2. Target-based virtual ligand screening has indicated that a series of marketed drugs, including the antibiotics cefamandole, chloramphenicol, and tigecycline, the anti-virus agents ribavirin, thymidine, and valganciclovir, and natural products such as platycodin D and catechin compounds, bind to PLpro with a high affinity, indicating their potential for SARS-CoV-2 treatment (*45*).

Darunavir, one of the second generation of HIV-1 protease inhibitors, drastically inhibited the replication of SAR-SCoV-2 *in vitro* (*49*). However, results from a randomized, open-labeled single-center, controlled phase III trial revealed that the combination of darunavir/cobicistat was not efficacious in reducing the duration of therapy or alleviating symptoms in patients with COVID-19 (NCT04252274). Further studied are need to evaluate the efficacy and safety of darunavir in the treatment of COVID-19.

3.2. Potential therapeutic agents targeting RdRp

RdRp is critical for the machinery of viral RNA transcription and replication. In addition to virus replication rates and fidelity, the virus' ability to mutate and adapt to new environments is determined by RdRp (*50*). At the protein level, the amino acid sequence of RdRp of SARS-CoV-2 is approximately 96% identical to that of SARS-CoV. Moreover, their protein structures are similar (*51*), indicating that potent inhibitors of the

RdRp of SARS-CoV are likely suppress SARS-CoV-2 RdRp (*52*). Thus, conserved RdRp has been recognized as a potential target for screening agents against SARS-CoV-2. The adenosine analogue remdesivir (GS-5734) was originally designed for the Ebola virus and exhibits broad-spectrum antiviral activity against several RNA viruses including SARS-CoV, MERS-CoV, and SARS-CoV-2 (*53,54*). Remdesivir can recognize the key component of RdRp nsp12 and join nascent viral RNA chains, leading to premature termination of RNA synthesis (*55*). Wang *et al.* found that micromolar concentrations of remdesivir can effectively block SARS-CoV-2 infection in Vero E6 cells, particularly in combination with chloroquine (*53*). A high intracellular concentration of remdesivir in its active form has been observed in rhesus monkeys and remdesivir retains its good pharmacokinetic properties, indicating its potential for clinical treatment of COVID-19. Since remdesivir has not been approved for treatment for any disease worldwide, it must be used compassionately or in enrolled clinical trials. One multicenter, double-blind, placebo-controlled, well-conducted RCT from China found that remdesivir reduced the time to clinical improvement in patients with COVID-19. However, the efficacy of remdesivir did not differ significantly from that of a placebo (*56*). The first American patient with COVID-19 received remdesivir and recovered in January 2020 (*57*). Remdesivir was also reported to reduce the time to recovery and tended to have a survival benefit for patients with COVID-19 in a clinical trial conducted by the Unites States National Institute of Health (*58*). Encouraged by these results, remdesivir was authorized by the United States Food and Drug Administration (FDA) for emergency use to treat inpatients with COVID-19 (*59*). Currently, a number of clinical trials to confirm the efficacy and safety of remdesivir for COVID-19 treatment are underway around the world (*10*).

Another nucleotide analogue suggested for COVID-19 treatment is favipiravir (Avigan, T-705), which has been approved for treatment of influenza in China and Japan (*49*). Favipiravir blocks the replication of RNA viruses by selectively inhibiting RdRp and is unlikely to generate resistant viruses (*60*). Since the RdRp gene of SARS-CoV-2 is similar to that of influenza virus, favipiravir may be a promising therapeutic for COVID-19 (*4*). The potential inhibitory effect of favipiravir on SARS-CoV-2 was demonstrated in Vero E6 cells *in vitro* (*53*). Preliminary results of clinical trials have indicated that favipiravir is effective at improving clinical outcomes for patients with COVID-19 (*61*). Compared to lopinavir/ritonavir, favipiravir resulted in faster improvement of chest images and faster viral clearance with fewer adverse effects during the treatment of patients with COVID-19 (*62*). Another randomized, multi-center, open labeled study revealed that favipiravir effectively decreased the incidence of cough and pyrexia and improved 7-day clinical recovery in inpatients with moderate-to-severe COVID-19 (*63*). However, there were no significant differences between groups receiving favipiravir and umifenovir. Although more clear evidence of the efficacy and safety of favipiravir is being assembled in multiple clinical trials (*10*), favipiravir may be one of the most promising anti-SARS-CoV-2 drugs and it has a relatively high level of patient compliance (*49*).

The guanosine analogue ribavirin has been proposed as a potent drug to treat SARS-CoV-2. Although there several RCTs to test its efficacy are underway, ribavirin is not recommended to treat patients with COVID-19 because of its apparent inactivity and hemolytic toxicity. In China, the latest treatment guidelines for COVID-19 (*30*), recommend a combination of ribavirin and lopinavir/ritonavir or interferon. However, use of ribavirin or lopinavir/ritonavir alone to treat COVID-19 is not recommended.

Computer-aided drug screening is being extensively used to discover new drugs and repurpose existing ones targeting RdRp in order to treat COVID-19. *in silico* virtual screening by Pokhrel *et al.* indicated that quinupristin bound across the conserved RNA tunnel of RdRp, possibly resulting in the arrest of viral replication (*64*). Elfiky cited ribavirin, sofosbuvir, remdesivir, tenofovir, galidesivir, and the guanosine derivative (IDX-184) as potent drugs for COVID-19 therapy since they tightly bind to SARS-CoV-2 RdRp in a model (*65*). In a target-based virtual ligand screening study, some marketed drugs such as the anti-bacterial agent novobiocin, the anti-fungal drug itraconazole, the muscle relaxant drug pancuronium bromide, and natural products or derivatives exhibited a high binding affinity to the RdRp of SARS-CoV-2 (*45*). The approved anti-HCV drug elbasvir was predicted to bind tightly and preferentially to RdRp, PLpro, and helicase of SARS-CoV-2, suggesting it could efficiently stop virus replication alone or in combination with other agents (*66*).

4. Discovery of potential therapeutic agents based on host immune responses

Pneumonia, lymphocyte exhaustion and peripheral lymphopenia, and a cytokine storm are the typical features of severe COVID-19 (*67*). When SARS-CoV-2 infects the host cell, the innate and adaptive immune responses are activated in the host's body. A variety of antibodies are produced to fight the virus. The uncontrolled inflammatory innate responses may induce a storm of pro-inflammatory cytokines including IL-1β, IL-6, and TNF, which cause tissue damage, leading to acute respiratory distress syndrome (ARDS). Thus, the host immune response provides a therapeutic avenue to treat COVID-19.

Based on experience with other viral diseases, the most direct but potentially effective treatment for

COVID-19 is using convalescent plasma (CP), which can be obtained from patients who have fully recovered from the SARS-CoV-2 infection (*68,69*). Patients who have recovered from SARS-CoV-2 have developed viral antibodies against SARS-CoV-2 at a high titre (*70*). Antibodies in the CP can neutralize the virus directly, suppress viremia, and boost the immunity of the patient. Studies in China have found that CP shows promising in improving the clinical condition of patients with severe COVID-19 (*69,71*). Hospitals in New York City are preparing to use CP as a promising treatment for COVID-19. Currently, a number of RCTs examining CP in the treatment of COVID-19 are underway in various countries. The human monoclonal neutralizing antibody CR3022, isolated from a convalescent patient with SARS-CoV, was reported to strongly bind to the conserved receptor-binding domain (RBD) in SARS-CoV-2 and SARS-CoV (*72*). CR3022 might be a potential therapeutic candidate to prevent and treat COVID-19, and especially for patients in life-threatening condition.

Neutralizing mAbs and small molecule inhibitors targeting pro-inflammatory cytokines and downstream signaling components may also useful in controlling the cytokine storm and alleviating immune injury (*29,67*). Tocilizumab, a recombinant human anti-IL-6 receptor antibody, has being investigated for off-label use in patients with severe COVID-19. Studies from China and Italy showed that tocilizumab potentially controlled fever and improved respiratory function in patients with severe COVID-19 (*73,74*). A number of RCTs are underway to evaluate the efficacy of tocilizumab, alone or in combination, in severely ill patients with COVID-19 (10). Other anti-IL-6 receptor antibodies studied for the treatment of COVID-19 include the humanized monoclonal antibody TZLS-501, sarilumab, and the recombinant human-mouse chimeric monoclonal antibody siltuximab (*75*). TZLS-501 has been shown to significantly reduce circulating levels of IL-6 in the blood (*75*). Clinical trials to test the safety and efficacy of siltuximab and sarilumab in patients with severe COVID-19 have begun (*10*). Several RCTs to study the efficacy of recombinant human IL-1 receptor antagonist anakinra in COVID-19 therapy are planned. The JAK1/2 inhibitor ruxolitinib and the anti-IL-1β monoclonal antibody canakinumab are compassionately used for COVID-19 treatment in Italy (*10*). Moreover, NLRP3 (NOD-, LRR-, and pyrin domain-containing 3) inflammasome, which plays an important role in inflammatory cytokine production, and its inhibitors have garnered attention as potential agents to treat SARS-CoV-2 (*76*).

In China, the latest treatment guidelines for COVID-19 recommend immunotherapies with CP and intravenous human immunoglobulin and tocilizumab to treat severe cases with rapid progression or a high level of IL-6 (*30*).

5. Other potential therapeutic agents with multiple mechanisms

Chloroquine (CQ) and its derivative hydroxychloroquine (HCQ), used to treat malaria and autoimmune diseases, have gained greater attention as promising therapeutic agents for the treatment of COVID-19 (*77,78*). To date, these agents have shown therapeutic activity against several viruses such as SARS-CoV and MERS-COV, suggesting they could be effective in treating SARS-CoV-2 infection (*79*). Proposed mechanisms by which CQ/HCQ combats SARS-CoV-2 include blocking virus entry into host cells, arresting viral replication, assembly, and budding, attenuating the inflammatory reaction, and inhibiting autophagy (*80,81*).

CQ/HCQ are weak bases and can elevate endosomal pH, thereby interfering with virus-host cell fusion during SARS-CoV-2 endocytosis (*78*). Another mechanism by which CQ/HCQ blocks SARS-CoV-2 entry into host cells is by inhibiting glycosylation of the ACE2 receptor and viral envelope glycoproteins (*53,79*). CQ/HCQ may arrest SARS-CoV-2 replication and budding by inhibiting specific enzymes that are necessary for virions assembly and budding from the cell membrane (*81*).

Another reason why CQ/HCQ may be a potential therapeutic agent for COVID-19 is because of their profound anti-inflammatory action to reduce pro-inflammatory cytokine and superoxide release, presumably by inhibiting the Toll-like receptor (TLR) pathway and upregulating the cyclin dependent kinase inhibitor p21 (*82,83*). Studies with Vero E6 cells have shown that CQ/HCQ has a potent antiviral effect against SARS-CoV-2 (*53,77*), with HCQ having relatively higher potency (*84*). That said, results from clinical trials of CQ/HCQ to treat patients with COVID-19 are inconsistent. A Chinese study with more than 100 patients showed that CQ is superior to the control in improving lung imaging findings, increasing the negative conversion rate, and shortening the duration of treatment (*85*). Two clinical trials suggested that HCQ improved clinical outcomes for patients with COVID-19 (*86*). However, HCQ did not improve viral clearance in another study with 30 patients with COVID-19 (*87*). The macrolide antibiotic azithromycin was shown to significantly enhance HCQ efficacy by increasing the virologic cure rate and reducing the duration of therapy in one case series from France (*88*). In contrast, another case series in France reported that a combination of HCQ and azithromycin had disappointing results in critically-ill patients with COVID-19 (*89*). Moreover, a retrospective analysis study from the US (*90*) found that the risk of mechanical ventilation for inpatients with COVID-19 could not be reduced by HCQ alone or in combination with azithromycin. Furthermore, increased overall mortality was found to be related to HCQ treatment alone. Therefore, there is a dire need for quality scientific evidence to confirm the efficacy

and safety of CQ/HCQ alone or in combination with azithromycin for the treatment of COVID-19. A large number of RCTs are ongoing (*80*). Interestingly, CQ/HCQ can induce the uptake of zinc into the cell cytosol, which has been shown to halt coronavirus replication by targeting RdRp (*91*). Thus, synergistic zinc supplementation may be necessary to improve the therapeutic effects of CQ/HCQ in patients with COVID-19 (*92*). Currently, many protocols have approved HCQ for the treatment of COVID-19, and especially when combined with other antiviral drugs (*78,84*). Instead of HCQ, chloroquine phosphate is recommended for the treatment of COVID-19 in the latest Chinese treatment guidelines (*30*). Post-exposure prophylaxis against SARS-CoV-2 with CQ/HCQ is not recommended in light of safety concerns (such as worsening vision, QT prolongation, hypoglycemia, and development of a rash).

Interferons (IFN) have antiviral activity by inhibiting viral replication and immunomodulatory action by interacting with toll-like receptors (*93*). IFN-α and IFN-β have been found to have potent inhibitory activity against SARS-CoV and MERS-CoV (*94,95*). Compared to SARS-CoV, SARS-CoV-2 was found to be more susceptible to IFNs and inhalation of IFN-α 2b significantly reduced the infection rate. Thus, IFN-α 2b can be used for prophylaxis against the SARS-CoV-2 infection (*96*). In China, IFN-α is recommended for treatment of COVID-19 alone or in combination with ribavirin and the antiviral drugs lopinavir/ritonavir (*30*). The efficacy and safety of this COVID-19 treatment strategy is being evaluated in a trial in China (ChiCTR2000029387). Reduced INF-β was reported to be directly associated with increased susceptibility to developing severe respiratory diseases in patients with a viral infection (*97*). The SARS-CoV-2 infection was found to decrease INF-β production in body (*98*). One study has suggested that a combination of INF-β and ribavirin offers promise as a treatment for SARS-CoV-2 (*99*). Clinical trials using IFN-β or inhaled IFN-β (SNG001) to treat COVID-19 are ongoing in the UK (*100*).

6. Conclusion

Effective therapeutic agents are urgently needed to globally combat the ongoing COVID-19 pandemic. This review has summarized potential therapeutic drugs targeting SARS-CoV-2 entry and replication and the host response to the infection. Although some of the drugs mentioned have yielded promising results, no specific drug is capable of treating COVID-19 according to a substantial amount of quality scientific evidence. The combination of antiviral and anti-inflammatory drugs may be more effective. Drug safety, a high level of efficacy, and availability should be full considered in COVID-19 therapy. Findings from ongoing clinical trials and advances in vaccine research will be critical to defeating the SARS-CoV-2 infection.

Funding: None.

Conflict of Interest: The authors have no conflict of interest to disclose.

References

1. Sozucan Y, Kalender ME, Sari I, Suner A, Oztuzcu S, Arman K, Yumrutas O, Bozgeyik I, Cengiz B, Igci YZ, Balakan O, Camci C. TRP genes family expression in colorectal cancer. Exp Oncol. 2015; 37:208-212.
2. Pushpakom S, Iorio F, Eyers PA, Escott KJ, Hopper S, Wells A, Doig A, Guilliams T, Latimer J, McNamee C, Norris A, Sanseau P, Cavalla D, Pirmohamed M. Drug repurposing: progress, challenges and recommendations. Nat Rev Drug Discov. 2019; 18:41-58.
3. Lu R, Zhao X, Li J, *et al.* Genomic characterisation and epidemiology of 2019 novel coronavirus: implications for virus origins and receptor binding. Lancet. 2020; 395:565-574.
4. Zhu N, Zhang D, Wang W, *et al.* A novel coronavirus from patients with pneumonia in China, 2019. N Engl J Med. 2020; 382:727-733.
5. Chan JF, Kok KH, Zhu Z, Chu H, To KK, Yuan S, Yuen KY. Genomic characterization of the 2019 novel human-pathogenic coronavirus isolated from a patient with atypical pneumonia after visiting Wuhan. Emerg Microbes Infect. 2020; 9:221-236.
6. Gralinski LE, Menachery VD. Return of the coronavirus: 2019-nCoV. Viruses. 2020; 12:135.
7. Hoffmann M, Kleine-Weber H, Schroeder S, Krüger N, Herrler T, Erichsen S, Schiergens TS, Herrler G, Wu NH, Nitsche A, Müller MA, Drosten C, Pöhlmann S. SARS-CoV-2 cell entry depends on ACE2 and TMPRSS2 and is blocked by a clinically proven protease inhibitor. Cell. 2020; 181:271-280.e278.
8. Zhou H, Fang Y, Xu T, Ni WJ, Shen AZ, Meng XM. Potential therapeutic targets and promising drugs for combating SARS-CoV-2. Br J Pharmacol. 2020; 177:3147-3161.
9. Sternberg A, McKee DL, Naujokat C. Novel drugs targeting the SARS-CoV-2/COVID-19 machinery. Curr Top Med Chem. 2020; 20:1423-1433.
10. Potì F, Pozzoli C, Adami M, Poli E, Costa LG. Treatments for COVID-19: emerging drugs against the coronavirus. Acta Biomed. 2020; 91:118-136.
11. Tortorici MA, Veesler D. Structural insights into coronavirus entry. Adv Virus Res. 2019; 105:93-116.
12. Ahmed SF, Quadeer AA, McKay MR. Preliminary identification of potential vaccine targets for the COVID-19 coronavirus (SARS-CoV-2) based on SARS-CoV immunological studies. Viruses. 2020; 12:254.
13. Pandey P, Rane JS, Chatterjee A, Kumar A, Khan R, Prakash A, Ray S. Targeting SARS-CoV-2 spike protein of COVID-19 with naturally occurring phytochemicals: an *in silico* study for drug development. J Biomol Struct Dyn. 2020.
14. Hasan A, Paray BA, Hussain A, Qadir FA, Attar F, Aziz FM, Sharifi M, Derakhshankhah H, Rasti B, Mehrabi M, Shahpasand K, Saboury AA, Falahati M. A review on

the cleavage priming of the spike protein on coronavirus by angiotensin-converting enzyme-2 and furin. J Biomol Struct Dyn. 2020.
15. Yan R, Zhang Y, Li Y, Xia L, Guo Y, Zhou Q. Structural basis for the recognition of SARS-CoV-2 by full-length human ACE2. Science. 2020; 367:1444-1448.
16. Zhang G, Pomplun S, Loftis AR, Loas A, Pentelute BL. The first-in-class peptide binder to the SARS-CoV-2 spike protein. bioRxiv. 2020.
17. Wrapp D, Wang N, Corbett KS, Goldsmith JA, Hsieh CL, Abiona O, Graham BS, McLellan JS. Cryo-EM structure of the 2019-nCoV spike in the prefusion conformation. Science. 2020; 367:1260-1263.
18. Liu S, Xiao G, Chen Y, He Y, Niu J, Escalante CR, Xiong H, Farmar J, Debnath AK, Tien P, Jiang S. Interaction between heptad repeat 1 and 2 regions in spike protein of SARS-associated coronavirus: implications for virus fusogenic mechanism and identification of fusion inhibitors. Lancet. 2004; 363:938-947.
19. Xia S, Liu M, Wang C, *et al.* Inhibition of SARS-CoV-2 (previously 2019-nCoV) infection by a highly potent pan-coronavirus fusion inhibitor targeting its spike protein that harbors a high capacity to mediate membrane fusion. Cell Res. 2020; 30:343-355.
20. Xia S, Yan L, Xu W, Agrawal AS, Algaissi A, Tseng CK, Wang Q, Du L, Tan W, Wilson IA, Jiang S, Yang B, Lu L. A pan-coronavirus fusion inhibitor targeting the HR1 domain of human coronavirus spike. Sci Adv. 2019; 5:eaav4580.
21. Monteil V, Kwon H, Prado P, *et al.* Inhibition of SARS-CoV-2 infections in engineered human tissues using clinical-grade soluble human ACE2. Cell. 2020; 181:905-913.e907.
22. Kruse RL. Therapeutic strategies in an outbreak scenario to treat the novel coronavirus originating in Wuhan, China. F1000Res. 2020; 9:72.
23. Maggio R, Corsini GU. Repurposing the mucolytic cough suppressant and TMPRSS2 protease inhibitor bromhexine for the prevention and management of SARS-CoV-2 infection. Pharmacol Res. 2020; 157:104837.
24. Elmezayen AD, Al-Obaidi A, Şahin AT, Yelekçi K. Drug repurposing for coronavirus (COVID-19): *in silico* screening of known drugs against coronavirus 3CL hydrolase and protease enzymes. J Biomol Struct Dyn. 2020.
25. Wang K, Chen W, Zhou Y-S, *et al.* SARS-CoV-2 invades host cells *via* a novel route: CD147-spike protein. bioRxiv. 2020.
26. Bian H, Zheng Z-H, Wei D, *et al.* Meplazumab treats COVID-19 pneumonia: an open-labelled, concurrent controlled add-on clinical trial. medRxiv. 2020.
27. Li J, Xing J, Yang Y, *et al.* Adjuvant (131)I-metuximab for hepatocellular carcinoma after liver resection: a randomised, controlled, multicentre, open-label, phase 2 trial. Lancet Gastroenterol Hepatol. 2020; 5:548-560.
28. Haviernik J, Štefánik M, Fojtíková M, Kali S, Tordo N, Rudolf I, Hubálek Z, Eyer L, Ruzek D. Arbidol (umifenovir): a broad-spectrum antiviral drug that inhibits medically important arthropod-norne flaviviruses. Viruses. 2018; 10:184.
29. Ahsan W, Javed S, Bratty MA, Alhazmi HA, Najmi A. Treatment of SARS-CoV-2: How far have we reached? Drug Discov Ther. 2020; 14:67-72.
30. Boccardo F, Decensi A, Guarneri D, Rubagotti A, Martorana G, Giberti C, Cerruti GB, Tani F, Zanollo A, Germinale T, *et al.* Long-acting (depot) D-TRP-6 LH-RH (Decapeptyl) in prostate cancer. An Italian multicentric trial. Am J Clin Oncol. 1988; 11 (Suppl 2):S129-131.
31. Richardson P, Griffin I, Tucker C, Smith D, Oechsle O, Phelan A, Rawling M, Savory E, Stebbing J. Baricitinib as potential treatment for 2019-nCoV acute respiratory disease. Lancet. 2020; 395:e30-e31.
32. Thiel V, Herold J, Schelle B, Siddell SG. Viral replicase gene products suffice for coronavirus discontinuous transcription. J Virol. 2001; 75:6676-6681.
33. Zhang L, Lin D, Sun X, Curth U, Drosten C, Sauerhering L, Becker S, Rox K, Hilgenfeld R. Crystal structure of SARS-CoV-2 main protease provides a basis for design of improved α-ketoamide inhibitors. Science. 2020; 368:409-412.
34. Dai W, Zhang B, Jiang XM, *et al.* Structure-based design of antiviral drug candidates targeting the SARS-CoV-2 main protease. Science. 2020; 368:1331-1335.
35. Cvetkovic RS, Goa KL. Lopinavir/ritonavir: a review of its use in the management of HIV infection. Drugs. 2003; 63:769-802.
36. Chu CM, Cheng VC, Hung IF, Wong MM, Chan KH, Chan KS, Kao RY, Poon LL, Wong CL, Guan Y, Peiris JS, Yuen KY, Group HUSS. Role of lopinavir/ritonavir in the treatment of SARS: initial virological and clinical findings. Thorax. 2004; 59:252-256.
37. Sheahan TP, Sims AC, Leist SR, *et al.* Comparative therapeutic efficacy of remdesivir and combination lopinavir, ritonavir, and interferon beta against MERS-CoV. Nat Commun. 2020; 11:222.
38. Choy KT, Wong AY, Kaewpreedee P, Sia SF, Chen D, Hui KPY, Chu DKW, Chan MCW, Cheung PP, Huang X, Peiris M, Yen HL. Remdesivir, lopinavir, emetine, and homoharringtonine inhibit SARS-CoV-2 replication *in vitro*. Antiviral Res. 2020; 178:104786.
39. Lim J, Jeon S, Shin HY, Kim MJ, Seong YM, Lee WJ, Choe KW, Kang YM, Lee B, Park SJ. Case of the index patient who caused tertiary transmission of COVID-19 infection in Korea: the application of lopinavir/ritonavir for the treatment of COVID-19 infected pneumonia monitored by quantitative RT-PCR. J Korean Med Sci. 2020; 35:e79.
40. Liu F, Xu A, Zhang Y, Xuan W, Yan T, Pan K, Yu W, Zhang J. Patients of COVID-19 may benefit from sustained lopinavir-combined regimen and the increase of Eosinophil may predict the outcome of COVID-19 progression. Int J Infect Dis. 2020; 95:183-191.
41. Cao B, Wang Y, Wen D, *et al.* A trial of lopinavir-ritonavir in adults hospitalized with severe Covid-19. N Engl J Med. 2020; 382:1787-1799.
42. Li Y, Xie Z, Lin W, *et al.* Efficacy and safety of lopinavir/ritonavir or arbidol in adult patients with mild/moderate COVID-19: An exploratory randomized controlled trial. Med (N Y). 2020.
43. Liu S, Zheng Q, Wang Z. Potential covalent drugs targeting the main protease of the SARS-CoV-2 coronavirus. Bioinformatics. 2020; 36:3295-3298.
44. Kandeel M, Al-Nazawi M. Virtual screening and repurposing of FDA approved drugs against COVID-19 main protease. Life Sci. 2020; 251:117627.
45. Wu C, Liu Y, Yang Y, Zhang P, Zhong W, Wang Y, Wang Q, Xu Y, Li M, Li X, Zheng M, Chen L, Li H. Analysis of therapeutic targets for SARS-CoV-2 and discovery of potential drugs by computational methods. Acta Pharm Sin B. 2020; 10:766-788.

46. Jin Z, Du X, Xu Y, *et al.* Structure of M(pro) from SARS-CoV-2 and discovery of its inhibitors. Nature. 2020; 582:289-293.
47. Ton AT, Gentile F, Hsing M, Ban F, Cherkasov A. Rapid identification of potential inhibitors of SARS-CoV-2 main protease by deep docking of 1.3 billion compounds. Mol Inform. 2020; 39:e2000028.
48. Harcourt BH, Jukneliene D, Kanjanahaluethai A, Bechill J, Severson KM, Smith CM, Rota PA, Baker SC. Identification of severe acute respiratory syndrome coronavirus replicase products and characterization of papain-like protease activity. J Virol. 2004; 78:13600-13612.
49. Dong L, Hu S, Gao J. Discovering drugs to treat coronavirus disease 2019 (COVID-19). Drug Discov Ther. 2020; 14:58-60.
50. Hukowska-Szematowicz B. Genetic variability and phylogenetic analysis of Lagovirus europaeus strains GI.1 (RHDV) and GI.2 (RHDV2) based on the RNA-dependent RNA polymerase (RdRp) coding gene. Acta Biochim Pol. 2020; 67:111-122.
51. Lung J, Lin YS, Yang YH, Chou YL, Shu LH, Cheng YC, Liu HT, Wu CY. The potential chemical structure of anti-SARS-CoV-2 RNA-dependent RNA polymerase. J Med Virol. 2020; 92:693-697.
52. Kirchdoerfer RN, Ward AB. Structure of the SARS-CoV nsp12 polymerase bound to nsp7 and nsp8 co-factors. Nat Commun. 2019; 10:2342.
53. Wang M, Cao R, Zhang L, Yang X, Liu J, Xu M, Shi Z, Hu Z, Zhong W, Xiao G. Remdesivir and chloroquine effectively inhibit the recently emerged novel coronavirus (2019-nCoV) *in vitro*. Cell Res. 2020; 30:269-271.
54. Sheahan TP, Sims AC, Graham RL, *et al.* Broad-spectrum antiviral GS-5734 inhibits both epidemic and zoonotic coronaviruses. Sci Transl Med. 2017; 9:eaal3653.
55. Gordon CJ, Tchesnokov EP, Woolner E, Perry JK, Feng JY, Porter DP, Götte M. Remdesivir is a direct-acting antiviral that inhibits RNA-dependent RNA polymerase from severe acute respiratory syndrome coronavirus 2 with high potency. J Biol Chem. 2020; 295:6785-6797.
56. Wang Y, Zhang D, Du G, *et al.* Remdesivir in adults with severe COVID-19: a randomised, double-blind, placebo-controlled, multicentre trial. Lancet. 2020; 395:1569-1578.
57. Holshue ML, DeBolt C, Lindquist S, *et al.* First Case of 2019 Novel Coronavirus in the United States. N Engl J Med. 2020; 382:929-936.
58. Ramos-Torres A, Bort A, Morell C, Rodriguez-Henche N, Diaz-Laviada I. The pepper's natural ingredient capsaicin induces autophagy blockage in prostate cancer cells. Oncotarget. 2016; 7:1569-1583.
59. Jang JJ, Cho KJ, Lee YS, Bae JH. Different modifying responses of capsaicin in a wide-spectrum initiation model of F344 rat. J Korean Med Sci. 1991; 6:31-36.
60. Shiraki K, Daikoku T. Favipiravir, an anti-influenza drug against life-threatening RNA virus infections. Pharmacol Ther. 2020; 209:107512.
61. Mori A, Lehmann S, O'Kelly J, Kumagai T, Desmond JC, Pervan M, McBride WH, Kizaki M, Koeffler HP. Capsaicin, a component of red peppers, inhibits the growth of androgen-independent, p53 mutant prostate cancer cells. Cancer Res. 2006; 66:3222-3229.
62. Cai Q, Yang M, Liu D, *et al.* Experimental treatment with favipiravir for COVID-19: An open-label control study. Engineering (Beijing). 2020.
63. Chen C, Zhang Y, Huang J, Yin P, Cheng Z, Wu J, Chen S, Zhang Y, Chen B, Lu M, Luo Y, Ju L, Zhang J, Wang X. Favipiravir versus arbidol for COVID-19: A randomized clinical trial. medRxiv. 2020.
64. Pokhrel R, Chapagain P, Siltberg-Liberles J. Potential RNA-dependent RNA polymerase inhibitors as prospective therapeutics against SARS-CoV-2. J Med Microbiol. 2020; 69:864-873.
65. Elfiky AA. Anti-HCV, nucleotide inhibitors, repurposing against COVID-19. Life Sci. 2020; 248:117477.
66. Balasubramaniam M, Reis RJS. Computational target-based drug repurposing of elbasvir, an antiviral drug predicted to bind multiple SARS-CoV-2 proteins. ChemRxiv. 2020.
67. Cao X. COVID-19: immunopathology and its implications for therapy. Nat Rev Immunol. 2020; 20:269-270.
68. Chen L, Xiong J, Bao L, Shi Y. Convalescent plasma as a potential therapy for COVID-19. Lancet Infect Dis. 2020; 20:398-400.
69. Shen C, Wang Z, Zhao F, *et al.* Treatment of 5 critically ill patients with COVID-19 with convalescent plasma. Jama. 2020; 323:1582-1589.
70. Li G, Fan Y, Lai Y, Han T, Li Z, Zhou P, Pan P, Wang W, Hu D, Liu X, Zhang Q, Wu J. Coronavirus infections and immune responses. J Med Virol. 2020; 92:424-432.
71. Duan K, Liu B, Li C, *et al.* Effectiveness of convalescent plasma therapy in severe COVID-19 patients. Proc Natl Acad Sci U S A. 2020; 117:9490-9496.
72. Tian X, Li C, Huang A, Xia S, Lu S, Shi Z, Lu L, Jiang S, Yang Z, Wu Y, Ying T. Potent binding of 2019 novel coronavirus spike protein by a SARS coronavirus-specific human monoclonal antibody. Emerg Microbes Infect. 2020; 9:382-385.
73. Zhang C, Wu Z, Li JW, Zhao H, Wang GQ. Cytokine release syndrome in severe COVID-19: interleukin-6 receptor antagonist tocilizumab may be the key to reduce mortality. Int J Antimicrob Agents. 2020; 55:105954.
74. Cellina M, Orsi M, Bombaci F, Sala M, Marino P, Oliva G. Favorable changes of CT findings in a patient with COVID-19 pneumonia after treatment with tocilizumab. Diagn Interv Imaging. 2020; 101:323-324.
75. Rayner CR, Smith PF, Hershberger K, Wesche D. Optimizing COVID-19 candidate therapeutics: Thinking without borders. Clin Transl Sci. 2020; 13:830-834.
76. Shah A. Novel coronavirus-induced NLRP3 inflammasome activation: A potential drug target in the treatment of COVID-19. Front Immunol. 2020; 11:1021.
77. Liu J, Cao R, Xu M, Wang X, Zhang H, Hu H, Li Y, Hu Z, Zhong W, Wang M. Hydroxychloroquine, a less toxic derivative of chloroquine, is effective in inhibiting SARS-CoV-2 infection *in vitro*. Cell Discov. 2020; 6:16.
78. Colson P, Rolain JM, Lagier JC, Brouqui P, Raoult D. Chloroquine and hydroxychloroquine as available weapons to fight COVID-19. Int J Antimicrob Agents. 2020; 55:105932.
79. Devaux CA, Rolain JM, Colson P, Raoult D. New insights on the antiviral effects of chloroquine against coronavirus: what to expect for COVID-19? Int J Antimicrob Agents. 2020; 55:105938.
80. Shukla AM, Archibald LK, Wagle Shukla A, Mehta HJ, Cherabuddi K. Chloroquine and hydroxychloroquine in the context of COVID-19. Drugs Context. 2020; 9:2020-4-5.
81. Mauthe M, Orhon I, Rocchi C, Zhou X, Luhr M, Hijlkema KJ, Coppes RP, Engedal N, Mari M, Reggiori

F. Chloroquine inhibits autophagic flux by decreasing autophagosome-lysosome fusion. Autophagy. 2018; 14:1435-1455.
82. van den Borne BE, Dijkmans BA, de Rooij HH, le Cessie S, Verweij CL. Chloroquine and hydroxychloroquine equally affect tumor necrosis factor-alpha, interleukin 6, and interferon-gamma production by peripheral blood mononuclear cells. J Rheumatol. 1997; 24:55-60.
83. Schrezenmeier E, Dörner T. Mechanisms of action of hydroxychloroquine and chloroquine: implications for rheumatology. Nat Rev Rheumatol. 2020; 16:155-166.
84. Yao X, Ye F, Zhang M, *et al. in vitro* antiviral activity and projection of optimized dosing design of hydroxychloroquine for the treatment of severe acute respiratory syndrome coronavirus 2 (SARS-CoV-2). Clin Infect Dis. 2020; 71:732-739.
85. Gao J, Tian Z, Yang X. Breakthrough: Chloroquine phosphate has shown apparent efficacy in treatment of COVID-19 associated pneumonia in clinical studies. Biosci Trends. 2020; 14:72-73.
86. Chen Z, Hu J, Zhang Z, Jiang S, Han S, Yan D, Zhuang R, Hu B, Zhang Z. Efficacy of hydroxychloroquine in patients with COVID-19: results of a randomized clinical trial. medRxiv. 2020.
87. Chen J, Liu D, Liu L, Liu P, Xu Q, Xia L, Ling Y, Huang D, Song S, Zhang D, Qian Z, Li T, Shen Y, Lu H. A pilot study of hydroxychloroquine in treatment of patients with moderate COVID-19. Zhejiang Da Xue Xue Bao Yi Xue Ban. 2020; 49:215-219.
88. Gautret P, Lagier JC, Parola P, *et al.* Clinical and microbiological effect of a combination of hydroxychloroquine and azithromycin in 80 COVID-19 patients with at least a six-day follow up: A pilot observational study. Travel Med Infect Dis. 2020; 34:101663.
89. Molina JM, Delaugerre C, Le Goff J, Mela-Lima B, Ponscarme D, Goldwirt L, de Castro N. No evidence of rapid antiviral clearance or clinical benefit with the combination of hydroxychloroquine and azithromycin in patients with severe COVID-19 infection. Med Mal Infect. 2020; 50:384.
90. Magagnoli J, Narendran S, Pereira F, Cummings T, Hardin JW, Sutton SS, Ambati J. Outcomes of hydroxychloroquine usage in United States veterans hospitalized with Covid-19. medRxiv. 2020.
91. Kaushik N, Subramani C, Anang S, Muthumohan R, Shalimar, Nayak B, Ranjith-Kumar CT, Surjit M. Zinc salts block hepatitis E virus replication by inhibiting the activity of viral RNA-dependent RNA polymerase. J Virol. 2017; 91.
92. Shittu MO, Afolami OI. Improving the efficacy of chloroquine and hydroxychloroquine against SARS-CoV-2 may require zinc additives - A better synergy for future COVID-19 clinical trials. Infez Med. 2020; 28:192-197.
93. Uematsu S, Akira S. Toll-like receptors and type I interferons. J Biol Chem. 2007; 282:15319-15323.
94. Falzarano D, de Wit E, Rasmussen AL, Feldmann F, Okumura A, Scott DP, Brining D, Bushmaker T, Martellaro C, Baseler L, Benecke AG, Katze MG, Munster VJ, Feldmann H. Treatment with interferon-α2b and ribavirin improves outcome in MERS-CoV-infected rhesus macaques. Nat Med. 2013; 19:1313-1317.
95. Barnard DL, Day CW, Bailey K, Heiner M, Montgomery R, Lauridsen L, Chan PK, Sidwell RW. Evaluation of immunomodulators, interferons and known *in vitro* SARS-coV inhibitors for inhibition of SARS-coV replication in BALB/c mice. Antivir Chem Chemother. 2006; 17:275-284.
96. Lokugamage KG, Hage A, Schindewolf C, Rajsbaum R, Menachery VD. SARS-CoV-2 is sensitive to type I interferon pretreatment. bioRxiv. 2020.
97. Sallard E, Lescure FX, Yazdanpanah Y, Mentre F, Peiffer-Smadja N. Type 1 interferons as a potential treatment against COVID-19. Antiviral Res. 2020; 178:104791.
98. Lu H. Drug treatment options for the 2019-new coronavirus (2019-nCoV). Biosci Trends. 2020; 14:69-71.
99. Zhang L, Liu Y. Potential interventions for novel coronavirus in China: A systematic review. J Med Virol. 2020; 92:479-490.
100. Uddin M, Mustafa F, Rizvi TA, Loney T, Suwaidi HA, Al-Marzouqi AHH, Eldin AK, Alsabeeha N, Adrian TE, Stefanini C, Nowotny N, Alsheikh-Ali A, Senok AC. SARS-CoV-2/COVID-19: Viral genomics, epidemiology, vaccines, and therapeutic interventions. Viruses. 2020; 12:526.

Received September 15, 2020; Revised October 11, 2020; Accepted October 14, 2020.

**Address correspondence to:*
Cuirong Zhao, Department of Pharmacy, Shandong Provincial Hospital Affiliated to Shandong First Medical University, Ji'nan, Shandong 250021, China.
E-mail: xiaozhao511@163.com

Released online in J-STAGE as advance publication October 25, 2020.

Review

DOI: 10.5582/bst.2020.03240

Systemic treatment of advanced or recurrent biliary tract cancer

Wei Zhang[1,2,*], Hongyuan Zhou[1,2], Yingying Wang[1,2], Zewu Zhang[1,2], Guangtai Cao[3], Tianqiang Song[1,2], Ti Zhang[1,2], Qiang Li[1,2]

[1] Department of Hepatobiliary Cancer, Tianjin Medical University Cancer Institute and Hospital, Tianjin, China;
[2] National Clinical Research Center for Cancer, Key Laboratory of Cancer Prevention and Therapy, Tianjin. Tianjin's Clinical Research Center for Cancer, Tianjin, China;
[3] Cangzhou Hospital of Integrated TCM-WM Cangzhou, Hebei, China.

SUMMARY Biliary tract cancer (BTC) is a disease entity comprising diverse epithelial tumors with features of cholangiocyte differentiation, and it includes cholangiocarcinoma (CCA) and gallbladder cancer (GBC). Depending on its anatomical location, cholangiocarcinoma is categorized as intrahepatic (iCCA), perihilar (pCCA), or distal (dCCA). Nearly two-thirds of patients with biliary tract cancer present with advanced disease at diagnosis and in 68-86% of resections the cancer eventually recurs either loco-regionally or at a distance. Chemotherapy is the first-line therapy for advanced or recurrent BTC. With the development of next-generation sequencing (NGS)-guided molecular targeted therapy, more options are available for treatment of advanced BTC. Chemotherapy, and especially a triplet regimen based on gemcitabine/cisplatin/nab-paclitaxel, has had the most significant effect, and fluorouracil, leucovorin, irinotecan plus oxaliplatin (FOLFIRINOX) combined with bevacizumab is promising. Molecular targeted therapy should be based on genome sequencing and appears essential to precision medicine. Fibroblast growth factor receptor (FGFR) inhibitors and isocitrate dehydrogenase (IDH) inhibitors are promising emerging targeted therapies mainly for iCCA. Other targeted therapies such as anti-human epidermal growth factor receptor-2 (HER2) therapies, MEK inhibitors, BRAF inhibitors, and poly ADP ribose polymerase (PARP) inhibitors had tentatively displayed efficacy. Further evaluations of combination strategies in particular are needed. An immune checkpoint inhibitor (ICI) alone is less efficacious, but an ICI in addition to chemotherapy or radiotherapy has resulted in a response according to many case series. However, ICIs are still being evaluated in several ongoing studies. Combination therapies have garnered attention because of interactions between signaling pathways of carcinogenesis in BTC.

Keywords biliary tract cancer, chemotherapy, targeted therapy, immune checkpoint inhibitor, next-generation sequencing

1. Introduction

Biliary tract cancer (BTC) is a disease entity comprising diverse epithelial tumors with features of cholangiocyte differentiation, and it includes cholangiocarcinoma (CCA) and gallbladder cancer (GBC). Depending on its anatomical location, cholangiocarcinoma is categorized as intrahepatic (iCCA), perihilar (pCCA), or distal (dCCA) (*1*). The overall incidence of BTC has increased progressively worldwide over the past four decades (*2-6*). Unfortunately, the prognosis remains poor, with a 5-year survival rate of around 5-15% (*7*). Surgical resection remains the mainstay of potentially curative treatment for all three disease subtypes, whereas liver transplantation after neoadjuvant chemoradiation is restricted to a subset of patients with early-stage pCCA (*1,8*). However, nearly two-thirds of patients with CCA present with advanced disease at diagnosis and in 68-86% of resections the cancer eventually recurs either loco-regionally or at a distance (*9-11*). Chemotherapy is the first-line therapy for advanced or recurrent BTC. With the development of next-generation sequencing (NGS)-guided molecular targeted therapy, more options are available for treatment of advanced BTC, and a growing number of studies have reported achieving a partial response or even a complete response (CR) after molecular targeted therapy or immune checkpoint inhibitors (ICIs). Systemic treatment of advanced or recurrent BTC is summarized here.

2. Chemotherapy and beyond

2.1. Chemotherapy: The first-line and the second line

Chemotherapy is the standard systemic therapy for BTC. Since 2010, the landmark UK ABC-02 trial established the doublet cisplatin and gemcitabine (GEMCIS) as the first-line standard of care for advanced CCA (*12*). In this randomized phase III study, 410 patients with BTC were randomly allocated to receive gemcitabine alone or gemcitabine combined with cisplatin. The doublet regimen conferred a statistically significant overall survival (OS) advantage over gemcitabine alone (11.7 *vs.* 8.1 months; HR, 0.64; 95% CI, 0.52-0.80; $P < 0.001$). In addition, cisplatin plus gemcitabine was well tolerated, and adverse events were similar between the treatment arms (Table 1).

After the ABC-02 trial, many gemcitabine-based regimens have been developed, including the gemcitabine plus oxaliplatin (GEMOX) regimen, the gemcitabine plus S-1 regimen (GS), and the gemcitabine plus nab-paclitaxel regimen (Table 1). The GEMOX regimen, which substitutes oxaliplatin for cisplatin, represents a valuable alternative as the first-line option in patients ineligible or unwilling to receive cisplatin based on promising results from a non-randomized phase II study (*13*), with fewer adverse reactions compared to GEMCIS. According to the Japanese experience, Morizane *et al.* (*14*) conducted a phase III clinical trial and found that GS is comparable to the GEMCIS regimen. The median progression-free survival (PFS) was 5.8 months with GC and 6.8 months with GS (HR: 0.86, 95% CI: 0.70-1.07). The median OS was 13.4 months with GEMCIS and 15.1 months with GS (HR: 0.945, 95% CI: 0.777-1.149, p for non-inferiority = 0.0459 < 0.05). In a phase II clinical trial where nab-paclitaxel and gemcitabine were administered as first-line treatment of advanced or metastatic cholangiocarcinoma, patients received intravenous nab-paclitaxel followed by gemcitabine on days 1, 8, and 15 of each 28-day treatment cycle until disease progression or unacceptable toxicities. Median OS was 12.4 months (95% CI, 9.2-15.9), and median time to progression was 7.7 months (95% CI, 6.1-13.1). The confirmed best overall response rate was 30% and the disease control rate was 66% (*15,16*). Although the trial did not meet its primary efficacy end point, its results indicated that a nab-paclitaxel plus gemcitabine regimen was well tolerated and may be an alternative to the current therapeutic approaches for advanced BTC.

Compared to the duplet gemcitabine, the triplet regimen based on GEMCIS resulted in a more objective response (Table 1). Shroff *et al.* (*17*) investigated the addition of nab-paclitaxel to standard doublet therapy (known as the GAP regimen: gemcitabine, nab-paclitaxel [Abraxane], and cisplatin [Platinol]). In this open-label, single-arm, phase II clinical trial, 60 patients with advanced BTC were treated with gemcitabine, cisplatin, and nab-paclitaxel. A point worth noting is that the standard starting doses of gemcitabine and nab-paclitaxel were reduced from 1000 mg/m^2 and 125 mg/m^2 to 800 mg/m^2 and 100 mg/m^2, respectively. The majority of

Table 1. Summary of first-line chemotherapy for advanced BTC

Study, Year	Study design	N	Chemotherapy regimen	Objective response (PR or CR)	PFS (months)	OS (months)
Valle (*12*), 2010	Advanced BTC Phase III (ABC-02)	410	GEMCIS *vs.* GEM; GEM: 1000 mg/m^2; CIS: ^{2}5 mg/ m^2	PR: 26.1% *vs.* 15% DCR:81.4% *vs.* 71.8%	8 *vs.* 5 4m-PFS 70% in CIS/GEM	11.7 *vs.* 8.1
Andre´ T (*13*), 2008	Advanced BTC Phase II	67	GEMOX gemcitabine 1000 mg/m^2 (day 1) and oxaliplatin 100 mg/m^2 (day 2), every 2 weeks	ORR: 20.5% in non-GBC 4.3% in GBC	3.4	8.8
Morizane (*14*), 2019	Unresectable locally advanced BTC, Phase III, FUGA-BT (JCOG1113)	354	GS (141 cases) *vs.* GEMCIS (148 cases); S-1 60/80/100 mg/day	ORR: 29.8% (42/141) *vs.* 32.4% (48/148)	6.8 *vs.* 5.8	15.1 *vs.* 13.4
Sahai V (*15*), 2019	Metastatic CCA Phase II	74	Gemcitabine, nab-paclitaxel on days 1, 8, and 15 of each 28-day treatment cycle	ORR 30%; DCR 66%	7.7 (6-m PFS: 61%)	12.4
Shroff (*17*), 2019	Phase II 63% iCCA 78% metastatic disease	60	GAP regimen (gemcitabine, nab-paclitaxel, cisplatin]): Gemcitabine and nab-paclitaxel were reduced from 1000 mg/m^2 and 125 mg/m^2 to 800 mg/m^2 and 100 mg/m^2.	ORR: 48.3%; PRR: 45%; DCR 84%. CR was achieved in 2 patients. Conversion to resectable: 20%(12/60)	11.8	19.2
Belkouz (*18*), 2020	Advanced BTC (salvage)	40	FOLFIRINOX-single arm Oxaliplatin (85 mg/m^2), LV (400 mg/m^2), irinotecan (180 mg/m^2), and FU bolus (400 mg/m^2) then FU (2400 mg/m^2) over 46 h, 12 cycles	ORR: 10%	6.2	10.7

BTC, biliary tract cancer. CCA, cholangiocarcinoma. iCCA, intrahepatic cholangiocarcinoma. GBC, gallbladder cancer. LV, leucovorin. FU, fluorouracil. GEM, gemcitabine. CIS, cisplatin. Oxa, Oxaliplatin. GS, gemcitabine plus S-1. PFS, progression-free survival. OS, overall survival. PR, partial response. CR, complete response. ORR, objective response rate. DCR, disease control rate. na, not available.

patients (63%) had intrahepatic cholangiocarcinoma, and 78% of the entire cohort had metastatic disease. PFS was 11.8 months (*vs.* 8.0 months for ABC-02) and median OS was 19.2 months (*vs.* 11.7 months for ABC-02). Moreover, the triplet regimen allowed conversion to resectable disease in 12 patients, and a pathologic complete remission was achieved in 2 of those patients. SWOG 1815 is a phase III trial currently underway comparing the gemcitabine/cisplatin/nab-paclitaxel regimen to the GEMCIS regimen (*16*) and if it yields positive results, it has the potential to establish a new standard of care.

Another triplet regimen is fluorouracil, leucovorin, irinotecan plus oxaliplatin (FOLFIRINOX), which is the standard therapy for pancreatic duct adenocarcinoma (PDAC). However, a single arm of FOLFIRINOX (*18*) to treat advanced BTC resulted in an objective response rate (ORR) of only 10% and a PFS of 6.2 months and an OS of 10.7 months, indicating that it was less efficacious than GEMCIS. A trial of modified FOLFIRINOX versus GEMCIS as first-line chemotherapy for locally advanced non resectable or metastatic BTC (AMEBICA)-PRODIGE 38 (NCT02591030) is now underway (*19*). This is a randomized controlled multicenter phase II/III study aiming to clarify the efficacy or FOLFIRINOX over GEMCIS.

Ten years ago when ABC-02 was published, there were fewer than 50 trials listed for this disease site on ClinicalTrials.gov. Currently, there are over 400 hundred BTC trials listed all over the world. More phase III clinical trials of different regimens are expected to help eradicate this aggressive disease.

2.2. Chemotherapy combined with antiangiogenic therapies

Antiangiogenic inhibitors, such as cabozantinib (*20*) or sunitinib (*21*), did not have better efficacy when used alone (not in combination with chemotherapy), and adverse reactions to cabozantinib and sunitinib precluded their combination with chemotherapy. Gemcitabine plus sorafenib provided comparable disease control and survival to GEMCIS (*22*). The best result came from a phase II study, which revealed that FOLFIRI plus bevacizumab (*23*) resulted in a PFS of 8 months and an OS of 20 months. In the future, the combination of chemotherapy with bevacizumab may offer hope.

2.3. Chemotherapy combined with anti-EGFR therapy

Combining GEMCIS with an epidermal growth factor receptor (EGFR) antibody, such as panitumumab (*24-26*), cetuximab (*27*), or erlotinib (*28*), did not provide a survival benefit compared to GEMCIS alone. Although the addition of erlotinib to gemcitabine and oxaliplatin had antitumor activity in advanced BTC as indicated by a higher ORR (30% *vs.* 16%) and a prolonged PFS (5.9 *vs.* 3.0 months, $p = 0.049$) (*28*), no significant difference in OS was noted between erlotinib/GEMCIS and GEMCIS groups. One possible reason for the lack of aq benefit could be because these trials were conducted in unselected populations. Further development of anti-EGFR therapy for cholangiocarcinoma should include a biomarker-driven approach.

3. Molecular targeted therapy

There is no standard second-line treatment for advanced cholangiocarcinoma. With the development of NGS, more driven genes are being identified, helping to explain the underlying mechanism of the pathogenesis of BTC and to develop new therapies (*29*). BTCs are clinically and genetically heterogeneous. Different forms of NGS have been reported to yield different results.

Wardell *et al.* (*30*) examined 412 BTC samples from Japanese and Italian populations including 136 of iCCA, 101 of dCCA, 109 of pCCA, and 66 of GBC. They identified 32 significantly mutated genes, some of which negatively affected prognosis. TP53 (26%), KRAS (17%), SMAD4 (8%), NF1 (6%), ARID1A (6%), PBRM1 (6%), ATR (6%), PIK3CA (5%), and ERBB3 (5%) are among the 32 significantly and commonly mutated genes. Nakamura *et al.* (*31*) performed comprehensive whole-exome and transcriptome sequencing in a large cohort of 260 patients with BTC, including 145 with iCCA, 86 with pCCA/dCCA, and 29 with GBC. The repertoire of genetic alterations varied across the different cholangiocarcinoma subtypes. For example, recurrent mutations in IDH1, IDH2, FGFR1, FGFR2, FGFR3, EPHA2, and BAP1 were noted predominantly in iCCA, whereas ARID1B, ELF3, PBRM1, PRKACA, and PRKACB mutations occurred preferentially in iCCA/pCCA/dCCA (*31*).

Lowery *et al.* (*32*) reported that the most commonly altered genes in iCCA were IDH1 (30%), followed by ARID1A (23%), BAP1 (20%), TP53 (20%), and FGFR2 gene fusions (14%).

In a cohort of 80 Chinese patients with eCCA, Xue *et al.* (*33*) reported that the most frequently altered genes were TP53 (68%), followed by KRAS (46%), SMAD4 (22%), ARID1A (20%), and CDKN2A (19%). The top three actionable alterations included CDKN2A ($n = 11$), BRAF ($n = 5$), and ERBB2 ($n = 4$). Montal *et al.* (*34*) identified KRAS (36.7%), TP53 (34.7%), ARID1A (14.0%), and SMAD4 (10.7%) as the prevalent mutations in 189 patients with BTC (76% had pCCA and 24% had dCCA) in the US and Europe, while recurrent chromosomal amplifications were observed in YEATS4 (6.0%), MDM2 (4.7%), CCNE1 (2.7%), CDK4 (1.3%), and ERBB2 (1.3%).

Paraffin-embedded tumors from a cohort of 108 Chinese and 107 American patients with GBC were subjected to comprehensive genomic profiling (CGP) with an NGS panel (*35*). The most frequent alterations

were TP53 (69.4%), followed by CDKN2A/B (26%), ERBB2 (18.5%), PIK3CA (17%), and CCNE1 (13%) in the Chinese cohort, and TP53 (57.9%), CDKN2A/B (25%), SMAD4 (17%), ARID1A (14%), PIK3CA (14%), and ERBB2 (13.1%) in American patients.

In patients with BTC, the disease is highly targetable, thus allowing precision medicine. In a study by Lowery *et al.* (*36*) with a total of 195 patients of iCCA/pCCA/dCCA, genetic alterations with potential therapeutic implications were identified in 47% of the patients, leading to biomarker-directed therapy or clinical trial enrollment in 16%. Nakamura *et al.* (*31*) also found potentially targetable genetic driver alterations in ~40% of the patients. With the development of NGS-guided molecular targeted therapy, many inhibitors of molecular targets are reported to achieve a PR or even a CR (*36*).

3.1. Targeting FGFR

Several studies have consistently identified fibroblast growth factor receptor (FGFR) fusions in patients with BTC, and especially patients with iCCA (*29*). FGFR2 fusion events have been identified in 5.5% (31) to 28% (*37*) of patients with iCCA. Clinically, FGFR2 fusion-positive status was associated with a shorter OS. A few therapies targeting FGFR-fusions have yielded promising results, including BGJ398 (infigratinib; QED Therapeutics), INCB54828 (pemigatinib; Incyte), ARQ-087 (derazantinib; Arqule), and TAS-120 (Table 2).

BGJ398 (infigratinib) is an orally bioavailable, selective, ATP-competitive pan-FGFR kinase inhibitor with activity in tumor models harboring FGFR alterations. A phase II study of BGJ398 (infigratinib; QED Therapeutics) (*38*) involved patients with pFGFR-altered advanced cholangiocarcinoma, and it found that the overall response rate was 14.8% (18.8% FGFR2 fusions only), the disease control rate was 75.4% (83.3% FGFR2 fusions only), and the estimated median PFS was 5.8 months (95% CI, 4.3 to 7.6 months). Adverse events included hypophosphatemia (72.1% all grade), fatigue (36.1%), stomatitis (29.5%), and alopecia (26.2%). A phase III clinical trial is ongoing (*39*).

Derazantinib (ARQ087) is an orally bioavailable, multikinase inhibitor with potent pan-FGFR activity. In a multicenter, open-label, phase I-II trial, Mazzaferro *et al.* (*40*) enrolled 29 patients with unresectable intrahepatic cholangiocarcinoma with FGFR2 fusion. The overall response rate was 20.7% and the disease control rate was 82.8%.

Pemigatinib (INCB54828; Incyte) is a selective, potent, oral inhibitor of FGFR1-3. A multicenter, open-label, phase II study (*41*) obtained an objective response (a CR in 3, a PR in 35, and a disease control rate of 82%) in 38 (35.5%) of 107 patients with FGFR2 fusions or rearrangements. Despite the low level of resistance caused by pemigatinib, tumor heterogeneity associated with acquired drug resistance remains a major barrier

Table 2. Small molecule inhibitor targeting FGFR

Study, Year	Study design	N	Chemotherapy regimen	PR or CR	PFS	OS (months)
Javle M (*39*), 2018	FGFR-altered advanced CCA	61	BGJ398 (infigratinib, a pan FGFR inhibitor) 125 mg once daily for 21 days, then 7 days off (28-day cycles) FGFR2 fusion (n = 48), mutation (n = 8), or amplification (n = 3)	ORR: 18.8% (FGFR2 fusions) DCR: 83.3% (FGFR2 fusions)	5.8	na
Mazzaferro (*40*), 2019	Unresectable iCCA with FGFR2 fusion Phase II, previously treated, locally	29	Derazantinib (ARQ 087), a potent pan-FGFR inhibitor	ORR: 20.7% DCR: 82.8%	5.7	na
Ghassan Abou-Alfa (*41*), 2020	advanced or metastatic CCA	107	Pemigatinib (INCB054828, highly selective FGFR-1, 2, and 3 TKI) (the FIGHT-202 trial) 13.5 mg once daily (21-day cycle; 2 weeks on, 1 week off) in 38/107 (35.5%) of patients with FGFR2 fusions or rearrangements	ORR: 35.5% (38/107, CR achieved in 3 patients, PR in 35)	6.9	21.1
Meric-Bernstam F (*44*), 2018	CCA previously treated with chemotherapy and another FGFR inhibitor	45	TAS120 (a FGFR 1-4 inhibitor)	PR 25%, SD 53%, CR 0. DCR 79%	na	na

CCA, cholangiocarcinoma. iCCA, intrahepatic cholangiocarcinoma. PFS, progression-free survival. OS, overall survival. PR, partial response. CR, complete response. ORR, objective response rate. DCR, disease control rate. na, not available. FGFR, fibroblast growth factor receptor.

to the long-term use of targeted therapy. Recent studies have noted the emergence of recurrent secondary single-nucleotide variants in FGFR following the inhibition of FGFR; these variants desensitize tumor cells to such therapies (*42*). Therefore, the mutations that develop in response to FGFR inhibition need to be comprehensively identified in order to investigate novel inhibitors (*43*).

TAS-120 is an irreversible FGFR inhibitor. A phase I study evaluated the efficacy of TAS-120 (*44*) in patients with cholangiocarcinoma and FGFR pathway alterations who previously received chemotherapy and other FGFR inhibitors. Forty-five patients with CCA (intra-hepatic $n = 41$) harboring FGF/FGFR aberrations were treated with 16 mg ($n = 24$), 20 mg ($n = 14$), and 24 mg ($n = 7$) QD. The tumor shrank in 20 (71%) of 28 patients with FGFR2 gene fusion, and a PR was achieved in 7. The ORR was 25%. Of the 7 responders, 6 remain on treatment, including 1 patient with an ongoing PR of > 1 year. SD was achieved in 15 (54%) of the 28 patients, and this was their best response. Seven patients are still on treatment. The overall disease control rate was 79%.

In conclusion, FGFR2 inhibitors resulted in the highest ORR and DCR among different targeted therapies, and those inhibitors offer promise for the future development of targeted therapies. In addition, combining FGFR inhibitors with chemotherapy or immunotherapy could increase survival benefits in patients with advanced or metastatic cholangiocarcinoma; this approach requires further investigation.

3.2. Targeting IDH1/2

Isocitrate dehydrogenase (IDH) is part of the Krebs cycle; this enzyme converts isocitrate to alpha-ketoglutarate (AKG). Various enzymes such as DNA and histone modifiers require AKG as a cofactor. Mutations in the IDH1 and IDH2 genes occur in about 15-20% of iCCA, with R132 and R172 being the most frequently mutated codons, respectively. An IDH mutation is found exclusively in iCCA, and the prognostic significance of an IDH mutation in advanced iCCA is a subject of debate. Goyal *et al.* (*45*) reported that the median OS did not differ significantly between patients with an IDH mutant and wild-type IDH (15.0 *vs.* 20.1 months, respectively; $p = 0.17$), but that patients with iCCA and an IDH mutant had a lower median serum CA19-9. Jiao *et al.* (*46*) reported that the status of IDH gene mutations was significantly associated with a worse prognosis: subjects with an IDH mutation had a 3-year survival of 33% compared to a 3-year survival of 81% for subjects with wild-type IDH genes ($P = 0.0034$). However, Wang *et al.* (*47*) found that mutations in IDH1 or IDH2 were associated with a longer OS ($p = 0.028$) and were independently associated with a longer time to tumor recurrence after intrahepatic cholangiocarcinoma resection according to multivariate analysis ($p = 0.021$).

Molecular targeted therapy for mutant IDH1 or IDH2 in cholangiocarcinoma is limited. Ivosidenib (AG-120) (Tibsovo; Agios) is an oral, targeted mutant IDH1 inhibitor that was approved for the treatment of IDH1 mutant acute myeloid leukemia by the FDA on July 20, 2018 (*48*). Lowery *et al.* (*49*) conducted a phase I study on IDH1-mutant iCCA. Seventy-three patients with IDH1-mutant cholangiocarcinoma were enrolled and received ivosidenib. A PR was achieved in 4 patients (5%). Median PFS was 3.8 months, 6-month PFS was 40.1%, and 12-month PFS was 21.8%. Median OS was 13.8 months, though data were censored for 48 patients (66%).

The ClarIDHy phase III clinical trial (NCT02989857) (*50*) evaluated the role of ivosidenib in patients with IDH1 mutant (R132C/L/G/H/S mutation variants) cholangiocarcinoma following progression during prior chemotherapy. PFS was significantly improved by ivosidenib in comparison to a placebo (median 2.7 months *vs.* 1.4 months; HR: 0.37; 95% CI: 0.25-0.54; one-sided $p < 0.0001$). However, data on survival time have not been available up to this point.

Other IDH inhibitors are also undergoing clinical trials. A phase I-II, multicenter, open-label, dose-escalation study of enasidenib (AG-221/CC-90007), a selective inhibitor of mutant-IDH2 enzymes, is underway in patients with advanced solid tumors including intrahepatic cholangiocarcinoma (NCT02273739). Patients with advanced malignancies that harbor IDH1R132 mutations are now being recruited for a study of IDH305 (targeted inhibitor of IDH1).

3.3. Targeting MEK1

A mutation in the MAP kinase signaling cascade, *i.e.* the RAS/RAF/MEK/ERK signaling pathway, is commonly found in BTC and occurs by multiple mechanisms including ERBB2 overexpression and KRAS, BRAF, and NRAS mutations. A few therapies that target MEK-1 have yielded preliminary results, including selumetinib, trametinib, and binimetinib. A combination of MEK-1 inhibitor and chemotherapy seems better, but the efficacy of MEK1 inhibitors still needs to be improved (Table 3).

Furuse *et al.* (*51*) reported the results of a phase II study of selumetinib in patients with metastatic biliary cancer. Selumetinib is an inhibitor of MEK1/2 targeting the RAS/RAF/MEK/extracellular signal-related kinase pathway. A PR was achieved in 3 of 28 patients, representing a response rate of 12%. The median PFS was 3.7 months and the median OS was 9.8 months. All toxicities were manageable and reversible. Bridgewater *et al.* (*52*) conducted a phase Ib study of selumetinib combined with cisplatin/gemcitabine. Objective response (Response Evaluation Criteria in Solid Tumors, RECIST v1.1) was evaluable in 8 patients: PR was achieved in 3 and SD was achieved in 5, with an ORR 25%. The median PFS was 6.4 months. Toxicities related to selumetinib were mostly edema and a rash of grade 1-2

Table 3. MEK1 inhibitors

Study, Year	Study design	N	Chemotherapy regimen	PR or CR	PFS	OS (months)
Furuse J (*51*), 2011	Phase II	28	Selumetinib	PR was achieved in 3 patients (ORR: 12%)	3.7	9.8
Bridgewater J (*52*), 2016	Phase Ib	12	The ABC-04 study: Selumetinib (75 mg bid) + cisplatin/gemcitabine (GEMCIS)	PR was achieved in 3 patients (ORR 25%); SD was achieved in 5 (objective response was evaluable in 8 patients) (RECIST v1.1)	6.4	Two patients remained on treatment at 14 and 19 months post registration.
Kim RD (*53*), 2020	Phase II trial (SWOG S1310)	44 (24 *vs.* 20)	Trametinib (arm 1) versus 5-fluorouracil or capecitabine (arm 2)	ORR: 8% *vs.* 10%	1.4 *vs.* 3.3	4.3 *vs.* 6.6
Shroff RT (*54*), 2017	advanced cholangiocarcinoma	25	Pazopanib and trametinib	ORR: 5%; DCR 75%	3.6	6.4
Finn RS (*55*), 2018	Phase Ib	25	Binimetinib monotherapy	SD was achieved in 12 patients (43%); CR in 1; PR 1; ORR: 2/25 (8%); DCR: 14/25(56%)	na	na
Kim JW (*56*), 2019	Phase Ib	34	Binimetinib + capecitabine	ORR: 20.6%; DCR:76.5%	4.1	7.8
Lowery MA (*32*), 2019	Phase II	35	Binimetinib + GEMCIS The efficacy signals observed were modest and not superior to GEMCIS alone	ORR: 36% (12/35) CR was achieved in 3 patients; PR in 9; SD in 14; PD in 7. DCR: 74.2%	6; PFS 6 = 54%	13.3

MEK1, mitogen-activated protein kinase kinase 1.GEM, gemcitabine. CIS, cisplatin. na, not available. RECIST, Response Evaluation Criteria in Solid Tumors. PFS, progression-free survival. OS, overall survival. PR, partial response. CR, complete response. ORR, objective response rate. DCR, disease control rate. na, not available.

and manageable.

Another MER-1 inhibitor, trametinib, was less efficacious than selumetinib. Kim *et al.* (*53*) studied a total of 44 eligible patients with cholangiocarcinoma (68%) and GBC (32%) who were randomly assigned to treatment arms (24 patients in arm 1 and 20 in arm 2). The response rate was 8% in arm 1 versus 10% in arm 2 ($p > 0.99$). Median OS was 4.3 months for arm 1 and 6.6 months for arm 2. The median PFS was 1.4 months for arm 1 and 3.3 months for arm 2. Shroff RT (*54*) reported that a combination of trametinib and pazopanib, a VEGF receptor inhibitor, improved DCR but not ORR in advanced cholangiocarcinoma.

Binimetinib monotherapy resulted in an ORR of 8% and a DCR of 56% (*55*), and a combination of binimetinib and chemotherapy resulted in an ORR of 20.6% and a DCR of 36% (*32,56)*. Using an MSK-IMPACT 410-gene panel, Lowery *et al.* (*32*) found aberrations in the RAS-RAF-MEK-ERK pathway and mutations in PIK3CA, AKT2, PIK3CG, BRAF, and MAP3K1 in responders. Binimetinib with gemcitabine and cisplatin did not improve the 6-month PFS or ORR. However, the recruiting criteria were not based on molecular signatures in those clinical trials. Molecular profiling may help to select patients who may benefit from MEK-1 targeted therapy.

3.4. Targeting BRAF-V600E

Several other solid tumors with a BRAF mutation have benefited from a combination of BRAF and MEK inhibitors. Planchard *et al.* (*57*) conducted an open-label phase II trial examining the efficacy of dabrafenib plus trametinib in patients with BRAFV600E-mutant metastatic non-small-cell lung cancers that were previously untreated. Thirty-six 36 patients were enrolled. Twenty-three patients had an overall response (64%, 95% CI 46-79); a CR was achieved in 2 (6%) and a PR in 21 (58%). Robert *et al.* (*58*) reported the first-line treatment with dabrafenib plus trametinib led to a long-term benefit in approximately one-third of patients who had unresectable or metastatic melanoma with a BRAF V600E or V600K mutation. A CR, which was associated with an improved long-term outcome, was achieved in 109 patients (19%). The overall survival rate at 5 years was 71% (95% CI, 62 to 79).

Only case reports have evaluated dabrafenib plus trametinib in advanced BTC (Table 4). Bunyatov *et al.* (*59*) described a rare case with poorly differentiated cholangiocarcinoma with an atypical genetic mutation in the BRAF V600E gene; the cancer was stage T4N1M0, and a successful outcome was obtained. A 38-year-old female patient underwent surgery at the National Surgery Institute for iCCA of the left lobe of the liver with invasion of the anterior abdominal wall, the diaphragm, and the pericardium. Liver resection, lymph node dissection, and pericardial resection were performed.

Table 4. Targeting BRAF V600E

Study, Year	Study design	N	Chemotherapy regimen	PR or CR	PFS	OS (months)
Kocsis J (*62*), 2017	Case report, a 59-year-old female with chemotherapy-refractory metastatic eCCA	eCCA (n = 1)	Dabrafenib + Trametinib Next-generation sequencing (NGS) revealed a BRAF V600E mutation	1 CR	3	At 12 weeks, PET CT confirmed further tumor regression with complete regression of multiple cerebral metastases.
Bunyatov T (*59*), 2019	Case report, iCCA of the left lobe of the liver with invasion of the anterior abdominal wall, the diaphragm, and the pericardium	iCCA (n = 1)	Dabrafenib + Trametinib Mutation in the BRAF V600E gene	1 CR	na	The patient has been tumor-free for 2 years with no signs of recurrence.
Lavingia V (*60*), 2016	Case report	iCCA (n = 2)	Dabrafenib and trametinib Mutation in the BRAF V600E gene	1 CR 1 PR	6 5	CR was achieved at 6 months in 1 patient who died at 9 months. PR was achieved at 2 months in 1 patient who had a PFS for 5 months.
Loaiza-Bonilla A (*61*), 2014	Case report	iCCA (n = 1)	Dabrafenib + Trametinib Mutation in the BRAF V600E gene	1 PR	na	Symptomatic and sustained near-complete radiological improvement.

iCCA, intrahepatic cholangiocarcinoma. eCCA, extra-hepatic cholangiocarcinoma. PFS, progression-free survival. OS, overall survival. PR, partial response. CR, complete response. na, not available.

Adjuvant chemotherapy (GEMOX) did not yield any results. Treatment with pembrolizumab did not result in any improvement, either. NGS and molecular profiling of the tumor revealed the mutation in BRAF V600E gene. Target therapy with dabrafenib and trametinib was initiated and resulted in a full response. The patient has been tumor-free for 2 years with no signs of recurrence.

Lavingia *et al.* (*60*) reported on 2 cases of BRAF V600E refractory iCCA treated with dual BRAF and MEK inhibitors (dabrafenib and trametinib) with an excellent clinical and radiological response to therapy and a protracted duration of disease control. A CR was achieved in 1 patient after 6 months of treatment, and disease progression ultimately occurred at 9 months. PR was achieved in the second patient 2 months after treatment, and that patient has been progression-free 5 months after treatment.

Loaiza-Bonilla *et al.* (*61*) reported on a 47-year-old woman diagnosed with chemotherapy and radiation-refractory BRAF V600E mutant, poorly differentiated iCCA. The patient was stage IV and had multiple metastatic lesions in the liver, lungs, pleura, and bone. NGS genomic information suggested that the patient was a suitable candidate for dual BRAF and MEK inhibition therapy. After dual therapy with dabrafenib and trametinib, the patient's tumor almost disappeared completely, as confirmed by computed tomography, but the patient is still symptomatic.

The outcome of the dual targeting therapy appears superior to that of BRAF inhibition alone and cytotoxic chemotherapy. Given the poor outlook and refractoriness of BRAF mutant iCCA, future studies should focus on early integration of BRAF/MEK inhibition.

3.5. Targeting HER-2

HER family receptors (EGFR/HER1, HER2neu, HER3, and HER4) trigger multiple signaling cascades, including the mitogen-activated protein kinase (MAPK) cascade phosphatidylinositol 3-kinase (PI3K)/AKT pathway and signal transducer and activator of transcription (STAT) transcription factor, leading to various phenomena, including cell proliferation, cell differentiation, angiogenesis, metastasis, and inhibition of apoptosis, that are involved in the development of several carcinomas. HER2 alterations, including overexpression, amplifications, and other mutations, are found in a variety of solid tumors (*63*). In BTC, HER2 overexpression is observed in ~ 5% of intrahepatic CCA, ~20% of extrahepatic CCA, and ~19% of GBC.

HER-2 inhibitors include trastuzumab, pertuzumab, lapatinib, neratinib, and afatinib. Trastuzumab plus chemotherapy is the first-line therapy for patients with HER2-positive gastric cancer, although trials involving pertuzumab, lapatinib, and T-DM1 have failed to improve outcomes.

Lapatinib monotherapy (*64*) or afatinib plus GEMCIS

(*65*) has failed to yield any survival benefit in advanced BTC. However, these studies were not treating patients with specific molecular biomarkers. Moreover, a PR was achieved in 2 patients with metastatic GBC who received HER-2 inhibitors with amplification of the ERBB2 gene (*66,67*). Furthermore, treatment of advanced GBC and CCA with HER2/neu genetic aberrations or protein overexpression with monotherapy or a combination of two HER-2 inhibitors resulted in an ORR ranging from 22-55% (*64-70*) (Table 5). In the future, both novel antibody-drug conjugates and bispecific antibodies targeting HER2 and HER2-targeted therapies in combination with immune-checkpoint inhibition will be tested in clinical trials (*67*).

3.6. PARP inhibitors targeting BRAC1/2, BAP1, and ATM

Poly [ADP-ribose] polymerase (PARP) inhibitors are involved in cell repair. Somatic mutations of the tumor-suppressor genes BRCA1 and BRCA2 have been reported in cholangiocarcinomas (*31*). BRCA-mutated tumors are often sensitive to PARP inhibitors. Accordingly, a retrospective clinical analysis of patients with BRCA-mutated cholangiocarcinoma (n = 18) found that a sustained disease response was achieved in 1 of 4 patients who received PARP inhibitors, with a PFS of 42.6 months; the OS for patients with stage III/IV cancer was 25 months (*71*). Although PARP inhibitors and inhibitors of ataxia-telangiectasia mutated (ATM), another DNA repair protein, are currently being evaluated in multiple clinical trials on BRCA-mutated breast cancer, they need to be prospectively evaluated in patients with cholangiocarcinoma. Zhang *et al.* (*72*) reported on the efficacy of olaparib in a patient with gallbladder cancer with an ATM-inactivating mutation. SD was achieved, and the patient survived for 16 months on olaparib. A phase II trial of the PARP inhibitor niraparib is planned in patients with advanced-stage malignancies, including cholangiocarcinoma, and with known mutations in BAP1 and other DNA double-strand break repair pathway genes – excluding BRCA1/2 mutations (NCT03207347).

3.7. Immune checkpoints inhibitors (ICI) for BTC

Immune checkpoints inhibitors (ICI) targeting programmed cell death protein 1 (PD-1) or its ligand PD-L1 or cytotoxic T-lymphocyte associated antigen 4 (CTLA-4) checkpoints have demonstrated the potential to target tumor-specific immune suppression. According to data from the literature, inhibition of immune checkpoints has yielded promising results in several malignancies such as melanoma (*73,74*), non-small cell lung cancer (*75*), urothelial carcinoma (*76*), renal cell carcinoma (*77*), head and neck cancer (*78*) and hepatocellular carcinoma (*79*). Thus far, the clinical data

Table 5. Targeting HER2/ERBB2

Study, Year	Study design	N	Chemotherapy regimen	PR or CR	PFS	OS (months)
Moehler M (*64*), 2019	advanced BTC	9	Afatinib + GEMCIS	failed to have a survival benefit in combination with GEMCIS	6.0	7.7
Ramanathan RK (*65*), 2009	Advanced BTC and HCC, Phase II	BTC 17, HCC 40	Lapatinib	The response was 0% in BTC and 5% in HCC	1.8 *vs.* 2.3	5.2 *vs.* 6.2
Czink E (*66*), 2016	metastatic GBC with ERBB2 gene mplification	1	Pertuzumab and trastuzumab in combination with nab-paclitaxel	1 case report of PR	> 12	> 12
Ye MF (*67*), 2019	HER2 amplification in GBC	1	Trastuzumab and lapatinib	1 case report of PR	na	na
Hyman DM (*70*), 2018	SUMMIT; phase II; Second-line or later. ERBB2 and/or ERBB3 alterations identified using NGS	11	Neratinib (a pan-HER-kinase inhibitor)	ORR 22%	na	na
Hainsworth JD (*69*), 2018	MyPathway Second-line or later. HER2-IHC 3+ and/or ISH-positive; Phase IIa (basket study)	11	Trastuzumab + pertuzumab	PR in 2/7 patients (ORR: 29%), SD in 3/7 >120 days. PR in 4/11, SD in 3/11, ORR: 36%	na	na
Javle M (*68*), 2015	advanced GBC and CCA with HER2/neu genetic aberrations or protein overexpression	14	HER2/neu-directed therapy (trastuzumab, lapatinib, or pertuzumab)	9 cases of GBC: CR was achieved in 1, PR in 4, SD in 3, MR (mixed response) in 1, ORR: 55%. 5 cases of CCA: PD was achieved in 5 patients	na	8-178 weeks 7-29weeks

BTC, biliary tract cancer. GBC, gall bladder cancer. CCA, cholangiocarcinoma. HCC, hepatocellular carcinoma. GEM, gemcitabine. CIS, cisplatin. PFS, progression-free survival. OS, overall survival. PR, partial response. CR, complete response. SD, stable disease. na, not available. HER2, human epidermal growth factor receptor-2. ERBB2, erythroblastic leukemia viral oncogene homolog 2.

on immunotherapy for CCA and other BTCs are limited, and several trials are underway; they are exploring, for instance, the role of the monoclonal antibodies ipilimumab or tremelimumab (anti-CTLA4) or antibodies targeting PD-L1 or PD-1, such as pembrolizumab or nivolumab (*80*).

Gou *et al.* (*81*) reported on 30 patients with metastatic BTC who voluntarily received nivolumab. CR was achieved in 1 patient, a PR in 5, SD in 12, and PD in 12. ORR was 20%, DCR was 60%, and PFS was 3.1 months. Fifty-four patients with BTC included 59% with iCCA, 11% with eCCA and 30% with GBC who received nivolumab monotherapy; ORR was 22%, median PFS was 3.8 months, and median OS was 10.3 months (*82*). Durvalumab monotherapy has also displayed limited efficacy. In a phase I study of 42 patients, ORR was only 4.8%, median PFS was 1.6 months, and median OS was 8.1 months (*83*).

The efficacy of pembrolizumab monotherapy is also limited. The PD-L1 inhibitor pembrolizumab was administered to 104 patients with advanced BTC. Pembrolizumab achieved a PR in 6 patients, resulting in an ORR of 5.8%. Median PFS was 2.0 months, and median OS was 9.1 months (*84*). Kang *et al.* (*85*) conducted a prospective cohort study in 40 patients with PDL1-positive BTC that progressed despite first-line gemcitabine plus cisplatin. Pembrolizumab 200 mg was administered intravenously every 3 weeks. The ORR was 10% according to RECIST v1.1 and 12.5% according to the immune-modified RECIST (imRECIST). The median PFS was 1.5 months, and OS was 4.3 months. This checkpoint inhibitor is currently being tested in combination with cisplatin and gemcitabine in the phase II ABC-09 trial (NCT03260712).

Combining two ICIs does not look promising. Arkenau *et al.* (*86*) reported that ramucirumab plus pembrolizumab in patients with advanced or metastatic BTC had limited efficacy even in the patients with biomarker-unselected progressive BTC, with an ORR of 4%, a median PFS of 1.6 months, and an OS of 6.4 months.

A combination of an ICI and chemotherapy resulted in a better ORR and DCR compared to an ICI alone. Nivolumab combined with chemotherapy resulted in a better tumor response and patient survival than nivolumab monotherapy. Ueno *et al.* (*87*) conducted a multicenter, open-label, phase I trial at four cancer centers in Japan. Thirty patients were enrolled in each cohort. In the monotherapy cohort, median OS was 5.2 months, median PFS was 1.4 months, and a PR was achieved in 1 of the 30 patients. In the combined therapy cohort, median OS was 15.4 months, median PFS was 4.2 months, and a PR was achieved in 11 of the 30 patients. Phase II studies are ongoing: patients with BTC are receiving either nivolumab alone (NCT02829918), or in combination with chemotherapy (gemcitabine/cisplatin) or with another immunotherapy (ipilimumab; NCT03101566).

Numerous case series have involved patients receiving immunotherapy with PD-1/PD-L1 inhibitors combined with radiotherapy or chemotherapy that achieved a CR or PR (Table 6). Clinical trials studying immunotherapy combinations designed to augment the immune antitumor response are also underway. Hyperactivated PD1/PD-L1 signals in tumor tissues are a negative prognostic marker for iCCA after resection (*88*). In addition, PD-L1 expression in both cancer and stroma cells of patients with CCA was an independent predictor of poor OS (*89*). However, evidence of PD-L1 expression was not always related to a longer PFS in contrast to a lack of PD-L1 expression (*81*). PD-L1 protein expression is determined using the tumor proportion score (TPS), which is the percentage of viable tumor cells with partial or complete membrane staining at any intensity. The TPS is an indicator of the degree of PD-L1 immunostaining. Some studies have reported that patients with a TPS $\geq$ 50% (*85*) had a higher rate of tumor response to ICI than patients with a TPS $<$ 50%. Immunotherapy could become an important part of treatment of iCCA in the future. Future studies of immunotherapies need to collect and report information on important clinical covariates, such as the anatomical site, along with blood and tumor samples. In addition, potential biomarkers including MSI, MMR, TMB, and PD-L1 and tumor somatic mutations (TMB) should be quantified in order to identify those patients who are most likely to benefit from immunotherapy (*80,90*).

4. Conclusion and perspectives for the future

In conclusion, advanced BTC has a poor prognosis. Chemotherapy, and especially a triplet GAP regimen based on GEMCIS, has the most significant effect on that cancer, and FOLFIRINOX combined with bevacizumab is promising. Molecular targeted therapy based on genome sequencing appears essential to precision medicine. FGFR inhibitors and IDH inhibitors are promising emerging targeted therapies mainly for iCCA. Other targeted therapies such as anti-HER2 therapies or MEK-1/2 or BRAF inhibitors should be used in accordance with biomarkers. Further evaluation of combination strategies in particular is needed. Case series have reported that ICIs combined with chemotherapy or radiotherapy result in a good response, though this is still being evaluated in several studies. Combination therapies have garnered attention because of interactions between signaling pathways of carcinogenesis in BTC

Acknowledgements

This study was supported by: *1*) The National Natural Fund Project, 81572434. *2*) A Major Special Science and Technology Project of the Ministry of Science and Technology: Prevention and Treatment of Major

Table 6. Summary of cases of biliary tract cancer where PR/CR was achieved with immune checkpoint inhibitors.

NO.	Author, Year	Tumor type	Stage	TMB	PD-L1	MS status	Pre-treatment	Treatment	Response	PFS/DFS
1	Chen (*91*), 2019	iCCA	IV	18.46	< 1%	na	Liver tumor recurred 5 months after surgery	Nivolumab + lenvatinib	PR	> 21 m
2	Liu (*92*), 2019	iCCA	IVA	1.2	< 1%	MSS, pMMR	na	SBRT (Cyberknife) +Nivolumab*15cycles	PR	7 m
3	Liu (*92*), 2019	iCCA	IIIA	3.8	< 1%	MSS, pMMR	Lapatinib*3cycles	Cyberknife + Pembrolizumab* 5 cycles	PR	5 m
4	Alshari (*93*), 2019	iCCA	IIIB	0.98	< 1%	MSS, pMMR	11 months after surgery, liver tumor recurred with LNM	Cyberknife + Pembrolizumab* 16 cycles. Furflucil* 6 cycles, Endostatin* 4 cycles	CR	11 m
5	Sui (*94*), 2018	iCCA	IIIB	2.95	< 5%	MSS, pMMR	11 month after surgery, liver tumor recurred with LNM	Cyberknife + Tegafur* 3 cycles + Pembrolizumab* 15 cycles	CR	16 m
6	Sui (*94*), 2019	iCCA	IIIB	7.09	< 5%	MSS, pMMR	3 months after surgery, liver tumor recurred with LNM	Tegafur continuous + Pembrolizumab* 6 cycles	CR	13 m
7	Mou (*95*), 2018	iCCA	IIIB	19.3	80%	pMMR	na	Pembrolizumab + SOX* 8 cycles, Pembrolizumab monotherapy for 6 months	CR	10 m
8	Alshari (*93*), 2019	GBC	IVB	na	na	na	Liver tumor recurred with LNM	Pembrolizumab* 8 cycles	CR	24 m

iCCA, intrahepatic cholangiocarcinoma. GBC, gall bladder cancer. LNM, lymph node metastasis. SOX, S-1 plus oxaliplatin. SBRT, stereotactic body radiation therapy. PR, partial response. CR, complete response. PFS, progression-free survival. DFS, disease-free survival. na, not available. MS, microsatellite status. MSS, microsatellite stable. MMR, mismatch repair status. TMB, tumor mutational burden.

Infectious Diseases such as AIDS and Viral Hepatitis, 2018ZX10723204-007-001. *3*) "Young Medical Leaders", Tianjin Health Commission, 2018-2-8. *4*) "Young Innovative Personnel", Tianjin Medical University Cancer Institute and Hospital, 2017-1-35.

References

1. Rizvi S, Khan SA, Hallemeier CL, Kelley RK, Gores GJ. Cholangiocarcinoma – Evolving concepts and therapeutic strategies. Nat Rev Clin Oncol. 2018; 15:95-111.
2. Saha SK, Zhu AX, Fuchs CS, Brooks GA. Forty-year trends in cholangiocarcinoma incidence in the U.S.: Intrahepatic disease on the rise. Oncologist. 2016; 21:594-599.
3. Raoof M, Singh G. Rising trends in intrahepatic cholangiocarcinoma incidence and mortality: getting at the root cause. Hepatobil Surg Nutr. 2019; 8:301-303.
4. Taylor-Robinson SD, Toledano MB, Arora S, Keegan TJ, Hargreaves S, Beck A, Khan SA, Elliott P, Thomas HC. Increase in mortality rates from intrahepatic cholangiocarcinoma in England and Wales 1968-1998. Gut. 2001; 48:816-820.
5. Yamamoto S. Biliary tract cancer mortality rates by prefectures in Japan. Jpn J Clin Oncol. 2000; 30:576.
6. Florio AA, Ferlay J, Znaor A, Ruggieri D, Alvarez CS, Laversanne M, Bray F, McGlynn KA, Petrick JL. Global trends in intrahepatic and extrahepatic cholangiocarcinoma incidence from 1993 to 2012. Cancer. 2020; 126:2666-2678.
7. DeOliveira ML, Cunningham SC, Cameron JL, Kamangar F, Winter JM, Lillemoe KD, Choti MA, Yeo CJ, Schulick RD. Cholangiocarcinoma: Thirty-one-year experience with 564 patients at a single institution. Ann Surg. 2007; 245:755-762.
8. Cai Y, Cheng N, Ye H, Li F, Song P, Tang W. The current management of cholangiocarcinoma: A comparison of current guidelines. Biosci Trends. 2016; 10:92-102.
9. Jeong S, Cheng Q, Huang L, Wang J, Sha M, Tong Y, Xia L, Han L, Xi Z, Zhang J, Kong X, Gu J, Xia Q. Risk stratification system to predict recurrence of intrahepatic cholangiocarcinoma after hepatic resection. BMC Cancer. 2017; 17:464.
10. Komaya K, Ebata T, Shirai K, Ohira S, Morofuji N, Akutagawa A, Yamaguchi R, Nagino M. Recurrence after resection with curative intent for distal cholangiocarcinoma. Br J Surg. 2017; 104:426-433.
11. Komaya K, Ebata T, Yokoyama Y, Igami T, Sugawara G, Mizuno T, Yamaguchi J, Nagino M. Recurrence after curative-intent resection of perihilar cholangiocarcinoma: Analysis of a large cohort with a close postoperative follow-up approach. Surgery. 2018; 163:732-738.
12. Valle J, Wasan H, Palmer DH, Cunningham D, Anthoney A, Maraveyas A, Madhusudan S, Iveson T, Hughes S, Pereira SP, Roughton M, Bridgewater J. Cisplatin plus gemcitabine versus gemcitabine for biliary tract cancer. N Engl J Med. 2010; 362:1273-1281.
13. Andre T, Reyes-Vidal JM, Fartoux L, Ross P, Leslie M, Rosmorduc O, Clemens MR, Louvet C, Perez N, Mehmud F, Scheithauer W. Gemcitabine and oxaliplatin in advanced biliary tract carcinoma: A phase II study. Br J Cancer. 2008; 99:862-867.

14. Morizane C, Okusaka T, Mizusawa J, *et al.* Combination gemcitabine plus S-1 versus gemcitabine plus cisplatin for advanced/recurrent biliary tract cancer: The FUGA-BT (JCOG1113) randomized phase III clinical trial. Ann Oncol. 2019; 30:1950-1958.
15. Sahai V, Catalano PJ, Zalupski MM, Lubner SJ, Menge MR, Nimeiri HS, Munshi HG, Benson AB, 3rd, O'Dwyer PJ. Nab-paclitaxel and gemcitabine as first-line treatment of advanced or metastatic cholangiocarcinoma: A phase 2 clinical trial. JAMA Oncol. 2018; 4:1707-1712.
16. Roth MT, Goff LW. Gemcitabine, cisplatin, and nab-paclitaxel for patients with advanced biliary tract cancer: Closing the GAP. JAMA Oncol. 2019; 5:831-832.
17. Shroff RT, Javle MM, Xiao L, Kaseb AO, Varadhachary GR, Wolff RA, Raghav KPS, Iwasaki M, Masci P, Ramanathan RK, Ahn DH, Bekaii-Saab TS, Borad MJ. Gemcitabine, cisplatin, and nab-paclitaxel for the treatment of advanced biliary tract cancers: A phase 2 clinical trial. JAMA Oncol. 2019; 5:824-830.
18. Belkouz A, de Vos-Geelen J, Mathot RAA, Eskens F, van Gulik TM, van Oijen MGH, Punt CJA, Wilmink JW, Klumpen HJ. Efficacy and safety of FOLFIRINOX as salvage treatment in advanced biliary tract cancer: An open-label, single arm, phase 2 trial. Br J Cancer. 2020; 122:634-639.
19. Phelip JM, Edeline J, Blanc JF, Barbier E, Michel P, Bourgeois V, Neuzillet C, Malka D, Manfredi S, Desrame J. Modified FOLFIRINOX versus CisGem first-line chemotherapy for locally advanced non resectable or metastatic biliary tract cancer (AMEBICA)-PRODIGE 38: Study protocol for a randomized controlled multicenter phase II/III study. Dig Liver Dis. 2019; 51:318-320.
20. Goyal L, Zheng H, Yurgelun MB, Abrams TA, Allen JN, Cleary JM, Knowles M, Regan E, Reardon A, Khachatryan A, Jain RK, Nardi V, Borger DR, Duda DG, Zhu AX. A phase 2 and biomarker study of cabozantinib in patients with advanced cholangiocarcinoma. Cancer. 2017; 123:1979-1988.
21. Yi JH, Thongprasert S, Lee J, Doval DC, Park SH, Park JO, Park YS, Kang WK, Lim HY. A phase II study of sunitinib as a second-line treatment in advanced biliary tract carcinoma: A multicentre, multinational study. Eur J Cancer. 2012; 48:196-201.
22. Moehler M, Maderer A, Schimanski C, *et al.* Gemcitabine plus sorafenib versus gemcitabine alone in advanced biliary tract cancer: A double-blind placebo-controlled multicentre phase II AIO study with biomarker and serum programme. Eur J Cancer. 2014; 50:3125-3135.
23. Guion-Dusserre JF, Lorgis V, Vincent J, Bengrine L, Ghiringhelli F. FOLFIRI plus bevacizumab as a second-line therapy for metastatic intrahepatic cholangiocarcinoma. World J Gastroenterol. 2015; 21:2096-2101.
24. Ferraro D, Goldstein D, O'Connell RL, *et al.* TACTIC: A multicentre, open-label, single-arm phase II trial of panitumumab, cisplatin, and gemcitabine in biliary tract cancer. Cancer Chemother Pharmacol. 2016; 78:361-367.
25. Vogel A, Kasper S, Bitzer M, *et al.* PICCA study: Panitumumab in combination with cisplatin/gemcitabine chemotherapy in KRAS wild-type patients with biliary cancer-A randomised biomarker-driven clinical phase II AIO study. Eur J Cancer. 2018; 92:11-19.
26. Leone F, Marino D, Cereda S, *et al.* Panitumumab in combination with gemcitabine and oxaliplatin does not prolong survival in wild-type KRAS advanced biliary tract cancer: A randomized phase 2 trial (Vecti-BIL study). Cancer. 2016; 122:574-581.
27. Malka D, Cervera P, Foulon S, *et al.* Gemcitabine and oxaliplatin with or without cetuximab in advanced biliary-tract cancer (BINGO): A randomised, open-label, non-comparative phase 2 trial. Lancet Oncol. 2014; 15:819-828.
28. Lee J, Park SH, Chang HM, *et al.* Gemcitabine and oxaliplatin with or without erlotinib in advanced biliary-tract cancer: A multicentre, open-label, randomised, phase 3 study. Lancet Oncol. 2012; 13: 181-188.
29. Adeva J, Sangro B, Salati M, Edeline J, La Casta A, Bittoni A, Berardi R, Bruix J, Valle JW. Medical treatment for cholangiocarcinoma. Liver Int. 2019; 39 Suppl 1:123-142.
30. Wardell CP, Fujita M, Yamada T, *et al.* Genomic characterization of biliary tract cancers identifies driver genes and predisposing mutations. J Hepatol. 2018; 68:959-969.
31. Nakamura H, Arai Y, Totoki Y, *et al.* Genomic spectra of biliary tract cancer. Nat Genet. 2015; 47:1003-1010.
32. Lowery MA, Bradley M, Chou JF, *et al.* Binimetinib plus gemcitabine and cisplatin phase I/II trial in patients with advanced biliary cancers. Clin Cancer Res. 2019; 25:937-945.
33. Xue L, Guo C, Zhang K, Jiang H, Pang F, Dou Y, Liu X, Lin H, Dong X, Zhao S, Yao M, Wang K, Feng Y, Gu W. Comprehensive molecular profiling of extrahepatic cholangiocarcinoma in Chinese population and potential targets for clinical practice. Hepatobiliary Surg Nutr. 2019; 8:615-622.
34. Montal R, Sia D, Montironi C, *et al.* Molecular classification and therapeutic targets in extrahepatic cholangiocarcinoma. J Hepatol. 2020; 73:315-327.
35. Yang P, Javle M, Pang F, *et al.* Somatic genetic aberrations in gallbladder cancer: Comparison between Chinese and US patients. Hepatobiliary Surg Nutr. 2019; 8:604-614.
36. Lowery MA, Ptashkin R, Jordan E, *et al.* Comprehensive molecular profiling of intrahepatic and extrahepatic cholangiocarcinomas: Potential targets for intervention. Clin Cancer Res. 2018; 24:4154-4161.
37. Goyal L, Saha SK, Liu LY, *et al.* Polyclonal secondary FGFR2 mutations drive acquired resistance to FGFR inhibition in patients with FGFR2 fusion-positive cholangiocarcinoma. Cancer Discov. 2017; 7:252-263.
38. Javle M, Lowery M, Shroff RT, *et al.* Phase II Study of BGJ398 in patients with FGFR-altered advanced cholangiocarcinoma. J Clin Oncol. 2018; 36 276-282.
39. Javle M, Borbath I, Clarke S, *et al.* Phase 3 multicenter, open-label, randomized study of infigratinib versus gemcitabine plus cisplatin in the first-line treatment of patients with advanced cholangiocarcinoma with FGFR2 gene fusions/translocations: The PROOF trial. Ann Oncol. 2019; 30 Suppl 4: iv62.
40. Mazzaferro V, El-Rayes BF, Droz Dit Busset M, *et al.* Derazantinib (ARQ 087) in advanced or inoperable FGFR2 gene fusion-positive intrahepatic cholangiocarcinoma. Br J Cancer. 2019; 120:165-171.
41. Abou-Alfa GK, Sahai V, Hollebecque A, *et al.* Pemigatinib for previously treated, locally advanced or metastatic cholangiocarcinoma: A multicentre, open-label, phase 2 study. Lancet Oncol. 2020; 21:671-684.
42. Krook MA, Lenyo A, Wilberding M, *et al.* Efficacy of

FGFR inhibitors and combination therapies for acquired resistance in FGFR2-fusion cholangiocarcinoma. Mol Cancer Ther. 2020; 19:847-857.
43. Yang T, Liang L, Wang MD, Shen F. FGFR inhibitors for advanced cholangiocarcinoma. Lancet Oncol. 2020; 21:610-612.
44. Goyal L, Shi L, Liu LY, *et al.* TAS-120 overcomes resistance to ATP-competitive FGFR inhibitors in patients with FGFR2 fusion-positive intrahepatic cholangiocarcinoma. Cancer Discovery. 2019; 9:1064-1079.
45. Goyal L, Govindan A, Sheth RA, *et al.* Prognosis and clinicopathologic features of patients with advanced stage isocitrate dehydrogenase (IDH) mutant and IDH wild-type intrahepatic cholangiocarcinoma. Oncologist. 2015; 20:1019-1027.
46. Jiao Y, Pawlik TM, Anders RA, *et al.* Exome sequencing identifies frequent inactivating mutations in BAP1, ARID1A and PBRM1 in intrahepatic cholangiocarcinomas. Nat Genet. 2013; 45:1470-1473.
47. Wang P, Dong Q, Zhang C, *et al.* Mutations in isocitrate dehydrogenase 1 and 2 occur frequently in intrahepatic cholangiocarcinomas and share hypermethylation targets with glioblastomas. Oncogene. 2013; 32:3091-3100.
48. Kucukyurt S, Eskazan AE. New drugs approved for acute myeloid leukaemia in 2018. Br J Clin Pharmacol. 2019; 85:2689-2693.
49. Lowery MA, Burris HA 3rd, Janku F, *et al.* Safety and activity of ivosidenib in patients with IDH1-mutant advanced cholangiocarcinoma: A phase 1 study. Lancet Gastroenterol Hepatol. 2019; 4:711-720.
50. Abou-Alfa GK, Macarulla T, Javle MM, *et al.* Ivosidenib in IDH1-mutant, chemotherapy-refractory cholangiocarcinoma (ClarIDHy): A multicentre, randomised, double-blind, placebo-controlled, phase 3 study. Lancet Oncol. 2020; 21:796-807.
51. Furuse J, Nagashima F. Inhibitor of MEK1/2, selumetinib, for biliary tract cancer. Expert Rev Gastroenterol Hepatol. 2011; 5:579-581.
52. Bridgewater J, Lopes A, Beare S, Duggan M, Lee D, Ricamara M, McEntee D, Sukumaran A, Wasan H, Valle JW. A phase 1b study of selumetinib in combination with cisplatin and gemcitabine in advanced or metastatic biliary tract cancer: The ABC-04 study. BMC Cancer. 2016; 16:153.
53. Kim RD, McDonough S, El-Khoueiry AB, Bekaii-Saab TS, Stein SM, Sahai V, Keogh GP, Kim EJ, Baron AD, Siegel AB, Barzi A, Guthrie KA, Javle M, Hochster H. Randomised phase II trial (SWOG S1310) of single agent MEK inhibitor trametinib versus 5-fluorouracil or capecitabine in refractory advanced biliary cancer. Eur J Cancer. 2020; 130:219-227.
54. Shroff RT, Yarchoan M, O'Connor A, Gallagher D, Zahurak ML, Rosner G, Ohaji C, Sartorius-Mergenthaler S, Parkinson R, Subbiah V, Zinner R, Azad NS. The oral VEGF receptor tyrosine kinase inhibitor pazopanib in combination with the MEK inhibitor trametinib in advanced cholangiocarcinoma. Br J Cancer. 2017; 116:1402-1407.
55. Finn RS, Ahn DH, Javle MM, Tan BR, Jr., Weekes CD, Bendell JC, Patnaik A, Khan GN, Laheru D, Chavira R, Christy-Bittel J, Barrett E, Sawyer MB, Bekaii-Saab TS. Phase 1b investigation of the MEK inhibitor binimetinib in patients with advanced or metastatic biliary tract cancer. Invest New Drugs. 2018; 36:1037-1043.
56. Kim JW, Lee KH, Suh KJ, Nam AR, Bang JH, Bang YJ, Oh DY. Enhanced antitumor effect of binimetinib in combination with capecitabine for biliary tract cancer patients with mutations in the RAS/RAF/MEK/ERK pathway: Phase Ib study. Br J Cancer. 2019; 121:332-339.
57. Planchard D, Smit EF, Groen HJM, Mazieres J, Besse B, Helland A, Giannone V, D'Amelio AM, Jr., Zhang P, Mookerjee B, Johnson BE. Dabrafenib plus trametinib in patients with previously untreated BRAF (V600E)-mutant metastatic non-small-cell lung cancer: An open-label, phase 2 trial. Lancet Oncol. 2017; 18:1307-1316.
58. Robert C, Grob JJ, Stroyakovskiy D, *et al.* Five-year outcomes with dabrafenib plus trametinib in metastatic melanoma. N Engl J Med. 2019; 381:626-636.
59. Bunyatov T, Zhao A, Kovalenko J, Gurmikov B, Vishnevsky V. Personalised approach in combined treatment of cholangiocarcinoma: A case report of healing from cholangiocellular carcinoma at stage IV. J Gastrointest Oncol. 2019; 10:815-820.
60. Lavingia V, Fakih M. Impressive response to dual BRAF and MEK inhibition in patients with BRAF mutant intrahepatic cholangiocarcinoma-2 case reports and a brief review. J Gastrointest Oncol. 2016; 7:E98-E102.
61. Loaiza-Bonilla A, Clayton E, Furth E, O'Hara M, Morrissette J. Dramatic response to dabrafenib and trametinib combination in a BRAF V600E-mutated cholangiocarcinoma: Implementation of a molecular tumour board and next-generation sequencing for personalized medicine. Ecancermedicalscience. 2014; 8:479.
62. Kocsis J, Arokszallasi A, Andras C, Balogh I, Beres E, Deri J, Petak I, Janvary L, Horvath Z. Combined dabrafenib and trametinib treatment in a case of chemotherapy-refractory extrahepatic BRAF V600E mutant cholangiocarcinoma: Dramatic clinical and radiological response with a confusing synchronic new liver lesion. J Gastrointest Oncol. 2017; 8:E32-E38.
63. Oh DY, Bang YJ. HER2-targeted therapies – A role beyond breast cancer. Nat Rev Clin Oncol. 2020; 17:33-48.
64. Moehler M, Maderer A, Ehrlich A, Foerster F, Schad A, Nickolay T, Ruckes C, Weinmann A, Sivanathan V, Marquardt JU, Galle PR, Woerns M, Thomaidis T. Safety and efficacy of afatinib as add-on to standard therapy of gemcitabine/cisplatin in chemotherapy-naive patients with advanced biliary tract cancer: An open-label, phase I trial with an extensive biomarker program. BMC Cancer. 2019; 19:55.
65. Ramanathan RK, Belani CP, Singh DA, Tanaka M, Lenz HJ, Yen Y, Kindler HL, Iqbal S, Longmate J, Mack PC, Lurje G, Gandour-Edwards R, Dancey J, Gandara DR. A phase II study of lapatinib in patients with advanced biliary tree and hepatocellular cancer. Cancer Chemother Pharmacol. 2009; 64:777-783.
66. Czink E, Heining C, Weber TF, Lasitschka F, Schemmer P, Schirmacher P, Weiss KH, Glimm H, Brors B, Weichert W, Jager D, Frohling S, Springfeld C. Durable remission under dual HER2 blockade with trastuzumab and pertuzumab in a patient with metastatic gallbladder cancer. Z Gastroenterol. 2016; 54:426-430. (in German).
67. Ye M, Lv J, Xu G, Wang W, Jing Y, Sun A, Lu Z, Wu X, Liu Y, Shao YW, Liu F, Tao F. Dual-targeting strategy using trastuzumab and lapatinib in a patient with HER2 gene amplification in recurrent metachronous metastatic

gallbladder carcinoma. J Int Med Res. 2019; 47:2768-2777.
68. Javle M, Churi C, Kang HC, Shroff R, Janku F, Surapaneni R, Zuo M, Barrera C, Alshamsi H, Krishnan S, Mishra L, Wolff RA, Kaseb AO, Thomas MB, Siegel AB. HER2/neu-directed therapy for biliary tract cancer. J Hematol Oncol. 2015; 8:58.
69. Hainsworth JD, Meric-Bernstam F, Swanton C, Hurwitz H, Spigel DR, Sweeney C, Burris H, Bose R, Yoo B, Stein A, Beattie M, Kurzrock R. Targeted therapy for advanced solid tumors on the basis of molecular profiles: Results from MyPathway, an open-label, phase IIa multiple basket study. J Clin Oncol. 2018; 36:536-542.
70. Hyman DM, Piha-Paul SA, Won H, *et al.* HER kinase inhibition in patients with HER2- and HER3-mutant cancers. Nature. 2018; 554:189-194.
71. Golan T, Raitses-Gurevich M, Kelley RK, Bocobo AG, Borgida A, Shroff RT, Holter S, Gallinger S, Ahn DH, Aderka D, Apurva J, Bekaii-Saab T, Friedman E, Javle M. Overall survival and clinical characteristics of BRCA-associated cholangiocarcinoma: A multicenter retrospective study. Oncologist. 2017; 22:804-810.
72. Zhang W, Shi J, Li R, Han Z, Li L, Li G, Yang B, Yin Q, Wang Y, Ke Y, Li Q. Effectiveness of olaparib treatment in a patient with gallbladder cancer with an ATM-inactivating mutation. Oncologist. 2020; 25:375-379.
73. Ascierto PA, Long GV, Robert C, *et al.* Survival outcomes in patients with previously untreated BRAF wild-type advanced melanoma treated with nivolumab therapy: Three-year follow-up of a randomized phase 3 trial. JAMA Oncol. 2019; 5:187-194.
74. Robert C, Long GV, Brady B, *et al.* Nivolumab in previously untreated melanoma without BRAF mutation. N Engl J Med. 2015; 372:320-330.
75. Borghaei H, Paz-Ares L, Horn L, *et al.* Nivolumab versus docetaxel in advanced nonsquamous non-small-cell lung cancer. N Engl J Med. 2015; 373:1627-1639.
76. Sharma P, Retz M, Siefker-Radtke A, *et al.* Nivolumab in metastatic urothelial carcinoma after platinum therapy (CheckMate 275): A multicentre, single-arm, phase 2 trial. Lancet Oncol. 2017; 18:312-322.
77. Motzer RJ, Escudier B, McDermott DF, *et al.* Nivolumab versus everolimus in advanced renal-cell carcinoma. N Engl J Med. 2015; 373:1803-1813.
78. Ferris RL, Blumenschein G Jr., Fayette J, *et al.* Nivolumab for recurrent squamous-cell carcinoma of the head and neck. N Engl J Med. 2016; 375:1856-1867.
79. El-Khoueiry AB, Sangro B, Yau T, *et al.* Nivolumab in patients with advanced hepatocellular carcinoma (CheckMate 040): An open-label, non-comparative, phase 1/2 dose escalation and expansion trial. Lancet. 2017; 389:2492-2502.
80. Kelley RK, Bridgewater J, Gores GJ, Zhu AX. Systemic therapies for intrahepatic cholangiocarcinoma. J Hepatol. 2020; 72:353-363.
81. Gou M, Zhang Y, Si H, Dai G. Efficacy and safety of nivolumab for metastatic biliary tract cancer. Onco Targets Ther. 2019; 12:861-867.
82. Kim RD, Chung V, Alese OB, El-Rayes BF, Li D, Al-Toubah TE, Schell MJ, Zhou JM, Mahipal A, Kim BH, Kim DW. A phase 2 multi-institutional study of Nivolumab for patients with advanced refractory biliary tract cancer. JAMA oncology. 2020; doi: 10.1001/jamaoncol.2020.0930.
83. Ioka T, Ueno M, Oh DY, Fujiwara Y, Chen JS, Doki Y, Mizuno N, Park K, Asagi A, Hayama M, Nii M, Komuro K, Sugimoto M, Vlahovic G, Keda M. Evaluation of safety and tolerability of durvalumab (D) with or without tremelimumab (T) in patients (pts) with biliary tract cancer (BTC). Gastrointestinal Cancers Symposium; 2019; San Francisco, CA. J Clin Oncol. 2019; 37:suppl 387-387.
84. Piha-Paul SA, Oh DY, Ueno M, *et al.* Efficacy and safety of Pembrolizumab for the treatment of advanced biliary cancer: results from the KEYNOTE-158 and KEYNOTE-028 studies. Int J Cancer 2020; May 2. doi: 10.1002/ijc.33013.
85. Kang J, Jeong JH, Hwang HS, *et al.* Efficacy and safety of Pembrolizumab in patients with refractory advanced biliary tract cancer: tumor proportion score as a potential biomarker for response. Cancer research and treatment. 2020; 52:594-603.
86. Arkenau HT, Martin-Liberal J, Calvo E, Penel N, Krebs MG, Herbst RS, Walgren RA, Widau RC, Mi G, Jin J, Ferry D, Chau I. Ramucirumab plus pembrolizumab in patients with previously treated advanced or metastatic biliary tract cancer: Nonrandomized, open-label, phase I trial (JVDF). Oncologist. 2018; 23:1407-e1136.
87. Ueno M, Ikeda M, Morizane C, Kobayashi S, Ohno I, Kondo S, Okano N, Kimura K, Asada S, Namba Y, Okusaka T, Furuse J. Nivolumab alone or in combination with cisplatin plus gemcitabine in Japanese patients with unresectable or recurrent biliary tract cancer: A non-randomised, multicentre, open-label, phase 1 study. Lancet Gastroenterol Hepatol. 2019; 4:611-621.
88. Lu JC, Zeng HY, Sun QM, *et al.* Distinct PD-L1/PD1 Profiles and clinical implications in intrahepatic cholangiocarcinoma patients with different risk factors. Theranostics. 2019; 9:4678-4687.
89. Kitano Y, Yamashita YI, Nakao Y, *et al.* Clinical significance of PD-L1 expression in both cancer and stroma cells of cholangiocarcinoma patients. Ann Surg Oncol. 2020; 27:599-607.
90. Yu F, Gong L, Mo Z, Wang W, Wu M, Yang J, Zhang Q, Li L, Yao J, Dong J. Programmed death ligand-1, tumor infiltrating lymphocytes and HLA expression in Chinese extrahepatic cholangiocarcinoma patients: Possible immunotherapy implications. Biosci Trends. 2019; 13:58-69.
91. Chen WX, Li GX, Hu ZN, Zhu P, Zhang BX, Ding ZY. Significant response to anti-PD-1 based immunotherapy plus lenvatinib for recurrent intrahepatic cholangiocarcinoma with bone metastasis: A case report and literature review. Medicine (Baltimore). 2019; 98:e17832.
92. Liu X, Yao J, Song L, Zhang S, Huang T, Li Y. Local and abscopal responses in advanced intrahepatic cholangiocarcinoma with low TMB, MSS, pMMR and negative PD-L1 expression following combined therapy of SBRT with PD-1 blockade. J Immunother Cancer. 2019; 7:204.
93. Alshari OM, Dawaymeh TA, Tashtush NA, Aleshawi AJ, Al Manasra ARA, Obeidat KA. Completely resolved advanced biliary tract cancer after treatment by pembrolizumab: A report of two cases. Onco Targets Ther. 2019; 12:5293-5298.
94. Sui M, Li Y, Wang H, Luo Y, Wan T, Wang X, Hu B, Cheng Y, Lv X, Xin X, Xu Q, Wang G, Lu S. Two cases of intrahepatic cholangiocellular carcinoma with high insertion-deletion ratios that achieved a complete

response following chemotherapy combined with PD-1 blockade. J Immunother Cancer. 2019; 7:125.
95. Mou H, Yu L, Liao Q, Hou X, Wu Y, Cui Q, Yan N, Ma R, Wang L, Yao M, Wang K. Successful response to the combination of immunotherapy and chemotherapy in cholangiocarcinoma with high tumour mutational burden and PD-L1 expression: A case report. BMC Cancer. 2018; 18:1105.

Received June 30, 2020; Revised August 15, 2020; Accepted August 19, 2020.

*Address correspondence to:
Wei Zhang, Department of Hepatobiliary Cancer, Tianjin Medical University Cancer Institute and Hospital; National Clinical Research Center for Cancer, Key Laboratory of Cancer Prevention and Therapy, Tianjin; Tianjin's Clinical Research Center for Cancer. Huan Hu Xi Road, Tianjin, 300060, China.
E-mail: zhangweitjch@163.com

Released online in J-STAGE as advance publication August 24, 2020.

Mini-Review

DOI: 10.5582/bst.2020.03253

Rheumatoid arthritis-associated bone erosions: evolving insights and promising therapeutic strategies

Minglu Yan[1], Jianling Su[2], Yang Li[2,*]

[1] Department of Immunology, Graduate School of Medicine and Faculty of Medicine, The University of Tokyo, Tokyo, Japan
[2] Department of Rheumatology and Immunology, The Second Affiliated Hospital of Harbin Medical University, Harbin, Heilongjiang, China

SUMMARY The human immune system has evolved to recognize and eradicate pathogens, a process that is known as "host defense". If, however, the immune system does not work properly, it can mistakenly attack the body's own tissues and induce autoimmune diseases. Rheumatoid arthritis (RA) is such an autoimmune disease in which the synovial joints are predominately attacked by the immune system. Moreover, RA is associated with bone destruction and joint deformity. Although biologic agents have propelled RA treatment forward dramatically over the past 30 years, a considerable number of patients with RA still experience progressive bone damage and joint disability. That is to be expected since current RA therapies are all intended to halt inflammation but not to alleviate bone destruction. A better understanding of bone erosions is crucial to developing a novel strategy to treat RA-associated erosions. This review provides insights into RA-associated bone destruction and perspectives for future clinical interventions.

Keywords rheumatoid arthritis, bone erosions, RANKL, synovial fibroblasts

1. Introduction

Rheumatoid arthritis (RA) is a chronic autoimmune disease associated with bone destruction that affects up to 1% of the general population all over the world (*1*). The autoimmunity triggers inflammatory responses that are evident in most of the clinical features of RA, such as joint redness, warmth, swelling, tenderness, and stiffness. Besides inflammation, RA also causes bone destruction and leads to progressive disability.

Bone damage is more likely within the first 2 years after the onset of disease, and it is more common in the synovial-lined peripheral joints of hands and feet, such as the metacarpophalangeal and metatarsophalangeal joints, as well as the knee joints. Intriguingly, synovial joints such as hip are rarely affected by RA (*2*). This specific anatomical distribution of joint involvement occurs even if immune system indices and genetic and environmental factors are the same, suggesting that a local predisposing factor within the joints is involved in the course of RA-associated bone destruction. Several studies using high-throughput sequencing have revealed joint-specific characteristics in terms of genomics, epigenomics, and even functions (*3-5*).

In arthritic joints, the synovium becomes hyperplastic. Synovium with an aggressive phenotype has the capacity to invade and destroy bone, which is mediated by bone-resorbing osteoclasts, the formation of which is significantly favored by the inflammatory milieu in arthritic joints (*6*). Recent studies have indicated that not only increased osteoclastic bone resorption but also suppressive osteoblastic bone formation is associated with bone damage due to RA (*7*). Synovial tissue is thought to be associated with the joint specificity of RA.

Over the past 30 years, therapies for RA have changed dramatically, as reflected in both their clinical goals and strategies. The development and current routine use of biologic agents can help to achieve disease remission in patients with RA, which is a feasible goal. Although there are differences between individuals, many patients with RA fail to respond and continue to suffer structural damage even if in remission (*8*). Therefore, a better understanding of bone destruction is urgently needed to optimize the avenues for future treatment of RA. Here, recent advances in the understanding of RA-associated bone destruction summarized and perspectives for bone-directed therapies are described.

2. Key features of RA

RA is a systemic autoimmune disease as evinced by the appearance of various autoantibodies such as rheumatoid factor (RF) and anti-citrullinated protein

antibodies (ACPAs). ACPAs in particular are highly specific to RA and thus are most widely used to diagnose RA at present (*1,9,10*). ACPAs positivity is strongly associated with structural damage in patients with RA (*11*), and immune complexes including ACPAs have been found to directly stimulate osteoclast formation (*12*). ACPAs are produced during autoimmune responses to citrullinated proteins. Thanks to the development of proteomic technology, over 100 citrullinated proteins have been identified in RA samples (*13,14*). The generation of citrullinated proteins requires citrullinating enzymes, mostly known as peptidylarginine deiminases (PADs). In arthritic joints, neutrophil extracellular traps (NETs) released from the activated neutrophils were thought to be one of the potential sources of PADs (*15*). Citrullinated proteins are immunogenic in RA, and the ensuing immune responses target these proteins, inducing inflammation and thus leading to tissue damage. However, protein citrullination indeed plays a critical role in many physiological processes such as skin moisturization (*16*) and hair follicle formation (*17*), suggesting that the autoimmune reactions to citrullinated proteins rather than their presence alone are relatively pathogenic in RA.

Autoimmune reactions in RA are thought to be closely associated with genetic risks and environmental factors, such as microbial activity at mucosal sites (18-20). These factors are likely to interact in a synergistic manner to drive autoimmune responses. However, numerous studies have found that autoantibodies appear years before the onset of clinically apparent arthritis (*21,22*), indicating that autoimmune responses are pathogenic in RA but that they alone may not cause joint disease. Further studies are needed to address what triggers the transition from pre-symptomatic autoimmunity to clinically erosive arthritis.

In addition to autoimmunity, a hallmark of RA is progressive bone destruction and joint deformities. As mentioned earlier, autoimmunity alone may not suffice to trigger bone destruction. Nevertheless, a point worth noting is that RA due to autoimmunity primarily affects the synovial joints and tissue, and arthritic synovium is capable of damaging bone.

The synovium is specialized connective tissue where synovial fluid is produced. This tissue primarily functions to lubricate and nourish the synovial joints and to support the joint structure by producing an extracellular matrix (*23*). A healthy synovium is typically acellular, while during the course of RA, the synovium becomes inflamed and hyperplastic due to both the influx of inflammatory cells and local proliferation of synovial fibroblasts (SFs). As a result, arthritic synovium is a common place for the formation of bone-resorbing osteoclasts, which directly cause bone destruction in RA.

3. RA-associated bone destruction

Owing to the advances in high-throughput technologies, researchers have become more aware of the process of bone destruction. RA-associated bone destruction is due to both excessive bone resorption by osteoclasts and defective bone formation by osteoblasts (Figure 1).

3.1. Excessive bone resorption by osteoclasts

Osteoclasts are multi-nucleated cells of hematopoietic origin that are derived from myeloid lineage precursor

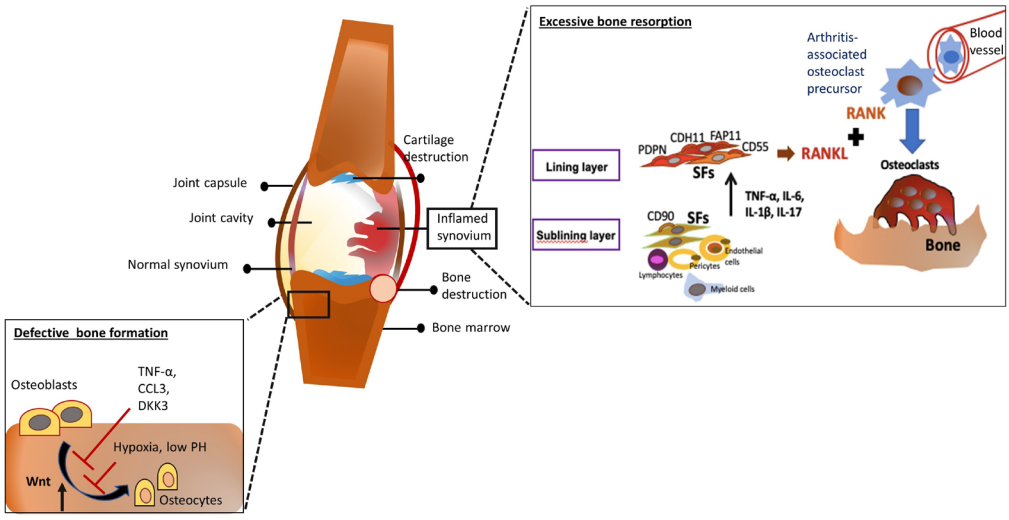

Figure 1. Potential mechanisms involved in RA-associated bone damage. Arthritic bone damage is caused by both excessive bone resorption by osteoclasts and by defective bone formation by osteoblasts. In the course of osteoclastic bone resorption, the osteoclast precursors in RA come from circulating blood and not synovial macrophages. Like RANKL-expressing SFs, osteoclast-supporting cells are thought to proliferate locally, and especially in the layer of cells lining bone. In RA, bone-forming osteoblasts are compromised by impaired Wnt signaling, which is negatively affected by intense inflammation in arthritic joints.

cells. The primary function of osteoclasts is to resorb bone. The essential roles of osteoclasts in RA-associated bone erosions have been identified in a series of human and genetically modified animal studies (*24,25*).

Osteoclasts are exclusively found attached to an area of bone resorption area in both patients with RA and murine models of arthritis. These findings lead to the question of whether or not osteoclasts cause arthritic erosions. A series of osteoclast-free models of arthritis have provided in vivo evidence. Transgenic mice that express human TNF (hTNFtg) failed to develop bone erosions when were crossed with c-fos-deficient mice, of which the functional osteoclasts were completely absent. A point worth noting is that the clinical signs of arthritis were equivalent between the hTNFtg and c-fos-knockout hTNFtg mice, indicating osteoclasts did function in bone erosions but not in inflammation (*25*).

Where do these osteoclasts come from? Osteoclast precursors can come from both circulating blood and resident cells in synovial tissue. Only recently did a study find that arthritic osteoclasts come from myeloid cells circulating in the blood and not the synovium (*26*). Remarkably, these arthritic osteoclast precursors are distinct in the transcriptome profile, compared to conventional osteoclast precursors that are responsible for physiological bone remodeling. This indicates that precisely targeting these arthritic osteoclasts could be a way to treat RA-associated bone erosions.

3.1.1. RANKL signaling governs osteoclast formation

Osteoclasts destroy bone in RA, so how osteoclasts are generated needs to be thoroughly investigated.

The receptor activator of the NF-κB ligand (RANKL), encoded by the Tnfsf11 gene, is essential for osteoclast formation and was identified in 1998 (*27*). The receptor of RANKL is RANK (encoded by the Tnfsf11a gene), which is highly expressed on osteoclast precursor cells. RANKL binds to RANK, inducing osteoclast formation. Mutations in the RANKL and RANK genes have been respectively identified in patients with osteopetrosis and familial expansile osteolysis (*28,29*). In addition, mice lacking either the RANKL or RANK gene display severe osteopetrosis due to a complete absence of osteoclasts. The same phenomenon occurs in arthritis. RANKL-deficient mice are protected from bone destruction even when attempts are made to induce arthritis, although they do have joint inflammation to a similar extent (*30*).

3.1.2. SFs are the major source of RANKL

In arthritic joints, which cells are responsible for RANKL production? Although RANKL was primarily reported to be expressed on activated T cells, in arthritic joints, SFs in synovial tissue are believed to be the major source of RANKL and thus primarily responsible for arthritic bone erosions (*31*). Because of their prominent role in RA-associated bone destruction, SFs have often been a topic of considerable interest in the past.

RA-SFs are mesenchymal lineage cells marked by the high expression of podoplanin (PDPN), cadherin 11 (CDH11), and fibroblast activation protein α (FAPα), all of which are barely expressed in a healthy individual (*32,33*). More recently, SFs within the rheumatoid synovium have been found to be heterogeneous, as evinced by different anatomical locations and protein markers as well as by specific functions (*32-37*). A single-cell RNA-seq analysis identified two functionally distinct SFs subsets. Lining layer SFs, which predominately express CD55 but lack CD90, cause bone destruction in arthritic mice via high levels of RANKL expression while sublining SFs that highly express CD90 are pro-inflammatory (*34*). That study demonstrated for the first time that functional distinct SFs subsets do exist in arthritic joints. The importance of SF heterogeneity may directly contribute to the distinctive features of RA. However, further studies are needed to clarify whether the two types of SFs are truly distinct cell subsets or just a single population. Are the distinct phenotypes only exhibited temporarily to cope with surrounding stimulatory signals and environmental insults? Inflammatory cytokines, such as tumor necrosis factor α (TNF-α), IL-6, IL-1β, and IL-17, are abundant in the inflammatory milieu of joints and are thought to be the most potent RANKL-inducing factors. In addition, biomechanical stimuli within joints, such as mechanical stress, have also been found to potentially induce RANKL expression (*38*).

3.2. Compromised bone formation by osteoblasts

Osteoblasts are derived from mesenchymal precursor cells in bone marrow and have the capacity to differentiate into osteocytes to form new bone. In RA, bone formation is compromised.

First, inflammation inhibits bone formation. TNF-α is considered to occupy the top position in the inflammatory cytokine cascade. As early as 1986, pioneering researchers reported that monocyte-derived TNF-α directly inhibited bone collagenase synthesis in osteoblast cultures (*39*). In addition, formation of mineralized bone at sites of inflammation decreased significantly compared to that at sites without inflammation in serum-transferred arthritic mice. Moreover, damaged bone could be repaired by osteoblasts if inflammation was eliminated (*40,41*). Enhanced bone formation in patients with RA was also observed after anti-TNF therapy (*42*). More recently, B cells located in the subchondral and endosteal bone marrow (BM) have been found to be involved in the mechanisms of RA-compromised osteoblasts since those B cells secrete TNF-α and CCL3 (*43*). This may partially explain clinical benefits in the form of

improved bone mineral density (BMD) and changes in bone turnover after treatment with rituximab (a CD20 blocker) in patients with RA.

Besides inflammation, localized hypoxia and a low PH environment in arthritic joints also affect osteoblast functions (*44*). Hypoxia suppresses the Wnt pathway, which is important for signaling bone formation in osteoblasts. A low PH directly prevents skeletal tissue mineralization, a process by which bone matrix is filled with calcium phosphate, thus improving bone strength. Noticeably, hypoxia and a low PH are commonly aggravated by the inflammatory milieu within arthritic joints. Accordingly, repaired bone is seen only when systemic inflammation is completely controlled.

4. Current treatment of RA-associated bone erosions and horizons for the future

4.1. Current treatment

Over the past few decades, the treatment of RA has changed dramatically due to the improved understanding of this disease (Figure 2).

Drug treatment options for RA have evolved from the era of nonsteroidal anti-inflammatory drugs (NSAIDs) in the 1930s, to glucocorticoid therapy in the 1950s, to disease-modifying anti-rheumatic drugs (DMARDs) in the 1980s, to biologics since the 2000s, and more recently to small-molecule DMARDs, which are mainly Janus kinase inhibitors (JAKis). The significant change in RA management has coincided with improved clinical outcomes.

NSAIDs only help with symptoms and pain relief, and DMARDs modify disease activity but do not affect structural alterations. Biologics, together with DMARDs, dramatically slow disease progression but still do not cure RA. JAKis target broad cytokine- and hormone-mediated signaling, so their long-term efficacy and safety remain unclear.

Biologics that inhibit key components of the immune system, such as inflammatory cytokines and activated immune cells, are the mainstay of current RA management and have resulted in significant structural improvements in patients with RA. In inflamed joints, inflammatory cytokines and activated immune cells fuel osteoclastic bone destruction and impair osteoblastic bone formation. One of the clearest examples of biologic agents that affect bone is TNF blockers. TNF directly regulates the osteoclast-intrinsic pathway and it stimulates RANKL expression on SFs to indirectly facilitate osteoclast formation. There are six different TNF blockers currently approved for treatment of RA, consisting of both monoclonal anti-TNF antibodies and soluble TNF receptors. TNF blockers have displayed the potential to arrest structural progression in RA, but nonetheless some patients are unresponsive or resistant to anti-TNF therapies (*45*).

JAKis, such as tofacitinib, baricitinib, and upadacitinib, regulate distinct cytokine- and hormone-mediated pathways and are currently approved for treatment of RA (*46*). Recent evidence has emerged to suggest that these JAKis play a role in bone biology. JAKis ameliorate bone loss by enhancing osteoblastic bone formation rather than by affecting osteoclastic bone erosions in models of both osteoporosis and arthritis (*47*). In patients with RA receiving 5 mg of tofacitinib twice daily for 2 years, bone formation is induced as revealed by high-resolution peripheral quantitative CT (*48*).

Denosumab (DMab), a fully human monoclonal antibody targeting RANKL, is the only anti-erosion agent that is currently available for treatment of RA. The clinical benefits of DMab therapy in patients with RA are the prevention of bone erosions as well as the alleviation osteoporosis (*49*). Thus, DMab has been approved for

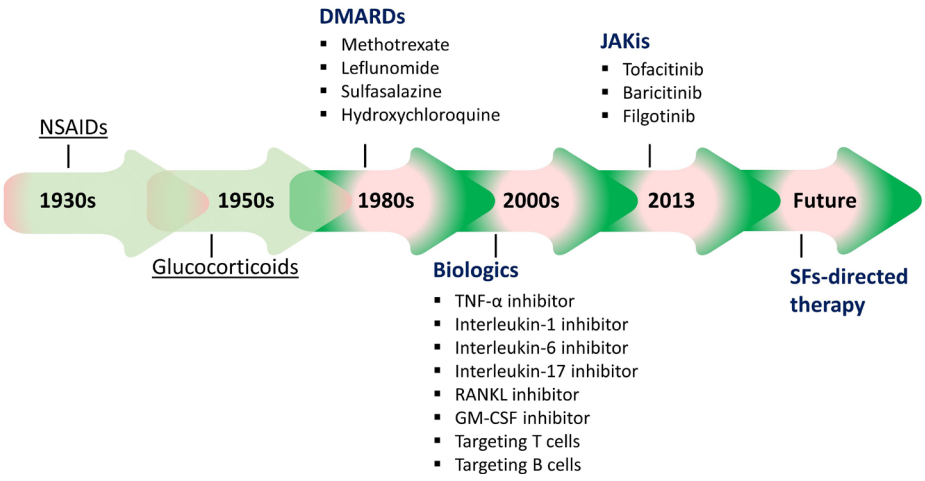

Figure 2. Key milestones during the evolution of treatments for RA. Drugs that are available for treatment of RA have dramatically evolved over the past few decades, though they cannot cure RA yet. Future SFs-directed therapies may potentially optimize the avenue for treatment of RA.

treatment of RA in Japan.

4.2. Horizons for the future

Researchers have increasingly recognized that RANKL-expressing SFs absolutely contribute to osteoclastic bone erosions. Perhaps lessons could be learned from experience with cancer-associated fibroblast-directed therapies. One such option is to target the surface proteins expressed on RA-SFs. Indeed, an early phase of a clinical trial of CDH11 therapy in patients with RA is now underway. In addition, RA-SFs in arthritic joints appear to be epigenetically imprinted, which potentially contributes to persistent aggressive phenotypes (*3*). Accordingly, histone-modifying inhibitors such as BET inhibitors may remodel RA-SFs to a normal landscape. However, one must keep in mind that there is still no unique cell marker with which to define erosive SFs, and the same challenge remains in relation to histone modifiers.

Targeting bone-destructive osteoclasts directly is also a potential strategy. For instance, a small molecule inhibitor of cathepsin K (CTSK) directly inhibits osteoclastic-bone resorption (*50*). Moreover, osteoclasts utilize oxidative phosphorylation to fulfill the energy demands for their resorptive functions (*51*), so targeting metabolic pathways may be another therapeutic option.

5. Conclusion

Despite vast improvement in the treatment of RA, achieving remission without medication is still impractical at present. In fact, most patients with RA do not respond optimally to these current therapies, particularly in terms of bone damage and joint deformities.

Bone destruction is a key feature of RA. Surprisingly, clinical therapeutic strategies to treat bone destruction are not being considered at present; most current therapies are based on a simplistic view and reductionist understanding. The complexity of RA-associated bone destruction has become increasingly clear: osteoclast-intrinsic mechanisms and the inflammatory milieu in joints both contribute to erosions. Most of the drugs available for RA are designed to modulate inflammation but not to treat bone directly. Structural damage may continue to progress even when inflammation diminishes since immune-suppressive drugs directly target neither osteoclasts nor RANKL-expressing SFs. Given the signature of this disease, a combined therapy that targets both the osteoclastic-intrinsic pathways and RA-related inflammation is expected to yield better clinical benefits.

Acknowledgement

This study was supported by the Bethune Medical Research Fund of China (TY153EN).

References

1. Klareskog L, Catrina AI, Paget S. Rheumatoid arthritis. Lancet. 2009; 373:659-672.
2. O'dell Jr. Treating rheumatoid arthritis early: A window of opportunity? Arthritis Rheum. 2002; 46:283-285.
3. Frank-Bertoncelj M, Trenkmann M, Klein K, Karouzakis E, Rehrauer H, Bratus A, Kolling C, Armaka M, Filer A, Michel BA, Gay RE, Buckley CD, Kollias G, Gay S, Ospelt C. Epigenetically-driven anatomical diversity of synovial fibroblasts guides joint-specific fibroblast functions. Nat Commun. 2017; 8:14852.
4. Ai R, Hammaker D, Boyle DL, Morgan R, Walsh AM, Fan S, Firestein GS, Wang W. Joint-specific DNA methylation and transcriptome signatures in rheumatoid arthritis identify distinct pathogenic processes. Nat Commun. 2016; 7:11849.
5. Kraan MC, Reece RJ, Smeets TJ, Veale DJ, Emery P, Tak PP. Comparison of synovial tissues from the knee joints and the small joints of rheumatoid arthritis patients: Implications for pathogenesis and evaluation of treatment. Arthritis Rheum. 2002; 46:2034-2038.
6. Bottini N, Firestein GS. Duality of fibroblast-like synoviocytes in RA: Passive responders and imprinted aggressors. Nat Rev Rheumatol. 2013; 9:24-33.
7. Tsukasaki M, Takayanagi H. Osteoimmunology: Evolving concepts in bone-immune interactions in health and disease. Nat Rev Immunol. 2019; 19:626-642.
8. Upchurch KSs, Kay J. Evolution of treatment for rheumatoid arthritis. Rheumatology (Oxford). 2012; Suppl 6:vi28-36.
9. Wasserman AM. Diagnosis and management of rheumatoid arthritis. Am Fam Physician. 2011; 84:1245-1252.
10. Fox DA. Citrullination: A specific target for the autoimmune response in rheumatoid arthritis. J Immunol. 2015; 195:5-7.
11. Bongi SM, Manetti R, Melchiorre D, Turchini S, Boccaccini P, Vanni L, Maggi E. Anti-cyclic citrullinated peptide antibodies are highly associated with severe bone lesions in rheumatoid arthritis anti-CCP and bone damage in RA. Autoimmunity. 2004; 37:495-501.
12. Krishnamurthy A, Joshua V, Haj Hensvold A, *et al.* Identification of a novel chemokine-dependent molecular mechanism underlying rheumatoid arthritis-associated autoantibody-mediated bone loss. Ann Rheum Dis. 2016; 75:721-729.
13. Mathsson L, Mullazehi M, Wick MC, Sjöberg O, Van Vollenhoven R, Klareskog L, Rönnelid J. Antibodies against citrullinated vimentin in rheumatoid arthritis: Higher sensitivity and extended prognostic value concerning future radiographic progression as compared with antibodies against cyclic citrullinated peptides. Arthritis Rheum. 2008; 58:36-45.
14. Alexiou I, Germenis, Koutroumpas A, Kontogianni A, Theodoridou K, Sakkas LI. Anti-cyclic citrullinated peptide-2 (CCP2) autoantibodies and extra-articular manifestations in Greek patients with rheumatoid arthritis. Clin Rheumatol. 2008; 27:511-513.
15. Khandpur R, Carmona-Rivera C, Vivekanandan-Giri A, Gizinski A, Yalavarthi S, Knight JS, Friday S, Li S, Patel RM, Subramanian V, Thompson P, Chen P, Fox DA, Pennathur S, Kaplan MJ. NETs are a source of citrullinated autoantigens and stimulate inflammatory responses in rheumatoid arthritis. Sci Transl Med. 2013;

5:178ra140.
16. Chavanas S, Méchin MC, Nachat R, Adoue V, Coudane F, Serre G, Simon M. Peptidylarginine deiminases and deimination in biology and pathology: Relevance to skin homeostasis. J Dermatol Sci. 2006; 44:63-72.
17. Kizawa K, Unno M, Heizmann C, Takahara H. Importance of citrullination on hair protein molecular assembly during trichocytic differentiation. In: Protein Deimination in Human Health and Disease. (Nicholas, AP, Bhattacharya, SK, eds). Springer New York, NY, 2014; pp 129-148.
18. Deane KD, Demoruelle MK, Kelmenson LB, Kuhn KA, Norris JM, Holers VM. Genetic and environmental risk factors for rheumatoid arthritis. Best Pract Res Clin Rheumatol. 2017; 31:3-18.
19. Demoruelle MK. Mucosa biology and the development of rheumatoid arthritis: Potential for prevention by targeting mucosal processes. Clin Ther. 2019; 41:1270-1278.
20. Holers VM, Demoruelle Mk, Kuhn KA, Buckner JH, Robinson WH, Okamoto Y, Norris JM, Deane KD. Rheumatoid arthritis and the mucosal origins hypothesis: Protection turns to destruction. Nat Rev Rheumatol. 2018; 14:542-557.
21. Bos WH, Van De Stadt LA, Sohrabian A, Rönnelid J, Van Schaardenburg D. Development of anti-citrullinated protein antibody and rheumatoid factor isotypes prior to the onset of rheumatoid arthritis. Arthritis Res Ther. 2014; 16:405.
22. Darrah E, Andrade F. Rheumatoid arthritis and citrullination. Curr Opin Rheumatol. 2018; 30:72-78.
23. Lindblad S, Hedfors E. The synovial membrane of healthy individuals--Immunohistochemical overlap with synovitis. Clin Exp Immunol. 1987; 69:41-47.
24. Takayanagi H, Iizuka H, Juji T, Nakagawa T, Yamamoto A, Miyazaki T, Koshihara Y, Oda H, Nakamura K, Tanaka S. Involvement of receptor activator of nuclear factor kappaB ligand/osteoclast differentiation factor in osteoclastogenesis from synoviocytes in rheumatoid arthritis. Arthritis Rheum. 2000; 43:259-269.
25. Redlich K, Hayer S, Ricci R, David JP, Tohidast-Akrad M, Kollias G, Steiner G, Smolen JS, Wagner EF, Schett G. Osteoclasts are essential for TNF-alpha-mediated joint destruction. J Clin Invest. 2002; 110:1419-1427.
26. Hasegawa T, Kikuta J, Sudo T, Matsuura Y, Matsui T, Simmons S, Ebina K, Hirao M, Okuzaki D, Yoshida Y, Hirao A, Kalinichenko VV, Yamaoka K, Takeuchi T, Ishii M. Identification of a novel arthritis-associated osteoclast precursor macrophage regulated by FoxM1. Nat Immunol. 2019; 20:1631-1643.
27. Yasuda H, Shima N, Nakagawa N, *et al.* Osteoclast differentiation factor is a ligand for osteoprotegerin/osteoclastogenesis-inhibitory factor and is identical to TRANCE/RANKL. Proc Natl Acad Sci U S A. 1998; 95:3597-3602.
28. Douni E, Rinotas V, Makrinou E, Zwerina J, Penninger JM, Eliopoulos E, Schett G, Kollias G. A RANKL G278R mutation causing osteopetrosis identifies a functional amino acid essential for trimer assembly in RANKL and TNF. Hum Mol Genet. 2012; 21:784-798.
29. Hughes AE, Ralston SH, Marken J, Bell C, Macpherson H, Wallace RG, Van Hul W, Whyte MP, Nakatsuka K, Hovy L, Anderson DM. Mutations in TNFRSF11A, affecting the signal peptide of RANK, cause familial expansile osteolysis. Nat Genet. 2000; 24:45-48.
30. Pettit AR, Ji H, Von Stechow D, Müller R, Goldring SR, Choi Y, Benoist C, Gravallese EM. TRANCE/RANKL knockout mice are protected from bone erosion in a serum transfer model of arthritis. Am J Pathol. 2001; 159:1689-1699.
31. Danks L, Komatsu N, Guerrini MM, Sawa S, Armaka M, Kollias G, Nakashima T, Takayanagi H. RANKL expressed on synovial fibroblasts is primarily responsible for bone erosions during joint inflammation. Ann Rheum Dis. 2016; 75:1187-1195.
32. Agarwal SK, Lee DM, Kiener HP, Brenner MB. Coexpression of two mesenchymal cadherins, cadherin 11 and N-cadherin, on murine fibroblast-like synoviocytes. Arthritis Rheum. 2008; 58:1044-1054.
33. Desanti GE, Saghir AN, Naylor AJ, Kemble S, Falconer J, Wehmeyer C, Marshall JL, Nakamura K, Goodall M, Navarro-Núñez L, Watson SP, Buckley CD. O014 Podoplanin (GP38), a marker of synovial inflammation, is an excellent therapeutic target in mouse collagen-induced arthritis. Ann Rheum. Dis 2018; 77:A7-A8.
34. Zhang F, Wei K, Slowikowski K, *et al.* Defining inflammatory cell states in rheumatoid arthritis joint synovial tissues by integrating single-cell transcriptomics and mass cytometry. Nat Immunol. 2019; 20:928-942.
35. Croft AP, Campos J, Jansen K, *et al.* Distinct fibroblast subsets drive inflammation and damage in arthritis. Nature. 2019; 570:246-251.
36. Mizoguchi F, Slowikowski K, Wei K, *et al.* Functionally distinct disease-associated fibroblast subsets in rheumatoid arthritis. Nat Commun. 2018; 9:789.
37. Wei K, Korsunsky I, Marshall Jl, *et al.* Notch signalling drives synovial fibroblast identity and arthritis pathology. Nature. 2020; 582:259-264.
38. Deschner J, Wypasek E, Ferretti M, Rath B, Anghelina M, Agarwal S. Regulation of RANKL by biomechanical loading in fibrochondrocytes of meniscus. J Biomech. 2006; 39:1796-1803.
39. Bertolini DR, Nedwin GE, Bringman TS, Smith DD, Mundy GR. Stimulation of bone resorption and inhibition of bone formation in vitro by human tumour necrosis factors. Nature. 1986; 319:516-518.
40. Matzelle MM, Gallant MA, Condon KW, Walsh NC, Manning CA, Stein GS, Lian JB, Burr DB, Gravallese EM. Resolution of inflammation induces osteoblast function and regulates the Wnt signaling pathway. Arthritis Rheum. 2012; 64:1540-1550.
41. Walsh NC, Reinwald S, Manning Ca, Condon KW, Iwata K, Burr DB, Gravallese EM. Osteoblast function is compromised at sites of focal bone erosion in inflammatory arthritis. J Bone Miner Res. 2009; 24:1572-1585.
42. Seriolo B, Paolino S, Sulli A, Ferretti V, Cutolo M. Bone metabolism changes during anti-TNF-alpha therapy in patients with active rheumatoid arthritis. Ann N Y Acad Sci. 2006; 1069:420-427.
43. Sun W, Meednu N, Rosenberg A, Rangel-Moreno J, Wang V, Glanzman J, Owen T, Zhou X, Zhang H, Boyce BF, Anolik JH, Xing L. B cells inhibit bone formation in rheumatoid arthritis by suppressing osteoblast differentiation. Nat Commun. 2018; 9:5127.
44. Quiñonez-Flores CM, González-Chávez SA, Pacheco-Tena C. Hypoxia and its implications in rheumatoid arthritis. J Biomed Sci. 2016; 23:62.
45. Schett G, Coates LC, Ash ZR, Finzel S, Conaghan PG. Structural damage in rheumatoid arthritis, psoriatic arthritis, and ankylosing spondylitis: Traditional views,

novel insights gained from TNF blockade, and concepts for the future. Arthritis Res Ther. 2011; 25:13.
46. Angelini J, Talotta R, Roncato R, Fornasier G, Barbiero G, Dal Cin L, Brancati S, Scaglione F. JAK-Inhibitors for the treatment of rheumatoid arthritis: A focus on the present and an outlook on the future. Biomolecules. 2020; 10:1002.
47. Adam S, Simon N, Steffen U, Andes FT, Scholtysek C, Müller DIH, Weidner D, Andreev D, Kleyer A, Culemann S, Hahn M, Schett G, Krönke G, Frey S, Hueber AJ. JAK inhibition increases bone mass in steady-state conditions and ameliorates pathological bone loss by stimulating osteoblast function. Sci Transl Med. 2020; 12:eaay4447.
48. Clarke J. JAK inhibitors boost bone formation. Nat Rev Rheumatol. 2020; 16:249.
49. Takeuchi T, Tanaka Y, Ishiguro N, Yamanaka H, Yoneda T, Ohira T, Okubo N, Genant HK, Van Der Heijde D. Effect of denosumab on Japanese patients with rheumatoid arthritis: A dose-response study of AMG 162 (denosumab) in patients with rheumatoid arthritis on methotrexate to validate inhibitory effect on bone Erosion (DRIVE)-A 12-month, multicentre, randomised, double-blind, placebo-controlled, phase II clinical trial. Ann Rheum Dis. 2016; 75:983-990.
50. Drake MT, Clarke BL, Oursler MJ, Khosla S. Cathepsin K inhibitors for osteoporosis: Biology, potential clinical utility, and lessons learned. Endocr Rev. 2017; 38:325-350.
51. Lemma S, Sboarina M, Porporato PE, Zini N, Sonveaux P, Di Pompo G, Baldini N, Avnet S. Energy metabolism in osteoclast formation and activity. Int J Biochem Cell Biol. 2016; 79:168-180.

Received July 8, 2020; Revised August 22, 2020; Accepted September 3, 2020.

Address correspondence to:
Yang Li, Department of Rheumatology and Immunology, The Second Affiliated Hospital of Harbin Medical University, Harbin 150000, Heilongjiang, China.
E-mail: liyang@hrbmu.edu.cn

Released online in J-STAGE as advance publication September 10, 2020.

Mini-Review

DOI: 10.5582/bst.2020.03267

Advances in personalized neoantigen vaccines for cancer immunotherapy

Changbo Sun, Shun Xu*

Department of Thoracic Surgery, the First Hospital of China Medical University, Shenyang, Liaoning, China.

SUMMARY Immunotherapy, which targets T cell inhibitory receptors (immune checkpoints), is now being widely used to treat a variety of types of cancer combined with surgery, chemotherapy, or radiotherapy. However, immune checkpoint inhibitors are highly dependent on the ability to present diverse tumor antigens to T cells. Neoantigens, arising from somatic mutations and specifically targeting tumor cells, have the potential to stimulate a highly specific immune anti-tumor response. Technological advances such as genomic sequencing and bioinformatics algorithms for epitope prediction have directly facilitated the development of neoantigen vaccines for individual cancers. Currently, several preclinical studies and early clinical trials using neoantigen in combination with checkpoint inhibitors have resulted in robust T cell responses and antitumor action. In the future, efforts will be made to optimize effective personalized neoantigen vaccines targeting individual tumors and to elucidate the immune mechanisms underlying tumor evolution.

Keywords personalized neoantigen, immune response, cancer vaccine, immunotherapy

1. Introduction

Immune checkpoint therapy with antibodies targeting cytotoxic T lymphocyte-associated antigen 4 (CTLA4) or programmed death 1/ligand 1(PD1)/(PDL1) has overcome immune suppression and induced sustained regression of disease in a subset of patients with cancer. However, tumor cells are able to evade the immune system due to their weak immunogenicity, leading to reduced efficacy or immunotherapeutic failure in many patients (10 to 60% of treated patients respond, depending on the type of cancer) (*1*). A recent study has reported that immune checkpoint inhibitors are highly dependent on the ability to present diverse tumor antigens to T cells (*2*). Hence, the effective identification of antigens with strong immunogenicity in tumor cells has become a priority in immunotherapy, and better understanding of mechanisms has suggested that immunogenicity and tumorigenicity are synchronous processes resulting from mutagenesis.

Neoantigens are mainly generated from peptide fragments of mutant proteins that derive from mutated genes, which are commonly involved in carcinogenesis (Figure 1) (*3*). Neoantigens are expressed exclusively in tumor cells with individual specificity and provide the immune system with potential target antigens. Neoantigens can be presented to T cells by major histocompatibility complex (MHC) molecules and stimulate lymphocyte-mediated anti-cancer immunity to eradicate cancer cells. They are presumed to be more highly immunogenic than non-mutated self-antigens, due to the minimized influence from thymic selection, central and peripheral tolerance, and the risk of autoimmunity (*4*).

Technological advances such as high-throughput sequencing of whole cancer genomes and the improvement of prediction algorithms have facilitated the development of personalized neoantigen vaccines (*5*). Recent studies have demonstrated the potential role of neoantigens in cancer immunotherapy and cancer evolution (*6,7*). This mini-review briefly summarizes advances brought about by recent neoantigen-directed studies to provide a better understanding of their mechanisms in order to improve cancer immunotherapy.

2. Neoantigen identification and selection

Neoantigens are highly individual-specific and are derived from driver mutations or passenger mutations in cancer cells. Prioritizing cancer-specific neoantigens is crucial to successful tumor vaccine therapy (*8*). Theoretically, potential neoantigens are generated from tumor somatic mutations based on the assumption that a mutated sequence can be translated into a protein, which is then processed into a peptide with a binding affinity for an MHC molecule that results in a mutant

peptide-MHC complex that is recognized by T cell receptors (*9*). To create a personalized cancer vaccine, neoantigens must be computationally predicted based on matched tumor-normal sequencing data and then ranked (prioritized) according to their predicted capability to stimulate a T cell response. This process of predicting potential neoantigens involves multiple steps, including somatic mutation identification, human leukocyte antigen (HLA) typing, peptide processing, and peptide-MHC binding prediction. The general workflow is shown in Figure 2. Finally, the antigenicity of the synthesized neoantigens is determined using standard immunological assays (*10*).

Short peptides and long peptides comprise the sequence of neoantigens with different lengths. The former generally refers to peptides of 8-11 amino acids in length that are recognized directly by $CD8^+$ T cells as potential epitopes. Short peptides directly bind to MHC class I molecules expressed by all nucleated cells, most of which are not specialized for antigen presentation, leading to weak T-cell priming or immune tolerance (*11*). Long peptides, which are 15-

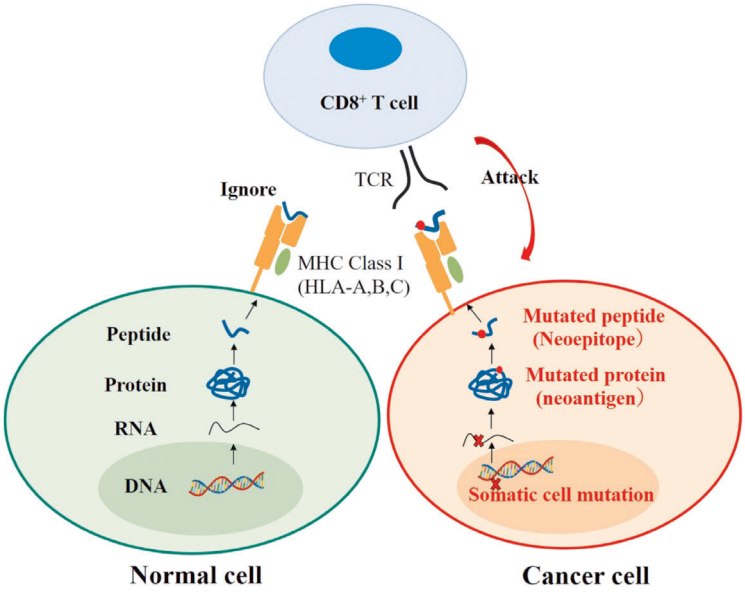

Figure 1. Peptide neoantigen. Variant peptides from mutated proteins (neoantigens) derived from somatic tumor-specific mutations can be presented as a mutant peptide-MHC complex on the cancer cell surface and can be recognized by T cell receptors (TCRs) to elicit an immune response.

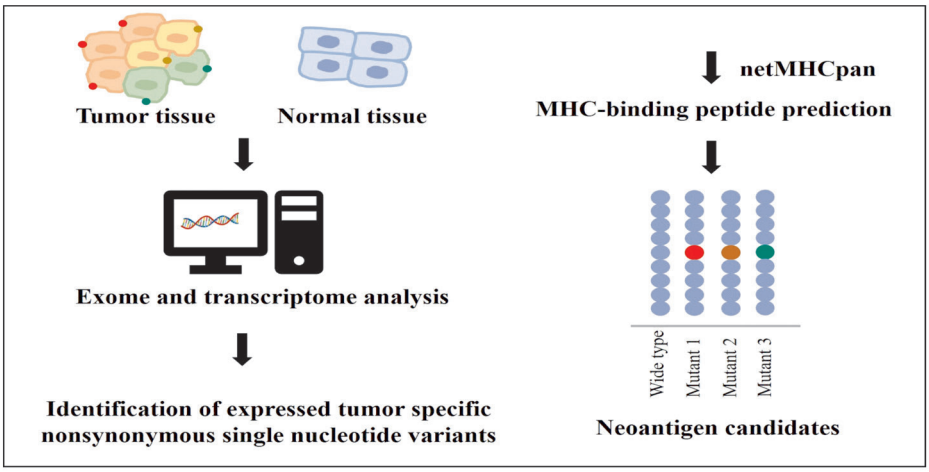

Figure 2. Diagram of the workflow for personalized neoantigen prediction. Clonal neoantigens can be expressed by intratumor heterogeneous mutations in tumor cells. Exome sequencing data from tumor tissue are compared with those from normal tissue to detect the full range of genomic alterations within a tumor. The expression of mutated antigens in the tumor is determined using transcriptome analysis. Then, the binding capacity to MHC molecules from mutations that encode a mutant protein is ranked using algorithms such as netMHCpan. The recognition of potential neoantigens is determined using standard immunological assays.

31 amino acids in length, are taken up and processed by professional antigen-presenting cells (APCs) for presentation and elicit MHC class I and MHC class II T cell activation (*12*). Studies have demonstrated that long peptides, which are superior to short peptides, can induce both $CD4^+$ and $CD8^+$ T cell responses (*6,7*). Clearly, both $CD8^+$ and $CD4^+$ T cells are critical to respectively recognizing antigens bound by MHC class I and II molecules on the cell surface. However, the challenge is to accurately identify optimal long peptides and to analyze MHC class II neoepitopes using current algorithms, as has been summarized elsewhere (*13,14*). Future developments may leverage artificial intelligence or machine learning with high-throughput sequencing and larger datasets of cancer-specific HLA ligands, T cell epitopes, and clinical responses to improve neoantigen prediction reliability (*13,15*).

In addition to the precise identification of highly expressed tumor-specific antigens, another step is to determine the therapeutic efficacy of neoantigens. That efficacy relies on a highly immunogenic environment including recruitment of professional APCs to the site of tumor antigen expression, uptake of the antigens by APCs, and maturation, activation, and trafficking of APCs to vaccine-draining lymph nodes where T cell activation occurs (*16*).

3. Clonal neoantigens and tumor evolution

The interplay of the adaptive immune system and evolving tumors is ongoing during the development and progression of tumors. On one hand, mutations provide fitness through the activation of key driver events or loss of tumor suppressor genes during evolution. On the other hand, a minority of mutations may result in neoantigens and provide targets for the immune system to inhibit the evolving tumor. Tumor cells undergo clonal selection pressure due to a variety of genetic and microenvironmental factors, which induce mutation frequencies that vary markedly within tumors (*17*).

Genomic heterogeneity including mutational burden and types, which might render tumors refractory to treatment, has also been found to correlate with heterogeneous immune cell infiltration. The interaction between an evolving cancer and a dynamic immune microenvironment was investigated by the TRACER-x consortium (*18*). Two hundred and fifty-eight regions from 88 early-stage, untreated non-small-cell lung cancers were analyzed and the immune cells, cancer mutations, and epigenetic marks were identified in these regions. The study found that sparsely infiltrated tumors exhibited a waning of neoantigen editing during tumor evolution, while immune-infiltrated tumor regions exhibited ongoing immunoediting, with either loss of heterozygosity in human leukocyte antigens or depletion of expressed neoantigens. That study revealed that local tumor-infiltrating lymphocytes influence the evolution of cancer through immunoediting of neoantigens.

Another study explored the relevance of the neoantigen burden, clonal neoantigen heterogeneity, and prognosis in patients with early-stage non-small-cell lung cancer included in the Cancer Genome Atlas project (*19*). In an immunotherapy-naïve setting, these patients were found to have significantly longer overall survival if their tumors contained a high number of clonal neoantigens and exhibited low levels of neoantigen heterogeneity. Gene-expression analysis revealed a subset of immune-related genes that were upregulated in the high clonal neoantigen group, indicating an inflammatory tumor microenvironment. That study demonstrated that the underlying mechanism of why the tumor overall mutation burden was not an optimal biomarker for checkpoint blockades in clinical settings since the clonal expression of neoantigens by tumor cells, rather than the overall mutational burden, determines the response to checkpoint blockade therapy (*20*).

The aforementioned study by the TRACER-x consortium found that immunogenicity could be lost through serial transplantation, while these tumors maintained their malignant potential according to different selective pressures (*18*). These fundamental findings have led to a basic understanding of the mechanism of neoantigens: due to the occurrence of T cell-mediated neoantigen immunoediting, a broad neoantigen-specific T cell response should be sought to avoid tumor resistance (*21*).

4. Neoantigen quality and quantity

Intratumor neoantigen heterogeneity, owing to the evolving tumor mutational landscape, poses a major problem to the management of early and advanced cancers. Neoantigen vaccines can only induce T cells to target a small number of tumor cells if the neoantigens are derived from mutated subclones, thus limiting the clinical efficacy of neoantigens (*22*). Because of their quantity and quality, clonal neoantigens are currently becoming a focus of immune-mediated control (*23*).

Previous research on cancer immunotherapy investigated the class I antigen processing pathway that elicits $CD8^+$ T cells to extensively kill cancer cells. However, there is mounting evidence of the promising efficacy of class II-specific neoantigens in cancer immunotherapies (*24,25*). In addition to CD8 T cells, the CD4 T cells are also required and may be crucial determinants of a successful response to immunotherapy (*26*). A recent study demonstrated that a successful immune response depends on the presence of neoantigens that trigger responses from both CD4 and CD8 T cells (*27*). Therefore, quality neoantigens should include both MHC class I and MHC class II epitopes to ensure CD8 cytotoxic T lymphocyte priming and CD4 T cell help for a robust immune response.

In the context of neoantigen-based cancer vaccines, mRNA/DNA or synthetic long peptides, encompassing both MHC class I and MHC class II epitopes, are typically used (*28*). Vaccination with a multi-epitope personalized neoantigen may be a promising strategy to induce intratumoral heterogeneous neoantigen-specific $CD4^+$ and $CD8^+$ T cell immune responses with a higher probability of antitumor efficacy (*29*). However, the challenge is to develop a general method for efficient stimulation of potent antitumor T cell responses (*30*). Direct injection of unformulated neoantigens has been tested in many studies (*7*). Nonetheless, the ultimate therapeutic efficacy of these peptide vaccines is limited by inefficient delivery to the desired lymphoid organs. Ex vivo-pulsed dendritic cell vaccines are promising but suffer from several limitations, including difficulties in preparation and expansion (*31*). In the future, engineered intelligent biomaterials, which can deliver several to several dozen neoantigens together with adjuvants to target APCs, are expected to achieve precise control of balanced MHC class I and II loading of antigens in order to elicit the most potent and broad T cell responses (*32*).

5. Neoantigen vaccine and checkpoint blockade therapy

If a neoantigen displayed on the surface of tumor cells bound to MHC molecules is recognized by a CD8 T cell, this cell can target and kill any tumor cells that express the same neoantigen. According to many studies, however, T cell priming neoantigen vaccines alone are not sufficient to trigger an effective immune response against the tumor because the cytotoxic response can be blocked by an immunosuppressive environment in the context of tumors (*33*).

Immune checkpoint therapy with antibodies targeting CTLA4 or PD1/PDL1 can overcome immune suppression across a variety of types of cancer (*34*). However, only a fraction of patients responds to immune checkpoint blockade with sustained regression. Given that the therapeutic benefit of an immune checkpoint blockade is currently limited to patients with pre-existing tumor-specific T cell responses, multifaceted approaches such as potent cancer vaccines specific to tumor neoantigens are anticipated to increase immune response in tumors treated with an immune checkpoint blockade (*35*). A study has demonstrated the nonsynonymous tumor mutation burden associated with the clinical benefit of anti–PD-1 therapy (*36*). Immune checkpoint blockades result in significant therapeutic responses to tumors with an increased mutation-associated neoantigen load. Importantly, studies on checkpoint blockades highlighted the positive correlation between the somatic mutation burden and the consequent emergence of clinically beneficial neoantigens (*37*). A recent study reported that acquired resistance to an immune checkpoint blockade can arise in association with the evolving landscape of mutations, some of which encode tumor neoantigens recognizable by T cells (*38*).

These findings imply that immune checkpoint blockades, which serve as vaccine adjuvants, are highly dependent on the ability to present diverse tumor antigens to T cells. Combining a blockade with neoantigen vaccines may improve antitumor efficacy or mitigate the development of acquired resistance. It is tempting to speculate that future studies involving the combination of T cell priming-neoantigen vaccines with T cell suppression-preventing checkpoint blockades may translate into a clinical benefit for patients with cold tumors (*39*).

6. Challenges for neoantigen vaccines

The broad range of neoantigens and their positive association with improved immune responses suggests their obvious advantages, including the possibility of mass production, easy monitoring of immune responses, and a tolerable safety profile. Nonetheless, the challenging aspects of anticancer vaccination are the identification of immunogenic neoantigens for vaccination and the difficulty of their intrinsic personalized nature: the bench-to-bedside timeframe. Therefore, the development of the accurate epitope-predicting algorithms and the optimization of efficient validation tools are currently top priorities for personalized neoantigen-based cancer immunotherapy. In addition, the development of an effective delivery strategy targeting multiple clonal neoantigens to elicit broad and potent T cell responses against tumor heterogenicity remains a challenge.

7. Conclusion

Personalized immunotherapy with neoantigens is one of the most promising approaches in cancer treatment. Precise identification of immunogenic neoantigens and an in-depth analysis of the immune-suppressive tumor microenvironment are required for an effective neoantigen-based cancer immunotherapy.

References

1. Kvistborg P, Yewdell JW. Enhancing responses to cancer immunotherapy. Science. 2018; 359:516-517.
2. Chowell D, Morris LGT, Grigg CM. *et al.* Patient HLA class I genotype influences cancer response to checkpoint blockade immunotherapy. Science. 2018; 359:582-587.
3. Kakimi K, Karasaki T, Matsushita H, Sugie T. Advances in personalized cancer immunotherapy. Breast Cancer. 2017; 24:16-24.
4. Peng M, Mo Y, Wang Y, Wu P, Zhang Y, Xiong F, Guo C, Wu X, Li Y, Li X, Li G, Xiong W, Zeng Z. Neoantigen vaccine: An emerging tumor immunotherapy. Mol Cancer.

2019; 18:128.
5. Kiyotani K, Chan HT, Nakamura Y. Immunopharmacogenomics towards personalized cancer immunotherapy targeting neoantigens. Cancer Sci. 2018; 109:542-549.
6. Sahin U, Derhovanessian E, Miller M. *et al.* Personalized RNA mutanome vaccines mobilize poly-specific therapeutic immunity against cancer. Nature. 2017; 547:222-226.
7. Ott PA, Hu Z, Keskin DB. *et al.* An immunogenic personal neoantigen vaccine for patients with melanoma. Nature. 2017; 547:217-221.
8. Schumacher TN, Schreiber RD. Neoantigens in cancer immunotherapy. Science. 2015; 348:69-74.
9. Liu XS, Mardis ER. Applications of immunogenomics to cancer. Cell. 2017; 168:600-612.
10. Chu Y, Liu Q, Wei J, Liu B. Personalized cancer neoantigen vaccines come of age. Theranostics. 2018; 8:4238-4246.
11. Rosenberg SA, Yang JC, Restifo NP. Cancer immunotherapy: Moving beyond current vaccines. Nat Med. 2004; 10:909-915.
12. Chen X, Yang J, Wang L, Liu B. Personalized neoantigen vaccination with synthetic long peptides: Recent advances and future perspectives. Theranostics. 2020; 10:6011-6023.
13. Richters MM, Xia H, Campbell KM, Gillanders WE, Griffith OL, Griffith M. Best practices for bioinformatic characterization of neoantigens for clinical utility. Genome Med. 2019; 11:56.
14. Lee CH, Yelensky R, Jooss K, Chan TA. Update on tumor neoantigens and their utility: Why it is good to be different. Trends Immunol. 2018; 39:536-548.
15. Zhang C, Ding H, Huang H, Palashati H, Miao Y, Xiong H, Lu Z. TCR repertoire intratumor heterogeneity of $CD4^+$ and $CD8^+$ T cells in centers and margins of localized lung adenocarcinomas. Int J Cancer. 2019; 144:818-827.
16. Chen DS, Mellman I. Oncology meets immunology: The cancer-immunity cycle. Immunity. 2013; 39:1-10.
17. Lawrence MS, Stojanov P, Polak P. *et al.* Mutational heterogeneity in cancer and the search for new cancer-associated genes. Nature. 2013; 499:214-218.
18. Rosenthal R, Cadieux EL, Salgado R. *et al.* Neoantigen-directed immune escape in lung cancer evolution. Nature. 2019; 567:479-485.
19. McGranahan N, Furness AJ, Rosenthal R. *et al.* Clonal neoantigens elicit T cell immunoreactivity and sensitivity to immune checkpoint blockade. Science. 2016; 351:1463-1469.
20. Spranger S. Tumor heterogeneity and tumor immunity: A chicken-and-egg problem. Trends Immunol. 2016; 37:349-351.
21. Verdegaal EM, de Miranda NF, Visser M, Harryvan T, van Buuren MM, Andersen RS, Hadrup SR, van der Minne CE, Schotte R, Spits H, Haanen JB, Kapiteijn EH, Schumacher TN, van der Burg SH. Neoantigen landscape dynamics during human melanoma-T cell interactions. Nature. 2016; 536:91-95.
22. McGranahan N, Favero F, de Bruin EC, Birkbak NJ, Szallasi Z, Swanton C. Clonal status of actionable driver events and the timing of mutational processes in cancer evolution. Sci Transl Med. 2015; 7:283ra254.
23. McGranahan N, Swanton C. Neoantigen quality, not quantity. Sci Transl Med. 2019; 11:eaax7918.
24. Borst J, Ahrends T, Babala N, Melief CJM, Kastenmuller W. $CD4^+$ T cell help in cancer immunology and immunotherapy. Nat Rev Immunol. 2018; 18:635-647.
25. Kreiter S, Vormehr M, van de Roemer N, Diken M, Lower M, Diekmann J, Boegel S, Schrors B, Vascotto F, Castle JC, Tadmor AD, Schoenberger SP, Huber C, Tureci O, Sahin U. Mutant MHC class II epitopes drive therapeutic immune responses to cancer. Nature. 2015; 520:692-696.
26. Linehan JL, Delamarre L. Teamwork by different T-cell types boosts tumour destruction by immunotherapy. Nature. 2019; 574:639-640.
27. Alspach E, Lussier DM, Miceli AP. *et al.* MHC-II neoantigens shape tumour immunity and response to immunotherapy. Nature. 2019; 574:696-701.
28. Melief CJ, van Hall T, Arens R, Ossendorp F, van der Burg SH. Therapeutic cancer vaccines. J Clin Invest. 2015; 125:3401-3412.
29. Keskin DB, Anandappa AJ, Sun J. *et al.* Neoantigen vaccine generates intratumoral T cell responses in phase Ib glioblastoma trial. Nature. 2019; 565:234-239.
30. Koshy ST, Mooney DJ. Biomaterials for enhancing anti-cancer immunity. Curr Opin Biotechnol. 2016; 40:1-8.
31. Sabado RL, Balan S, Bhardwaj N. Dendritic cell-based immunotherapy. Cell Res. 2017; 27:74-95.
32. Guo Y, Lei K, Tang L. Neoantigen vaccine delivery for personalized anticancer immunotherapy. Front Immunol. 2018; 9:1499.
33. Li L, Goedegebuure SP, Gillanders WE. Preclinical and clinical development of neoantigen vaccines. Ann Oncol. 2017; 28(suppl_12):xii11-xii17.
34. Buchbinder EI, Desai A. CTLA-4 and PD-1 Pathways: Similarities, differences, and implications of their inhibition. Am J Clin Oncol. 2016; 39:98-106.
35. Aldous AR, Dong JZ. Personalized neoantigen vaccines: A new approach to cancer immunotherapy. Bioorg Med Chem. 2018; 26:2842-2849.
36. Rizvi NA, Hellmann MD, Snyder A. *et al.* Cancer immunology. Mutational landscape determines sensitivity to PD-1 blockade in non-small cell lung cancer. Science. 2015; 348:124-128.
37. Gibney GT, Weiner LM, Atkins MB. Predictive biomarkers for checkpoint inhibitor-based immunotherapy. Lancet Oncol. 2016; 17:e542-e551.
38. Anagnostou V, Smith KN, Forde PM. *et al.* Evolution of neoantigen landscape during immune checkpoint blockade in non-small cell lung cancer. Cancer Discov. 2017; 7:264-276.
39. Galon J, Bruni D. Approaches to treat immune hot, altered and cold tumours with combination immunotherapies. Nat Rev Drug Discov. 2019; 18:197-218.

Received July 22, 2020; Revised September 1, 2020; Accepted September 4, 2020.

**Address correspondence to:*
Shun Xu, Department of Thoracic Surgery, the First Hospital of China Medical University, 155 North Nanjing Street, Heping District, Shenyang 110001, Liaoning, China.
E-mail: xushun610539@sina.com

Released online in J-STAGE as advance publication September 10, 2020.

Mini-Review

DOI: 10.5582/bst.2020.03308

CAR-expressing NK cells for cancer therapy: a new hope

Jufeng Xia (Shunichi Arai)[1,2,*], Shuichi Minamino[2], Kazuma Kuwabara[2]

[1] Graduate School of Frontier Science, The University of Tokyo, Chiba, Japan;
[2] Department of Immunology, Arai Japan Medical Institute, Tokyo, Japan.

SUMMARY Since the approval in 2017 and the amazing achievement of Kymriah and Yescarta, the number of basic researchers and clinical trials investigating the safety and efficacy of chimeric antigen receptor-expressing T cells (CAR-T cells) has been relentlessly increasing. Up to now, more than 200 clinical trials are listed on clinical trial database of NIH and the basic research is countless. However, the production of allogeneic CAR-T cells products is still expensive and has toxicity. Thus, more effort is needed to develop reliable off-the-shelf cellular therapeutic methods with safety and efficiency for the treatment of patients with cancer. As a kind of innate effector lymphocyte with potent antitumor activity, natural killer cells (NK cells) have attracted much attention. Until now, basic and clinical research has shown that chimeric antigen receptor-expressing NK cell (CAR-NK) therapy may play a significant anti-tumor role and its safety is higher than CAR-T cell therapy. In this review, we discuss advantages and shortages of employing CAR-NK cells as a novel cellular therapy against cancer.

Keywords CAR-NK, cancer, immunotherapy, clinical trial

1. Introduction

Natural killer (NK) cells, which were discovered over 45 years ago (*1*), are a type of cytotoxic lymphocyte critical to the innate immune system. NK cells launch rapid responses to virus-infected cells, acting at around 3 days after infection, and respond to tumor formation. Typically, immune cells detect the major histocompatibility complex (MHC) presented on infected cell surfaces, triggering cytokine release, causing the death of the infected cell by lysis or apoptosis. NK cells are unique, however, as they have the ability to recognize and kill stressed cells in the absence of antibodies and MHC, allowing for a much faster immune reaction. They were named "natural killers" because of the initial notion that they do not require activation to kill cells that are missing "self" markers of MHC class I. This role is especially important because harmful cells that are missing MHC I markers cannot be detected and destroyed by other immune cells, such as T lymphocyte cells (*2-4*). Previous research has suggested that lower activity of NK cells in peripheral blood is related to higher cancer risk, indicating that NK cells play a role in inhibiting cancer (*5,6*). NK cells in human peripheral blood are divided into two major subgroups: CD56bright and CD56dim NK cells. CD56bright NK cells are usually known as cytokine-producing cells with low cytotoxicity, while CD56dim NK cells are known for potential cytotoxicity (*7*). Since NK cells can identify and break up tumor cells, immunotherapy based on NK cells has been developed.

The chimeric antigen receptor (CAR) is a receptor protein that has been engineered to give immune cells the new ability to target a specific antigen protein. The receptors are chimeric because it is a fusion protein composed of an extracellular antigen binding domain, a transmembrane region, and intracellular activating signaling domains. The extracellular antigen binding domain, which is usually a single-chain variable fragment (scFv), can identify the specific antigen on the surface of tumor cells. Intracellular activating signaling domains, such as CD28, 4-1BB (CD137) and OX40, usually play a role of triggering the activation and killing effect of immune cells. CAR-expressing T cells can instantly identify the tumor surface antigen and then lyse the tumor cells. CAR-T cell immunotherapy has produced a great achievement in treating hematological tumors, such as acute lymphoblastic leukemia (ALL), chronic lymphocytic leukemia (CLL) and lymphoma. As we know, CD19 CAR-T therapy has shown complete remission rates as high as 90% in both children and adult patients with ALL (*8*). Although CAR-T cell immunotherapy has advanced rapidly, it still has several deficiencies in clinical application. CAR-T cell immunotherapy has shown a

low effect in the treatment of solid tumors (*9,10*). In addition, most CAR-T cell immunotherapies require autologous adoptive cell transfer because allogeneic T cells may cause graft-versus-host- disease (GVHD) unless addressing HLA barriers (*11,12*). Furthermore, CAR-T cell immunotherapy may lead to a few side effects, which may do harm to patients' lives, such as cytokine release syndrome. CAR-expressing NK cells have been reported to overcome the above deficiencies of CAR-T cells and showed a significant anti-tumor effect (*13,14*). In this review, we will discuss the opportunities provided by CAR-expressing NK cells and the challenges faced by CAR-NK cells.

2. Advantages of CAR-NK cell immunotherapy

Although the early success of CAR-T cell immunotherapy, especially in treating hematological tumors, the extensive clinical application of CAR-T cell immunotherapy may be limited by autologous adoptive cell transfer and various side effects, such as GVHD, neurologic toxicities and off-target effects. Based on these problems, NK cell therapy has been suggested to be superior to CAR-T cell therapy (*15*). Particularly, NK cells have a few advantages in CAR-expressing immunotherapy.

First, CAR-expressing NK cells immunotherapy would be safer than CAR-T cells immunotherapy in clinical application, and the safety of NK cells has been validated in a few clinical fields. For example, a few phase I/II trials revealed that allogeneic NK cell infusions are tolerated well and did not cause GVHD and significant toxicities (*16-18*). Hence, the NK cell is an adaptable CAR driver that is not limited to autologous cells. One of the major side effects in CAR-T cell immunotherapy are off-target effects owing to the persistence of CAR-T cells. For example, CD19-targeting CAR-T cells can lead to significant and long-term B lymphocyte deficiency due to the cellular memory effect of T lymphocytes and the challenge of mature or progenitor B lymphocytes (*19*). Conversely, CAR-NK cells have a short life duration, which causes few off-target effects. Otherwise, the kinds of cytokines produced by NK cells are much different from those produced by T lymphocytes. Active NK cells normally produce IFN-γ and Granulocyte-macrophage colony-stimulating factor (GMCSF), but CAR-T cells usually induce a cytokine storm by secreting pro-inflammatory cytokines, such as TNF-α, IL-1 and IL-6.

Second, besides inhibiting cancer cells *via* a CAR-related mechanism by which NK cells recognize the tumor surface antigen *via* scFv, NK cells can suppress cancer cells by identifying various ligands through a variety of receptors (*20,21*), such as natural cytotoxicity receptors (NKp46, NKp44, and NKp30), NKG2D and DNAM-1 (CD226). These NK cell receptors normally recognize stress-induced ligands expressed on tumor cells under the pressure of immune cells or long-lasting therapy. Moreover, NK cells induce antibody-dependent cytotoxicity by FcγRIII (CD16). Thus, CAR-expressing NK cells can inhibit cancer cells through both CAR-dependent and NK cell receptor-dependent pathways to eliminate either tumor antigen positive cancer cells or cancer cells expressing ligands for NK cell receptors. The clinical trials have suggested that CAR-T cells can't eliminate cancer cells which are highly heterogeneous (*22*), but CAR-expressing NK cells could be able to effectively kill residual tumor cells that may change their phenotypes after long-term treatment.

Finally, NK cells are abundant in clinical samples and can be produced from peripheral blood (PB), umbilical cord blood (UCB), human embryonic stem cells (hESCs), induced pluripotent stem cells (iPSCs), and even NK-92 cell lines. NK-92 cells provide a homogeneous cell population and can be easily expanded under proper culture conditions for extensive clinical applications (*23*). But, they must be irradiated before infusion owing to their tumor cell line origin. Conversely, active PB-NK cells express a broad range of receptors and could be utilized without irradiation, which enables them to be generated *in vivo*. NK cells derived from iPSCs or hESCs combine the merits of PB-NK and NK-92 cells for they show a phenotype similarity to PB-NK cells and are a homogeneous population. More importantly, CAR can be easily expressed in hESC- and/or iPSC-derived NK cells by employing non-viral transgenic methods (*24*).

3. Current status of CAR-NK cell immunotherapy

3.1. Hematologic cancer

Preclinical research has suggested that CD19-CAR-NK cells have high efficiency against hematological cancers and are easy to manufacture, which is a tremendous advance compared to current CAR-T cell immunotherapy (*25,26*). Clinical trials of CD19-CAR-T cell immunotherapy have revealed high complete responses in patients with hematological cancers (*27,28*). CD19-CAR modified NK cells are expected to show a better anti-tumor effect owing to the merits of CAR-NK cell immunotherapy in hematological cancers. Clinical trials have suggested that CD19-CAR-expressing NK cells could be a good therapeutic method for patients suffering from lymphoid malignancies (*29*). Besides CD19, CAR-NK cell clinical studies for lymphoma and leukemia also target CD7 (NCT02742727) and CD33 (NCT02944162). Although CAR-T cell immunotherapy has undergone a large number of clinical trials for hematological cancers, only several clinical CAR-NK cell therapies against hematological malignancies are under way (Table 1).

Tabel 1. Clinical trials of CAR-NK cell immunotherapy against cancers

Cancers	Targets	Origin	Phase	*Ref.*
Leukemia and lymphoma	CD19	Umbilical cord blood	I/II	NCT03579927
Leukemia and lymphoma	CD19	Umbilical cord blood	I/II	NCT03056339
Leukemia and lymphoma	CD19	NK-92	I/II	NCT02892695
Leukemia and lymphoma	CD7	NK-92	I/II	NCT02742727
Acute lymphocytic leukemia	CD19	Haploidentical donor NK cells	II	NCT01974479
Acute lymphocytic leukemia	CD19	Expanded donor NK cells	I	NCT00995137
Acute myeloid leukemia	CD33	NK-92	I/II	NCT02944162
Solid tumors	MUC1	Unknown	I/II	NCT02839954
Solid tumors	NKG2D ligands	Autologous or allogeneic NK cells	I	NCT03415100
Glioblastoma	HER2	NK-92	I	NCT03383978
Non-small cell lung cancer	Unknown	CCCR-NK-92	I	NCT03656705

Ref. resource: clinicaltrials.gov.

3.2. Solid tumors

In previous studies, it has been suggested that the NK-92 cell line can be effectively transduced with various CARs against different cancers for experiments in preclinical research and currently in clinical trials. CAR-NK-92 cells were extremely successful in targeting tumor cells and exerting anti-tumor cytotoxicity against several resistant solid tumors, such as epithelial cancers, by targeting human epidermal growth factor receptors (HER1, HER2), neuroectodermal tumors by GD2, brain tumors by HER1 and HER2, and ovarian cancers also by HER2 (*13,30-32*). But there are several limitations for using this cell line. For transformed NK-92 cell lines from undifferentiated NK-cell precursors (*33-35*), they are short of antibody-dependent cell-mediated cytotoxicity (ADCC)-inducing CD16 receptors, which share a similar situation with other NK cell lines (*36*). As a result, these NK cells fail to recognize tumor-targeted antigens by ADCC mechanisms. To supply these gaps, NK-92 cells were genetically modified to express the high-affinity V158 variant of the Fc-gamma receptor (FcγRIIIa/CD16a, termed haNKTM) and to produce endogenous, intracellularly retained IL-2 (*37,38*). In a phase I clinical trial underway it will be evaluated for safety and efficacy of haNKTM cells in treatment of patients with unresectable and locally advanced or metastatic solid tumors (NCT03027128; Table 1).

Another deficiency is the absence of some killer-cell immunoglobulin-like receptors (KIRs), with the absence of KIR2DL4 (CD158d) on the surface of NK-92 cells, which may lead to potential stimulation of GVHD (*39-41*). Therefore, attention should be paid that activated CAR-expressing NK-92 cells must be irradiated with at least 10 Gy before infusion into patients with cancers, resulting in a lower cell persistence and a loss of effector-mediated anti-tumor functions (*41*). Despite these deficiencies, preclinical research has suggested that CAR-expressing NK-92 cells could target a broad range of cancer antigens (*42,43*). Up to now, only a few clinical trials using CAR-expressing NK cells against Hematologic cancer and particularly against solid tumors have been launched (Table 1). Lately, a phase I/II trial has aimed to validate the safety and efficacy of CAR-NK cells in patients with overexpressed MUC1-positive solid tumors, particularly carcinomas (hepatocellular, pancreatic, breast, colorectal, gastric), non-small cell lung cancer (*31*), and glioblastoma (NCT02839954; Table 1).

4. Barriers to clinical application of CAR-NK cell immunotherapy

4.1. Mass production of NK cells

The first barrier to CAR-NK cell immunotherapy is the expansion of NK cells *in vitro*. The number of NK cells from a single-donor is insufficient for therapy, which makes the expansion and activation of NK cells very critical (*44*). This production process normally takes two to three weeks to culture NK cells with certain cytokines (IL-2 or in combination with IL-15 or anti-CD3 mAb) (*45*). The combination of IL-2 and IL-21 were also utilized to improve NK cells proliferation (*46,47*). The studies suggested that the combination of IL-2 and IL-21 showed a higher inhibitive effect on proliferation of cancer cells than employing IL-2 alone (*46,47*). In spite of irradiated K562-mb15-4-1BBL cells used as feeders could improve growth of cells in the production process of NK cells proliferation, the availability of donor cell number remains a barrier (*48*). In addition, T cells must be entirely eliminated to protect against GVHD. Achieving sufficient NK cells is critical for treatment of patients with cancers. However, owing to the production process limitations of expanding to a great number of cells, it is difficult to broadly perform in clinical applications.

4.2. The methods to transduce CAR into NK cells

For development of CAR-NK cell immunotherapy, it will be critical to choose the proper method to transduce CAR into NK cells. So far, viral vectors and non-viral

vectors have both been employed to transfer CAR.

Transfection vectors, including viral vectors and non-viral vectors, are broadly utilized in the production of CAR-NK cells because they can stably integrate into the human genome. Although the transfection efficiency of retroviral vectors is high, it may give rise to insertional mutagenesis, carcinogenesis and other adverse effects (*30*). Although lentiviral vectors show a lower incidence rate of insertion mutagenesis, their transfection efficiency is as low as 20% for NK cells from peripheral blood (*45*). The transfection efficiency of lentivirus vectors is high enough for NK cells from cord blood (*49*). However, the transfection efficiency of lentivirus for NK cells from peripheral blood has room for improvement. Previous research has suggested that suppressing the intracellular antiviral system may increase lentivirus transfection level of NK cells, providing an affordable and safe method for CAR transduction into NK cells (*50*).

Transfection with mRNA for CAR-NK cells has also been considered to be a practical and safe transduction method. Research has revealed that receptor expression level 24 hours after electroporation with the mRNA method was more than 80% and NK cells transfected with mRNA showed obvious cytotoxicity in a xenograft cancer model (*48*). Lately, a research result suggested that "on-target off-tumor" toxicity, which is an important limiting factor for the clinical application of CAR-modified immunotherapies, may be effectively avoided by transfection with mRNA (*51*). However, the antitumor effect of CAR-NK cells transfected with mRNA by electroporation method will be transitory because the expression level of CARs will last no more than three days (*52*).

5. Conclusion and outlook

Both cord blood and peripheral blood-derived CAR-NK cells and CAR-NK-92 cell line are comprehensive medicinal products combining critical characteristics: they are genetically modified and employed as cellular immunotherapy. The complete production process following Good Manufacturing Practice (GMP) requires ten days to several weeks using Teflon bags, flasks, continuous-flow devices, stirred-tank bioreactors and the Miltenyi's Prodigy system (*44*). Compared to CAR-T cells, CAR-NK cells have the merit of "off-the-shelf" production, but still are confronted with several challenges. These challenges include improvement in cell expansion, making the activation of cytotoxicity more efficient, and finally finding the best reconstruction methods for NK cells (*53*).

Although CAR-NK cell immunotherapy has been proved to be effective for inhibiting cancers, the long-term anti-cancer effect is still ambiguous. The combination therapy provides a novel prospect for CAR-based cell immunotherapy. In a few previous studies, researchers suggested chemotherapy may also improve the efficiency of CAR-NK cell immunotherapy. Chemotherapeutic drugs could not only eliminate the existing cell populations to establish new niches for the proliferation of NK cells, but also can lead to a genotoxic stress response to increase tumor cell sensitivity to NK cells (*54*). Clinical trials have revealed that the chemotherapeutic drugs could remarkably enhance the tumor inhibitive effect of CAR-NK cells (*55*). In a preclinical study, it has been reported that the combination of CAR-T cell immunotherapy and radiotherapy shows a synergistic effect against glioblastoma (*56*). However, the synergistic effects of CAR-NK cell immunotherapy and radiotherapy remain unclear (*57*). Thus, further research is needed to better understand the relationship between the two therapeutic methods. Moreover, the CRISPR/Cas9 technique has become an increasingly popular gene editing tool due to its advantages in editing the genomes of multiple organisms precisely (*58*). A few studies have suggested that editing a CAR by using the CRISPR/Cas9 technique could cause homogeneous CAR expression and improve cytotoxicity efficiency (*59*). If so, then the CRISPR/CAS9 technique may have the capacity to improve the efficiency and safety of CAR-NK cells by editing genes of primary NK cells and manufacturing stably transduced NK cells.

References

1. Kiessling R, Klein E, Wigzell H. "Natural" killer cells in the mouse. I. cytotoxic cells with specificity for mouse moloney leukemia cells. Specificity and distribution according to genotype. Eur J Immunol. 1975; 5:112-117.
2. Farag SS, Caligiuri MA. Human natural killer cell development and biology. Blood Rev. 2006; 20:123-137.
3. Konjević G, Vuletić A, Mirjačić Martinović K. Natural killer cell receptors: alterations and therapeutic targeting in malignancies. Immunol Res. 2016; 64: 25-35.
4. Benson DM Jr, Caligiuri MA. Killer immunoglobulin-like receptors and tumor immunity. Cancer Immunol Res. 2014; 2:99-104.
5. Imai K, Matsuyama S, Miyake S, Suga K, Nakachi K. Natural cytotoxic activity of peripheral-blood lymphocytes and cancer incidence: an 11-year follow-up study of a general population. Lancet. 2000; 356:1795-1799.
6. Orange JS, Ballas ZK. Natural killer cells in human health and disease. Clin Immunol. 2006; 118:1-10.
7. Björkström NK, Ljunggren HG, Michaëlsson J. Emerging insights into natural killer cells in human peripheral tissues. Nat Rev Immunol. 2016; 16:310-320.
8. Maude SL, Frey N, Shaw PA, *et al.* Chimeric antigen receptor T cells for sustained remissions in leukemia. N Engl J Med. 2014; 371:1507-1517.
9. Feng KC, Guo YL, Dai HR, Wang Y, Li X, Jia HJ, Han WD. Chimeric antigen receptor-modified T cells for the immunotherapy of patients with EGFR-expressing advanced relapsed/refractory non-small cell lung cancer. Sci China Life Sci. 2016; 59:468-479.
10. Gilham DE, Debets R, Pule M, Hawkins RE, Abken H. CAR-T cells and solid tumors: tuning T cells to challenge

an inveterate foe. Trends Mol Med. 2012; 18:377-384.
11. Kalaitsidou M, Kueberuwa G, Schütt A, Gilham DE. CAR T-cell therapy: Toxicity and the relevance of preclinical models. Immunotherapy. 2015; 7:487-497.
12. Qasim W. Allogeneic CAR T cell therapies for leukemia. Am J Hematol. 2019; 94:S50-S54.
13. Zhang C, Oberoi P, Oelsner S, Waldmann A, Lindner A, Tonn T, Wels WS. Chimeric antigen receptor-engineered NK-92 cells: an off-the-shelf cellular therapeutic for targeted elimination of cancer cells and induction of protective antitumor immunity. Front Immunol. 2017; 8:533.
14. Boissel L, Betancur-Boissel M, Lu W, Krause DS, Van Etten RA, Wels WS, Klingemann H. Retargeting NK-92 cells by means of CD19- and CD20-specific chimeric antigen receptors compares favorably with antibody-dependent cellular cytotoxicity. Oncoimmunology. 2013; 2:e26527.
15. Klingemann H. Are natural killer cells superior CAR drivers? Oncoimmunology. 2014; 3:e28147.
16. Miller JS, Soignier Y, Panoskaltsis-Mortari A, *et al.* Successful adoptive transfer and *in vivo* expansion of human haploidentical NK cells in patients with cancer. Blood. 2005; 105:3051-3057.
17. Rubnitz JE, Inaba H, Ribeiro RC, Pounds S, Rooney B, Bell T, Pui CH, Leung W. NKAML: a pilot study to determine the safety and feasibility of haploidentical natural killer cell transplantation in childhood acute myeloid leukemia. J Clin Oncol. 2010; 28:955-999.
18. Shaffer B, Le Luduec JB, Forlenza C, Jakubowski AA, Perales MA, Young JW, Hsu KC. Phase II study of haploidentical natural killer cell infusion for treatment of relapsed or persistent myeloid malignancies following allogeneic hematopoietic cell transplantation. Biol Blood Marrow Transplant. 2016; 22:705-709.
19. Kalos M, Levine BL, Porter DL, Katz S, Grupp SA, Bagg A, June CH. T cells with chimeric antigen receptors have potent antitumor effects and can establish memory in patients with advanced leukemia. Sci Transl Med. 2011; 3:95ra73.
20. Sun C, Sun HY, Zhang C, Tian ZG. NK cell receptor imbalance and NK cell dysfunction in HBV infection and hepatocellular carcinoma. Cell Mol Immunol. 2015; 12:292-302.
21. Sun C, Sun HY, Xiao WH, Zhang C, Tian ZG. Natural killer cell dysfunction in hepatocellular carcinoma and NK cell-based immunotherapy. Acta Pharmacol Sin. 2015; 36:1191-1199.
22. Maude SL, Frey N, Shaw PA, *et al.* Chimeric antigen receptor T cells for sustained remissions in leukemia. N Engl J Med. 2014; 371:1507-1517.
23. Tam YK, Martinson JA, Doligosa K, Klingemann K. *Ex vivo* expansion of the highly cytotoxic human natural killer-92 cell-line under current good manufacturing practice conditions for clinical adoptive cellular immunotherapy. Cytotherapy. 2003; 5:259-272.
24. Ni ZY, Knorr DA, Bendzick L, Allred J, Kaufman DS. Expression of chimeric receptor CD4ζ by natural killer cells derived from human pluripotent stem cells improves *in vitro* activity but does not enhance suppression of HIV infection *in vivo*. Stem Cells. 2014; 32:1021-1031.
25. Liu E, Tong Y, Dotti G, *et al.* Cord blood NK cells engineered to express IL-15 and a CD19-targeted CAR show long-term persistence and potent antitumor activity. Leukemia. 2018; 32:520-531.
26. Oelsner S, Friede ME, Zhang CC, Wagner J, Badura S, Bader P, Ullrich E, Ottmann OG, Klingemann H, Tonn T, Wels WS. Continuously expanding CAR NK-92 cells display selective cytotoxicity against B-cell leukemia and lymphoma. Cytotherapy. 2017; 19:235-249.
27. Levine BL. Performance-enhancing drugs: design and production of redirected chimeric antigen receptor (CAR) T cells. Cancer Gene Ther. 2015; 22:79-84.
28. Weiland J, Elder A, Forster V, Heidenreich O, Koschmieder S, Vormoor J. CD19: a multifunctional immunological target molecule and its implications for blineage acute lymphoblastic leukemia. Pediatr Blood Cancer. 2015; 62:1144-1148.
29. Romanski A, Uherek C, Bug G, Seifried E, Klingemann H, Wels WS, Ottmann OG, Tonn T. CD19-CAR engineered NK-92 cells are sufficient to overcome NK cell resistance in B-cell malignancies. J Cell Mol Med. 2016; 20:1287-1294.
30. Hu Y, Tian ZG, Zhang C. Chimeric antigen receptor (CAR)-transduced natural killer cells in tumor immunotherapy. Acta Pharmacol Sin. 2018; 39:167-176.
31. Zotto GD, Marcenaro E, Vacca P, Sivori S, Pende D, Chiesa MD, Moretta F, Ingegnere T, Mingari MC, Moretta A, Moretta L. Markers and function of human NK cells in normal and pathological conditions. Cytometry B Clin Cytom. 2017; 92:100-114.
32. Schönfeld K, Sahm C, Zhang CC, Naundorf S, Brendel C, Odendahl M, Nowakowska P, Bönig H, Köhl U, Kloess S, Köhler S, Holtgreve-Grez H, Jauch A, Schmidt M, Schubert R. Selective inhibition of tumor growth by clonal NK cells expressing an ErbB2/HER2-specific chimeric antigen receptor. Mol Ther. 2015; 23:330-338.
33. Tonn T, Becker S, Esser R, Schwabe D, Seifried E. Cellular immunotherapy of malignancies using the clonal natural killer cell line NK-92. J Hematother Stem Cell Res. 2001; 10:535-544.
34. Maki G, Klingemann HG, Martinson JA, Tam YK. Factors regulating the cytotoxic activity of the human natural killer cell line, NK-92. J Hematother Stem Cell Res. 2001; 10:369-383.
35. Gong JH, Maki G, Klingemann HG. Characterization of a human cell line (NK-92) with phenotypical and functional characteristics of activated natural killer cells. Leukemia. 1994; 8:652-658.
36. Matsuo Y, Drexler HG. Immunoprofiling of cell lines derived from natural killer-cell and natural killer-like T-cell leukemia-lymphoma. Leuk Res. 2003; 27:935-945.
37. Jochems C, Hodge JW, Fantini M, Fujii R, Morillon YM, Greiner JW, Padget MR, Tritsch ST, Tsang KY, Campbell KS, Klingemann H, Boissel L, Rabizadeh S, Soon-Shiong P, Schlom J. An NK cell line (haNK) expressing high levels of granzyme and engineered to express the high affinity CD16 allele. Oncotarget. 2016; 7:86359-86373.
38. Klingemann H, Boissel L, Toneguzzo F. Natural killer cells for immunotherapy - advantages of the NK-92 cell line over blood NK cells. Front Immunol. 2016; 7:91.
39. Cooley S, Xiao F, Pitt M, Gleason M, McCullar V, Bergemann TL, McQueen KL, Guethlein LA, Parham P, Miller JS. A subpopulation of human peripheral blood NK cells that lacks inhibitory receptors for self-MHC is developmentally immature. Blood. 2007; 110:578-586.
40. Faure M, Long EO. KIR2DL4 (CD158d), an NK cell-activating receptor with inhibitory potential. J Immunol. 2002; 168:6208-6214.
41. Suck G, Odendahl M, Nowakowska P, Seidl C, Wels

WS, Klingemann HG, Tonn T. NK-92: an 'off-the-shelf therapeutic' for adoptive natural killer cell-based cancer immunotherapy. Cancer Immunol Immunother. 2016; 65:485-492.
42. Boissel L, Betancur M, Wels WS, Tuncer H, Klingemann H. Transfection with mRNA for CD19 specific chimeric antigen receptor restores NK cell mediated killing of CLL cells. Leuk Res. 2009; 33:1255-1259.
43. Uherek C, Tonn T, Uherek B, Becker B, Schnierle B, Klingemann HG, Wels W. Retargeting of natural killer-cell cytolytic activity to ErbB2-expressing cancer cells results in efficient and selective tumor cell destruction. Blood. 2002; 100:1265-1273.
44. Klingemann H. Challenges of cancer therapy with natural killer cells. Cytotherapy. 2015; 17:245-249.
45. Shimasaki N, Coustan-Smith E, Kamiya T, Campana D. Expanded and armed natural killer cells for cancer treatment. Cytotherapy. 2016; 18:1422-1434.
46. Oberschmidt O, Morgan M, Huppert V, Kessler J, Gardlowski T, Matthies N, Aleksandrova K, Arseniev L, Schambach A, Koehl U, Kloess S. Development of automated separation, expansion, and quality control protocols for clinical-scale manufacturing of primary human NK cells and alpharetroviral chimeric antigen receptor engineering. Hum Gene Ther Methods. 2019; 30:102-120.
47. Granzin M, Stojanovic A, Miller M, Childs R, Huppert V, Cerwenka A. Highly efficient IL-21 and feeder cell-driven *ex vivo* expansion of human NK cells with therapeutic activity in a Xenograft mouse model of melanoma. Oncoimmunology. 2016; 5:e1219007.
48. Shimasaki N, Fujisaki H, Cho D, Masselli M, Lockey T, Eldridge P, Leung W, Campana D. A clinically adaptable method to enhance the cytotoxicity of natural killer cells against B-cell malignancies. Cytotherapy. 2012; 14:830-840.
49. Boissel L, Betancur M, Lu WQ, Wels WS, Marino T, Van Etten RA, KlingemannH. Comparison of mRNA and lentiviral based transfection of natural killer cells with chimeric antigen receptors recognizing lymphoid antigens. Leuk Lymphoma. 2012; 53: 958-965.
50. Sutlu T, Nyström S, Gilljam M, Stellan B, Applequist SE, Alici E. Inhibition of intracellular antiviral defense mechanisms augments lentiviral transduction of human natural killer cells: implications for gene therapy. Hum Gene Ther. 2012; 23:1090-1100.
51. Hung CF, Xu XQ, Li LH, Ma Y, Jin Q, Viley A, Allen C, Natarajan P, Shivakumar R, Peshwa MV, Emens LA. Development of anti-human mesothelin-targeted chimeric antigen receptor messenger RNA-transfected peripheral blood lymphocytes for ovarian cancer therapy. Hum Gene Ther. 2018; 29:614-625.
52. Li L, Liu LN, Feller S, Allen C, Shivakumar R, Fratantoni J, Wolfraim LA, Fujisaki H, Campana D, Chopas N, Dzekunov S, Peshwa M. Expression of chimeric antigen receptors in natural killer cells with a regulatory-compliant non-viral method. Cancer Gene Ther. 2010; 17:147-154.
53. Oberschmidt O, Kloess S, Koehl U. Redirected primary human chimeric antigen receptor natural killer cells as an "off-the-shelf immunotherapy" for improvement in cancer treatment. Front Immunol. 2017; 8:654.
54. Fine JH, Chen P, Mesci A, Allan DSJ, Gasser S, Raulet DH, Carlyle JR. Chemotherapy-induced genotoxic stress promotes sensitivity to natural killer cell cytotoxicity by enabling missing-self recognition. Cancer Res. 2010;70: 7102-7113.
55. Klapdor R, Wang S, Hacker U, Büning H, Morgan M, Dörk T, Hillemanns P, Schambach A. Improved killing of ovarian cancer stem cells by combining a novel chimeric antigen receptor-based immunotherapy and chemotherapy. Hum Gene Ther. 2017; 28:886-896.
56. Weiss W, Weller M, Guckenberger M, Sentman CL, Roth P. NKG2D-based CAR T cells and radiotherapy exert synergistic efficacy in glioblastoma. Cancer Res. 2018; 78:1031-1043.
57. Seyedin SN, Schoenhals JE, Lee DA, *et al.* Strategies for combining immunotherapy with radiation for anticancer therapy. Immunotherapy. 2015; 7:967-980.
58. Zhang F, Wen Y, Guo X. CRISPR/Cas9 for genome editing: progress, implications and challenges. Hum Mol Genet. 2014; 23:R40-46.
59. Eyquem J, Mansilla-Soto J, Giavridis T, van der Stegen SJC, Hamieh M, Cunanan KM, Odak A, Gönen M, Sadelain M. Targeting a CAR to the TRAC locus with CRISPR/Cas9 enhances tumour rejection. Nature. 2017; 543:113-117.

Received July 6, 2020; Revised August 27, 2020; Accepted September 3, 2020.

**Address correspondence to:*
Jufeng Xia, Graduate School of Frontier Science, The University of Tokyo, 5 Chome-1-5 Kashiwanoha, Kashiwa, Chiba 277-8561, Japan.
E-mail: xia-tky@umin.ac.jp

Released online in J-STAGE as advance publication September 6, 2020.

Original Article

DOI: 10.5582/bst.2020.03321

Transplantation of neural stem cells encapsulated in hydrogels improve functional recovery in a cauda equina lesion model

Zhiyi Fu[§], Huidong Wang[§], Yujie Wu[*], Tong Zhu[*]

Shanghai Key Laboratory of Orthopaedic Implants, Department of Orthopaedic Surgery, Shanghai Ninth People's Hospital, Shanghai Jiao Tong University School of Medicine, Shanghai, China.

SUMMARY This study explored the therapeutic effects of transplantation of neural stem cells (NSCs) encapsulated in hydrogels in a cauda equina lesion model. NSCs were isolated from neonatal dorsal root ganglion (nDRG) and cultured in three-dimensional porous hydrogel scaffolds. Immunohistochemistry, transmission electron microscopy and TUNEL assay were performed to detect the differentiation capability, ultrastructural and pathological changes, and apoptosis of NSCs. Furthermore, the functional recovery of sensorimotor reflexes was determined using the tail-flick test. NSCs derived from DRG were able to proliferate to form neurospheres and mainly differentiate into oligodendrocytes in the three-dimensional hydrogel culture system. After transplantation of NSCs encapsulated in hydrogels, NSCs differentiated into oligodendrocytes, neurons or astrocytes *in vivo*. Moreover, NSCs engrafted on the hydrogels decreased apoptosis and alleviated the ultrastructural and pathological changes of injured cauda equina. Behavioral analysis showed that transplanted hydrogel-encapsulated NSCs decreased the tail-flick latency and showed a neuroprotective role on injured cauda equina. Our results indicate transplantation of hydrogel-encapsulated NSCs promotes stem cell differentiation into oligodendrocytes, neurons or astrocytes and contributes to the functional recovery of injured cauda equina, suggesting that NSCs encapsulated in hydrogels may be applied for the treatment of cauda equina injury.

Keywords Cauda equina lesion, neural stem cells, neonatal dorsal root ganglion, Hydrogel

1. Introduction

Cauda equina syndrome (CES) is a neurological disease, which is usually caused by central lumbar disc herniation. The consequences of CES, such as neuropathic pain, lower extremity dysfunction, and sexual dysfunction adversely affect patients' life quality to various degrees, ranging from physical to mental conditions, and cause enormous economic loss to society. Although this disease has a low incidence in the population, ranging from 1:33,000 to 1:100,000 inhabitants, its sequelae still generate high public healthcare costs (*1*). Current treatment strategies include application of corticosteroid, surgical stabilization and decompression, although effective but with unsatisfied therapeutic efficacy (*2,3*). Surgery and neurotrophic drugs available for CES are limited because of the poor self-repair ability of nerve tissue, especially those in the central nervous system, the therapeutic effects of surgery and neurotrophic drugs on cauda equina injury-induced CES is limited.

Neural stem cells (NSCs) can make copies of themselves and generate different mature cell types. They are promising candidate cells for neural transplantation treatment of neurological disorders, such as brain trauma, spinal cord injury, and peripheral nerve injury (*4-6*). Many studies indicate that stem cells foster host axons to grow into the grafted spinal cord (*7-9*). In addition, induced pluripotent stem cells differentiate into astrocytes, neurons and oligodendrocytes and further improve functional recovery after spinal cord injury (*10*). Nevertheless, application of stem cell transplantation therapy is limited by poor cell survival at the injury site. Thus, development of novel approaches to maintain neural stem cell viability is important to achieve ideal therapeutic outcomes.

Recently, tissue engineering has been developed that could provide solutions to the problem of stem cell death during transplantation (*11*). Biopolymer hydrogels are designed to promote stem cell survival after cerebral transplantation, exhibiting a promising therapeutic role in central nervous system damage. One type of ionic hydrogel commonly used is made from polypeptide nanomaterials, which can be excited by Na^+ and K^+ to form solid or semi-solid (half-liquid) consolidated gel

products. Therefore, the gelation process of hydrogels can be initiated rapidly in the damaged part and used for damage repair. As previously reported by Singh *et al.* (*12*), neural stem cells derived from adult dorsal root ganglia not only retain multi-differentiation potential, but also tend to differentiate into sensory neurons after transplantation, supporting the premise that dorsal root ganglion neural stem cells (DRG NSCs) may be useful for repair of damaged cauda equina.

The nerve underneath lumbar 5-6 in rats (also called cauda equine nerve) is the sensorimotor nerve responsible for the tail of the rat. Therefore, in the present study, a rat CES model was established by application of compression to the site and NSCs were isolated from neonatal dorsal root ganglion (nDRG), encapsulated in three-dimensional porous hydrogel scaffolds, and used to repair damaged cauda equina in a rat model of CES.

2. Materials and Methods

2.1. Animals

Male Sprague-Dawley rats weighing 200-250 g and aged 6-8 weeks were purchased from the Animal Center of the Second Military Medical University. The surgical interventions for animal experiments were approved by the Ethical Committee of the Shanghai Jiao Tong University School of Medicine, and the animals were cared for in accordance with the Guide for the Care and Use of Laboratory Animals after surgery. This study was conducted according to the guidelines laid down in the Declaration of Helsinki.

2.2. Culture of DRG-NSCs

DRG were dissected from postnatal day 2 rats, mechanically dissociated in Hank's balanced saline solution, pH 7.4, and seeded in Dulbecco's modified Eagle's medium (DMEM)/F12 (Invitrogen) supplemented with 2% B27, 10 ng/mL epidermal growth factor (EGF), and 10 ng/mL basic fibroblast growth factor (bFGF). NSCs were cultured in a 6-well culture plate at a density of 50-100 cells/μL with 5% CO_2 at 37°C. The medium was changed 2-3 times a week. The dissociated DRG cells formed clusters or neurospheres within 72 h. The neurospheres and culture medium in the whole culture plate were transferred to a 15 mL centrifuge tube, centrifuged at 200 g for 5 min, and the supernatants were discarded. 2 mL trypsin was added to the cell preparation. Pasteur pipettes were used to gently blow the neurospheres, place them at 37°C for 20 min, then centrifugation, and the supernatant was discarded. The preparation was suspended in a small amount of medium, gently beaten and mixed, counted, then laid in a 6-well plate, and each hole had about 200-300 neurospheres (*13*). After 3 generations of subcloning, the NSCs were derived from the neurospheres.

2.3. Transfection of NSCs with GFP

Neurospheres were digested into single cells with trypsin (#0458, Genebase, Shanghai, China) and inoculated into 2-well plates (200,000/250 μL). Lenti-virus-GFP was dissolved and diluted to a suitable MOI (final MOI = 100) with complete culture medium. A volume of 10 μg/mL of Polybrene (working concentration: 5 μg/mL) was added to promote virus infection. The virus solution (250 μL) was added to the plate and cultured in a 37 °C incubator for 24 h, followed by the cells being transferred into normal virus-free medium for further culture.

2.4. Hydrogel preparation

3D Cell Culture Hydrogels were purchased from Beaver Nano-Technologies Co., Ltd, (China). The original solution of the hydrogel was pre-treated in an ultrasonic water bath for 30 min at room temperature to reduce the viscosity. Half-liquid or solid hydrogels were formed according to manufacturer's protocol. The NSCs suspension was centrifuged at low speed to remove the supernatant. 5 mL of 10% sterile sucrose solution was added to the collected cells to resuspend them. The cell suspension was centrifuged again, and the supernatant was discarded to remove the remaining ionic components in the protocell preparation. Then, the cells were resuspended with 50 μL 10% sterile sucrose solution to prepare the salt ion free isotonic cell suspension. The 50 μL pretreatment hydrogel solution was mixed lightly with 50 μL NSCs suspension. A volume of 100 μL phosphate buffer saline was slightly added to the upper layer of the mixture. Then, the PBS layer and the hydrogel layer were mixed evenly with a pipette, and finally 200 μL hydrogel cell mixture was obtained. The final concentration of the hydrogel was 0.25%.

2.5. Model establishment and NSC transplantation

Forty-eight SD rats were randomly divided into 3 groups: Sham, CES model+Hydrogel and NSCs+Hydrogel, n = 16 in each group. For the latter two groups, animals were anesthetized with chloral hydrate before laminectomy was performed at lumbar 4. A silicone band (10 mm long, 1 mm wide, and 1 mm thick) was placed under the laminae of the L5-6 vertebra to produce the CES animal model (*14,15*). A sham operation was performed with a simple laminectomy but without contusion injury. The NSCs+Hydrogel group was subjected to transplantation of NSCs when the silicone band was removed 7 days after the compression injury, and the rats were intrathecally injected with 12 μL 0.25% hydrogels containing approximately 1,000,000 NSCs (transfected with lentivirus vectors carrying GFP) using a micropulled pipette connected to a Hamilton syringe (20 μL, Envta Technology, China).

The model+Hydrogel group was subjected to 12 μL 0.25% hydrogel containing no NSCs and injected into the subarachnoid space. GFP-transfected cells were observed under a microscope (Olympus, Japan).

2.6. Immunohistochemistry assay

The rats were perfused with 4% paraformaldehyde as the fixative. The cauda equina was then extracted, placed in EDTA solution, and heated in an oven for antigen retrieval. Then, 15 μm thick sections of the cauda equina around the lesion site were prepared longitudinally. The tissue sections were permeabilized with 0.2% Triton X-100 and blocked in blocking solution for 1 hour at room temperature. In order to identify the results of neural stem cell differentiation, the sections were incubated with primary antibodies against O4 (#MAB1326, R&D, USA), βIII-tubulin (#5568, CST, USA), glial fibrillary acidic protein (GFAP) (#12389, CST, USA), S100 (#ab52642, ABcam, Cambridge, UK) overnight at 4°C followed by incubation with secondary antibodies for 1 hour at 37°C after rinsing with PBS. The slices were stained with Hoechst for 10 min and images were photographed using inverted fluorescence Leica DMi8 microscopy (Germany). The staining of NSCs *in vitro* was the same as the above method.

2.7. Ultrastructural imaging

For transmission electron microscopic (TEM) studies, the sections were fractured with liquid nitrogen and quenched in hydrogen peroxide solution. After rinsing in PBS, the sections were prepared for ultra-thin sectioning. Tissue sections were fixed in osmium tetroxide, dehydrated in ethanol, and embedded in resin. All samples were observed under TEM (H-9500, Hitachi, Japan).

2.8. TdT-mediated dUTP-biotin nick end labeling (TUNEL) staining

Apoptosis of cauda equina were measured using a TUNEL detection kit according to the manufacturer's instructions (Sigma, USA). In brief, paraffin-embedded tissue sections (4-mm-thick) were dewaxed, rehydrated, and incubated with reaction mixture of terminal deoxynucleotidyl transferase for 1 h. After rinsing in PBS, the sections were incubated with biotinylated antibody and ABC complex, and photographed using a light microscope (Zeiss, Germany) equipped with a digital camera.

2.9. Behavioral analysis

For the tail-flick test, the rats were immobilized for 20 mins before the test by using a cylinder tool provided together with a tail flick test instrument (SW-200, Techman Soft, China), and the tail was placed over a slit. A beam of light from a projection lamp (voltage of 18.5 V) was focused on the tail skin at the junction between the middle and distal 1/3 of the tail. The latency to respond was recorded with a maximal 15 s radiant heat stimulus (*13*).

2.10. Statistical analysis

Experimental data are presented as mean ± SD. One-Way ANOVA was used for comparison of different groups. Results were considered statistically significant when the *P* value was less than 0.05.

3. Results

3.1. Characterization of NSCs in hydrogel scaffolds

NSCs were isolated from the neonatal rat DRG and cultured in proliferation culture medium for different days. We observed that many cells floated in the medium and formed neurospheres (Figure 1A). Then, NSCs were successfully grown in 0.25% hydrogels, with neurospheres similarly observed (Figure 1B). After 7 days of differentiation in vitro, the neurospheres of neural progenitor cells (without GFP) attached to the hydrogel scaffolds, differentiated into different types of cells and were detected as previously described by Fu *et al.* (*13*). Consistent with their results, our results suggested most of the NSCs differentiated into oligodendrocytes (O4+), and only very few cells differentiated into Schwann cells (S100+), neurons (βIII-tubulin+) and astrocytes (GFAP+).

3.2. Transplantation of NSCs following in the injured cauda equina

To more easily track cells, we transfected NSCs with lentivirus vectors carrying green fluorescent protein (GFP) and cultured the cells on differentiation medium. Transfected NSCs displaying green fluorescence are shown in Figure 1C. Next, we successfully established the rat model of cauda equina injury as verified by the tail-flick test (Figure 2) and transplanted hydrogel-encapsulated NSCs (Figure 3A and 3B). To detect the viability of transplanted NSCs in the cauda equina, frozen sections were imaged by confocal microscopy after 7 days of transplantation. As expected, GFP-positive grafted NSCs were present in the injured cauda equina (Figure 3C).

3.3. Differentiation of NSCs in the injured cauda equina

To determine the differentiation status of NSCs *in vivo* after 7 days of transplantation, we further co-stained sagittal sections of the cauda equina with O4, S100, GFAP and βIII-tubulin respectively. The

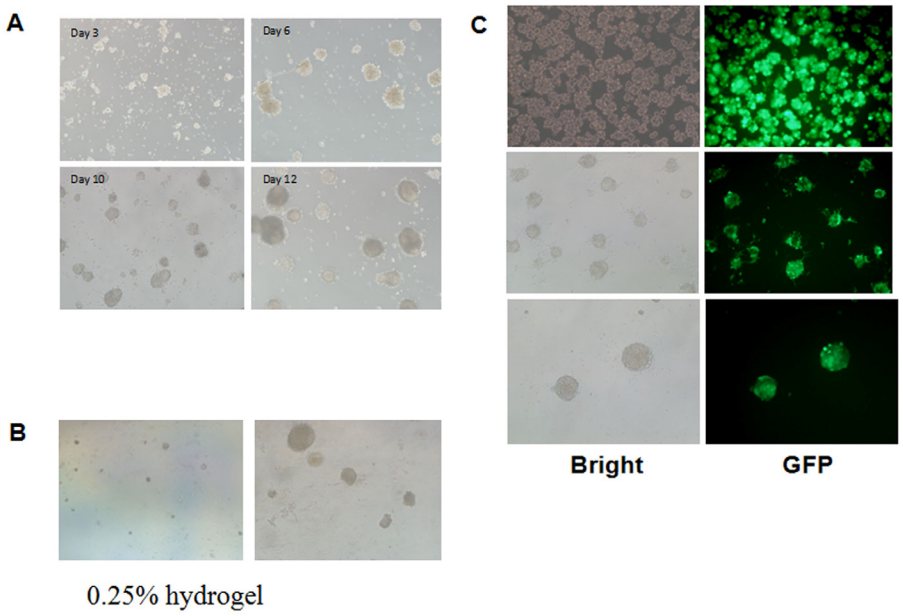

Figure 1. Characterization of NSCs in hydrogel scaffolds. (A) NSCs were isolated from the neonatal rat DRG and cultured on proliferation culture medium for different time points at 3, 6, 10 and 12 days. Magnification, ×100. **(B)** NSCs successfully grown on 0.25% hydrogels. Magnification, ×40, ×100. **(C)** NSCs transfected with lentivirus vectors carrying green fluorescent protein (GFP) and cultured on differentiation medium. Magnification, ×100.

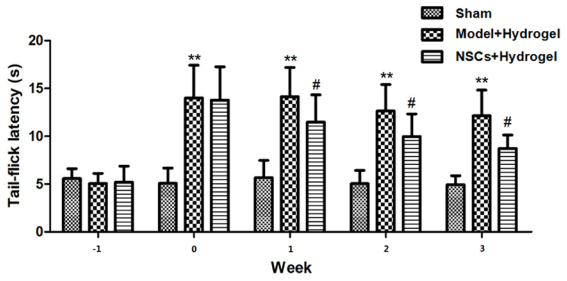

Figure 2. Functional recovery following transplantation of NSCs encapsulated in hydrogels. The functional recovery of sensorimotor reflexes in the sham, CES model+Hydrogel and NSCs+Hydrogel groups was determined using the tail-flick test. $^{**}p < 0.01$, compared *vs.* the sham group; $^{\#}p < 0.05$, *vs.* the CES model+Hydrogel group. Data are reported as means ± SD.

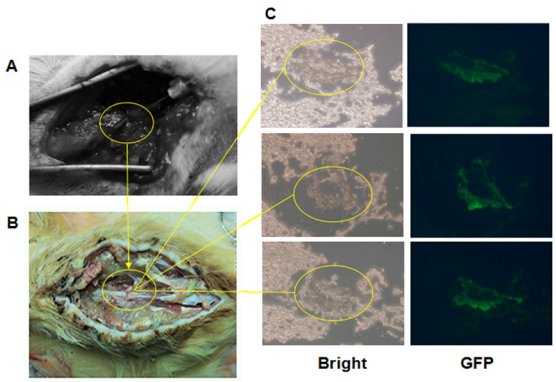

Figure 3. Transplantation of NSCs in the injured cauda equine. A rat model of cauda equina injury was established and transplanted with hydrogel-encapsulated NSCs **(A)**. After 7 days of transplantation, the frozen sections were imaged **(B)** and GFP-positive grafted NSCs in the injured cauda equina were observed in the bright and GFP channel respectively **(C)**.

outcomes demonstrated that NSCs differentiated into oligodendrocytes (O4+), neurons (βIII-tubulin+) or astrocytes (GFAP+) *in vivo* (Figure 4). However, there was no obvious detection of Schwann cells (S100+), which is an interesting result.

3.4. Functional recovery following NSC transplantation encapsulated in three-dimensional hydrogels

Fourteen days after transplantation, we investigated the regenerative effect of transplanted NSCs by examining cell apoptosis of DRG tissues and pathological morphology of cauda equina. Bilateral L5-6 DRG tissues were isolated from the rats and subjected to TUNEL staining. The results showed that the CES model+Hydrogel group led to a significant increase in apoptotic cells compared to the sham group (21.63% ± 2.08 *vs.* 1.41% ± 0.56, $p < 0.01$). By contrast, NSCs transplanted with three-dimensional hydrogels significanly decreased the apoptosis rate compared to the CES model+Hydrogel group (13.92% ± 3.67 *vs.* 21.63% ± 2.08, $p < 0.05$) (Figure 5A). Furthermore, TEM analysis showed in an organized state, normal axons, and intact myelin sheath of cauda equina nerve fibers. However, compression of cauda equina resulted in disorganized nerve fibers, swollen axons and myelin sheaths, and demyelination. These observations were alleviated after transplantation of NSCs encapsulated in hydrogels (Figure 5A). Additionally, G-ratio (inner

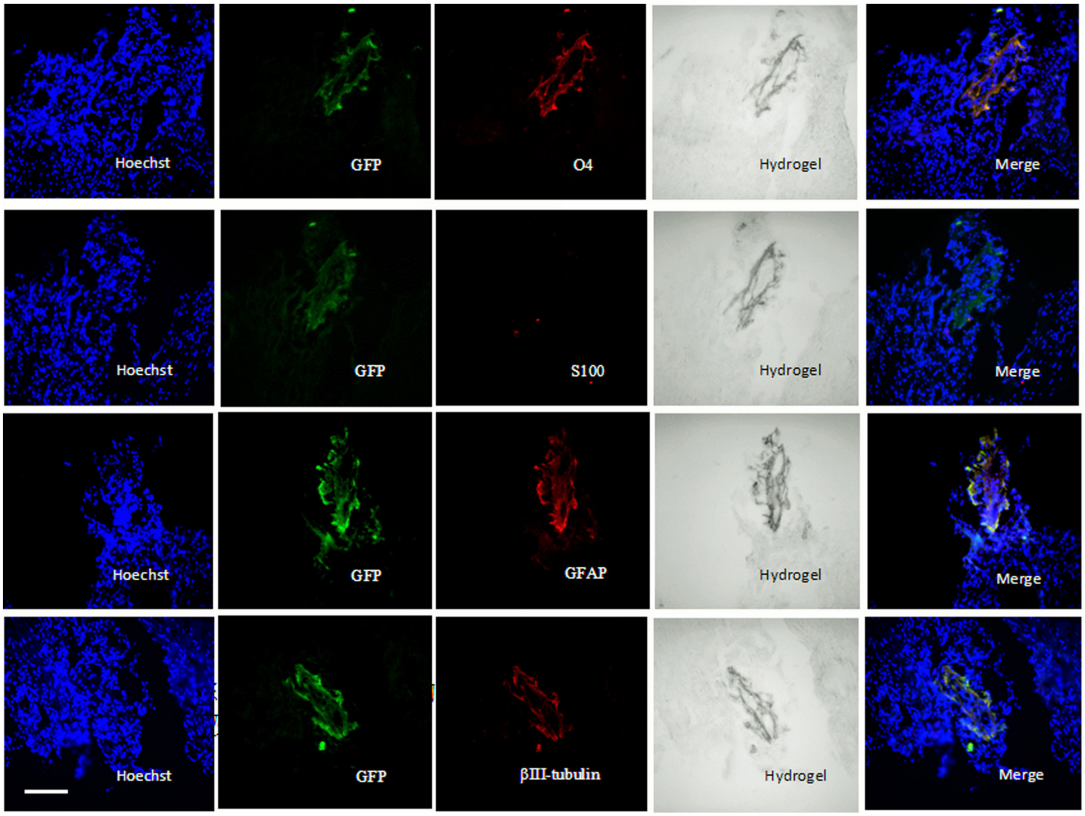

Figure 4. Differentiation of NSCs *in vivo*. After 7 days transplantation, the frozen sections were immunohistochemically stained with antibodies against O4, S100, βIII-tubulin, and GFAP, and co-stained with Hoechst for 10 min prior to images being taken using confocal microscopy. Magnification, ×200. Scale bar = 100μm.

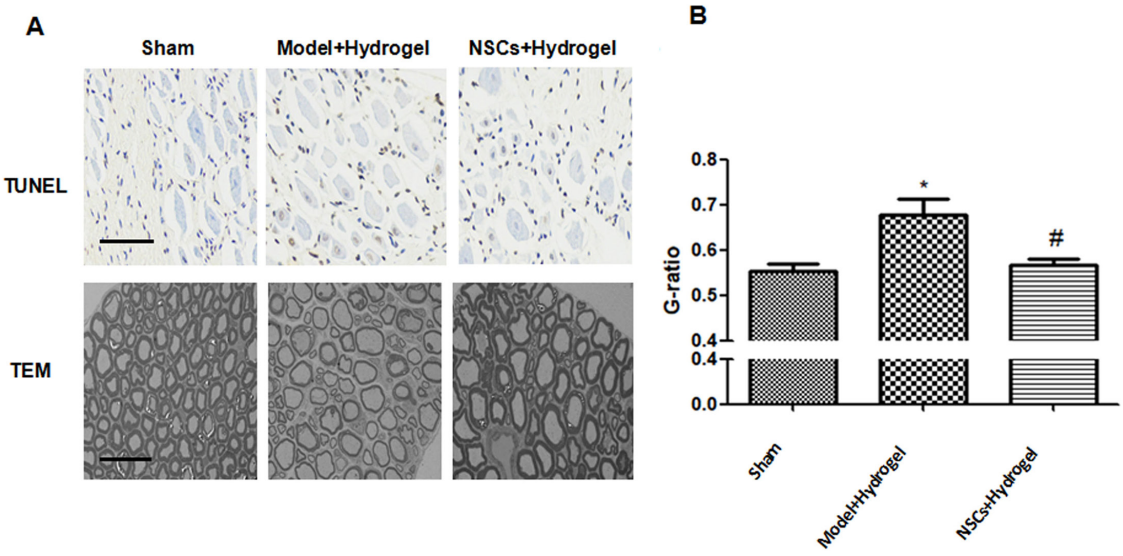

Figure 5. Ultrastructural and pathological changes of DRG after NSC transplantation. (A) The rat DRG tissues were subject to TUNEL and TEM. Magnification, ×200 (TUNEL), ×200 (TEM). **(B)** G-ratio (inner diameter/outer diameter of myelinated axons) was calculated. $^{*}p < 0.05$, *vs.* the sham group; $^{\#}p < 0.05$, *vs.* the CES model+Hydrogel group. Data are reported as means ± SD. Scale bar = 100 μm.

diameter/outer diameter of myelinated axons) was significantly higher in the model+Hydrogel group than the sham group, and then decreased in the grafted NSCs+Hydrogel animal group (Figure 5B).

We monitored the functional changes of sensorimotor reflexes of cauda equina using the tail-flick test before and after compression prior to transplantation, as well as on day 7, 14 and 21 of post-transplantation. After

compression for 7 days, we observed significantly higher tail flick latency (TFL) of the CES model+Hydrogel group than that of the sham group. This indicates the success of the CES model. This trend of the CES model+Hydrogel group was prolonged during the three weeks of post-transplantation, which corresponds with the phenotypes observed in TEM analysis fourteen days after transplantation (Figure 4A). Three weeks after transplantation, animals with cauda equina injury still exhibited a significant increase in tail-flick latency compared with those in the sham group. However, transplantation of hydrogel-encapsulated NSCs partly decreased tail-flick latency, exhibiting a neuroprotective activity on injured cauda equina (Figure 2).

4. Discussion

In the present study, we applied tissue engineering technology combined with NSCs transplantation, and explored the potential therapeutic effects on cauda equina injury. Consequently, our study demonstrated that transplantation of hydrogel-encapsulated NSCs can limitedly promote the differentiation of stem cells and improve the functional recovery of injured cauda equina.

CES is a rare neurological disorder characterized by low back pain, muscle weakness, and sensory disturbance (*16*). At the cellular level, DRG cells appear disorganized with some apoptotic bodies. In addition, CES will cause demyelination and swelling of myelin. Because of the poor self-repair ability of nerve tissue, especially those in the central nervous system, the therapeutic effects of surgery and neurotrophic drugs on cauda equina injury-induced CES is limited. Patients often have residual bladder and sexual dysfunction, and skin sensory disorder in the sella area. Although this disease has a low incidence in the population, ranging from 1: 33,000 to 1: 100,000 patients, its sequelae still generate high public healthcare costs (*1*). Thus, development of novel approaches to maintain neural stem cell viability is important to achieve ideal therapeutic outcomes. The functional recovery of CES is not satisfied because of the failure of axon regeneration and nerve damage.

Because the cauda equina is different from the spinal cord, it is impossible to transplant neural stem cells into the solid tissues. Our previous study showed that GFP-NSCs survived in the cerebrospinal fluid around the damaged cauda equina after intrathecal transplantation, but the surviving time was very short, *i.e.*, only one week (*13*). Based on the previous study, hydrogels were used to localize neural stem cells to the injured cauda equina to promote axon regeneration and remyelination of damaged cauda equina, eventually achieving the goal of neuron preservation and functional repair.

NSCs have shown promising and beneficial effects in the therapy of neurological disorders, such as spinal cord injury, brain trauma, and cauda equina lesion (*17*). Accumulating evidence demonstrates that transplanted NSCs successfully survive in the injured tissues and integrate into the host brain to achieve functional recovery (*18*). Moreover, the pluripotency of DRG has been reported by several research groups, including our group (*13,19,20*). The sensory branch in the cauda equina is composed of the central processes of DRG neurons. Thus, DRG-NSCs were used to repair the damaged cauda equina because of the homology of DRG-NSCs with cauda equina. The mechanisms by which NSCs exert their neuroprotective effects have begun to be elucidated. Increasing studies have shown that NSCs may synthesize a variety of neurotrophic cytokines stimulating nerve growth, such as vascular endothelial growth factor (VEGF), brain derived neurotrophic factor (BDNF), and nerve growth factor (NGF) (*21,22*). Previous studies showed that deficiency of endogenous neurotrophins is associated with poor neuronal survival and cell death (*23*). BDNF has very extensive neurotrophy and can maintain the survival of various kinds of neurons and directly promote their axon growth (*24*). Following a cervical spinal cord injury, administration of BDNF into the site of spinal cord injury promoted axonal regeneration and prevented axotomy-induced atrophy and/or death of rubrospinal neurons (*25,26*). Furthermore, cell transplantation may also enhance endogenous repair processes including neurogenesis, axonal sprouting, and angiogenesis (*27,28*). However, NSCs application is limited due to poor cell survival in host tissues. In our study, NSCs were successfully isolated and cultured in hydrogels. Moreover, we found the possibility of NSCs differentiating into oligodendrocytes, Schwann cells, neurons and astrocytes.

Tissue engineering may provide solutions to the challenges of stem cell death and damage associated with transplantation (*29*). Biopolymer hydrogels can promote stem cell survival, enhance stem cell engraftment, and minimize wound scar formation. Published studies have shown that hydrogels alter the survival and differentiation of stem cells both in vitro and *in vivo* (*30,31*). In the present study, we isolated NSCs from neonatal DRG to repair damaged cauda equina in a rat model of lumbar spinal canal stenosis. As a result, hydrogel-encapsulated NSCs presented high viability in the injured cauda equina and mainly differentiated to oligodendrocytes. Oligodendrocytes are known to be susceptible to spinal cord contusion and loss of oligodendrocytes may induce demyelination, disturb the functional recovery of damaged nerve tissues, and damage the conductive capacity of sensory nerves (*32*). Therefore, stem cell transplantation is helpful to improve myelination and enhance functional recovery after CNS injury (*33*). To evaluate the neuroprotective role of the hydrogel encapsulated NSCs, the tail-flick test was performed to measure the functional recovery of sensorimotor reflexes. As expected, NSCs engrafted on the hydrogels significantly decreased apoptosis of injured cauda equina tissue. Moreover, cauda equina nerve fibers

presented an organized state, normal axons, and intact myelin sheath. Additionally, transplanted hydrogel-encapsulated NSCs decreased the tail-flick latency and showed a neuroprotective role on injured cauda equina.

In summary, our study demonstrates that transplantation of hydrogel-encapsulated NSCs enhances the viability of transplanted cells, promotes stem cell differentiation into oligodendrocytes, thereby contributing to the functional recovery of injured cauda equina. These results implied that NSCs encapsulated in three-dimensional hydrogels may be used for the treatment of cauda equina disorder. Nevertheless, more related sensory and motor functions, time-dependence of the repair effect, or gender differences remain to be further investigated.

Our results indicate transplantation of hydrogel-encapsulated NSCs promotes stem cell differentiation into oligodendrocytes, neurons or astrocytes and contributes to the functional recovery of injured cauda equina, suggesting that NSCs encapsulated in hydrogels may be applied for the treatment of cauda equina injury.

Funding: This research is supported by the National Natural Science Foundation of China (grant #81400997), Shanghai Municipal Commission of Health and Family Planning (grant #201440326).

Conflict of Interest: The authors have no conflict of interest to disclose.

References

1. Dias ALN, Araújo FF, Cristante AF, Marcon RM, Barros Filho TEP, Letaif OB. Epidemiology of cauda equina syndrome. What changed until 2015. Rev Bras Ortop. 2017; 53:107-112.
2. Li X, Dou Q, Hu S, Liu J, Kong Q, Zeng J, Song Y. Treatment of cauda equina syndrome caused by lumbar disc herniation with percutaneous endoscopic lumbar discectomy. Acta Neurol Belg. 2016; 116:185-190.
3. Korse NS, Pijpers JA, van Zwet E, Elzevier HW, Vleggeert-Lankamp CLA. Cauda Equina Syndrome: presentation, outcome, and predictors with focus on micturition, defecation, and sexual dysfunction. Eur Spine J. 2017; 26:894-904.
4. Abe K. Therapeutic potential of neurotrophic factors and neural stem cells against ischemic brain injury. J Cereb Blood Flow Metab. 2000; 20:1393-1408.
5. Imitola J, Raddassi K, Park KI, Mueller FJ, Nieto M, Teng YD, Frenkel D, Li J, Sidman RL, Walsh CA, Snyder EY, Khoury SJ. Directed migration of neural stem cells to sites of CNS injury by the stromal cell-derived factor 1alpha/CXC chemokine receptor 4 pathway. Proc Natl Acad Sci U S A. 2004; 101:18117-18122.
6. Haus DL, López-Velázquez L, Gold EM, Cunningham KM, Perez H, Anderson AJ, Cummings BJ. Transplantation of human neural stem cells restores cognition in an immunodeficient rodent model of traumatic brain injury. Exp Neurol. 2016; 281:1-16.
7. Méndez-Olivos EE, Muñoz R, Larraín J. Spinal cord cells from pre-metamorphic stages differentiate into neurons and promote axon growth and regeneration after transplantation into the injured spinal cord of non-regenerative Xenopus laevis froglets. Front Cell Neurosci. 2017; 11:398.
8. Marei HE, Shouman Z, Althani A, Afifi N, A AE, Lashen S, Hasan A, Caceci T, Rizzi R, Cenciarelli C, Casalbore P. Differentiation of human olfactory bulb-derived neural stem cells toward oligodendrocyte. J Cell Physiol. 2018; 233:1321-1329.
9. Zhang LQ, Zhang WM, Deng L, Xu ZX, Lan WB, Lin JH. Transplantation of a peripheral nerve with neural stem cells plus lithium chloride injection promote the recovery of rat spinal cord injury. Cell Transplant. 2018; 27:471-484.
10. Levison SW, Druckman SK, Young GM, Basu A. Neural stem cells in the subventricular zone are a source of astrocytes and oligodendrocytes, but not microglia. Dev Neurosci. 2003; 25:184-196.
11. Wang A, Tang Z, Park IH, Zhu Y, Patel S, Daley GQ, Li S. Induced pluripotent stem cells for neural tissue engineering. Biomaterials. 2011; 32:5023-5032.
12. Singh RP, Cheng YH, Nelson P, Zhou FC. Retentive multipotency of adult dorsal root ganglia stem cells. Cell Transplant. 2009; 18:55-68.
13. Fu ZY, Shi JG, Liu N, Jia LS, Yuan W, Wang Y. Differentiation of neonatal dorsal root ganglion-derived neural stem cells into oligodendrocytes after intrathecal transplantation into a cauda equina lesion model. Genet Mol Res. 2013; 12:6092-6102.
14. Kim JH, Budde MD, Liang HF, Klein RS, Russell JH, Cross AH, Song SK. Detecting axon damage in spinal cord from a mouse model of multiple sclerosis. Neurobiol Dis. 2006; 21:626-632.
15. Liu X, Fu Z, Wu Y, Hu X Jr, Zhu T Jr, Jin C Jr. Neuroprotective effect of hydrogen sulfide on acute cauda equina injury in rats. Spine J. 2016; 16:402-407.
16. Ma B, Wu H, Jia LS, Yuan W, Shi GD, Shi JG. Cauda equina syndrome: a review of clinical progress. Chin Med J (Engl). 2009; 122:1214-1222.
17. Pluchino S, Zanotti L, Deleidi M, Martino G. Neural stem cells and their use as therapeutic tool in neurological disorders. Brain Res Brain Res Rev. 2005; 48:211-219.
18. Uchida K, Momiyama T, Okano H, Yuzaki M, Koizumi A, Mine Y, Kawase T. Potential functional neural repair with grafted neural stem cells of early embryonic neuroepithelial origin. Neurosci Res. 2005; 52:276-286.
19. Ogawa R, Fujita K, Ito K. Mouse embryonic dorsal root ganglia contain pluripotent stem cells that show features similar to embryonic stem cells and induced pluripotent stem cells. Biol Open. 2017; 6:602-618.
20. Hu H, Ding Y, Mu W, Li Y, Wang Y, Jiang W, Fu Y, Tou J, Chen W. DRG-Derived Neural Progenitors Differentiate into Functional Enteric Neurons Following Transplantation in the Postnatal Colon. Cell Transplant. 2019; 28:157-169.
21. Salewski RP, Mitchell RA, Li L, Shen C, Milekovskaia M, Nagy A, Fehlings MG. Transplantation of Induced Pluripotent Stem Cell-Derived Neural Stem Cells Mediate Functional Recovery Following Thoracic Spinal Cord Injury Through Remyelination of Axons. Stem Cells Transl Med. 2015; 4:743-754.
22. Upadhyay G, Shankar S, Srivastava RK. Stem Cells in Neurological Disorders: Emerging Therapy with Stunning Hopes. Mol Neurobiol. 2015; 52:610-625.

23. Nakamura M, Bregman BS. Differences in neurotrophic factor gene expression profiles between neonate and adult rat spinal cord after injury. Exp Neurol. 2001; 169:407-415.
24. McCall J, Weidner N, Blesch A. Neurotrophic factors in combinatorial approaches for spinal cord regeneration. Cell Tissue Res. 2012; 349:27-37.
25. Liu Y, Himes BT, Murray M, Tessler A, Fischer I. Grafts of BDNF-producing fibroblasts rescue axotomized rubrospinal neurons and prevent their atrophy. Exp Neurol. 2002; 178:150-164.
26. Tan J, Shi J, Shi G, Liu Y, Liu X, Wang C, Chen D, Xing S, Shen L, Jia L, Ye X, He H, Li J. Changes in compressed neurons from dogs with acute and severe cauda equina constrictions following intrathecal injection of brain-derived neurotrophic factor-conjugated polymer nanoparticles. Neural Regen Res. 2013; 8:233-243.
27. Daadi MM, Davis AS, Arac A, Li Z, Maag AL, Bhatnagar R, Jiang K, Sun G, Wu JC, Steinberg GK. Human neural stem cell grafts modify microglial response and enhance axonal sprouting in neonatal hypoxic-ischemic brain injury. Stroke. 2010; 41:516-523.
28. Andres RH, Horie N, Slikker W, Keren-Gill H, Zhan K, Sun G, Manley NC, Pereira MP, Sheikh LA, McMillan EL, Schaar BT, Svendsen CN, Bliss TM, Steinberg GK. Human neural stem cells enhance structural plasticity and axonal transport in the ischaemic brain. Brain. 2011; 134:1777-1789.
29. Kim H, Cooke MJ, Shoichet MS. Creating permissive microenvironments for stem cell transplantation into the central nervous system. Trends Biotechnol. 2012; 30:55-63.
30. Führmann T, Tam RY, Ballarin B, Coles B, Elliott Donaghue I, van der Kooy D, Nagy A, Tator CH, Morshead CM, Shoichet MS. Injectable hydrogel promotes early survival of induced pluripotent stem cell-derived oligodendrocytes and attenuates longterm teratoma formation in a spinal cord injury model. Biomaterials. 2016; 83:23-36.
31. Naghdi P, Tiraihi T, Ganji F, Darabi S, Taheri T, Kazemi H. Survival, proliferation and differentiation enhancement of neural stem cells cultured in three-dimensional polyethylene glycol-RGD hydrogel with tenascin. J Tissue Eng Regen Med. 2016; 10:199-208.
32. Nistor GI, Totoiu MO, Haque N, Carpenter MK, Keirstead HS. Human embryonic stem cells differentiate into oligodendrocytes in high purity and myelinate after spinal cord transplantation. Glia. 2005; 49:385-396.
33. Armstrong RC, Mierzwa AJ, Sullivan GM, Sanchez MA. Myelin and oligodendrocyte lineage cells in white matter pathology and plasticity after traumatic brain injury. Neuropharmacology. 2016; 110:654-659.

Received September 3, 2020; Revised October 10, 2020; Accepted October 17, 2020.

[§]These authors contributed equally to this work.

**Address correspondence to:*
Yujie Wu and Tong Zhu, Shanghai Key Laboratory of Orthopaedic Implants, Department of Orthopaedic Surgery, Shanghai Ninth People's Hospital, Shanghai Jiao Tong University School of Medicine, 639 Zhizaoju Rd, Shanghai 200011, China.
E-mail: 611240@sh9hospital.org.cn (Wu YJ); alphaf@163.com (Zhu T)

Released online in J-STAGE as advance publication October 25, 2020.

Original Article

DOI: 10.5582/bst.2020.03230

High platelet count as a poor prognostic factor for liver cancer patients without cirrhosis

Yutaka Midorikawa[1,*], Tadatoshi Takayama[1], Tokio Higaki[1], Osamu Aramaki[1], Kenichi Teramoto[1], Nao Yoshida[1], Shingo Tsuji[2], Tatsuo Kanda[3], Mitsuhiko Moriyama[3]

[1] Department of Digestive Surgery, Nihon University School of Medicine, Tokyo, Japan;
[2] Genome Science Division, Research Center for Advanced Science and Technology, University of Tokyo, Tokyo, Japan;
[3] Department of Gastroenterology and Hepatology, Nihon University School of Medicine, Tokyo, Japan.

SUMMARY A low platelet count, one of parameters of portal hypertension, is clinically a predictor of postoperative mortality, while platelets induce tumor development during growth factor secretion. In this study, we retrospectively investigated whether high platelet count negatively affects the survival of patients with hepatocellular carcinoma (HCC). Patients undergoing initial and curative resection for HCC were included. Surgical outcomes were compared between the high platelet (platelet count $\geq 20 \times 10^4/\mu L$) and control ($< 20 \times 10^4/\mu L$) groups in patients without cirrhosis and between the low platelet ($< 10 \times 10^4/\mu L$) and control ($\geq 10 \times 10^4/\mu L$) groups in patients with cirrhosis. Among patients without cirrhosis, tumor was larger ($P < 0.001$) and tumor thrombus was more frequent ($P < 0.001$) in the high-platelet group than in the control group. After a median follow-up period of 3.1 years (range 0.2-16.2), median overall survival was 6.3 years (95% confidence interval [CI], 5.3-7.8) and 7.6 years (6.6-10.9) in the high-platelet ($n = 273$) and control ($n = 562$) groups, respectively ($P = 0.027$). Among patients with cirrhosis, liver function was worse ($P < 0.001$) and varices were more frequent ($P < 0.001$) in the low-platelet group. The median overall survival of patients in the low-platelet group ($n = 172$) was significantly shorter than that of patients in the control group ($n = 275$) (4.5 years [95% CI, 3.7–6.0] *vs.* 5.9 years [4.5-7.5], $P = 0.038$). Taken together, thrombocytopenia indicates poor prognosis in HCC patients with cirrhosis, while thrombocytosis is a poor prognostic predictor for those without cirrhosis.

Keywords growth factor, hepatocellular carcinoma, platelet, portal hypertension, prognostic predictor

1. Introduction

Portal hypertension is clinically defined based on the presence of esophageal varices or splenomegaly and is associated with a platelet count of less than $10 \times 10^4/\mu L$ (*1*). Therefore, a low platelet count due to portal hypertension is one of the risk factors for patients undergoing resection for hepatocellular carcinoma (HCC). The surgical outcomes for these patients are worse, although these outcomes do not contradict with the postoperative outcomes for patients with cirrhosis (*2-4*). In addition to the cessation of bleeding and thrombosis induction, platelets play a direct role in hepatocyte proliferation by triggering the secretion of several growth factors such as platelet-derived growth factor, serotonin, transforming growth factor-ß, and hepatocyte growth factor (*5-7*). Clinically, platelets have been reported to support the regeneration of remnant liver after resection (*8,9*). A low platelet count has served as a predictor of postoperative dysfunction and postoperative mortality (*10,11*).

However, *in vitro* studies have shown that platelets also induce tumor growth, migration, and invasion through the secretion of growth factors (*12,13*) and could antagonize sorafenib- or regorafenib-mediated tumor growth suppression and apoptosis in HCC cells through epidermal growth factor and insulin-like growth factor 1 release (*14*). Clinically, early tumor recurrence and shorter survival of patients with HCC are associated with a high platelet count and serotonin level (*15,16*). Patients with a high platelet count or pretreatment platelet count are also at risk of extrahepatic recurrence of HCC after resection (*17,18*) or recurrence after living donor liver transplantation (*19*).

Given that platelet has multiple contrasting functions in patients with HCC and that portal hypertension negatively affects the platelet count, the clinical significance of the platelet count in HCC patients with

and without liver cirrhosis should be investigated in great detail. In this study, we focused on the clinical significance of platelet count in HCC patients undergoing liver resection. To avoid the strong effect of portal hypertension on the survival rate, patients with and without liver cirrhosis were analyzed separately in this series. We further compared surgical outcomes and tumor progression in patients with HCC on the basis of platelet count.

2. Materials and Methods

2.1. Patients

Patients who underwent initial and curative resection for HCC between 2000 and 2018 at Nihon University Itabashi Hospital (Tokyo, Japan) were included in this study. Each participant provided written informed consent, and this study was approved by the institutional review board of Nihon University (RK-200512-4). All clinical investigations were conducted according to the principles of the Declaration of Helsinki.

2.2. Indications for liver resection

The indications for liver resection and other treatments for patients with HCC were determined by assessing their liver functional reserve according to Guidelines on Liver Cancer Examination and Treatment in Japan (*20*). Briefly, patients with Child-Pugh A or B with up to three viable lesions were candidates for liver resection.

2.3. Patient groups

Among the patients who were histologically diagnosed as not having liver cirrhosis after the operation, those with a platelet count of $\geq 20 \times 10^4/\mu L$ were included in the high-platelet group. Among the patients with cirrhosis, those with a platelet count of $< 10 \times 10^4/\mu L$ were included in the low-platelet group. Clinical characteristics and surgical outcomes were compared between the high-platelet and control (platelet count $< 20 \times 10^4/\mu L$) groups in patients without cirrhosis and between the low-platelet and control (platelet count $\geq 10 \times 10^4/\mu L$) groups in patients with cirrhosis.

2.4. Surgical procedures

Open liver resection was performed in all patients according to the criteria based on the liver function (*21*). Patients with a preoperative platelet count of $< 10 \times 10^4/\mu L$ had platelet transfusion on the day of operation. Anatomical resection was the first-line treatment. Major resection included segmentectomy, hemihepatectomy, and trisegmentectomy, while anatomic resection was defined as liver resection over subsegmentectomy. The liver was transected under ultrasonographic guidance using the clamp-crushing method with the inflow-blood-occlusion technique (*22*). Curative resection was defined as the complete removal of recognizable viable HCC diagnosed preoperatively or intraoperatively with macroscopically tumor-free surgical margins. Postoperative complications were stratified according to the Clavien-Dindo classification (*23*), which defines morbidities as complications with a score of ≥ 3a. Complications specific to liver resection were defined as described previously (*24*).

2.5. Follow-up after operation

All patients were followed up for postoperative recurrence as described previously (*25*). Briefly, the levels of tumor markers including alpha-fetoprotein and des-gamma-carboxy prothrombin were measured, and imaging studies including computed tomography and ultrasonography were performed every three months in all patients. Tumor recurrence was diagnosed by dynamic computed tomography and/or magnetic resonance imaging. The date of recurrence was defined as the date of examination when the recurrent HCC was noted.

2.6. Statistical analysis

Data collected from each group were statistically analyzed with Fisher's exact test and Wilcoxon rank-sum test. Survival curves were generated using the Kaplan-Meier method and compared using the log-rank test. Prognostic factors for overall survival were identified with the Cox proportional hazards regression model. Statistical analyses were performed using JMP 12.0.1 statistical software (SAS Institute, Cary, NC, USA). $P < 0.05$ was considered to indicate significance.

3. Results

3.1. Patients

The 1,282 patients who underwent initial and curative resection for HCC were included (Figure 1). The median platelet count for 835 patients (65.1%) without cirrhosis was $18.6 \times 10^4/\mu L$ (range; 2.4-68.6). Two hundred seventy-three patients (32.6%) with a platelet count of $\geq 20 \times 10^4/\mu L$ were included into the high-platelet group. By contrast, among the 447 patients (34.8%) who were histologically diagnosed as having cirrhosis, the median platelet count was $11.1 \times 10^4/\mu L$ (range 3.2-66.0) and 172 patients (38.4%) with a platelet count of $< 10 \times 10^4/\mu L$ were included in the low-platelet group.

For patients without cirrhosis, hepatitis C virus infection ($P < 0.001$) and varices ($P = 0.011$) were less frequent, liver functions such as Child-Pugh classification ($P = 0.013$) and indocyanine green clearance rate at 15 minutes ($P < 0.001$) were better, and des-gamma-carboxy prothrombin was higher ($P < 0.001$) in the high-platelet

group than in the control group (Table 1). By contrast, for patients with cirrhosis, hepatitis C virus infection ($P < 0.001$) and varices ($P < 0.001$) were more frequent and liver function parameters were worse ($P < 0.001$) in the low-platelet group than in the control group (Table 2).

3.2. Operative data

For patients without cirrhosis, operation time was longer ($P < 0.001$), the amount of blood loss was higher ($P = 0.013$), and major resection ($P < 0.001$) and anatomic resection ($P < 0.001$) were more frequent in the high-platelet group than in the control group (Table 3), but complication rates except for bile leakage ($P = 0.014$) and respiratory complications ($P = 0.005$) were not significantly different between the two groups (Table 4). Histological findings showed that the tumor was in a more advanced stage in the high-platelet group than in the control group; the tumor was larger ($P < 0.001$) and the tumor thrombus was more frequent ($P < 0.001$).

For patients with cirrhosis, the amount of blood loss was higher ($P = 0.015$) and both major resection and anatomic resection were less frequent ($P < 0.001$) in the low-platelet group than in the control group (Table 5). Complication rates were not different between the two groups (Table 6). Histological findings were not significantly different between the low-platelet and control groups.

Coefficients of determination (R^2) between platelet count and tumor size were 0.164 and 0.015 in patients without cirrhosis ($P < 0.001$) and those with cirrhosis ($P = 0.008$), respectively (Figure 2).

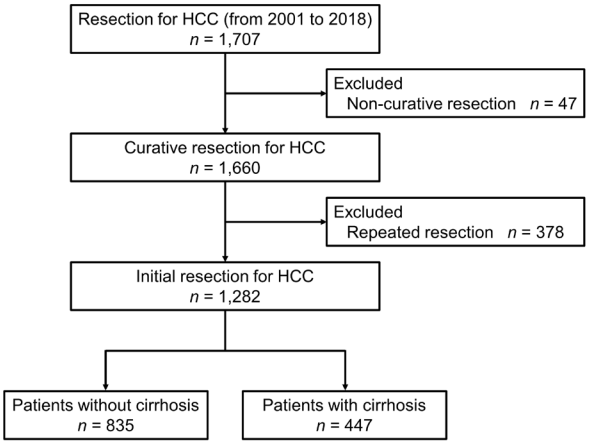

Figure 1. Flowchart for patient selection.

3.3. Survivals

For patients without cirrhosis, the median overall

Table 1. Patient background (without cirrhosis)

Items	High platelet ($n = 273$)	Control ($n = 562$)	P value
Age, years	69 (35-84)	70 (33-86)	0.314
Sex, male (%)	226 (82.7)	456 (81.1)	0.633
Alcoholic, n (%)	70 (25.6)	177 (31.4)	0.089
Diabetes mellitus, n (%)	90 (32.9)	190 (33.8)	0.875
HBV, n (%)	39 (14.2)	102 (18.1)	0.169
HCV, n (%)	77 (28.2)	267 (47.5)	< 0.001
Varices, n (%)	18 (6.5)	70 (12.4)	0.011
Child-Pugh, A (%)	256 (93.7)	496 (88.2)	0.013
ICGR15, %	9.4 (1.9-35.5)	12.4 (1.3-48.0)	< 0.001
Alpha-fetoprotein, ng/mL	8 (1-541,432)	11 (1-449,211)	0.725
DCP, mAU/mL	214 (9-75,000)	75 (1-75,000)	< 0.001

Data are presented as median with range, if not specified. HBV, hepatitis B virus; HCV, hepatitis C virus; ICGR15, indocyanine green clearance rate at 15 minutes; DCP, des-gamma carboxyprothrombin.

Table 2. Patient background (with cirrhosis)

Items	Low platelet ($n = 172$)	Control ($n = 275$)	P value
Age, years	68 (32-81)	68 (40-85)	0.783
Sex, male (%)	108 (62.7)	193 (70.1)	0.120
Alcoholic, n (%)	36 (20.9)	69 (25.0)	0.359
Diabetes mellitus, n (%)	55 (48.6)	96 (45.0)	0.560
HBV, n (%)	20 (11.6)	51 (18.5)	0.062
HCV, n (%)	130 (75.5)	161 (65.1)	< 0.001
Varices, n (%)	96 (55.8)	92 (33.4)	< 0.001
Child-Pugh, A (%)	99 (57.5)	228 (82.9)	< 0.001
ICGR15, %	19.4 (2.0-48.4)	14.4 (2.0-49.8)	< 0.001
Alpha-fetoprotein, ng/mL	32 (1-17,853)	18 (1-53,460)	0.182
DCP, mAU/mL	39 (7-35,203)	42 (1-60,300)	0.187

Data are presented as median with range, if not specified. HBV, hepatitis B virus; HCV, hepatitis C virus; ICGR15, indocyanine green clearance rate at 15 minutes; DCP, des-gamma carboxyprothrombin.

Table 3. Operative data (without cirrhosis)

Items	High platelet (*n* = 273)	Control (*n* = 562)	*P* value
Operation data			
Operation time, min	360 (107-855)	310 (97-1,004)	< 0.001
Bleeding, mL	298 (5-7,066)	252 (10-3,777)	0.013
Pringle time, min	80 (0-274)	68 (0-304)	< 0.001
Transfusion, *n* (%)	23 (8.4)	32 (5.6)	0.139
Major resection, *n* (%)	99 (36.2)	83 (14.7)	< 0.001
Anatomic resection, *n* (%)	149 (54.5)	224 (39.8)	< 0.001
Pathology			
Multiple, *n* (%)	61 (22.3)	134 (23.8)	0.663
Size, cm (range)	5.0 (0.8-21.0)	3.2 (0.5-20.0)	< 0.001
Differentiation grade, well, (%)	33 (12.0)	105 (18.6)	0.017
Vascular invasion, *n* (%)	105 (38.4)	147 (26.1)	< 0.001
Tumor exposure, *n* (%)	23 (8.4)	43 (8.2)	0.683

Data are presented as median, if not specified.

Table 4. Complications (without cirrhosis)

Items	High platelet (*n* = 273)	Control (*n* = 562)	*P* value
Overall, *n* (%)	84 (30.7)	194 (34.5)	0.309
Morbidity, *n* (%)	59 (21.6)	140 (24.9)	0.300
Intraperitoneal hemorrhage	1 (0.3)	5 (0.8)	0.669
Intraperitoneal abscess	8 (2.9)	13 (2.3)	0.639
Bile leakage	18 (6.5)	16 (2.8)	0.014
Ascites	2 (0.7)	3 (0.5)	0.664
Portal thrombus	1 (0.3)	1 (0.1)	0.547
Wound infection	11 (4.0)	23 (4.0)	1
Respiratory	13 (4.7)	55 (9.7)	0.005
Cardiovascular	1 (0.3)	2 (0.3)	1
Stroke	0	1 (0.1)	1
Liver failure	0	0	1
Variceal rapture	0	1 (0.1)	1
Ileus	0	4 (0.7)	0.309
Perforation	1 (0.3)	1 (0.1)	0.547
Others	3 (1.0)	15 (2.6)	0.203
Re-operation, *n* (%)	8 (2.9)	13 (2.3)	0.639
Mortality, *n* (%)	0 (0)	2 (0.3)	1.000

Morbidity was defined as complication with score of ≥ 3a.

Table 5. Operative data (with cirrhosis)

Items	Low platelet (*n* = 172)	Control (*n* = 275)	*P* value
Operation data			
Operation time, min	316 (130-705)	305 (113-655)	0.884
Bleeding, mL	315 (20-4,530)	275 (5-2,988)	0.015
Pringle time, min	64 (0-266)	69 (0-230)	0.824
Transfusion, *n* (%)	15 (8.7)	18 (6.5)	0.392
Major resection, *n* (%)	2 (1.1)	17 (6.1)	0.013
Anatomic resection, *n* (%)	33 (19.1)	88 (32)	0.003
Pathology			
Multiple, *n* (%)	55 (31.9)	75 (27.2)	0.287
Size, cm (range)	2.6 (0.7-10.5)	2.5 (0.7-18.0)	0.781
Differentiation grade, well (%)	38 (22.0)	56 (20.3)	0.720
Vascular invasion, *n* (%)	30 (17.4)	56 (20.3)	0.462
Tumor exposure, *n* (%)	21 (12.2)	19 (86.9)	0.062

Data are presented as median, if not specified.

survival of patients in the high-platelet group was 6.3 years (95% confidence interval [CI], 5.3-7.8), which was significantly shorter than that of patients in the control group (7.6 years; 95% CI, 6.6-10.9; $P = 0.027$) after a median follow-up period of 3.1 years (range 0.2-16.2) (Figure 3A). By contrast, there was no significant difference in the median recurrence-free survival between the two groups (1.9 years, [95% CI, 1.5-2.2]

vs. 2.1 years, [95% CI, 1.9-2.3]; $P = 0.904$) (Figure 3B). The overall survival and recurrence-free survival rates at five years were 60.5% and 30.6% in the high-platelet group, respectively, and 66.9% and 27.5% in the control group, respectively.

For patients with cirrhosis, the median overall survival of patients in the low-platelet group and the control group was 4.5 years (95% CI, 3.7-6.0) and 5.9 years (95% CI, 4.5-7.5; $P = 0.038$), respectively (Figure 4A). Recurrence-free survival was 1.8 years (95% CI, 1.5-2.0) and 2.0 years (95% CI, 1.6-2.4; $P = 0.268$), respectively (Figure 4B). The 5-year overall survival rates were 46.6% and 54.3%, and 5-year recurrence-free survival rates were 15.7% and 21.4% in the two groups, respectively.

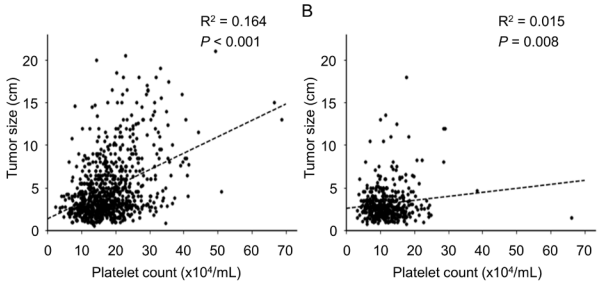

Figure 2. Scatter plots showing the correlation between tumor size and platelet count. (A) Tumor size weakly correlated with platelet count in patients without cirrhosis. **(B)** There was no correlation between tumor size and platelet count in patients with cirrhosis.

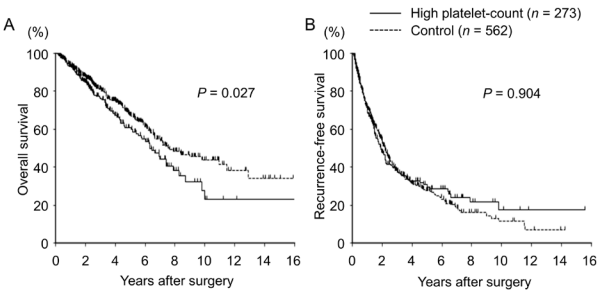

Figure 3. Survival outcomes following liver resection in patients without cirrhosis. (A) Overall survival of patients in the high-platelet count group was significantly shorter than that of patients in the control group ($P = 0.027$). **(B)** Recurrence-free survival was not significantly different between the two groups ($P = 0.904$). Study group sizes are indicated (n).

4. Discussion

Our data showed that a high platelet count was associated with liver cancer progression and, consequently, shorter survival and early recurrence in patients without cirrhosis who underwent resection for HCC. By contrast, a low platelet count indicated poorer prognosis due to the worse liver function in patients with cirrhosis. Thus, according to the background chronic liver disease status, platelet count harbored different predictive values for patients with HCC.

Both experimental and clinical studies demonstrated

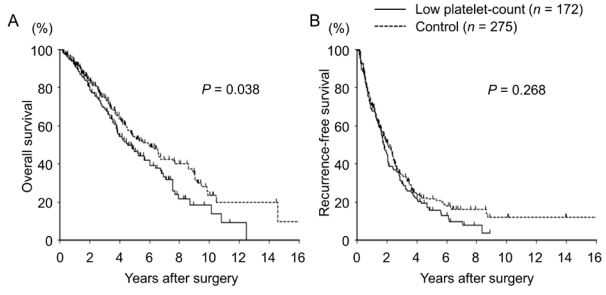

Figure 4. Survival outcomes following liver resection in patients with cirrhosis. (A) Overall survival of patients in the low-platelet count group was significantly shorter than that of patients in the control group ($P = 0.038$). **(B)** Recurrence-free survival was not significantly different between the two groups ($P = 0.268$). Study group sizes are indicated (n).

Table 6. Complications (with cirrhosis)

Items	Low platelet (n = 172)	Control (n = 275)	P value
Overall, n (%)	79 (45.9)	120 (43.6)	0.695
Morbidity, n (%)	61 (35.4)	92 (33.4)	0.682
Intraperitoneal hemorrhage	4 (2.3)	6 (2.1)	1
Intraperitoneal abscess	13 (7.5)	15 (5.4)	0.423
Bile leakage	3 (1.7)	8 (2.9)	0.542
Ascites	2 (1.1)	3 (1.0)	1
Portal thrombus	0	1 (0.3)	1
Wound infection	6 (3.4)	9 (3.2)	1
Respiratory	26 (15.1)	40 (14.5)	0.891
Cardiovascular	0	1 (0.3)	1
Stroke	0	0	1
Liver failure	3 (1.7)	1 (0.3)	0.161
Variceal rapture	0	0	0
Ileus	1 (0.5)	1 (0.3)	1
Perforation	1 (0.5)	0	0.384
Others	2 (1.1)	7 (2.5)	0.492
Re-operation, n (%)	9 (5.2)	7 (2.5)	0.187
Mortality, n (%)	0	0	1.000

Morbidity was defined as complication with score of ≥ 3a.

that platelets promoted HCC proliferation by secreting several types of growth factors (*12,13*). Therefore, platelets had positive induction of further tumor progression in patients with HCC, and a high platelet count in patients with HCC was associated with shorter overall survival (*26,27*). Consistent with the previous data, tumor size weakly correlated with platelet count in patients without cirrhosis, while there was no correlation between the two variables in patients with cirrhosis. Taken together, in the patients without cirrhosis, tumors were more advanced at the time of operation, and consequently, overall survival was shorter despite better parameters of liver function in the high-platelet group.

Recurrence-free survival was not significantly different in both cohorts, but the recurrence rates in the low-platelet group were relatively longer in patients with cirrhosis, although the differences between the low-platelet and control groups were not significant. By contrast, for patients without cirrhosis, recurrence-free survival curves in the high-platelet and control groups crossed at approximately three years, and recurrence rates at two years were higher in the high-platelet group (46.0%) than in the control group (52.3%), while those at five years were lower in the high-platelet group. The characteristics of HCC recurrence are generally understood as follows: most cases of tumor recurrence by metachronous intrahepatic metastasis occurred within two years (*28*), while most cases of recurrence two years after operation were due to multicentric origin, which was more remarkable in patients with poor liver function (*29,30*). Therefore, we assumed that platelets could contribute to the early recurrence by stimulating liver cancer cells through the secretion of growth factors, while low platelet count, both in patients with and without cirrhosis, indicated the possibility of the late-term recurrence. On the other hand, there was no significance of the recurrence-free survival rates between the low-platelet count and the control groups. However the recurrence-free survival tended to be shorter especially two years after surgery, which did not conflict the results of overall survival.

Thrombocytopenia is also one of the most important indicators of portal hypertension. Consistent with a previous report (*31*), liver function was worse and varices were more frequent in the low-platelet group, and therefore, a low preoperative platelet count was associated with poor survival after operation in patients with liver cirrhosis in this study.

Moreover, platelets play a pivotal role in the initiation of the coagulation cascade and reduce the amount of blood loss through bleeding during liver transection, leading to the low rate of postoperative complications (*32*). Platelets also have a strong proliferative effect on hepatocytes and induce liver regeneration by secreting growth factors (*5-7*). Consequently, a decrease in platelet counts was associated with morbidity such as postoperative liver dysfunction and rupture of varices after operation (*33,34*). To avoid massive bleeding during operation, patients with a preoperative platelet count of $< 10 \times 10^4/\mu L$ routinely had platelet transfusion on the day of operation in our institute. Consequently, there was no significant difference in postoperative complications between the low-platelet and control groups observed in this study.

In the previous reports, the cut-off value for platelet counts ranged from 6.8 to $10 \times 10^4/\mu L$, especially, $10 \times 10^4/\mu L$ seemed be the most frequent (*10,11,17,19,30*). Given that platelet counts were strongly affected by the liver status, the cut-off value should be separately determined according to whether the patients have liver cirrhosis or not. Therefore, we defined the cut-off value of the platelet counts ($20 \times 10^4/\mu L$ in the patients without cirrhosis and $10 \times 10^4/\mu L$ in those with cirrhosis) based on the median value ($18.6 \times 10^4/\mu L$ and $11.1 \times 10^4/\mu L$), which could be considered to be adequate.

This study had several limitations. First, concentrations of serotonin or other growth factors were not measured, and therefore, it is not clear whether the advanced stage of tumors in the high-platelet group was actually caused specifically by the growth factors secreted by platelets. If that is the case, we should observe the correlation between patient survival and the presence of growth factors in the serum with the expression of their respective receptors in tumors in future studies. Second, platelet count is easily affected by liver function. However, despite better liver function in the high-platelet group in patients without cirrhosis, survival time in these patients was shorter, and therefore, we assumed that a high platelet count could have negatively affected the survival of patients with HCC. Finally, it is clinically difficult to fully predict whether a patient has cirrhosis before operation. In this situation, it needs more consideration to apply these findings to clinical practice.

In conclusion, a high platelet count was an unfavorable prognostic factor and it negatively impacted the survival of HCC patients without cirrhosis because a high platelet count promoted liver cancer progression. By contrast, low platelet count negatively affected the surgical outcomes of patients with cirrhosis. Therefore, our findings suggest that platelet count has different implications for predicting patient survival based on the chronic liver disease status background.

Acknowledgements

This research was supported by AMED under Grant Number JP20hk0102049s0303 and a grants-in-aid of The 106th Annual Congress of JSS Memorial Surgical Research Fund, Tokyo, Japan. The funding body supported the data collection used in this study. The funding body has no role in the design of the study and analysis and interpretation of data and in writing the manuscript.

References

1. Forner A, Llovet JM, Bruix J. Hepatocellular carcinoma. Lancet. 2012; 379:1245-1255.
2. Cucchetti A, Ercolani G, Vivarelli M, Cescon M, Ravaioli M, Ramacciato G, Grazi GL, Pinna AD. Is portal hypertension a contraindication to hepatic resection? Ann Surg. 2009; 250:922-928.
3. Ishizawa T, Hasegawa K, Aoki T, Takahashi M, Inoue Y, Sano K, Imamura H, Sugawara Y, Kokudo N, Makuuchi M. Neither multiple tumors nor portal hypertension are surgical contraindications for hepatocellular carcinoma. Gastroenterology. 2008; 134:1908-1916.
4. Ohkubo T, Midorikawa Y, Nakayama H, Moriguchi M, Aramaki O, Yamazaki S, Higaki T, Takayama T. Liver resection of hepatocellular carcinoma in patients with portal hypertension and multiple tumors. Hepatol Res. 2018; 48:433-441.
5. Lesurtel M, Clavien PA. Platelet-derived serotonin: translational implications for liver regeneration. Hepatology. 2014; 60:30-33.
6. Padickakudy R, Pereyra D, Offensperger F, Jonas P, Oehlberger L, Schwarz C, Haegele S, Assinger A, Brostjan C, Gruenberger T, Starlinger P. Bivalent role of intra-platelet serotonin in liver regeneration and tumor recurrence in humans. J Hepatol. 2017; 67:1243-1252.
7. Lisman T, Porte RJ. Mechanisms of platelet-mediated liver regeneration. Blood. 2016; 128:625-629.
8. Han S, Park HW, Song JH, Gwak MS, Lee WJ, Kim G, Lee SK, Ko JS. Association Between Intraoperative Platelet Transfusion and Early Graft Regeneration in Living Donor Liver Transplantation. Ann Surg. 2016; 264:1065-1072.
9. Yamazaki S, Takayama T, Mitsuka Y, Aoki M, Midorikawa Y, Moriguchi M, Higaki T. Platelet recovery correlates parenchymal volume recovery after liver resection. Hepatol Res. 2020; 50:620-628.
10. Alkozai EM, Nijsten MW, de Jong KP, de Boer MT, Peeters PM, Slooff MJ, Porte RJ, Lisman T. Immediate postoperative low platelet count is associated with delayed liver function recovery after partial liver resection. Ann Surg. 2010; 251:300-306.
11. Li L, Wang H, Yang J, Jiang L, Yang J, Wang W, Yan L, Wen T, Li B, Xu M. Immediate Postoperative Low Platelet Counts After Living Donor Liver Transplantation Predict Early Allograft Dysfunction. Medicine (Baltimore). 2015; 94:e1373.
12. Carr BI, Cavallini A, D'Alessandro R, Refolo MG, Lippolis C, Mazzocca A, Messa C. Platelet extracts induce growth, migration and invasion in human hepatocellular carcinoma *in vitro*. BMC Cancer. 2014; 14:43.
13. Labelle M, Begum S, Hynes RO. Direct signaling between platelets and cancer cells induces an epithelial-mesenchymal-like transition and promotes metastasis. Cancer Cell. 2011; 20:576-590.
14. D'Alessandro R, Refolo MG, Lippolis C, Giannuzzi G, Carella N, Messa C, Cavallini A, Carr BI. Antagonism of sorafenib and regorafenib actions by platelet factors in hepatocellular carcinoma cell lines. BMC Cancer. 2014; 14:351.
15. Shu B, Wang S, Deng Y, Zhai M, Liu S. Intra-platelet serotonin in prognosis of tumorigenesis: Friend or foe? J Hepatol. 2018; 68:1333-1334.
16. Liu PH, Hsu CY, Su CW, Huang YH, Hou MC, Rich NE, Fujiwara N, Hoshida Y, Singal AG, Huo TI. Thrombocytosis is associated with worse survival in patients with hepatocellular carcinoma. Liver Int. 2020 (*in press*)
17. Morimoto Y, Nouso K, Wada N, Takeuchi Y, Kinugasa H, Miyahara K, Yasunaka T, Kuwaki K, Onishi H, Ikeda F, Miyake Y, Nakamura S, Shiraha H, Takaki A, Yamamoto K. Involvement of platelets in extrahepatic metastasis of hepatocellular carcinoma. Hepatol Res. 2014; 44:E353-359.
18. Lee CH, Lin YJ, Lin CC, Yen CL, Shen CH, Chang CJ, Hsieh SY. Pretreatment platelet count early predicts extrahepatic metastasis of human hepatoma. Liver Int. 2015; 35:2327-2336.
19. Han S, Lee S, Yang JD, Leise MD, Ahn JH, Kim S, Jung K, Gwak MS, Kim GS, Ko KJS. Risk of posttransplant hepatocellular carcinoma recurrence is greater in recipients with higher platelet counts in living donor liver transplantation. Liver Transpl. 2018; 24:44-55.
20. Kokudo N, Hasegawa K, Akahane M, *et al.* Evidence-based Clinical Practice Guidelines for Hepatocellular Carcinoma: The Japan Society of Hepatology 2013 update (3rd JSH-HCC Guidelines). Hepatol Res. 2015; 45:123-127.
21. Makuuchi M, Kosuge T, Takayama T, Yamazaki S, Kakazu T, Miyagawa S, Kawasaki S. Surgery for small liver cancers. Semin Surg Oncol. 1993; 9:298-304.
22. Takayama T, Makuuchi M, Kubota K, Harihara Y, Hui AM, Sano K, Ijichi M, Hasegawa K. Randomized comparison of ultrasonic *vs.* clamp transection of the liver. Arch Surg. 2001; 136:922-928.
23. Dindo D, Demartines N, Clavien PA. Classification of surgical complications: a new proposal with evaluation in a cohort of 6336 patients and results of a survey. Ann Surg. 2004; 240:205-213.
24. Midorikawa Y, Kubota K, Takayama T, Toyoda H, Ijichi M, Torzilli G, Mori M, Makuuchi M. A comparative study of postoperative complications after hepatectomy in patients with and without chronic liver disease. Surgery. 1999; 126:484-491.
25. Midorikawa Y, Takayama T, Shimada K, Nakayama H, Higaki T, Moriguchi M, Nara S, Tsuji S, Tanaka M. Marginal survival benefit in the treatment of early hepatocellular carcinoma. J Hepatol. 2013; 58:306-311.
26. Nouso K, Ito Y, Kuwaki K, Kobayashi Y, Nakamura S, Ohashi Y, Yamamoto K. Prognostic factors and treatment effects for hepatocellular carcinoma in Child C cirrhosis. Br J Cancer. 2008; 98:1161-1165.
27. Scheiner B, Kirstein M, Popp S, Hucke F, Bota S, Rohr-Udilova N, Reiberger T, Müller C, Trauner M, Peck-Radosavljevic M, Vogel A, Sieghart W, Pinter M. Association of Platelet Count and Mean Platelet Volume with Overall Survival in Patients with Cirrhosis and Unresectable Hepatocellular Carcinoma. Liver Cancer. 2019; 8:203-217.
28. Yamamoto S, Midorikawa Y, Nagae G, Tatsuno K, Ueda H, Moriyama M, Takayama T, Aburatani H. Spatial and temporal expansion of intrahepatic metastasis by molecularly-defined clonality in multiple liver cancers. Cancer Sci. 2020; 111:601-609.
29. Cucchetti A, Piscaglia F, Caturelli E, Benvegnù L, Vivarelli M, Ercolani G, Cescon M, Ravaioli M, Grazi GL, Bolondi L, Pinna AD. Comparison of recurrence of hepatocellular carcinoma after resection in patients with cirrhosis to its occurrence in a surveilled cirrhotic

population. Ann Surg Oncol. 2009; 16:413-422.
30. Sasaki K, Shindoh J, Margonis GA, Nishioka Y, Andreatos N, Sekine A, Hashimoto M, Pawlik TM. Effect of Background Liver Cirrhosis on Outcomes of Hepatectomy for Hepatocellular Carcinoma. JAMA Surg. 2017; 152:e165059.
31. Pang Q, Qu K, Zhang JY, Song SD, Liu SS, Tai MH, Liu HC, Liu C. The Prognostic Value of Platelet Count in Patients With Hepatocellular Carcinoma: A Systematic Review and Meta-Analysis. Medicine (Baltimore). 2015;94:e1431.
32. Aramaki O, Takayama T, Higaki T, Nakayama H, Ohkubo T, Midorikawa Y, Moriguchi M, Matsuyama Y. Decreased blood loss reduces postoperative complications in resection for hepatocellular carcinoma. J Hepatobiliary Pancreat Sci. 2014;21:585-591.
33. Takahashi K, Liang C, Oda T, Ohkohchi N. Platelet and liver regeneration after liver surgery. Surg Today. DOI: 10.1007/s00595-019-01890-x.
34. Nathan H, Herlong HF, Gurakar A, Li Z, Koteish AA, Bridges JF, Pawlik TM. Clinical decision-making by gastroenterologists and hepatologists for patients with early hepatocellular carcinoma. Ann Surg Oncol. 2014;21:1844-1851.

Received June 18, 2020; Revised July14, 2020; Accepted July 20, 2020.

*Address correspondence to:
Yutaka Midorikawa, Department of Digestive Surgery, Nihon University School of Medicine, 30-1 Oyaguchi Kami-machi, Itabashi-ku, Tokyo 173-8610, Japan.
E-mail: mido-tky@umin.ac.jp

Released online in J-STAGE as advance publication July 25, 2020.

Original Article

DOI: 10.5582/bst.2020.03293

Safety and feasibility of laparoscopic versus open liver resection with associated lymphadenectomy for intrahepatic cholangiocarcinoma

Jia Wu[1,§], Junjun Han[2,§], Yuhua Zhang[1], Lei Liang[1], Junjun Zhao[2], Fang Han[1], Changwei Dou[1], Yuanbiao Zhang[1], Jie Liu[1], Weiding Wu[1], Zhiming Hu[1], Chengwu Zhang[1,*]

[1] Department of Hepatobiliary and Pancreatic Surgery & Minimally Invasive Surgery, Zhejiang Provincial People's Hospital & Hangzhou Medical College affiliated People's Hospital, Hangzhou, Zhejiang, China;
[2] Graduate Department, Bengbu Medical College, Bengbu, Anhui, China.

SUMMARY The safety and feasibility of laparoscopic versus open liver resection (LLR *vs.* OLR) associated lymphadenectomy for intrahepatic cholangiocarcinoma (ICC) are still controversial. The aim of the present study was to compare short and long-term outcomes. We reviewed data on 43 consecutive patients who underwent curative liver resection with associated lymphadenectomy for ICC. The short-term outcomes including postoperative morbidity and mortality, and the long-term outcomes including overall survival (OS) and recurrence-free survival (RFS) were compared. The median survival, 1- and 3-year OS in LLR and OLR groups were 22.5 months, 76.9% and 47.1%, and 12.1 months, 43.1% and 20.0%, respectively. The median survival, 1- and 3-year RFS in LLR and OLR groups were 10.3 months, 27.8% and 0%, and 8.1 months, 24.0% and 4.0%, respectively. The results showed that LLR obviously reduced intraoperative blood loss (median, 375 *vs.* 500ml, $p = 0.016$) and postoperative hospital stay (median, 6 *vs.* 9 days, $p = 0.016$). Moreover, there was no significant difference in short-term outcomes including postoperative morbidity (including wound infection, bile leakage, liver failure and pneumonia) and mortality within 30 days, and long-term outcomes including OS and RFS between LLR and OLR. (all $p > 0.05$). Multivariate analysis showed that CA19-9 level, TNM stage, and tumor differentiation were independent risk factors for OS and RFS. LLR for ICC is safety and feasibility compared with OLR. The advantage of LLR was to reduce intraoperative blood loss and postoperative hospital stay.

Keywords laparoscopy, intrahepatic cholangiocarcinoma, lymphadenectomy, liver resection.

1. Introduction

Intrahepatic cholangiocarcinoma (ICC) is the second most common primary liver cancer after hepatocellular carcinoma, which accounts for 10% to 20% of newly diagnosed liver cancers (*1*). The incidence of ICC has been rising on a global scale over the last twenty years, which may reflect both a true increase and the trend of earlier detection of the disease. Previous studies reported a 5-year survival for ICC ranging from 15% to 40% (*2*). Several clinicopathologic parameters, including lymph node metastasis, vascular invasion and multiple tumors, have been raised as potential prognostic factors determining clinical outcomes (*3,4*).

Liver resection remains the first-line curative treatment. Laparoscopic liver resection (LLR), which has progressed over the last 20 years, has become a feasible choice for various kinds of liver lesions owing to the development of high-tech surgical techniques and equipment. In 1995 and 1996, the minimally invasive liver resection series were reported (*5,6*). Since then, a minimally invasive approach to liver resection has been used in the treatment of a myriad of conditions, and exponential dissemination has been experienced (*7*). However, the safety and feasibility of LLR for ICC are still controversial. Although ICC is not a contraindication for LLR, debates focusing on the risks of positive surgical margins, massive hemorrhage and difficulty with lymphadenectomy in LLR still exist. Nowadays, few reports referring to LLR for ICC are available (8-10). In 2015, Billy et al reported 11 patients with ICC underwent LLR, and 26 patients underwent open liver resection (OLR) (*8*). The results indicated that LLR was technically safe and the survival was comparable to OLR. However, most of them did not include enough relevant data, such as lymph node dissection, postoperative adjuvant chemotherapy, *et al.*

In the present study, we aimed to compare short-

term outcomes including postoperative morbidity and mortality, and long-term outcomes including overall survival (OS) and recurrence-free survival (RFS) between LLR and OLR with associated lymphadenectomy for ICC.

2. Materials and Methods

2.1. Patient selection

A retrospective study was conducted on consecutive patients with ICC, who underwent curative liver resection and associated lymphadenectomy from Jan 2010 to Dec 2017 in Zhejiang Provincial People's Hospital, China. Curative liver resection was defined as removal of all microscopic and macroscopic tumors with a microscopically clear margin of surgical specimens (R0 resection). The resected tumors with surrounding liver tissues were examined histopathologically. Inclusion criteria were (*i*) age between 18 and 80 years, (*ii*) ICC confirmed by postoperative pathological result; (*iii*) patients with associated lymphadenectomy; (*iv*) patients who received postoperative adjuvant chemotherapy. Exclusion criteria included: (*i*) distal metastasis or macroscopic tumor thrombus in major portal/hepatic veins before operation, (*ii*) hilar cholangiocarcinoma or gallbladder cancer, (*iii*) a history of preoperative anticancer treatment, including biliary drainage. Informed consent was obtained from all the enrolled patients for their data to be utilized in clinical research. The present study was conducted in accordance with the Declaration of Helsinki and the Ethical Guidelines for Clinical Studies by the Institutional Ethics Committee of Zhejiang Provincial People's Hospital.

2.2. Diagnosis and surgical procedure

Enhanced computerized tomography (CT) or magnetic resonance (MR) were used to identify the type of tumor, relationship with adjacent tissue or organ and evaluate lymph node status routinely. Elevated carbohydrate antigen 19-9 (CA19-9) and carcinoma embryonic antigen (CEA) were another indicator for diagnosis of ICC. All patients underwent liver resection, with the intention of complete removal of macroscopic tumors, provided that the volume of the future liver remnant was estimated to be sufficient on CT or MR imaging volumetry. All patients were allocated into LLR or OLR group according to the different surgical approach. Major hepatectomy was defined as resection of three or more Couinaud's segments, while minor hepatectomy was resection of fewer than three segments.

For LLR, pringle maneuver was a commonly used method to block inflow of blood stream in the process of liver transection when severe bleeding occurred, which was implemented using an 8F rubber catheter wrapping around hepatoduodenal ligament and tightening the catheter when necessary. Harmonic scalpel and Cavitron Ultrasonic Surgical Aspirator (CUSA) were employed during liver parenchymal transection. The branches of Glisson system or hepatic vein toward the resected liver were ligated by non-absorbable clips. Regional lymphadenectomy was carried out routinely, which included hepatoduodenal ligament lymph nodes (Site 12). Fine rubber tapes were employed to hang bile duct, hepatic artery and portal vein, which could make lymph node dissection easy. Resected specimens were put into a plastic bag and retrieved from the enlarged subumbilical incision. Typical liver resection and lymph node dissection is demonstrated in Figure 1.

All patients received six courses of postoperative preventive chemotherapy, which consisted of Gemcitabine (Day 1, Day 8) plus S-1 (Day1-14), cycled 3 weeks 6 times.

2.3. Data collection and postoperative follow-up

The patient- and liver-related variables included age, sex, comorbid illnesses (consists of diabetes mellitus, cardiovascular disease, chronic obstructive pulmonary disease, and renal dysfunction history), ASA score, abdominal surgical history, and preoperative serum total bilirubin (TBIL). The tumor-related variables included preoperative CA19-9 level, CEA level, maximum size of tumor, TNM stage by AJCC (8^{th} edition), nerve invasion, and tumor differentiation (well, moderately or poorly). The operative variables included range of hepatectomy (minor or major), number of lymphadenectomy (≥ 6 or < 6), intraoperative blood loss, and length of surgery.

The postoperative follow-up protocol included physical examination, serum tumor marker levels (CEA, CA19-9), CT or MR scan every month for the first 3 months, and then every 3 months for the initial 2 years and every 6 months for the following years. Recurrence and Metastasis were judged by PET/CT. The short outcomes including postoperative hospital stay, morbidity (including wound infection, bile leakage, liver failure and pneumonia) and mortality within 30 days. The long-term outcomes include OS and RFS. OS was calculated as the interval between the date of operation and death for any reason, with censoring at the date of last follow-up. RFS was calculated from the date of liver resection to the date of first ICC recurrence or the date of the last follow-up.

2.4. Statistical analysis

Statistical analysis was performed using SPSS statistical software (IBM SPSS, Inc., Chicago, IL, version 26.0). Survival curves were draw and compared by GraphPad (GraphPad Software, Inc. version 6.0). Continuous variables were presented as median ± interquartile range (IQR), and compared between groups by Mann-Whitney *U* test. Categorical variables were demonstrated as

absolute numbers and compared between groups using the χ^2 test. Kaplan-Meier method and log-rank test were employed to analyze the difference of OS and RFS between LLR and OLR groups. Statistical significance was inferred at a two-tailed *P* value of < 0.05.

3. Results

3.1. Baseline characteristics

A total of 43 patients undergoing curative liver resection and lymphadenectomy for diagnosed ICC met the inclusion criteria and were included. Among them, 18 patients received LLR, and 25 patients underwent OLR. The baseline characteristics of the patients in the two groups are listed in Table 1. Intraoperative blood loss of LLR group was less than OLR group (375 *vs.* 500 mL, $p = 0.016$). There was no other difference between LLR and OLR in the aspect of the patient- and liver-related variables, the tumor-related variables and the operative variables.

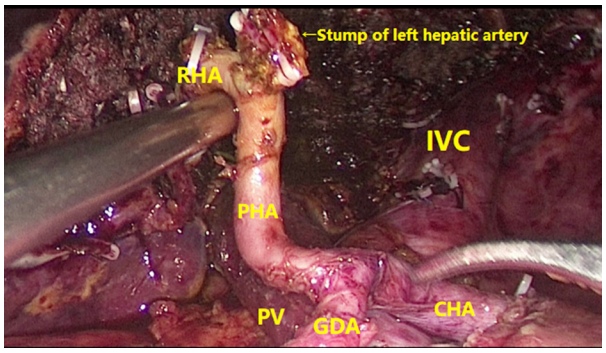

Figure 1. Typical figure of laparoscopic left hemi-hepatectomy and lymphadenectomy. RHA, right hepatic artery; IVC, inferior vein cava; PHA, primary hepatic artery; PV, portal vein; GDA, gastroduodenal artery; CHA, common hepatic artery.

3.2. Comparisons of short-term outcomes

The short outcomes including postoperative hospital stay, mortality (including wound infection, bile leakage, liver failure and pneumonia) and mortality within 30 days. As shown in Table 2, the results indicated that there was no significant difference in morbidity (including wound infection, bile leakage, liver failure and pneumonia) and mortality within 30 days (all $p > 0.05$). Moreover, the mortality was stratified by Dindo-Clavien classification (*11*), and the results also showed there were no significant differences between LLR and OLR groups ($p = 0.990$). In addition, compared to OLR, LLR obviously reduced postoperative hospital stay (6 *vs.* 9 days, $p = 0.016$).

3.3. Comparisons of the long-term OS and RFS

All 43 patients received six courses of postoperative preventive chemotherapy, which consisted of Gemcitabine (Day 1, Day 8) plus S-1 (Day1-14), cycled 3 weeks 6 times. The median survival time, 1- and 3-year overall survival (OS) in LLR and OLR groups were 22.5 months, 76.9% and 47.1%, and 12.1 months, 43.1% and 20.0%, respectively (Figure 2A). The median survival, 1- and 3-year recurrence-free survival (RFS) in LLR and OLR groups were 10.3 months, 27.8% and 0%, and 8.1 months, 24.0% and 4.0%, respectively (Figure 2B).

The site of recurrence included liver, lymph node, incisional or abdominal implantation, bone, *et al.* There was no obvious difference in recurrent site and rate between LLR and OLR groups (Table 2). Multivariate

Table 1. Baseline characteristics of the included patients

N, % or Median, IQR	LLR (18, 41.9%)	OLR (25, 58.1%)	*p*
The patient- and liver-related variables			
Age, years	64 (60-72)	61 (55-64)	0.100
Sex, male	12 (67)	10 (40)	0.084
Comorbid illnesses	5 (12)	7 (28)	0.987
ASA score, ≤ 2	15 (83)	19 (76)	0.839
Abdominal surgical history	3 (16)	7 (28)	0.616
Total bilirubin, > 24 μmol/L	3 (16)	8 (32)	0.648
The tumor-related variables			
CA19-9 level, > 200 U/mL	8 (44)	14 (56)	0.455
CEA level, > 5μg/L	7 (39)	10 (40)	0.914
TNM stage			
IA+IB	7 (39)	17 (68)	0.058
II+III	11 (61)	8 (32)	
Nerve invasion	4 (22)	9 (36)	0.332
Vascular invasion	4 (22)	9 (36)	0.332
Tumor differentiation, poor	14 (78)	17 (68)	0.480
The operative variables			
Range of hepatectomy, major	6 (33)	13 (52)	0.224
Number of lymphadenectomy, ≥ 6	6 (33)	8 (32)	0.927
Intraoperative blood loss, mL	375 (275-500)	500 (350-750)	0.016
Length of surgery, min	305 (207-390)	300 (257-392)	0.730

Table 2. Comparing the short and long-term outcomes between laparoscopic versus open liver resection

N, % or Median, IQR	LLR (18, 41.9%)	OLR (25, 58.1%)	*p*
Mortality within 30 days	0 (0)	1(4)	1.000
Postoperative hospital stays, days	6 (5-12)	9 (7-15)	0.001
Postoperative Complication			
Wound Infection	0 (0)	2 (8)	0.502
Bile Leakage	1 (6)	2 (8)	1.000
Liver Failure	0 (0)	1 (4)	1.000
Pneumonia	2 (11)	2 (8)	1.000
Dindo-Clavien classification			
1-2	17 (94)	23 (92)	0.990
3-4	1 (6)	2 (8)	1.000
Median OS, months	22.5	12.1	0.073
1-year OS, %	76.9	43.1	0.177
3-year OS, %	47.1	20.0	0.819
Median RFS, months	10.3	8.1	0.409
1-year RFS, %	27.8	24.0	0.348
3-year RFS, %	0	4.0	0.750
Postoperative Recurrence Site			
Liver	7 (39)	11 (44)	0.738
Lymph Node	3 (17)	3 (12)	1.000
Incisional or abdominal Implantation	4 (22)	3 (12)	1.000
Bone	1 (6)	4 (14)	0.567
Others	2 (11)	3 (12)	0.990

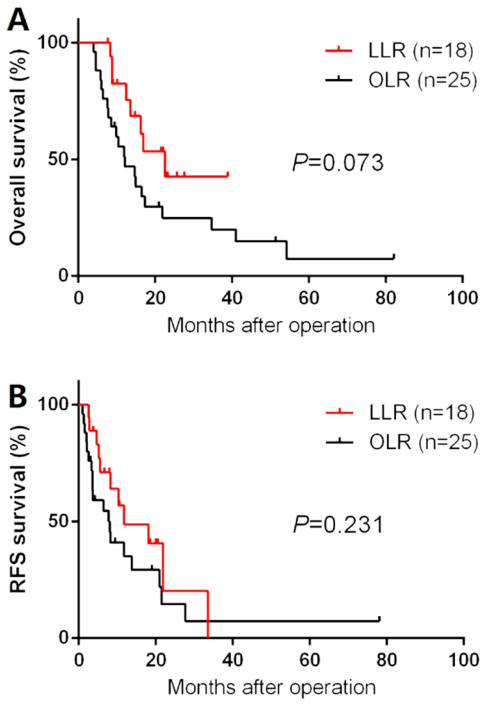

Figure 2. Comparisons of overall survival (A) and recurrence-free survival (B) curves between LLR and OLR groups.

analysis showed that CA19-9 level, TNM stage, and tumor differentiation were independent risk factors for the OS (Table 3) and RFS (Table 4).

3.4. Subgroup analysis of overall survival between LLR and OLR groups

We further analyzed the OS stratified by TNM stage (IA+IB, II+III), CA19-9 (≥ 200 U/mL, < 200 U/mL), number of lymphadenectomy (≥ 6, < 6) and differentiation grade (well or moderately, poor). The cut-off points of CA19-9 and number of dissected lymph nodes were set at 200U/mL and 6 respectively, which were considered as a high-risk factor and recommended number for postoperative staging (*12*) (Figure 3). The results from the subgroup analysis showed there were no significant differences between LLR and OLR groups (all $p > 0.05$).

4. Discussion

In the present study, 43 patients with ICC were retrospectively analyzed, who received liver resection and associated lymphadenectomy, and postoperative adjuvant chemotherapy in our hospital. The results showed that LLR obviously reduced intraoperative blood loss and postoperative hospital stay. Moreover, there was no significant difference in the short-term outcomes including postoperative morbidity (including wound infection, bile leakage, liver failure and pneumonia) and mortality within 30 days, and long-term outcomes (including OS and RFS) between LLR and OLR (all $p > 0.05$). Multivariate analysis showed that CA19-9 level, TNM stage, and tumor differentiation were independent risk factors for the OS and RFS.

The technology of laparoscopy has evolved rapidly in recent years, ultra-high definition (UHD) camera and display system and electrosurgical instruments were employed in the surgery, which could provide a clear field and better hemostatic control for the surgeons. By this Amplifying effect of laparoscopy, LLR achieved less intraoperative blood loss than OLR.

Table 3. Univariable and multivariable Cox-regression analyses on risk factors of overall survival

Variables	Comparison	UV		MV	
		HR (95%CI)	*p*	HR (95%CI)	*p*
Age, years	continuous, years	0.965 (0.916-1.016)	0.173		
Sex, male	male *vs.* female	1.403 (0.672-2.928)	0.367		
Comorbid illnesses	with *vs.* without	0.556 (0.267-1.157)	0.116		
ASA score	> 2 *vs.* ≤ 2	0.822 (0.332-2.036)	0.671		
Abdominal surgical history	with *vs.* without	1.253 (0.596-2.642)	0.550		
Total bilirubin	> 24 *vs.* ≤ 24 mmol/L	1.047 (0.474-2.309)	0.910		
CA19-9 level	> 200 *vs.* ≤ 200 U/mL	4.445 (1.791-11.034)	0.001	2.219 (1.632-3.017)	< 0.001
CEA level	> 5 *vs.* ≤ 5 μg/L	1.545 (0.742-3.204)	0.246		
TNM stage	II+III *vs.* IA+IB	2.357 (1.091-5.092)	0.029	2.098 (1.671-2.634)	< 0.001
Nerve invasion	with *vs.* without	1.590 (0.740-3.416)	0.235		
Vascular invasion	with *vs.* without	2.264 (0.990-5.180)	0.053		
Tumor differentiation	poor *vs.* well or moderately	2.865 (1.261-6.513)	0.012	1.524 (1.093-2.126)	0.013
Range of hepatectomy	major *vs.* minor	0.884 (0.422-1.851)	0.743		
Number of lymphadenectomy	< 6 *vs.* ≥ 6	1.916 (0.893-4.109)	0.095	NS	
Intraoperative blood loss	continuous, mL	0.999 (0.996-1.012)	0.532		
Length of surgery	continuous, min	1.000 (0.998-1.0)	0.905		

*Those variables found significant at $P < 0.10$ in univariable analyses were entered into multivariable analyses. HR, hazard ratio; UV, univariable; MV, multivariable; CI, Confidence interval; NS, no significance.

Table 4. Univariable and multivariable Cox-regression analyses on risk factors of recurrence-free survival

Variables	Comparison	UV		MV	
		HR (95%CI)	*p*	HR (95%CI)	*p*
Age, years	continuous, years	0.964(0.897-1.003)	0.169		
Sex, male	male *vs.* female	1.401(0.603-2.549)	0.369		
Comorbid illnesses	with *vs.* without	0.555(0.371-1.640)	0.115		
ASA score	> 2 *vs.* ≤ 2	0.821(0.370-2.123)	0.670		
Abdominal surgical history	with *vs.* without	1.253(0.371-1.719)	0.552		
Total bilirubin	> 24 *vs.* ≤ 24 mmol/L	1.046(0.414-2.127)	0.912		
CA19-9 level	> 200 *vs.* ≤ 200 U/mL	4.438(1.261-6.830)	0.001	3.405 (2.684-4.318)	< 0.001
CEA level	> 5 *vs.* ≤ 5 μg/L	1.545(0.784-3.476)	0.244		
TNM stage	II + III *vs.* IA+IB	2.362(0.964-4.212)	0.029	2.268 (1.840-2.795)	0.001
Nerve invasion	with *vs.* without	1.587(0.749-3.171)	0.236		
Vascular invasion	with *vs.* without	2.260(0.741-3.640)	0.053		
Tumor differentiation	poor *vs.* well or moderately	2.861(1.172-5.715)	0.012	1.885 (1.485-2.392)	0.029
Range of hepatectomy	major *vs.* minor	0.885(0.498-2.114)	0.747		
Number of lymphadenectomy	< 6 *vs.* ≥ 6	1.913(1.303-6.236)	0.096	NS	
Intraoperative blood loss	continuous, mL	0.999(0.996-1.010)	0.528		
Length of surgery	continuous, min	1.000(0.998-1.002)	0.898		

*Those variables found significant at $P < 0.1$ in univariable analyses were entered into multivariable analyses. HR, hazard ratio; UV, univariable; MV, multivariable; CI, Confidence interval; NS, no significance.

Masateru *et al.* reported intraoperative blood loss of LLR was less than OLR in patients of hepatocellular carcinoma with liver cirrhosis (*13*). Likewise, a similar outcome was confirmed by Cai *et al.*, who compared 145 cases of LLR with 190 cases OLR in recurrent hepatocellular carcinoma (*14*). Hadrien *et al.* suggested a pneumoperitoneum of 10-14 mmHg should be used as it allows good control of the bleeding, by which positive abdominal pressure could be seen as a factor to reduce intraoperative blood loss in LLR (*15*). More and more authors have reported their experience on LLR for ICC, and most of them have achieved satisfactory results, or at least not inferior (*9,16*). Billy *et al.* reported 6 patients with stage I and 5 patients with stage II/III (7th AJCC), who underwent laparoscopic liver resection and selectively LND. Finally, it suggested non-inferior oncological outcomes compared with 26 cases LLR (17 cases of stage I, 9 cases of stage II/III) (*8*) . In our study, 11 patients in stage I and 17 patients in stage I were involved in LLR and OLR groups respectively. and 7 patients underwent LLR and 8 patients underwent OLR in stage II/III. Moreover, all patients of LLR and OLR received regional lymphadenectomy (removed hepatoduodenal ligament lymph nodes). As a result, OS of LLR with regular lymphadenectomy group achieved identical outcomes with OLR compared with regular lymphadenectomy group, not only in the patients in stage I, but also those in stage II/III.

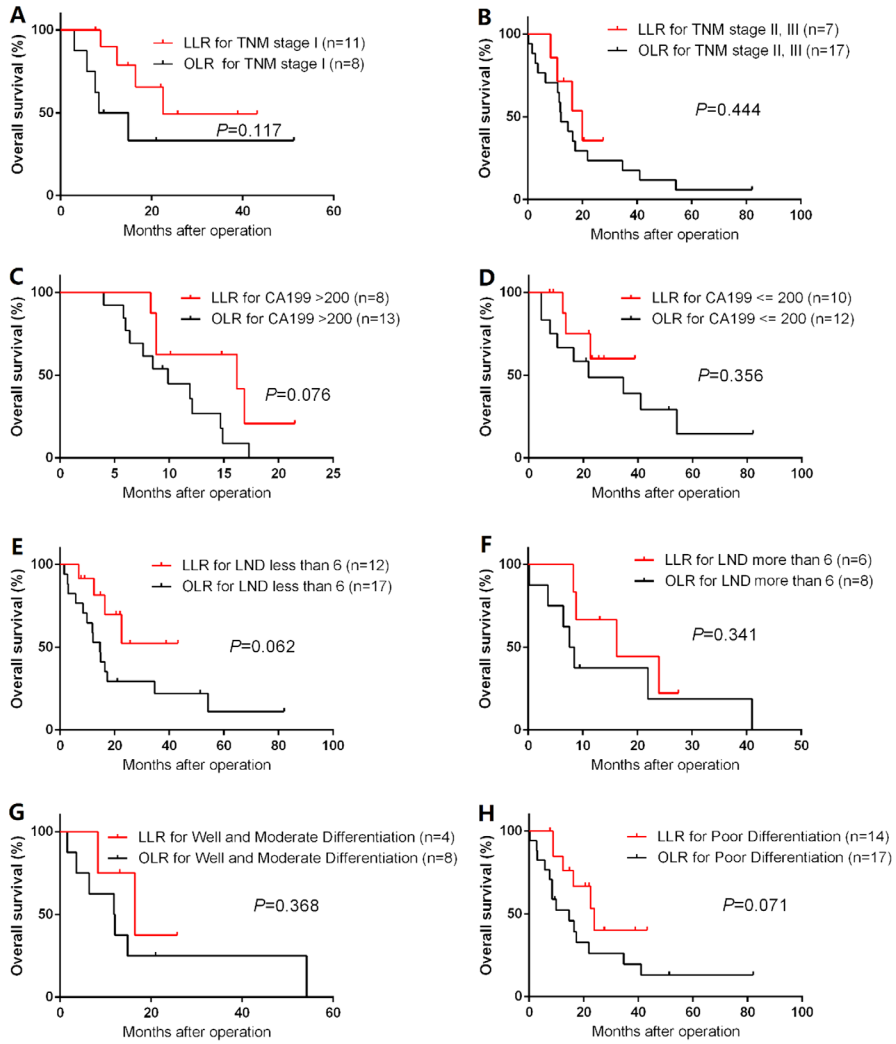

Figure 3. Subgroup analysis of overall survival stratified by TNM stage, CA19-9, number of lymphadenectomy and tumor differentiation.

Some published papers have demonstrated TNM stage, tumor differentiation, preoperative and CA19-9 level as important determinants of prognosis (*9,17*). The present study also indicated that TNM stage, tumor differentiation and preoperative CA19-9 level were independent risk factors associated with poor survival. We further analyzed the difference stratified by TNM stage, tumor differentiation and preoperative CA19-9 level between LLR and OLR groups. The results indicated that these risk factors did not influence the prognosis between LLR and OLR groups.

Whether to perform lymphadenectomy and the range of lymphadenectomy in LLR are still controversial. Li *et al.* suggested ICC patients without lymph node involvement and patients with multiple tumors and lymph node metastases may not benefit from aggressive lymphadenectomy (*18*). Consensus statement from AHPBA declared that regional lymphadenectomy should be considered a standard part of surgical therapy for patients undergoing resection of ICC (*19*), because the incidence of nodal disease was high, with some studies showing lymph node metastasis in as many as 40% of patients (*17,20,21*). However, some studies suggested that lymphadenectomy did not significantly improve prognosis, however, lymphadenectomy might be useful for nodal staging (*22,23*). Based on this experience, we performed lymphadenectomy regularly, and the results in this study also demonstrated that increasing retrieved lymph node count or extended lymph node dissection was not associated with a survival benefit among patients who underwent curative surgical resection for ICC. Lymph node status, however, was prognostically important as patients with lymph node metastasis had a markedly worse long-term prognosis. Retrieval of 6 lymph nodes at the time of surgery was associated with the identification of more lymph node positive patients and therefore should be used as the goal cut-off value to avoid under-staging patients with ICC. In the aspect of range of lymphadenectomy, consensus of AHPBA recommended that lymph nodes of hepatoduodenal ligament (site 12) and common hepatic duct (site 8a) should be removed in 2015.

Besides, for ICC originating from right hemiliver, the retropancreatic lymph nodes (site 13) may be involved; if ICC is located in left hemiliver, in addition to above-mentioned lymph nodes, the nodes around the cardiac portion of the stomach and along the lesser curvature (site 1 and 3) should also be removed. Similarly, Chinese experts recommended that lymphadenectomy for ICC should cover site 8, 12 and 13, which was suggested by Chinese Society of Clinical Oncology (CSCO) in 2019. The deadline for the cases we studied was 2017, and the majority of our cases (31/43) underwent their surgery before those consensuses were issued. To the best of our knowledge at that time, range of LND was limited in site 12.

CA19-9 ≥ 200U/mL was identified as a negative prognostic factor in patients without preoperative jaundice, according to 8th AJCC guideline. In our study, 18 patients in LLR group and 25 patients in OLR group divided into two subgroups by setting the cut-off point of CA19-9 at 200U/mL. OS in LLR group did not differ with the OLR group with and without this high-risk feature. Elevated preoperative CA19-9, thus, should not be considered as a contraindication of LLR for ICC patients. Poor differentiation has been demonstrated as another independent risk factor for prognosis. The underling mechanism may be that this kind of tumor cells are more likely to metastasize (*24*).

This study had several limitations. First, this study is not a randomized controlled trail and therefore biases in patient's selection may exist. Second, to make the results robust, only 43 patients were included. However, all patients were carefully selected to include only those with associated lymphadenectomy and postoperative adjuvant chemotherapy. Third, though all the patients received associated lymphadenectomy, we did not further analyze the number and range of positive lymph nodes. Fourth, though all the patients received 6 course of adjuvant chemotherapy, we did not further analyze the role and complication of chemotherapy, especially for different TNM stage. Fifth, there was no statistically significant difference in OS or RFS between the two groups in this study. However, the sample size of both groups was small, and the follow-up time of LLR group was short. Sixth, LLR has achieved equal OS with OLR, but proportion of TNM stage II/III of LLR was higher than OLR (61.1% *vs*. 32.0%, $p > 0.05$). Statistically, there was no significant difference between the two groups, this phenomenon may be associated with small-size sample, which could be affected by extremum easily. Moreover, shorter follow-up time of LLR was likely the cause.

In conclusion, the present study demonstrated LLR for ICC is safe and feasible compared with OLR. The advantage for LLR was to reduce intraoperative blood loss and postoperative hospital stay. Furthermore, future randomized controlled trials are still needed to better define the role of LLR.

References

1. Bergquist A, von Seth E. Epidemiology of cholangiocarcinoma. Best Pract Res Clin Gastroenterol. 2015; 29:221-232.
2. Bridgewater J, Galle PR, Khan SA, Llovet JM, Park JW, Patel T, Pawlik TM, Gores GJ. Guidelines for the diagnosis and management of intrahepatic cholangiocarcinoma. J Hepatol. 2014; 60:1268-1289.
3. Wang Y, Li J, Xia Y, Gong R, Wang K, Yan Z, Wan X, Liu G, Wu D, Shi L, Lau W, Wu M, Shen F. Prognostic nomogram for intrahepatic cholangiocarcinoma after partial hepatectomy. J Clin Oncol. 2013; 31:1188-1195.
4. Hwang S, Lee YJ, Song GW, Park KM, Kim KH, Ahn CS, Moon DB, Lee SG. Prognostic Impact of Tumor Growth Type on 7th AJCC Staging System for Intrahepatic Cholangiocarcinoma: a Single-Center Experience of 659 Cases. J Gastrointest Surg. 2015; 19:1291-1304.
5. Hashizume M, Takenaka K, Yanaga K, Ohta M, Kajiyama K, Shirabe K, Itasaka H, Nishizaki T, Sugimachi K. Laparoscopic hepatic resection for hepatocellular carcinoma. Surg Endosc. 1995; 9:1289-1291.
6. Kaneko H, Takagi S, Shiba T. Laparoscopic partial hepatectomy and left lateral segmentectomy: technique and results of a clinical series. Surgery. 1996; 120:468-475.
7. Ciria R, Cherqui D, Geller DA, Briceno J, Wakabayashi G. Comparative Short-term Benefits of Laparoscopic Liver Resection: 9000 Cases and Climbing. Ann Surg. 2016; 263:761-777.
8. Uy BJ, Han HS, Yoon YS, Cho JY. Laparoscopic liver resection for intrahepatic cholangiocarcinoma. J Laparoendosc Adv Surg Tech A. 2015; 25:272-277.
9. Lee W, Park JH, Kim JY, Kwag SJ, Park T, Jeong SH, Ju YT, Jung EJ, Lee YJ, Hong SC, Choi SK, Jeong CY. Comparison of perioperative and oncologic outcomes between open and laparoscopic liver resection for intrahepatic cholangiocarcinoma. Surg Endosc. 2016; 30:4835-4840.
10. Kinoshita M, Kanazawa A, Takemura S, Tanaka S, Kodai S, Shinkawa H, Shimizu S, Murata A, Nishio K, Hamano G, Ito T, Tsukamoto T, Kubo S. Indications for laparoscopic liver resection of mass-forming intrahepatic cholangiocarcinoma. Asian J Endosc Surg. 2020; 13:46-58.
11. Dindo D, Clavien PA. What is a surgical complication? World J Surg. 2008; 32:939-941.
12. Lee AJ, Chun YS. Intrahepatic cholangiocarcinoma: the AJCC/UICC 8th edition updates. Chin Clin Oncol. 2018; 7:52.
13. Yamamoto M, Kobayashi T, Oshita A, Abe T, Kohashi T, Onoe T, Fukuda S, Omori I, Imaoka Y, Honmyo N, Ohdan H. Laparoscopic versus open limited liver resection for hepatocellular carcinoma with liver cirrhosis: a propensity score matching study with the Hiroshima Surgical study group of Clinical Oncology (HiSCO). Surg Endosc. 2019.
14. Cai W, Liu Z, Xiao Y, Zhang W, Tang D, Cheng B, Li Q. Comparison of clinical outcomes of laparoscopic versus open surgery for recurrent hepatocellular carcinoma: a meta-analysis. Surg Endosc. 2019; 33:3550-3557.
15. Tranchart H, O'Rourke N, Van Dam R, Gaillard M, Lainas P, Sugioka A, Wakabayashi G, Dagher I. Bleeding control during laparoscopic liver resection: a review of literature. J Hepatobiliary Pancreat Sci. 2015; 22:371-378.
16. Waisberg DR, Pinheiro RS, Nacif LS, Rocha-Santos V, Martino RB, Arantes RM, Ducatti L, Lai Q, Andraus

W, D'Albuquerque LC. Resection for intrahepatic cholangiocellular cancer: new advances. Transl Gastroenterol Hepatol. 2018; 3:60.
17. Ribero D, Pinna AD, Guglielmi A, *et al.* Surgical Approach for Long-term Survival of Patients With Intrahepatic Cholangiocarcinoma: A Multi-institutional Analysis of 434 Patients. Arch Surg. 2012; 147:1107-1113.
18. Li DY, Zhang HB, Yang N, Quan Y, Yang GS. Routine lymph node dissection may be not suitable for all intrahepatic cholangiocarcinoma patients: results of a monocentric series. World J Gastroenterol. 2013; 19:9084-9091.
19. Weber SM, Ribero D, O'Reilly EM, Kokudo N, Miyazaki M, Pawlik TM. Intrahepatic cholangiocarcinoma: expert consensus statement. HPB (Oxford). 2015; 17:669-680.
20. Luo X, Yuan L, Wang Y, Ge R, Sun Y, Wei G. Survival outcomes and prognostic factors of surgical therapy for all potentially resectable intrahepatic cholangiocarcinoma: a large single-center cohort study. J Gastrointest Surg. 2014; 18:562-572.
21. Endo I, Gonen M, Yopp AC, *et al.* Intrahepatic cholangiocarcinoma: rising frequency, improved survival, and determinants of outcome after resection. Ann Surg. 2008; 248:84-96.
22. Shimada M, Yamashita Y, Aishima S, Shirabe K, Takenaka K, Sugimachi K. Value of lymph node dissection during resection of intrahepatic cholangiocarcinoma. Br J Surg. 2001; 88:1463-1466.
23. Kim DH, Choi DW, Choi SH, Heo JS, Kow AW. Is there a role for systematic hepatic pedicle lymphadenectomy in intrahepatic cholangiocarcinoma? A review of 17 years of experience in a tertiary institution. Surgery. 2015; 157:666-675.
24. Blok P, Craanen ME, Dekker W, Tytgat GN. Loss of E-cadherin expression in early gastric cancer. Histopathology. 1999; 34:410-415.

Received August 7, 2020; Revised September 4, 2020; Accepted September 8, 2020.

[§]These authors contributed equally to this work.

**Address correspondence to:*
Chengwu Zhang, Department of Hepatobiliary and Pancreatic Surgery & Minimally Invasive Surgery, Zhejiang Provincial People's Hospital & Hangzhou Medical College affiliated People's Hospital, 158 Shangtang RD, Hangzhou 310014, Zhejiang, China.
E-mail: zcwzry@163.com

Released online in J-STAGE as advance publication September 11, 2020.

Original Article

DOI: 10.5582/bst.2020.03303

Predictive value of perfusion CT for blood loss in liver resection

Shintaro Yamazaki, Tadatoshi Takayama*, Yusuke Mitsuka, Nao Yoshida, Atsuko Hosaka, Takaharu Kawai, Hayato Abe, Tokio Higaki

Department of Digestive Surgery, Nihon University School of Medicine, Tokyo, Japan.

SUMMARY Blood loss is associated with the degree of damage in liver stiffness. Severe liver steatosis is a matter of concern in liver surgery, but does not correlate with liver stiffness. This study aimed to assess the relationship between blood perfusion of the liver and blood loss in liver pathologies. Data from elective liver resection for liver cancer were analyzed. All patients underwent preoperative assessments including perfusion CT. Patients were divided into 4 groups in accordance with the pathological background of liver parenchyma. Relationships between portal flow as assessed by perfusion CT and perioperative variables were compared. Factors correlating with blood loss were analyzed. In 166 patients, portal flow from perfusion CT correlated positively with platelet count and negatively with indocyanine green retention rate at 15 min. Background liver pathology was normal liver (NL) in 43 cases, chronic hepatitis (CH) in 56, liver cirrhosis (LC) in 42, and liver steatosis (LS) in 25. Rates of hepatitis viral infection and pathological hepatocellular carcinoma were more frequent in LC and CH groups than in the other groups ($p < 0.05$). LC and LS showed significantly worse liver function than the NL and CH groups. Portal flow from perfusion CT correlated positively with damage to liver parenchyma and negatively with blood loss at liver transection. Low portal flow on perfusion CT predicts blood loss during liver transection.

Keywords liver perfusion, blood loss, liver steatosis

1. Introduction

The liver shows unique blood flow characteristics, with two sets of inflow vessels (hepatic artery and portal artery flows) and one set of outflow vessels (hepatic veins). The amount of blood flow changes depending on the background liver parenchyma damage, such as cirrhosis, liver fibrosis, chemotherapy-associated steatohepatitis (CASH) and obstacle jaundice (*1-3*). However, the hemodynamics of the diseased liver are complex and not yet fully understood.

Measurement of liver stiffness by MRI or ultrasonography is a convenient, less-stressful method to assess damage to the background liver parenchyma (*4,5*). During liver resection, a correlation has been confirmed between blood loss and liver stiffness and a significant relationship is known to exist between intraoperative blood loss and morbidity (*6-8*). Evaluation of the background liver damage is thus key to avoiding severe complications.

With colorectal metastasis, perioperative chemotherapy is a common strategy that sometimes results in severe liver steatosis (*9,10*). CASH involves secondary damage to the liver parenchyma from chemotherapy and represents a risk for liver resection (*10,11*). Differing from liver cirrhosis, the parenchyma of a liver showing severe steatosis is soft and fragile, making liver stiffness hard to assess by conventional testing (*4-8*). Perfusion CT enables estimation of blood flow and volume in independent vessels and the mean transit time of blood (*2,3,12*). This may contribute to a better understanding of the etiology of liver damage. The aim of this study was thus to clarify whether parameters from perfusion CT correlate with liver function and can predict blood loss during liver transection.

2. Materials and Methods

2.1. Study design

Between April 2012 and December 2013, perioperative data including perfusion CT were collected from patients who underwent hepatic resection for liver cancer. First, preoperative data concerning liver function (indocyanine green retention rate at 15 min ($ICGR_{15}$) and platelet count) were evaluated for correlations with parameters from perfusion CT. Portal blood flow from perfusion CT was assessed on the basis of the histological difference

of the background liver parenchyma. Finally, the relationship between portal flow from perfusion CT and intraoperative blood loss was analyzed. Written informed consent for clinical analysis was obtained from each patient. This clinical study was approved by the institutional review board of the Nihon University Itabashi Hospital (IRB. RK200114-10).

2.2. Perfusion CT analysis

A 320-detector row CT system (Aquilion One; Toshiba Medical Systems, Tochigi, Japan) was used for perfusion CT. Scan area of the perfusion CT was the whole liver, spleen and pancreas. To minimize respiratory-induced motion of the liver, each patient maintained natural breathing, but a crumpled towel was fixed to the subcostal abdominal wall using an elastic binder during scanning. Circular regions of interest (ROIs) were placed in the aorta, portal vein, right and left lobes of the liver, spleen and pancreas. The median value from five ROIs in the liver parenchyma was used as the representative value for the liver. The size of each ROI was ≥ 1.0 cm^2. Body Registration software (Toshiba Medical System, Tochigi, Japan) was used to automatically correct for the spatially inconsistent positions of each organ. Perfusion parameters (portal flow, arterial flow, perfusion index) were calculated on a pixel-by-pixel basis using the maximum slope model (Body Perfusion; Toshiba Medical System), with results expressed in units of milliliters per 100 milliliters per minute.

2.3. Blood loss measurement

The amount of blood loss was independently measured during liver transection. Blood loss per transection area of the liver (mL/cm^2) was estimated based on the shape of the transection plane, as traced onto a piece of paper that was digitally photographed (Adobe Photoshop Elements® 14 software; Adobe System, San Jose, CA). Blood loss per transection area (mL/cm^2) was calculated as blood loss divided by transection area.

2.4. Pathological evaluation

Patients were divided into four categories on the basis of the background liver parenchyma: normal liver (NL), chronic hepatitis (CH), liver cirrhosis (LC) and severe liver steatosis (LS), respectively. The New Inuyama classification was used to assess degree of fibrosis in the liver (grade 0-4) and inflammation (grade 0-3) by two independent pathologists (*13*). To assess the degree of liver steatosis, the Brunt scoring system (fat deposits in < 33%, 33-66%, or > 66% of hepatocytes) was used (*14*). Complications were defined according to the Clavien-Dindo classification and severe grade was defined as grade III or above (*15*).

2.5. Statistical analysis

Data are expressed as medians and ranges or as absolute values and percentages. Student's *t*-test, the χ^2 test, and Fisher's exact test were used, as appropriate. For multiple comparisons between different groups, the Bonferroni test was used. Values of $p < 0.05$ were considered indicative of statistical significance. Cutoff values and correlation coefficients for each variable were obtained from a receiver operating characteristic (ROC) curve. All analyses were performed using JMP version 13.2 statistical software (SAS Institute, Cary, NC, USA).

3. Results

3.1. Patients

Data from 301 patients who underwent hepatic resection for liver cancer between April 2012 and December 2013 were included. Of these, 99 patients were excluded because of unsuitability for imaging studies; repeat resection ($n = 64$), macrovascular invasion ($n = 23$) and large tumor > 10 cm in diameter or > 5 cm for bilobar tumors ($n = 12$). Among them, 36 patients were excluded because of other reasons; lack of or abnormal $ICGR_{15}$ data ($n = 11$), lack of informed consent obtained from patients ($n = 11$), placement of a drainage tube to treat obstructive jaundice ($n = 8$), and an inability to resect the tumor ($n = 6$). (Figure 1).

3.2. Preoperative data by background liver parenchyma

After pathological evaluation of the resected specimen, patients were divided into four groups on the basis of the background liver parenchyma: NL group ($n = 43$); CH group ($n = 56$); LC group ($n = 42$); and LS group ($n = 25$) (Table 1). Regarding the analysis of raw data, significant differences were observed in the rate of hepatocellular carcinoma ($p < 0.001$) and hepatitis viral infection ($p < 0.001$). In terms of liver function, significant differences were observed in preoperative platelet count and $ICGR_{15}$ ($p < 0.001$).

3.3. Relationship between portal flow and preoperative liver functions

In terms of preoperative data, patients were divided into 3 categories by platelet count (≤ 10^4/μL, 10^4-3 × 10^4/μL and > 3 × 10^4/μL) and compared in terms of portal flow on perfusion CT (Figure 2). Significant differences were evident between groups and significant positive correlations were apparent between platelet count and portal flow. Patients were divided into 4 categories by $ICGR_{15}$: ≤ 10%; 10-20%; 20-30%; and > 30% (Figure 3). Significant differences were seen between groups and a significant negative correlation was identified between platelet count and portal flow.

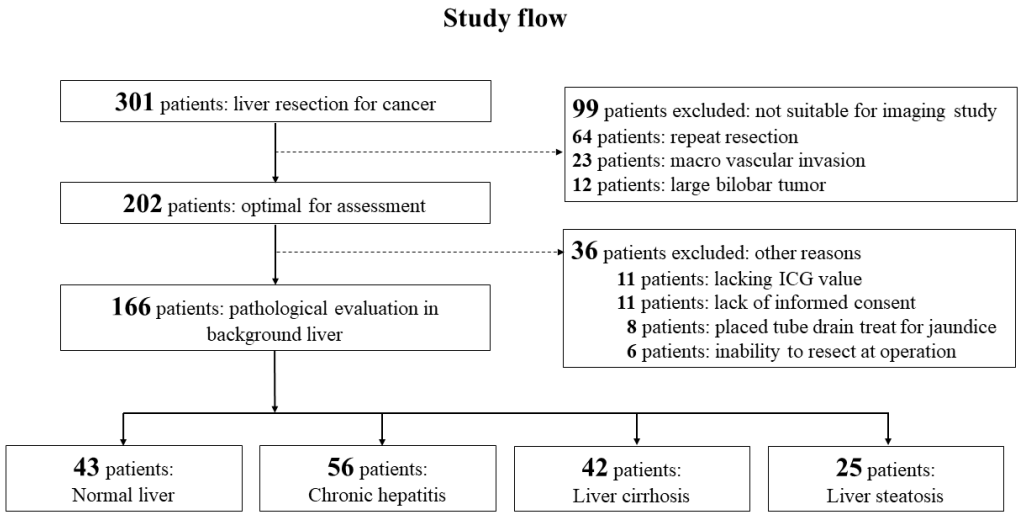

Figure 1. Study flow. Patients were divided into 4 groups based on the background liver. $ICGR_{15}$, indocyanine green retention rate at 15 min.

Table 1. Patient characteristics by back ground pathological liver parenchyma

	Normal liver (n = 43)	Chronic hepatitis (n = 56)	Liver cirrohsis (n = 42)	Liver steatosis (n = 25)	p-value
Gender (male, %)	27 (62.8)	44 (78.6)	29 (69.1)	19 (76.0)	0.340
Age (years)	66 (40-83)	69 (40-83)	68 (46-79)	67 (47-78)	0.870
Body mass index	22.3 (16.1-31.1)	23.6 (16.8-30.2)	23.4 (17.8-33.3)	24.3 (17.7-31.0)	0.621
Tumor diameter (mm)	30 (12-115)	25 (14-130)	26 (10-137)	28 (10-133)	0.416
Number of tumor	1 (1-11)	1 (1-5)	1 (1-3)	1 (1-3)	0.841
Hepatocellular carcinoma (%)	15 (34.9)	44 (78.6)	38 (90.0)	9 (36.0)	< 0.001
Colorectal metastasis	19 (44.2)	11 (19.6)	3 (7.1)	16 (64.0)	< 0.001
Gallbladder cancer	8 (18.6)	1 (1.8)	0	0	
Others	1 (2.3)	0	1 (2.4)	0	
Hepatitis viral infection (%)	9 (20.9)	21 (37.5)	23 (54.8)	3 (1.2)	< 0.001
History of chemotherapy	4 (9.3)	1 (1.8)	0	16 (64.0)	< 0.001
Aspartate aminotransferase (IU/L)	28 (14-93)	34.5 (13-118)	53 (21-205)	32 (14-222)	0.284
Alanine aminotransferase (IU/L)	20 (8-201)	32.7 (10-158)	47.5 (16-106)	29 (8-315)	0.128
Albumin (g/dL)	4.2 (2.9-4.9)	4.0 (3.1-4.8)	3.6 (2.7-4.4)	4.0 (3.3-4.8)	0.113
Bilirubin (mg/dL)	0.54 (0.26-1.59)	0.63 (0.23-1.87)	0.82 (0.27-1.96)	0.24 (0.24-1.74)	0.167
Prothrombin activity (%)	100 (47-100)	97.5 (38-100)	92.5 (63-100)	99 (36-100)	0.501
Platelet count (10^4/μL)	20.5 (10.9-44.3)	15.7 (4.3-74.2)	9.9 (4.0-19.5)	20.0 (7.3-39.5)	< 0.001
ICG-R15* (%)	8.1 (2.9-19.4)	3.3 (12.7-44.9)	17.8 (7.4-54.5)	11.7 (3.5-37.7)	< 0.001

Data are expressed as median (range), *; indocyanine green retention rate at 15 minutes

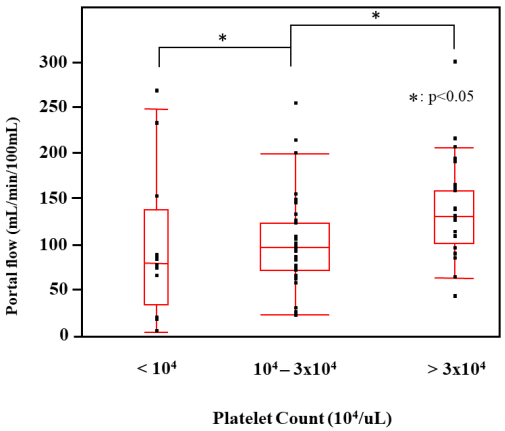

Figure 2. Relationship between portal flow and platelet count. Significant differences are apparent between portal flow and platelet count in each category ($p < 0.05$), and platelet count correlates positively with portal flow ($p < 0.05$).

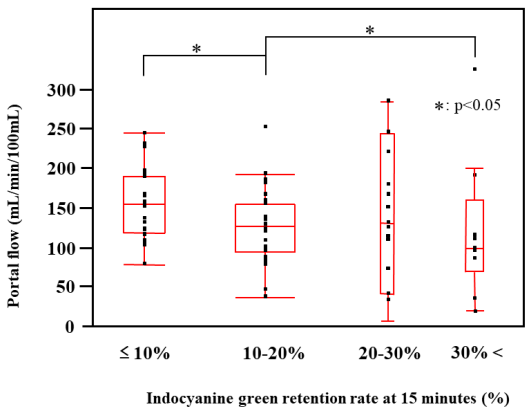

Figure 3. Relationship between portal flow and $ICGR_{15}$. Significant differences are observed between portal flow and $ICGR_{15}$ for each group ($p < 0.05$) and $ICGR_{15}$ correlates positively with portal flow ($p < 0.05$).

Table 2. Operation related variables by back ground pathological liver parenchyma

	Normal liver (n = 43)	Chronic hepatitis (n = 56)	Liver cirrohsis (n = 42)	Liver steatosis (n = 25)	p-value
Operation time (min)	316 (125-672)	321 (150-720)	368 (130-609)	358 (199-577)	0.675
Hepatic ischemia time (min)	121 (46-238)	119 (15-223)	111 (45-163)	127 (15-199)	0.511
Blood loss (mL)	193 (20-2398)	237.5 (15-4491)	404 (30-2158)	387 (54-1494)	0.041
Transection area (cm^2)	56.2 (4.7-219.8)	57.7 (7.3-225.1)	49.4 (7.2-242.1)	50.8 (4.7-152.8)	0.923
Complications (≥ Grade IIIb*) (%)	2 (4.7)	4 (7.1)	4 (9.5)	2 (8.3)	0.104
Mortality (%)	0 (0)	1 (0)	0 (0)	1 (0)	1.000

Data are expressed as median (range), *; Clavien-Dindo classification.

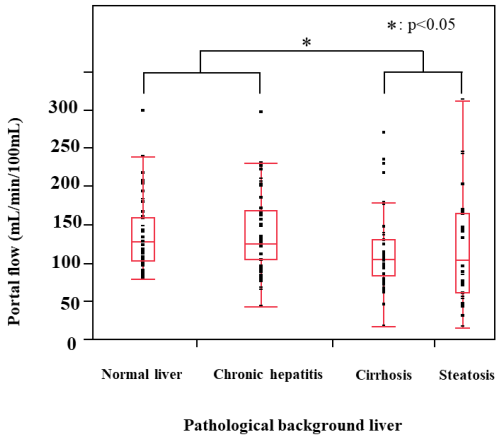

Figure 4. Trends in postoperative liver function. No significant difference in blood loss is evident between NL and CH or between CH and LS. A significant difference is observed between the former two groups and the latter two groups ($p < 0.05$).

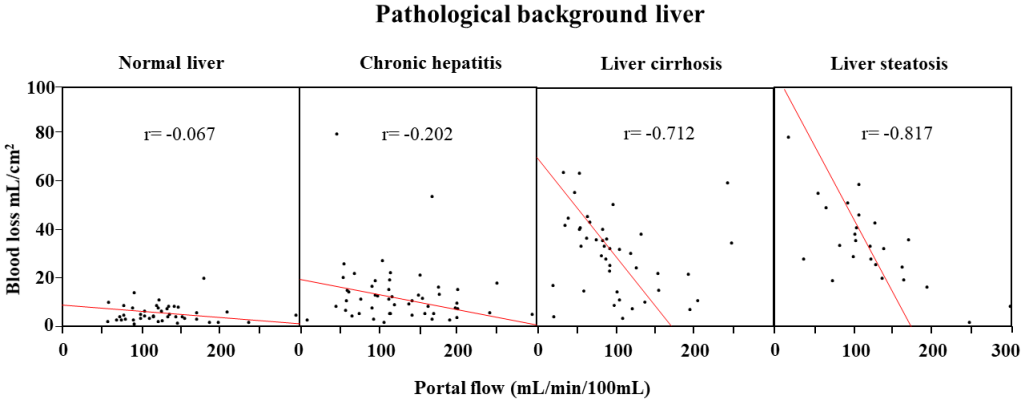

Figure 5. Recovery of parenchyma volume after liver resection. Very weak correlations are evident between portal blood flow and blood loss in NL (r = -0.067) and CH (r = -0202) groups. In contrast, strong correlations are observed in the LC (r = -0.712) and LS groups (r = -0.817).

3.4. Operation-related data by background liver parenchyma

Blood loss was significantly greater in the LC and LS groups than in the other two groups (p = 0.041) (Table 2). Operation time, hepatic ischemia time and transection area did not differ significantly between groups. No perioperative mortality was encountered and the rate of severe-grade complications did not differ between groups.

3.5. Correlation between portal flow and preoperative liver functions

No significant difference in blood loss was seen between NL and CH or between CH and LS. A significant difference was observed between the former and latter groups ($p < 0.05$) (Figure 4). Very weak correlations were apparent between portal blood flow and blood loss in the NL (r = -0.067) and CH (r = -0.202) groups. In contrast, strong correlations were observed in the LC (r = -0.712) and LS groups (r = -0.817) (Figure 5).

4. Discussion

This study showed that portal flow as measured by perfusion CT correlated significantly with $ICGR_{15}$

and platelet count, which are known to reflect liver functional reserve. Portal flow correlates with the degree of damage to the liver parenchyma and to blood loss during liver transection. Perfusion CT provides information not only on tumor status, but also on portal flow, which is predictive of blood loss.

A significant correlation between complications and damage to the liver parenchyma is well known (*7,8,16*). A positive relationship existed between intraoperative blood loss and outcomes (*17,18*). Many techniques have been devised to improve blood loss, including Pringle's maneuver, the total blood flow occlusion technique, hanging maneuver, and use of energy devices during liver transection (*19-21*). As blood loss during liver transection depends on the damage of background liver parenchyma, assessment of the liver parenchyma plays a key role in avoiding severe complications (*7,8,18*). Thus, liver stiffness measurement represents a useful preoperative option (*4-8*). In this study, portal blood flow from perfusion CT correlated positively with platelet count and negatively with $ICGR_{15}$. Moreover, a significant correlation was observed between portal flow and blood loss per transection square. This means that blood loss depends on liver stiffness as shown in previous studies using different imaging modalities, such as MRI and ultrasound (*4-8*).

In imaging studies, CASH is expressed as severe steatosis with splenomegaly (*22,23*). This implies the presence of portal hypertension while the liver parenchyma is soft and fragile at liver transection. As the underlying etiologies remain poorly recognized, standardized methods are lacking to assess liver function in severe steatosis, including CASH. Interestingly, in the LS group, even though the stiffness of the liver parenchyma differed from that in liver cirrhosis, the relationship between portal flow and blood loss resembled that in the LC group. The pathological features of CASH are known to involve "sinusoidal obstruction syndrome", as blood congestion caused by injury to the peripheral sinusoids (*1,9,10,22,23*). Therefore, one speculation is that together with fat deposition inside hepatocytes, severe parenchymal congestion results in decreased portal flow. Increased blood loss during liver transection under conditions such as liver cirrhosis is easily understood. Further investigation by perfusion CT should clarify the hemodynamics of severe steatosis.

We used a uniform procedure at the time of operation, but this study did not eliminate the variable influence of surgical factors such as blood flow control and the difference in central venous pressure during liver transection resembling previous studies (*4-8*). Even though the total number of patients included in this study was larger than another study of perfusion CT, the number of participants in each group was still small because of the 4 different pathological groups. This was the main limitation of the present study, and we therefore aim to analyze a larger number of participants in the future. In addition, two different types of steatosis were included: CASH and obesity. Hemodynamics in those subsets of patients may differ, and larger numbers of patients are required to properly assess each category. In addition, data were lacking to compare the results of portal flow as determined ultrasonographically. Assessment of blood flow is not objective and easily changes between operators, and more objective assessment of blood flow requires estimation from perfusion CT. Further study is needed to compare blood flow data between ultrasound and perfusion CT to determine which modality is more convenient and correct in clinical use.

In conclusion, parameters of perfusion CT enable the assessment of hemodynamics in the diseased liver. Portal flow from perfusion CT is predictive of blood loss at liver transection, and thus appears useful for planning liver resection.

References

1. Rubbia-Brandt L, Audard V, Sartoretti P, Roth AD, Brezault C, Le Charpentier M, Dousset B, Morel P, Soubrane O, Chaussade S, Mentha G, Terris B. Severe hepatic sinusoidal obstruction associated with oxaliplatin-based chemotherapy in patients with metastatic colorectal cancer. Ann Oncol. 2004; 15:460-466.
2. Ronot M, Asselah T, Paradis V, Michoux N, Dorvillius M, Baron G, Marcellin P, Van Beers BE, Vilgrain V. Liver fibrosis in chronic hepatitis C virus infection: differentiating minimal from intermediate fibrosis with perfusion CT. Radiology. 2010; 256:135-142.
3. Hashimoto K, Murakami T, Dono K, Hori M, Kim T, Kudo M, Marubashi S, Miyamoto A, Takeda Y, Nagano H, Umeshita K, Nakamura H, Monden M. Assessment of the severity of liver disease and fibrotic change: the usefulness of hepatic CT perfusion imaging. Oncol Rep. 2006; 16:677-683.
4. Zhao H, Chen J, Meixner DD, Xie H, Shamdasani V, Zhou S, Robert JL, Urban MW, Sanchez W, Callstrom MR, Ehman RL, Greenleaf JF, Chen S. Noninvasive assessment of liver fibrosis using ultrasound-based shear wave measurement and comparison to magnetic resonance elastography. J Ultrasound Med. 2014; 33:1597-1604.
5. Grgurevic I, Puljiz Z, Brnic D, Bokun T, Heinzl R, Lukic A, Luksic B, Kujundzic M, Brkljacic B. Liver and spleen stiffness and their ratio assessed by real-time two dimensional-shear wave elastography in patients with liver fibrosis and cirrhosis due to chronic viral hepatitis. Eur Radiol. 2015; 25:3214-3221.
6. Wong JS, Wong GL, Chan AW, Wong VW, Cheung YS, Chong CN, Wong J, Lee KF, Chan HL, Lai PB. Liver stiffness measurement by transient elastography as a predictor on posthepatectomy outcomes. Ann Surg. 2013; 257:922-928.
7. Sato N, Kenjo A, Kimura T, Okada R, Ishigame T, Kofunato Y, Shimura T, Abe K, Ohira H, Marubashi S. Prediction of major complications after hepatectomy using liver stiffness values determined by magnetic resonance elastography. Br J Surg. 2018; 105:1192-1199.
8. Hayato A, Midorikawa Y, Mitsuka Y, Aramaki O,

Higaki T, Matsumoto N, Moriyama M, Haradome H, Abe O, Sugitani M, Tsuji S, Takayama T. Predicting postoperative outcomes of liver resection by magnetic resonance elastography Surgery. 2017; 162:248-255.
9. Narita M, Oussoultzoglou E, Chenard MP, Fuchshuber P, Rather M, Rosso E, Addeo P, Jaeck D, Bachellier P. Liver injury due to chemotherapy-induced sinusoidal obstruction syndrome is associated with sinusoidal capillarization. Ann Surg Oncol. 2012; 19:2230-2237.
10. Zhao J, van Mierlo KMC, Gómez-Ramírez J, *et al.* Systematic review of the influence of chemotherapy-associated liver injury on outcome after partial hepatectomy for colorectal liver metastases. Br J Surg. 2017; 104:990-1002.
11. Wolf PS, Park JO, Bao F, Allen PJ, DeMatteo RP, Fong Y, Jarnagin WR, Kingham TP, Gönen M, Kemeny N, Shia J, D'Angelica MI. Preoperative chemotherapy and the risk of hepatotoxicity and morbidity after liver resection for metastatic colorectal cancer: a single institution experience. J Am Coll Surg. 2013; 216:41-49.
12. Shin J, Yoon H, Cha YJ, Han K, Lee MJ, Kim MJ, Shin HJ. Liver stiffness and perfusion changes for hepatic sinusoidal obstruction syndrome in rabbit model. World J Gastroenterol. 2020; 26:706-716.
13. Ichida F, Tsuji T, Omata M, Ichida T, Inoue K, Kamimura T, Yamada G, Hino K, Yokosuka O, Suzuki H. New Inuyama Classification for histological assessment of chronic hepatitis. Hepatol Commun 1996; 6:112-119.
14. Brunt EM, Janney CG, Di Bisceglie AM, Neuschwander-Tetri BA, Bacon BR. Nonalcoholic steatohepatitis: a proposal for grading and staging the histological lesions. Am J Gastroenterol. 1999; 94:2467-2474.
15. Dindo D, Demartines N, Clavien PA. Classification of surgical complications: a new proposal with evaluation in a cohort of 6336 patients and results of a survey. Ann Surg. 2004; 240:205-213.
16. Fung J, Poon RT, Yu WC, Chan SC, Chan AC, Chok KS, Cheung TT, Seto WK, Lo CM, Lai CL, Yuen MF. Use of liver stiffness measurement for liver resection surgery: correlation with indocyanine green clearance testing and post-operative outcome PLoS One 2013; 8:e72306.
17. Aramaki O, Takayama T, Higaki T, Nakayama H, Ohkubo T, Midorikawa Y, Moriguchi M, Matsuyama Y. Decreased blood loss reduces postoperative complications in resection for hepatocellular carcinoma. J Hepatobiliary Pancreat Sci. 2014; 21:585-591.
18. Kim MS, Lee JR. Assessment of liver stiffness measurement: novel intraoperative blood loss predictor? World J Surg. 2013; 37:185-191.
19. Kokudo N, Imamura H, Sano K, Zhang K, Hasegawa K, Sugawara Y, Makuuchi M. Ultrasonically assisted retrohepatic dissection for a liver hanging maneuver. Ann Surg. 2005; 242:651-654.
20. Rahbari NN, Koch M, Zimmermann JB, Elbers H, Bruckner T, Contin P, Reissfelder C, Schmidt T, Weigand MA, Martin E, Büchler MW, Weitz J. Infrahepatic inferior vena cava clamping for reduction of central venous pressure and blood loss during hepatic resection: a randomized controlled trial. Ann Surg. 2011; 253:1102-1110.
21. Ichida A, Hasegawa K, Takayama T, Kudo H, Sakamoto Y, Yamazaki S, Midorikawa Y, Higaki T, Matsuyama Y, Kokudo N. Randomized clinical trial comparing two vessel-sealing devices with crush clamping during liver transection. Br J Surg. 2016; 103:1795-1803.
22. Rubbia-Brandt L. Sinusoidal obstruction syndrome. Clin Liver Dis. 2010; 14:651-668.
23. Stevenson HL, Prats MM, Sasatomi E. Chemotherapy-induced sinusoidal injury (CSI) score: a novel histologic assessment of chemotherapy-related hepatic sinusoidal injury in patients with colorectal liver metastasis. BMC Cancer. 2017; 17:35.

Received August 8, 2020; Revised August 26, 2020; Accepted August 28, 2020.

**Address correspondence to:*
Tadatoshi Takayama, Department of Digestive Surgery, Nihon University School of Medicine, 30-1 Oyaguchikami-machi, Itabashi-ku, Tokyo 173-8610, Japan.
E-mail: takayama.tadatoshi@nihon-u.ac.jp

Released online in J-STAGE as advance publication September 6, 2020.

Original Article

DOI: 10.5582/bst.2020.01048

Methyl-CpG binding domain protein 3: a new diagnostic marker and potential therapeutic target of melanoma

Takayuki Ishibashi[1], Ikko Kajihara[1], Satoru Mizuhashi[1], Haruka Kuriyama[1], Toshihiro Kimura[1], Hisashi Kanemaru[1], Katsunari Makino[1], Azusa Miyashita[1], Jun Aoi[1], Takamitsu Makino[1], Satoshi Fukushima[1,*], Kanako Kita[2,*], Hironobu Ihn[1]

[1] Department of Dermatology and Plastic Surgery, Graduate School of Medical Sciences, Kumamoto University, Kumamoto, Japan;
[2] Department of Molecular Pathology, Graduate School of Medical Sciences, Kumamoto University, Kumamoto, Japan.

SUMMARY Methyl-CpG binding domain protein 3 (MBD3) belongs to the methyl-CpG binding protein family. MBD3 facilitates the initiation of neural stem cell reprogramming. Melanoma originates in melanocytes derived from neural crest stem cells; therefore, we investigated the role of MBD3 in melanoma. MBD3 was overexpressed in melanoma compared with pigmented nevi. MBD3 knockdown had no effect on the proliferation of melanoma cells (A375 and A2058 cells). Contrarily, it significantly reduced the migration and invasion of A375 cells, but had no significant effect on A2058 cells. Furthermore, MBD3 knockdown reduced N-cadherin protein levels and matrix metalloproteinase-2 (MMP-2) activity in A375 cells, but had no significant effect on A2058 cells. Based on these results, the MBD3 expression level may be a useful biomarker for the diagnosis of melanoma. Thus, MBD3 has potential as a novel therapeutic target for some melanoma patients.

Keywords MBD3, melanoma, N-cadherin, MMP-2

1. Introduction

Although immune checkpoint inhibitors (ICIs) improve the prognosis of patients with advanced melanoma, the response rate to ICIs is approximately 30-40% (*1*). In addition, only approximately 30% of Japanese melanoma patients have a BRAF mutation, which is required for treatment with BRAF inhibitors (*1*). As such, the currently available therapies are not suitable for all melanoma patients. Therefore, novel therapeutic molecular targets for advanced melanoma need to be identified. Furthermore, it is not always possible to make a differential diagnosis between a nevus and a melanoma. This is due to the fact that the representative melanoma markers, including melanoma antigen recognized by T cells 1 (MART-1) and gp100, are also present in pigmented nevi. Therefore, they are not useful for differential diagnoses.

Methyl-CpG binding domain protein 3 (MBD3) is approximately 35 kDa and belongs to the methyl-CpG-binding protein family. MBD3 acts as a transcriptional repressor through its interaction with nucleosome remodeling deacetylase (NuRD) (*2*). MBD3 is essential for the formation and stability of the NuRD complex (*3*). It is contained within this complex, where it binds to hydroxymethylated DNA (*4*). DNA hydroxymethylation is an epigenetic mechanism that modifies the C-5 position of cytosine by adding a hydroxymethyl group, resulting in the regulation of gene expression levels (*5,6*). MBD3 binds to hydroxymethylated DNA and suppresses gene expression (*4*). MBD3 protein has been previously detected in neural stem cells using two-dimensional fluorescence differential gel electrophoresis targeting nuclear phosphorylated proteins after stimulation with fibroblast growth factor 2 (*7*). MBD3 is involved in the regulation of neural stem cell reprogramming and differentiation (*8*). Moreover, melanoma originates from melanocytes derived from neural crest cells (*9*).

Although the expression levels of MBD3 are high in several cancers, there is a divergence in terms of its function according to the type of cancer. MBD3 suppresses tumor growth in lung cancer (*10*) and pancreatic cancer (*11*) but promotes tumor growth in breast cancer (*12*). However, the role of MBD3 in melanoma has not yet been clarified. Therefore, we investigated the role of MBD3 in melanoma and whether the inhibition of MBD3 has an antitumor effect.

2. Material and Methods

2.1. Clinical assessment and patient samples

In accordance with the Declaration of Helsinki, institutional review board approval and written informed consent was obtained from patients before their enrollment in this study. Skin samples were collected from 20 patients with melanoma and 19 patients with pigmented nevi.

2.2. Cell culture

Human melanoma cell lines were obtained from the Cell Resource Center for Biomedical Research Institute of Development, Aging and Cancer, Tohoku University (Sendai, Miyagi, Japan) or the American Type Culture Collection (Manassas, VA, USA). Normal human epidermal melanocytes (NHEM) were purchased from Lonza (Basel, Switzerland). Human melanoma cell lines were maintained in Dulbecco's modified Eagle medium, supplemented with 20% fetal bovine serum (FBS) under 5% CO_2 and 95% air. NHEM in CSF-4HM-500D culture medium, supplemented with human melanocyte growth supplements, were maintained under 5% CO_2 and 95% air.

2.3. Immunofluorescent staining

Immunofluorescent staining of MBD3 and Melan-A proteins in patient tissues and cultured cell lines was performed using an anti-MBD3 antibody at a dilution of 1:100 (ab157464; Abcam, Cambridge, UK) or an anti-Melan-A antibody at 1:100 (mouse monoclonal) (ab731; Abcam), respectively. Slides were counterstained with Fluoroshield mounting medium with 4′,6-diamidino-2-phenylindole (DAPI) (ab104139; Abcam) and images were captured using fluorescence microscopy (BZ-X 710; Keyence, Osaka, Japan). The intensity of staining was classified as follows: (–), same or weaker than the adjacent epidermis; (+), stronger than the adjacent epidermis; (++), much stronger than the adjacent epidermis.

2.4. Western blotting

Equal amounts of proteins (10 μg) were separated using SDS polyacrylamide gels and were electrotransferred to polyvinylidene fluoride (PVDF) membranes (Bio-Rad Laboratories, Hercules, CA, USA). The membranes were immunoblotted overnight at 4°C with primary antibodies, followed by their respective secondary antibodies, anti-MBD3 (1:1,000; Abcam), anti-N-cadherin (1:1,000; Abcam), and anti-β-actin (1:2,000; Cell Signaling Technology, Beverly, MA, USA).

2.5. Gene silencing using small interfering RNA

An MBD3-specific small interfering RNA (siRNA) and a scrambled control siRNA were purchased from Dharmacon (Lafayette, CO, USA). The target sequences of the MBD3-specific siRNA are the following four sequences: CCUGAACGCCUUCGACAUU, UGAGCA AGAUGAACAAGAG, UCAAGCAGCCGGUGACCA A, CCAACCAGGUCAAGGGCAA. Human melanoma cell lines were transfected using Lipofectamine RNAiMAX transfection reagent (Invitrogen Corporation, Carlsbad, CA, USA) for 6 h following manufacturer's instructions. The final concentration of MBD3-specific siRNA and scrambled control siRNA were 100 nM.

2.6. Cell proliferation assay

A375 (low metastatic melanoma cell line) and A2058 (high metastatic melanoma cell line) (*13*) cells were seeded at 5.0×10^4 cells/well in 6-well plates and transfected with either an *MBD3*-specific siRNA or a scrambled control siRNA using Lipofectamine RNAiMAX. After incubating for 48 hours, the transfected cells were stained with Trypan blue and counted under a light microscope. Each experiment was performed in triplicate.

2.7. Migration and invasion assays

Migration and invasion assays were performed to evaluate the migrative and invasive ability of A375 and A2058 cells transfected with either an MBD3-specific siRNA or a scrambled control siRNA using Lipofectamine RNAiMAX. For migration assay, a 24-well plate containing Permeable Support with 8.0 μm Transparent PET Membrane (Corning Inc., Corning, NY, USA), was prepared and for invasion assay, a 24-well plate containing 8 μm pore size transwell inserts pre-coated with Matrigel (Corning Inc.) was prepared. After serum starved incubation with serum-free Dulbecco's Modified Eagle Medium (DMEM) in 5% CO_2 atmosphere at 37ºC for 24 h, the cells were seeded into the upper chamber of the insert at 5×10^4/well in 500 μL serum-free DMEM. The lower chamber was filled with 750 μL DMEM supplemented with 20% fetal bovine serum as a chemoattractant. After incubating the cells at 37ºC for 48 h, the cells on the upper chamber of the insert were removed with a cotton swab. Subsequently, the cells on the bottom of the insert were fixed with paraformaldehyde for 15 min. Using an inverted microscope, the migrated and invaded cells were counted in five different fields at 200× magnification.

2.8. MMP-2 activity assay

Supernatants were collected from melanoma cells (A375 and A2058 cells) and cultured in 6-well plates for 48 hours. MMP-2 activity was measured using a commercially available assay (QuickZyme Biosciences, Leiden, Netherlands), according to the manufacturer's protocol.

2.9. Statistical analysis

Data are presented as bar graphs with the mean ± standard deviation (SD) of at least three independent experiments. Statistical analyses were performed using the Mann-Whitney *U*-test to compare medians. The immunofluorescent staining results were analyzed using the Chi-squared test. A p-value < 0.05 was considered to be statistically significant.

3. Results

3.1. MBD3 was overexpressed in melanoma

Western blotting was performed to examine the MBD3 expression levels in melanoma *in vitro*. The MBD3 levels were higher in melanoma cell lines than in NHEM (Figure 1a). Immunofluorescent staining showed results similar to western blotting (Figure 1b). In addition, we measured the expression levels of MBD3 in melanoma tissues by immunofluorescence. A representative MBD3 immunofluorescence experiment is shown in Figure 2a. The tissue samples were classified as negative, slightly positive, or strongly positive based on MBD3 immunoreactivity (Figure 2b). MBD3 staining was significantly more intense in melanoma samples than in pigmented nevi (Table 1). Moreover, when the patients were evaluated by the staining results of MBD3, neither lymph node metastasis nor organ metastasis was observed in all three cases of melanoma negative for MBD3 (Table 2).

3.2. An MBD3-specific small interfering RNA inhibited the migration and invasion of A375 cells

We investigated the effect of an MBD3-specific siRNA in melanoma cell lines (A375 and A2058 cells) to determine the role of MBD3 in the pathogenesis of melanoma. The expression level of MBD3 was down-regulated by the MBD3-specific siRNA, as shown in Figure 3a. MBD3 knockdown did not affect the proliferation of neither A375 nor A2058 cells (Figure

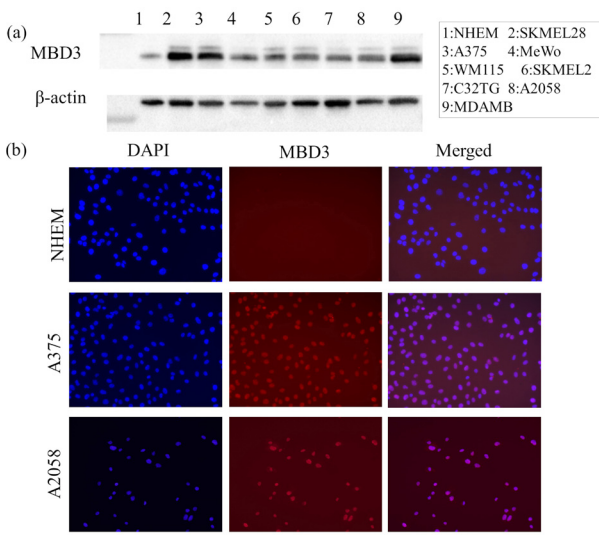

Figure 1. (a) Expression levels of methyl-CpG binding domain protein 3 (MBD3) protein in melanoma and normal human epidermal melanocyte (NHEM) cell lines using immunoblotting. **(b)** Immunofluorescent staining. Expression of MBD3 protein in A375, A2058, and NHEM cell lines. MART-1 is shown in green. MBD3 is shown in red. DNA is stained blue (DAPI).

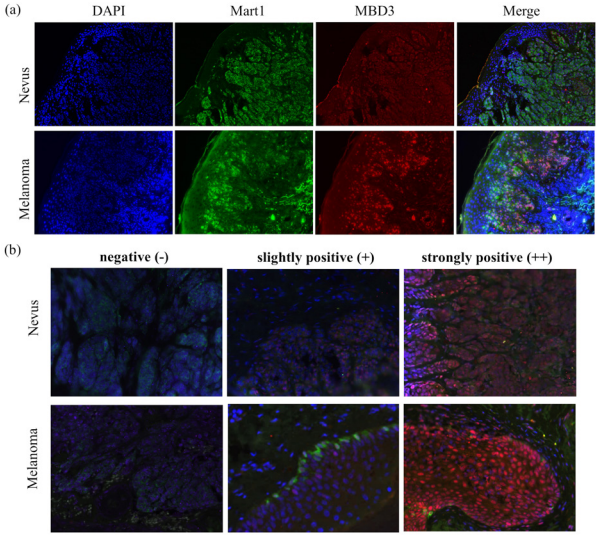

Figure 2. Immunofluorescent staining in melanoma and pigmented nevi. (a) Representative images of immunofluorescent staining of nuclei (DAPI, blue), MART-1 protein (green), and MBD3 protein (red) in melanoma and nevus tissue samples. (400× magnification). **(b)** Representative images of semiquantitative scoring of immunofluorescent staining. The intensity of staining was classified as follows: (–), same or weaker than the adjacent epidermis; (+), stronger than the adjacent epidermis; or (++), much stronger than the adjacent epidermis.

Table 1. Results of the immunofluorescent analysis of MBD3

Items	*n*	–	+	++
Pigmented nevus	19	16	2	1
Melanoma	20	3	1	16

The tissue samples were classified as negative (–), slightly positive (+), or strongly positive (++) based on MBD3 immunoreactivity. MBD3 staining was significantly more intense in melanoma samples than in pigmented nevi.

Table 2. Correlation between MBD3 immunofluorescent staining and clinical features of melanoma patients

Items	Negative (n = 3)	Positive (n = 17)	p-value
Sex (Male:Female)	2:1	8:9	1
Age (years), mean ± SD	74.9 ± 11.7	63.3 ± 21.7	0.175
Lymph node metastasis (No:Yes)	3:0	9:8	0.242
Organ metastasis (No:Yes)	3:0	15:2	1

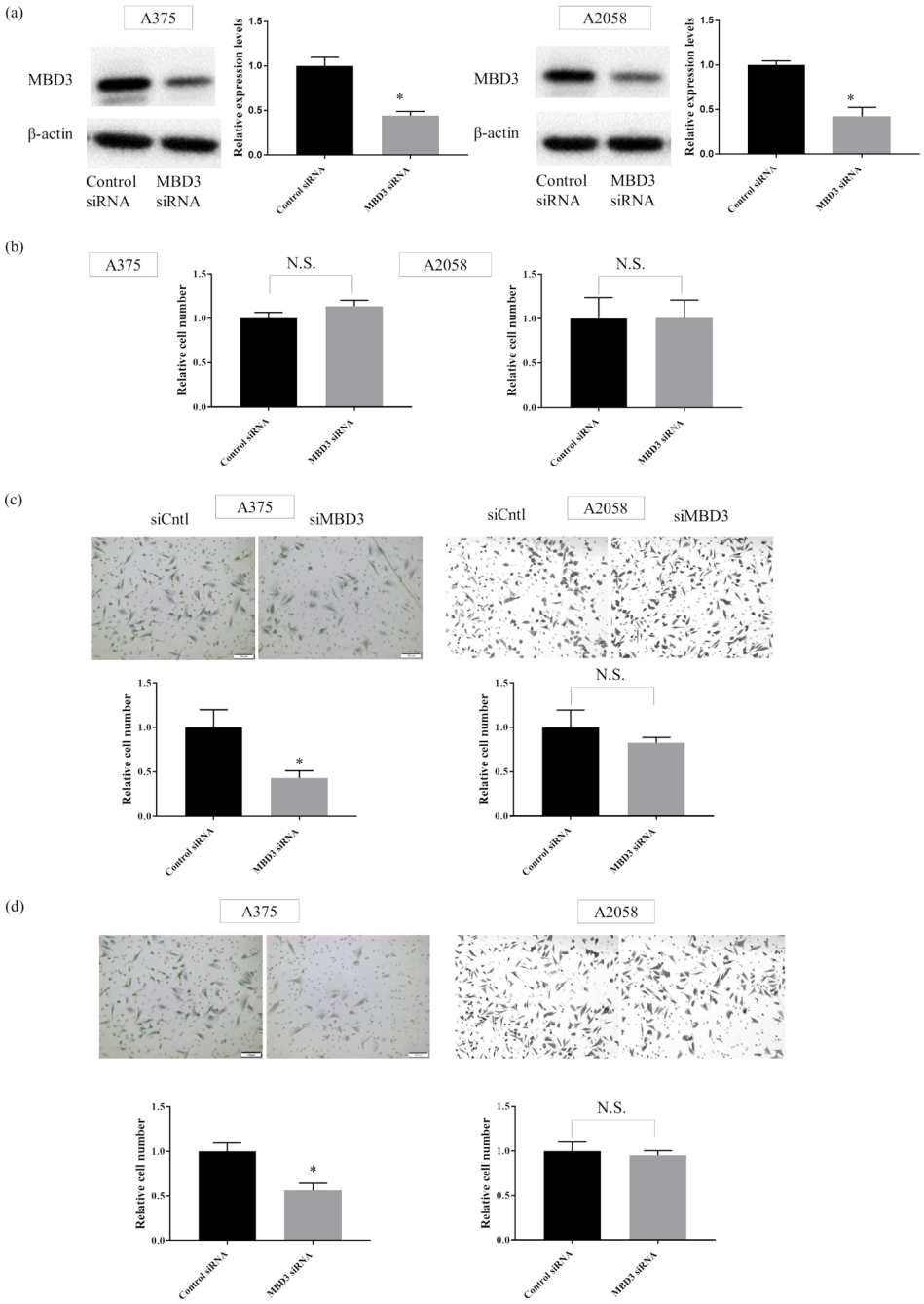

Figure 3. Knockdown of MBD3 affected cell growth, migration, and invasion in melanoma. (a) Down-regulation of MBD3 expression by small interfering RNA (siRNA). A375 and A2058 cells were transfected with a control or MBD3-specific siRNA. After treatment for 48 hours, we evaluated cell proliferation, migration, and invasion. Data represent the mean ± SD from three independent experiments. **(b)** The number of melanoma cells was counted using a particle counter. **(c)** Cell migration was evaluated using transwell inserts without a Matrigel coating. **(d)** Cell invasion was evaluated using transwell inserts coated with Matrigel. Diff-Quick staining of melanoma cells treated with a control or MBD3-specific siRNA. Magnification, 400×. Data are expressed as the mean ± SD of three independent experiments. $^{*}p < 0.05$ versus controls.

3b). We also evaluated the effect of the MBD3-specific siRNA on the migration and invasion of melanoma cells. Migration/invasion assays showed that MBD3 silencing significantly inhibited the migration and invasion of A375 cells, but had no statistically significant effect on the migration or invasion of A2058 cells (Figures 3c and 3d).

3.3. MBD3 knockdown suppressed N-cadherin expression and MMP-2 activity in A375 cells

N-cadherin promotes the migration of melanocytes and is involved in the migratory ability of melanoma *(14)*. MMP-2 has the ability to degrade type IV collagen and is associated with the migration and invasion of cancer (*15*). To clarify the mechanism of migration and invasion related to MBD3, we examined whether MBD3 knockdown affected N-cadherin expression levels and MMP-2 activity in melanoma cell lines. As shown in Figure 4a-b, MBD3 knockdown significantly suppressed N-cadherin expression and MMP-2 activity

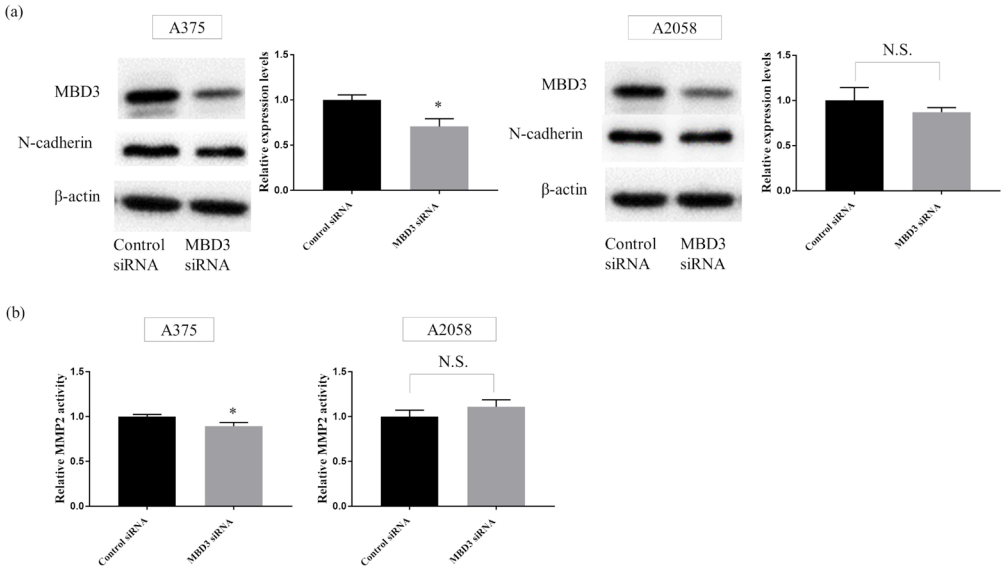

Figure 4. Knockdown of MBD3 down-regulated N-cadherin and inhibited MMP-2 activity in A375 cells, but not A2058 cells. A375 and A2058 cells were transfected with a control or MBD3-specific siRNA. All results were analyzed after 48 hours of treatment. The levels of N-cadherin expression (**a**, western blotting) and MMP-2 activity **(b)** in A375 and A2058 cells. Data are expressed as the mean ± SD of three independent experiments. $^{*}p < 0.05$ versus controls. N.S., not significant.

in A375 cells, but had no effect on these parameters in A2058 cells.

4. Discussion

In this study, we revealed two major findings. Firstly, MBD3 was found to be strongly expressed in the cultured melanoma cells and tissues of melanoma patients. In addition, as shown in Figure 2b and Table 1, the MBD3 levels were significantly higher in melanoma compared with pigmented nevi. These results demonstrated that MBD3 may be useful for the differential diagnosis of melanoma and pigmented nevus.

Secondly, the role of MBD3 in the progression of melanoma was found to vary depending on the cell line. MBD3 knockdown did not affect the proliferative ability of A375 or A2058 cells. However, MBD3 knockdown significantly reduced the migration and invasion of A375 cells, but had no significant effect on A2058 cells. Furthermore, the knockdown of MBD3 reduced the N-cadherin protein levels and MMP-2 activity in A375 cells, but had no significant effect on A2058 cells. These findings suggested that MBD3 may promote migration and invasion by regulating N-cadherin and MMP-2 in A375 cells. The reason of the finding that the migration and invasion of A2058 cells were not affected by an MBD3-specific siRNA, was suggested to depend on the presence of PTEN. A2058 cells have been established from metastatic lymph node and reported to be PTEN-deficient, while A375 cells have wild-type PTEN (*16,17*). PTEN is a negative regulator of PI3K, and the inactivation of PTEN can promote the metastatic progression of melanoma (*18*). The progression of melanoma has characteristic features of epithelial to mesenchymal transition (EMT), including the disruption of the adherent junctions caused by the upregulation of N-cadherin. The PI3K /PTEN pathway transcriptionally regulates this cadherin regulation (*19*). It has been reported that PTEN was repressed through the epigenetic repressor NuRD complex (*20*). MBD3 is essential for the formation and stability of the NuRD complex. The knockdown of MBD3 may only suppress EMT in tumor cells with PTEN. Therefore, we suggest that the migration and invasion of PTEN-deficient A2058 cells were not affected by an MBD3-specific siRNA. However, this should be confirmed using a greater number of different cell lines in future studies.

In conclusion, although the differential diagnosis of pigmented nevus and melanoma is sometimes difficult, the assessment of MBD3 protein expression levels may solve this problem. Although heterogeneity was observed depending on the type of cell line, MBD3 has potential for use as a therapeutic target for the treatment of advanced melanoma.

Acknowledgements

This work was supported by a JSPS Grant (grant numbers 15K09772 and 18K08301).

References

1. Nakamura Y, Asai J, Igaki H, *et al*. Japanese Dermatological Association Guidelines: Outlines of guidelines for cutaneous melanoma 2019. J Dermatol. 2020; 47:89-103.
2. Dos Santos RL, Tosti L, Radzisheuskaya A, Caballero IM,

Kaji K, Hendrich B, Silva JCR. MBD3/NuRD Facilitates Induction of Pluripotency in a Context-Dependent Manner. Cell Stem Cell. 2014; 15:102-110.
3. Wade PA, Gegonne A, Jones PL, Ballestar E, Aubry F, Wolffe AP. Mi-2 complex couples DNA methylation to chromatin remodelling and histone deacetylation. Nat Genet. 1999; 23:62-66.
4. Yildirim O, Li R, Hung JH, Chen PB, Dong X, Ee LS, Weng Z, Rando OJ, Fazzio TG. Mbd3/NURD complex regulates expression of 5-hydroxymethylcytosine marked genes in embryonic stem cells. Cell. 2011; 147:1498-1510.
5. Wu H, Zhang Y. Tet1 and 5-hydroxymethylation: A genome-wide view in mouse embryonic stem cells. Vol. 10, Cell Cycle. Taylor and Francis Inc., 2011; pp. 2428-2436.
6. Mendonca A, Chang EH, Liu W, Yuan C. Hydroxymethylation of DNA influences nucleosomal conformation and stability *in vitro*. Biochim Biophys Acta. 2014; 1839:1323-1329.
7. Niimori-Kita K, Tamamaki N, Koizumi D, Niimori D. Matrin-3 is essential for fibroblast growth factor 2-dependent maintenance of neural stem cells. Sci Rep. 2018; 8:13412.
8. Kaji K, Caballero IM, MacLeod R, Nichols J, Wilson VA, Hendrich B. The NuRD component Mbd3 is required for pluripotency of embryonic stem cells. Nat Cell Biol. 2006; 8:285-292.
9. Kohler C, Nittner D, Rambow F, Radaelli E, Stanchi F, Vandamme N, Baggiolini A, Sommer L, Berx G, van den Oord JJ, Gerhardt H, Blanpain C, Marine JC. Mouse cutaneous melanoma induced by mutant B-Raf arises from expansion and dedifferentiation of mature pigmented melanocytes. Cell Stem Cell. 2017; 21:679-693.e6.
10. Noh EJ, Jang ER, Jeong G, Lee YM, Min CK, Lee JS. Methyl CpG-binding domain protein 3 mediates cancer-selective cytotoxicity by histone deacetylase inhibitors *via* differential transcriptional reprogramming in lung cancer cells. Cancer Res. 2005; 65:11400-11410.
11. Xu M, He J, Li J, Feng W, Zhou H, Wei H, Zhou M, Lu Y, Zeng J, Peng W, Du F, Gong A. Methyl-CpG-binding domain 3 inhibits epithelial-mesenchymal transition in pancreatic cancer cells via TGF-beta/Smad signalling. Br J Cancer. 2017; 116:91-99.
12. Cui J, Duan B, Zhao X, Chen Y, Sun S, Deng W, Zhang Y, Du J, Chen Y, Gu L. MBD3 mediates epigenetic regulation on EPAS1 promoter in cancer. Tumor Biol. 2016; 37:13455-13467.
13. Kim HY, Lee H, Kim SH, Jin H, Bae J, Choi HK. Discovery of potential biomarkers in human melanoma cells with different metastatic potential by metabolic and lipidomic profiling. Sci Rep. 2017; 7:8864.
14. Li G, Satyamoorthy K, Herlyn M. N-cadherin-mediated intercellular interactions promote survival and migration of melanoma cells. Cancer Res. 2001; 61:3819-3825.
15. Pereira AMM, Strasberg-Rieber M, Rieber M. Invasion-associated MMP-2 and MMP-9 are up-regulated intracellularly in concert with apoptosis linked to melanoma cell detachment. Clin Exp Metastasis. 2005; 22:285-295.
16. Pap M, Bátor J, Szeberényi J. Sensitivity of human malignant melanoma cell lines to Newcastle disease virus. Anticancer Res. 2015; 35:5401-5406.
17. Chatterjee N, Pazarentzos E, Mayekar MK, *et al*. Synthetic Essentiality of Metabolic Regulator PDHK1 in PTEN-Deficient Cells and Cancers. Cell Rep. 2019; 28:2317-2330.e8.
18. Kim M. Cooperative interactions of PTEN deficiency and RAS activation in melanoma metastasis. Small GTPases. 2010; 1:161.
19. Hao L, Ha JR, Kuzel P, Garcia E, Persad S. Cadherin switch from E- to N-cadherin in melanoma progression is regulated by the PI3K/PTEN pathway through Twist and Snail. Br J Dermatol. 2012; 166:1184-1197.
20. Lu J, Jeong HW, Kong N, Yang Y, Carroll J, Luo HR, Silberstein LE, Yupoma, Chai L. Stem cell factor SALL4 represses the transcriptions of PTEN and SALL1 through an epigenetic repressor complex. PLoS One. 2009; 4:e5577.

Received February 18, 2020; Revised August 29, 2020; Accepted September 7, 2020.

**Address correspondence to:*
Satoshi Fukushima, Department of Dermatology and Plastic Surgery, Faculty of Life Sciences, Kumamoto University, 1-1-1 Honjo, Kumamoto, Japan.
E-mail: satoshi.fukushima.tb@gmail.com

Kanako Kita, Department of Comprehensive Molecular Medicine, Faculty of Life Sciences, Kumamoto University, 1-1-1 Honjo, Kumamoto, Japan.
E-mail: kitakana@kumamoto-u.ac.jp

Released online in J-STAGE as advance publication September 18, 2020.

Letter

DOI: 10.5582/bst.2020.03365

The development of a quarantine strategy is an important path to a normalized response to COVID-19

Han Zhu[1,2], Hongzhou Lu[1,*]

[1] Department of Infectious Diseases, Shanghai Public Health Clinical Center, Fudan University, Shanghai, China;
[2] School of Public Health, Bengbu Medical College, Bengbu, Anhui, China.

SUMMARY The ongoing pandemic of coronavirus disease 19 (COVID-19) is still in a global pandemic that has affected more than 200 countries. When prevention and control of COVID-19 is gradually normalized, communication between countries needs to be gradually restored due to development needs. There are 34 vaccines in the clinical evaluation stage and 145 vaccines in the preclinical evaluation stage in the global COVID-19 vaccine research and development program, but the rate and process of vaccination may not be sufficient to meet the current needs of society for restoring development and communication. Studies have found that chloroquine, favipiravir, remdesivir and other drugs are useful for COVID-19, but currently there is no specific drug for the treatment of COVID-19. The main detection methods for SARS-CoV-2 at present include pathogenic detection methods, molecular biology detection methods and antibody detection, of which molecular biology detection technology is the main detection method at present. There are some more convenient and rapid detection methods. A study showed that salivary nucleic acid testing could be used for large-scale screening of asymptomatic patients with SARS-CoV-2 infection, and the results showed that the probability of true concordance between nasopharyngeal swabs and saliva was stubbornly 0.998 (90% CI: 0.996-0.999). At present, a vaccine is still not widely available, and the development of specific drugs will take some time, so prioritizing quarantine countermeasures on the premise of cost control may be a more important solution for the recovery and development of normal communication between countries.

Keywords COVID-19, vaccines, specific drugs, quarantine countermeasures

1. Status of the epidemic

According to Worldometer data, as of October 9, Beijing time, a total of 36,706,900 cases of coronavirus disease-19(COVID-19) had been diagnosed worldwide, with a cumulative total of 1,065,646 deaths and more than 10 thousand cases diagnosed in 105 countries. The first case of COVID-19 was detected in December 2019 (*1*), and the epidemic is still in a global pandemic that has affected more than 200 countries. It poses a serious threat to the life and health of the population of all countries and affects the normal social order and development. The mortality rate of COVID-19 varies significantly by age. With hospital mortality rates below 5% among patients under 40 years of age, 35% among patients aged 70-79 years, and over 60% among patients aged 80-89 years (*2*). The epidemic has also caused a sharp decline in communication between countries, with the transnational flow of goods, people and services temporarily halted to reduce the spread of the neo-crown virus. With the gradual control of the epidemic, the prevention and control of COVID-19 will be gradually normalized, and the communication between countries will be gradually restored due to development needs.

2. Control situation

WHO concluded on March 10, 2020, that "the outbreak in China is ending". As of October 8, 21 new confirmed cases have been reported nationwide, all of which were imported from overseas (*3*), Figure 1. At present, the epidemic in China has gradually come under control, and in order to promote social development and international contacts as soon as possible, it is necessary to start from the three aspects of prevention, treatment and quarantine, in order to restore economics and communication while keeping the possibility of virus transmission to a minimum level.

2.1. Vaccines

According to World Health Organization (WHO) data

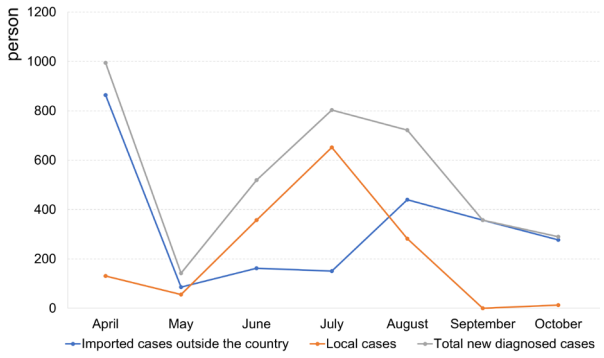

Figure 1. Trend of new cases in 2020. Local cases started to show an increasing trend in May and gradually decreased in July, while the number of imported cases from abroad gradually increased in July. At present, the new confirmed cases are mainly imported from overseas, and quarantine should be the mainstay of prevention and control to prevent overseas importation.

(*4*), as of September 8, 2020, there are 34 vaccines in the clinical evaluation stage and 145 vaccines in the preclinical evaluation stage in the global COVID-19 vaccine research and development program, and a total of four vaccines in China have entered phase III clinical trials. The results of the Phase II clinical trial of recombinant COVID-19 vaccine (adenovirus vector) developed by Chen Wei showed that 99.5% of subjects produced specific antibodies, 95.3% produced neutralizing antibodies, and 89% produced specific T-cell immune reactions 28 days after a single vaccination, which can meet the technical requirements for emergency use (*5*). Although breakthroughs have been achieved, the rate and process of vaccination may not be sufficient to meet the current needs of society for restoring development and communication.

2.2. New drugs and specific drugs

There is no specific drug for the treatment of COVID-19. Studies have shown that chloroquine has an inhibitory effect on severe acute respiratory syndrome coronavirus 2 (SARS-CoV-2) (*6*), and its derivative chloroquine phosphate has been recommended for the antiviral treatment of COVID-19. Some studies have found that *in vitro* application of favipiravir significantly inhibits COVID-19 and accelerates viral clearance (*6-7*). Favipiravir and its generics have been included in treatment protocols in India and Russia respectively (*8-9*). Remdesivir is an antiviral drug developed for the Ebola virus, and was found to have anti- SARS-CoV-2 effects when used *in vitro* (*6*), and a clinical trial in the United States showed that remdesivir shortened recovery time in hospitalized patients with SARS-CoV-2 infection of the lower respiratory tract (*10*). Although effective antiviral drugs have been developed by targeting viral proteases, polymerases and host proteins in the Middle East Respiratory Syndrome and SARS epidemics, there are no specific antiviral drugs for SARS-CoV-2.

2.3. Detection technology

The rapid and accurate detection of SARS-CoV-2 is an important tool to control the spread of the epidemic, and the main detection methods for SARS-CoV-2 at present include pathogenic detection methods, molecular biology detection methods and antibody detection, of which molecular biology detection technology is the main detection method at present. CRISPR-based assays and flow-immunochromatography have the advantages of rapid testing, low cost and high sensitivity, which can be used for field testing (*11*). Due to the persistence and extensiveness of the epidemic, continuous investment and testing have been carried out to continuously update the detection technology and explore more convenient and rapid detection methods. The University of Helsinki, Finland, conducted a SARS-CoV-2 test using the odor discrimination ability of dogs (*12*), which showed that 10 screened dogs could accurately identify neocrown-positive odors. The first batch "COVID-19 Detection Dogs" are now in use at Finnish airports, where they can detect an abnormality by sniffing the wipes on the arms of test subjects, which takes only 10 seconds. Takanori Teshima et al. (*13*) showed that salivary nucleic acid testing could be used for large-scale screening of asymptomatic patients with SARS-CoV-2 infection. 1924 people were included in the study to compare the sensitivity and specificity of SARS-CoV-2 nucleic acid testing of nasopharyngeal swabs and saliva, and the results showed that the probability of true concordance between nasopharyngeal swabs and saliva was stubbornly 0.998 (90% CI: 0.996-0.999), with a high correlation between nasopharyngeal swabs and saliva for SARS-CoV-2 load in SARS-CoV-2 nucleic acid-positive patients. Quarantine countermeasures are of great practical importance due to the specificity of the exchange situation under the normalized demands of social development.

In conclusion, the full-blown COVID-19 epidemic has affected countries in many ways, but there is still a developmental need in society. At present, the vaccine is still not widely available, and the development of specific drugs will take some time, so the rapid detection of SARS-CoV-2 infection in asymptomatic people is the key to prevent and control the outbreak of SARS-CoV-2 epidemic, and prioritizing quarantine countermeasures on the premise of cost control may be a more important solution for the recovery and development of normal communication between countries. Therefore, while developing vaccines and specific drugs, quarantine countermeasures should be explored under the premise of cost control.

Funding: This study was funded by Efficacy and Safety of Hydroxychloroquine Sulfate in Treating Pneumonia Caused by Novel Coronavirus Infection from Shanghai Municipal Science and Technology Commission

(20431900103); Research on Clinical Diagnosis and Treatment Standards of Pneumonia with Novel Coronavirus Infection from Fudan University.

Conflict of Interest: The authors have no conflict of interest to disclose.

References

1. Malik YS, Sircar S, Bhat S, Sharun K, Dhama K, Dadar M, Tiwari R, Chaicumpa W. Emerging novel coronavirus (2019-nCoV)-current scenario, evolutionary perspective based on genome analysis and recent developments. Vet Q. 2020; 40:68-76.
2. Richardson S, Hirsch JS, Narasimhan M, *et al*. the Northwell COVID-19 Research Consortium. Presenting characteristics, comorbidities, and outcomes among 5700 patients hospitalized with COVID-19 in the New York City area. JAMA. 2020; 323:2052-2059.
3. National Health Commission of the People's Repulic of China. An update of Novel Coronavirus Pneumonia break out as of 24:00 on 9 October. *http://www.nhc.gov.cn/xcs/yqtb/202010/b4298767b6104a80a15ec7e8e477e322.shtml* (accessed October 14, 2020). (in Chinese)
4. World Health Organization. Timeline of WHO's response to COVID-19, Last updated 9 September 2020. *https://www.who.int/news/item/29-06-2020-covidtimeline* (accessed October 14, 2020).
5. Zhu FC, Wurie AH, Hou LH, *et al*. Safety and immunogenicity of a recombinant adenovirus type-5 vector-based Ebola vaccine in healthy adults in Sierra Leone: a single-centre, randomised, double-blind, placebo-controlled, phase 2 trial. Lancet. 2017; 389:621-628.
6. Wang M, Cao R, Zhang L, Yang X, Liu J, Xu M, Shi Z, Hu Z, Zhong W, Xiao G. Remdesivir and chloroquine effectively inhibit the recently emerged novel coronavirus (2019-nCoV) in vitro. Cell Res. 2020; 30:269-271.
7. Cai Q, Yang M, Liu D, *et al.* Experimental Treatment with Favipiravir for COVID-19: An Open-Label Control Study. Engineering (Beijing). 2020; doi: 10.1016/j.eng.2020.03.007.
8. Russian Direct Investment Fund. RDIF and ChemRar Announce Increased Production of Avifavir for Treatment of Coronavirus and Begin Export Deliveries. *https://www.prnewswire.com/ae/news-releases/rdif-and-chemrar-announce-increased-production-of-avifavir-for-treatment-of-coronavirus-and-begin-export-deliveries-832625464.html* (accessed October 14, 2020).
9. Glenmark gets India approval for favipiravir as Covid-19 treatment. *https://www.hindustantimes.com/business-news/glenmark-gets-india-approval-for-favipiravir-as-covid-19-treatment/story-nfUZfzToLISJa2LEE7lsbK.html* (accessed October 14, 2020).
10. Paladugu S, Donato AA. Remdesivir improved time to recovery in adults hospitalized with COVID-19 and lower respiratory tract involvement. Ann Intern Med. 2020; 173:JC4.
11. Gootenberg JS, Abudayyeh OO, Lee JW, *et al.* Nucleic acid detection with CRISPR- Cas13a/C2c2. Science. 2017; 356:438-442.
12. Daily Mail. Meet British dogs trained sniff coronavirus airports. *https://www.dailymail.co.uk/femail/article-8770311/Meet-British-dogs-trained-sniff-coronavirus-airports.html* (accessed October 14, 2020).
13. Yokota I, Shane PY, Okada K, Unoki Y, Yang Y, Inao T, Sakamaki K, Iwasaki S, Hayasaka K, Sugita J, Nishida M, Fujisawa S, Teshima T. Mass screening of asymptomatic persons for SARS-CoV-2 using saliva. Clin Infect Dis. 2020; ciaa1388. doi: 10.1093/cid/ciaa1388.

Received October 2, 2020; Revised October 20, 2020; Accepted October 22, 2020.

**Address correspondence to:*
Hongzhou Lu, Department of Infectious Diseases, Shanghai Public Health Clinical Center, Fudan University, 2901 Caolang Road, Jinshan District, Shanghai 201508, China.
E-mail: luhongzhou@fudan.edu.cn

Released online in J-STAGE as advance publication October 25, 2020.

BST
BioScience Trends

Guide for Authors

1. Scope of Articles

BioScience Trends (Print ISSN 1881-7815, Online ISSN 1881-7823) is an international peer-reviewed journal. *BioScience Trends* devotes to publishing the latest and most exciting advances in scientific research. Articles cover fields of life science such as biochemistry, molecular biology, clinical research, public health, medical care system, and social science in order to encourage cooperation and exchange among scientists and clinical researchers.

2. Submission Types

Original Articles should be well-documented, novel, and significant to the field as a whole. An Original Article should be arranged into the following sections: Title page, Abstract, Introduction, Materials and Methods, Results, Discussion, Acknowledgments, and References. Original articles should not exceed 5,000 words in length (excluding references) and should be limited to a maximum of 50 references. Articles may contain a maximum of 10 figures and/or tables. Supplementary Data are permitted but should be limited to information that is not essential to the general understanding of the research presented in the main text, such as unaltered blots and source data as well as other file types.

Brief Reports definitively documenting either experimental results or informative clinical observations will be considered for publication in this category. Brief Reports are not intended for publication of incomplete or preliminary findings. Brief Reports should not exceed 3,000 words in length (excluding references) and should be limited to a maximum of 4 figures and/or tables and 30 references. A Brief Report contains the same sections as an Original Article, but the Results and Discussion sections should be combined.

Reviews should present a full and up-to-date account of recent developments within an area of research. Normally, reviews should not exceed 8,000 words in length (excluding references) and should be limited to a maximum of 10 figures and/or tables and 100 references. Mini reviews are also accepted, which should not exceed 4,000 words in length (excluding references) and should be limited to a maximum of 5 figures and/or tables and 50 references.

Policy Forum articles discuss research and policy issues in areas related to life science such as public health, the medical care system, and social science and may address governmental issues at district, national, and international levels of discourse. Policy Forum articles should not exceed 3,000 words in length (excluding references) and should be limited to a maximum of 5 figures and/or tables and 30 references.

Communications are short, timely pieces that spotlight new research findings or policy issues of interest to the field of global health and medical practice that are of immediate importance. Depending on their content, Communications will be published as "Comments" or "Correspondence". Communications should not exceed 1,500 words in length (excluding references) and should be limited to a maximum of 2 figures and/or tables and 20 references.

Editorials are short, invited opinion pieces that discuss an issue of immediate importance to the fields of global health, medical practice, and basic science oriented for clinical application. Editorials should not exceed 1,000 words in length (excluding references) and should be limited to a maximum of 10 references. Editorials may contain one figure or table.

News articles should report the latest events in health sciences and medical research from around the world. News should not exceed 500 words in length.

Letters should present considered opinions in response to articles published in *BioScience Trends* in the last 6 months or issues of general interest. Letters should not exceed 800 words in length and may contain a maximum of 10 references. Letters may contain one figure or table.

3. Editorial Policies

For publishing and ethical standards, BioScience Trends follows the Recommendations for the Conduct, Reporting, Editing, and Publication of Scholarly Work in Medical Journals (*http://www.icmje.org/recommendations*) issued by the International Committee of Medical Journal Editors (ICMJE), and the Principles of Transparency and Best Practice in Scholarly Publishing (*https://doaj.org/bestpractice*) jointly issued by the Committee on Publication Ethics (COPE), the Directory of Open Access Journals (DOAJ), the Open Access Scholarly Publishers Association (OASPA), and the World Association of Medical Editors (WAME).

BioScience Trends will perform an especially prompt review to encourage innovative work. All original research will be subjected to a rigorous standard of peer review and will be edited by experienced copy editors to the highest standards.

Ethics: *BioScience Trends* requires that authors of reports of investigations in humans or animals indicate that those studies were formally approved by a relevant ethics committee or review board. For research involving human experiments, a statement that the participants gave informed consent before taking part (or a statement that it was not required and why) should be indicated. Authors should also state that the study conformed to the provisions of the Declaration of Helsinki (as revised in 2013). When reporting experiments on animals, authors should indicate whether the institutional and national guide for the care and use of laboratory animals was followed.

Conflict of Interest: All authors are required to disclose any actual or potential conflict of interest including financial interests or relationships with other people or organizations that might raise questions of bias in the work reported. If no conflict of interest exists for each author, please state "There is no conflict of interest to disclose".

Submission Declaration: When a manuscript is considered for submission to *BioScience Trends*, the authors should confirm that 1) no part of this manuscript is currently under consideration for publication elsewhere; 2) this manuscript does not contain the same information in whole or in part as manuscripts that have been published, accepted, or are under review elsewhere, except in the form of an abstract, a letter to

the editor, or part of a published lecture or academic thesis; 3) authorization for publication has been obtained from the authors' employer or institution; and 4) all contributing authors have agreed to submit this manuscript.

Cover Letter: The manuscript must be accompanied by a cover letter prepared by the corresponding author on behalf of all authors. The letter should indicate the basic findings of the work and their significance. The letter should also include a statement affirming that all authors concur with the submission and that the material submitted for publication has not been published previously or is not under consideration for publication elsewhere. The cover letter should be submitted in PDF format. For example of Cover Letter, please visit: Download Centre (*https://ircabssagroup.com/downcentre*).

Copyright: When a manuscript is accepted for publication in *BioScience Trends*, the transfer of copyright is necessary. A JOURNAL PUBLISHING AGREEMENT (JPA) form will be e-mailed to the authors by the Editorial Office and must be returned by the authors as a scan. Only forms with a hand-written signature are accepted. This copyright will ensure the widest possible dissemination of information. Please note that your manuscript will not proceed to the next step in publication until the JPA Form is received. In addition, if excerpts from other copyrighted works are included, the author(s) must obtain written permission from the copyright owners and credit the source(s) in the article.

Peer Review: *BioScience Trends* uses single-blind peer review, which means that reviewers know the names of the authors, but the authors do not know who reviewed their manuscript. The external peer review is performed for research articles by at least two reviewers, and sometimes the opinions of more reviewers are sought. Peer reviewers are selected based on their expertise and ability to provide high quality, constructive, and fair reviews. For research manuscripts, the editors may, in addition, seek the opinion of a statistical reviewer. Consideration for publication is based on the article's originality, novelty, and scientific soundness, and the appropriateness of its analysis.

Suggested Reviewers: A list of up to 3 reviewers who are qualified to assess the scientific merit of the study is welcomed. Reviewer information including names, affiliations, addresses, and e-mail should be provided at the same time the manuscript is submitted online. Please do not suggest reviewers with known conflicts of interest, including participants or anyone with a stake in the proposed research; anyone from the same institution; former students, advisors, or research collaborators (within the last three years); or close personal contacts. Please note that the Editor-in-Chief may accept one or more of the proposed reviewers or may request a review by other qualified persons.

Language Editing: Manuscripts prepared by authors whose native language is not English should have their work proofread by a native English speaker before submission. If not, this might delay the publication of your manuscript in *BioScience Trends*.

The Editing Support Organization can provide English proofreading, Japanese-English translation, and Chinese-English translation services to authors who want to publish in *BioScience Trends* and need assistance before submitting a manuscript. Authors can visit this organization directly at *http://www.iacmhr.com/iac-eso/support.php?lang=en*. IAC-ESO was established to facilitate manuscript preparation by researchers whose native language is not English and to help edit works intended for international academic journals.

4. Manuscript Preparation

Manuscripts are suggested to be prepared in accordance with the "Recommendations for the Conduct, Reporting, Editing, and Publication of Scholarly Work in Medical Journals", as presented at *http://www.ICMJE.org*.

Manuscripts should be written in clear, grammatically correct English and submitted as a Microsoft Word file in a single-column format. Manuscripts must be paginated and typed in 12-point Times New Roman font with 24-point line spacing. Please do not embed figures in the text. Abbreviations should be used as little as possible and should be explained at first mention unless the term is a well-known abbreviation (*e.g.* DNA). Single words should not be abbreviated.

Title page: The title page must include 1) the title of the paper (Please note the title should be short, informative, and contain the major key words); 2) full name(s) and affiliation(s) of the author(s), 3) abbreviated names of the author(s), 4) full name, mailing address, telephone/fax numbers, and e-mail address of the corresponding author; and 5) conflicts of interest (if you have an actual or potential conflict of interest to disclose, it must be included as a footnote on the title page of the manuscript; if no conflict of interest exists for each author, please state "There is no conflict of interest to disclose"). Please visit Download Centre and refer to the title page of the manuscript sample.

Abstract: The abstract should briefly state the purpose of the study, methods, main findings, and conclusions. For articles that are Original Articles, Brief Reports, Reviews, or Policy Forum articles, a one-paragraph abstract consisting of no more than 250 words must be included in the manuscript. For Communications, Editorials, News, or Letters, a brief summary of main content in 150 words or fewer should be included in the manuscript. Abbreviations must be kept to a minimum and non-standard abbreviations explained in brackets at first mention. References should be avoided in the abstract. Three to six key words or phrases that do not occur in the title should be included in the Abstract page.

Introduction: The introduction should be a concise statement of the basis for the study and its scientific context.

Materials and Methods: The description should be brief but with sufficient detail to enable others to reproduce the experiments. Procedures that have been published previously should not be described in detail but appropriate references should simply be cited. Only new and significant modifications of previously published procedures require complete description. Names of products and manufacturers with their locations (city and state/country) should be given and sources of animals and cell lines should always be indicated. All clinical investigations must have been conducted in accordance with Declaration of Helsinki principles. All human and animal studies must have been approved by the appropriate institutional review board(s) and a specific declaration of approval must be made within this section.

Results: The description of the experimental results should be succinct but in sufficient detail to allow the experiments to be analyzed and interpreted by an independent reader. If necessary, subheadings may be used for an orderly presentation. All figures and tables must be referred to in the text.

Discussion: The data should be interpreted concisely without repeating material already presented in the Results section. Speculation is permissible, but it must be well-founded, and discussion of the wider implications of the findings is encouraged. Conclusions derived from the study should be included in this section.

Acknowledgments: All funding sources should be credited in the Acknowledgments section. In addition, people who contributed to the work but who do not meet the criteria for authors should be listed along with their contributions.

References: References should be numbered in the order in which they appear in the text. Citing of unpublished results, personal communications, conference abstracts, and theses in the reference list is not recommended but these sources may be mentioned in the text. In the reference list, cite the names of all authors when there are fifteen or fewer authors; if there are sixteen or more authors, list the first three followed by *et al*. Names of journals should be abbreviated in the style used in PubMed. Authors are responsible for the accuracy of the references. The EndNote Style of *BioScience Trends* could be downloaded at **EndNote** (*https://ircabssagroup.com/examples/BioScience_Trends.ens*).

Examples are given below:

Example 1 (Sample journal reference):

Inagaki Y, Tang W, Zhang L, Du GH, Xu WF, Kokudo N. Novel aminopeptidase N (APN/CD13) inhibitor 24F can suppress invasion of hepatocellular carcinoma cells as well as angiogenesis. Biosci Trends. 2010; 4:56-60.

Example 2 (Sample journal reference with more than 15 authors):

Darby S, Hill D, Auvinen A, *et al*. Radon in homes and risk of lung cancer: Collaborative analysis of individual data from 13 European case-control studies. BMJ. 2005; 330:223.

Example 3 (Sample book reference):

Shalev AY. Post-traumatic stress disorder: Diagnosis, history and life course. In: Post-traumatic Stress Disorder, Diagnosis, Management and Treatment (Nutt DJ, Davidson JR, Zohar J, eds.). Martin Dunitz, London, UK, 2000; pp. 1-15.

Example 4 (Sample web page reference):

World Health Organization. The World Health Report 2008 – primary health care: Now more than ever. *http://www.who.int/whr/2008/whr08_en.pdf* (accessed September 23, 2010).

Tables: All tables should be prepared in Microsoft Word or Excel and should be arranged at the end of the manuscript after the References section. Please note that tables should not in image format. All tables should have a concise title and should be numbered consecutively with Arabic numerals. If necessary, additional information should be given below the table.

Figure Legend: The figure legend should be typed on a separate page of the main manuscript and should include a short title and explanation. The legend should be concise but comprehensive and should be understood without referring to the text. Symbols used in figures must be explained. Any individually labeled figure parts or panels (A, B, *etc*.) should be specifically described by part name within the legend.

Figure Preparation: All figures should be clear and cited in numerical order in the text. Figures must fit a one- or two-column format on the journal page: 8.3 cm (3.3 in.) wide for a single column, 17.3 cm (6.8 in.) wide for a double column; maximum height: 24.0 cm (9.5 in.). Please make sure that the symbols and numbers appeared in the figures should be clear. Please make sure that artwork files are in an acceptable format (TIFF or JPEG) at minimum resolution (600 dpi for illustrations, graphs, and annotated artwork, and 300 dpi for micrographs and photographs). Please provide all figures as separate files. Please note that low-resolution images are one of the leading causes of article resubmission and schedule delays.

Units and Symbols: Units and symbols conforming to the International System of Units (SI) should be used for physicochemical quantities. Solidus notation (*e.g*. mg/kg, mg/mL, mol/mm^2/min) should be used. Please refer to the SI Guide *www.bipm.org/en/si/* for standard units.

Supplemental data: Supplemental data might be useful for supporting and enhancing your scientific research and *BioScience Trends* accepts the submission of these materials which will be only published online alongside the electronic version of your article. Supplemental files (figures, tables, and other text materials) should be prepared according to the above guidelines, numbered in Arabic numerals (*e.g.*, Figure S1, Figure S2, and Table S1, Table S2) and referred to in the text. All figures and tables should have titles and legends. All figure legends, tables and supplemental text materials should be placed at the end of the paper. Please note all of these supplemental data should be provided at the time of initial submission and note that the editors reserve the right to limit the size and length of Supplemental Data.

5. Submission Checklist

The Submission Checklist will be useful during the final checking of a manuscript prior to sending it to *BioScience Trends* for review. Please visit Download Centre and download the Submission Checklist file.

6. Online Submission

Manuscripts should be submitted to *BioScience Trends* online at *http://www.biosciencetrends.com*. The manuscript file should be smaller than 5 MB in size. If for any reason you are unable to submit a file online, please contact the Editorial Office by e-mail at *office@biosciencetrends.com*

7. Accepted Manuscripts

Proofs: Galley proofs in PDF format will be sent to the corresponding author *via* e-mail. Corrections must be returned

to the editor (*proof-editing@biosciencetrends.com*) within 3 working days.

Offprints: Authors will be provided with electronic offprints of their article. Paper offprints can be ordered at prices quoted on the order form that accompanies the proofs.

Page Charge: Page charges will be levied on all manuscripts accepted for publication in *BioScience Trends* ($140 per page for black white pages; $340 per page for color pages). Under exceptional circumstances, the author(s) may apply to the editorial office for a waiver of the publication charges at the time of submission.

Misconduct: *BioScience Trends* takes seriously all allegations of potential misconduct and adhere to the ICMJE Guideline (*http://www.icmje.org/recommendations*) and COPE Guideline (*http://publicationethics.org/files/Code_of_conduct_for_journal_editors.pdf*). In cases of suspected research or publication misconduct, it may be necessary for the Editor or Publisher to contact and share submission details with third parties including authors' institutions and ethics committees. The corrections, retractions, or editorial expressions of concern will be performed in line with above guidelines.

(As of June 2020)

BioScience Trends
Editorial and Head Office
Pearl City Koishikawa 603,
2-4-5 Kasuga, Bunkyo-ku,
Tokyo 112-0003, Japan.
E-mail: office@biosciencetrends.com